# SATELLITE POWER SYSTEM

DOE/ER-0023

# Concept Development and Evaluation Program

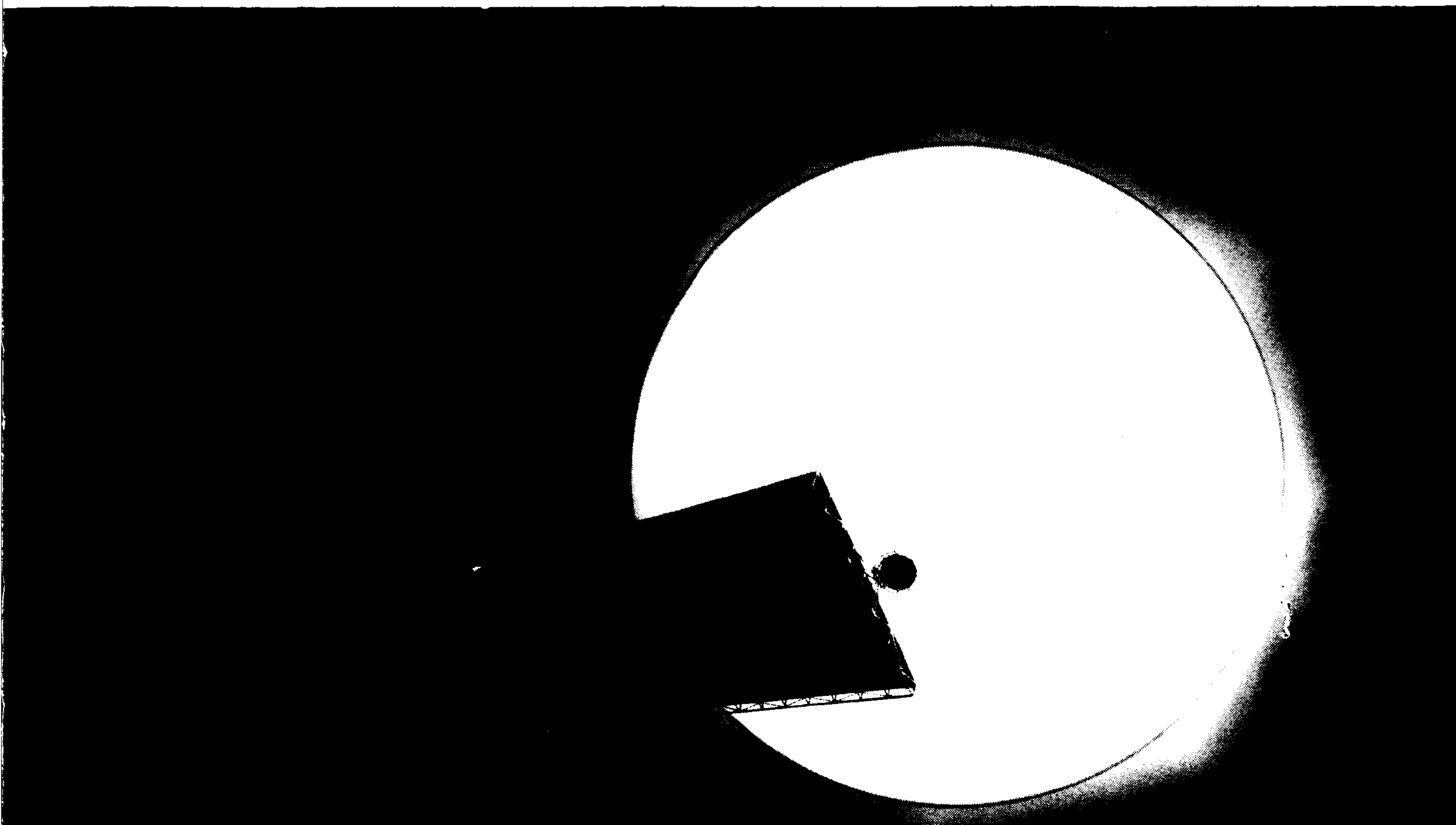


(NASA-TM-80413 SATELLITE POWER SYSTEM: CONCEPT DEVELOPMENT AND EVALUATION PROGRAM, REFERENCE SYSTEM REPORT (National Aeronautics and Space Administration) 321 p HC A14/MF A01 CSCL 10B G3/44

N79-21538

Unclas 19832



US Department of Energy and the National Aeronautics and Space Administration


**Reference System Report**

October 1978

Available from:

National Technical Information Service (NTIS)
U.S. Department of Commerce
5285 Port Royal Road
Springfield, Virginia 22161

Price: Printed copy: $11.75
Microfiche: $3.00

DOE/ER-0023
Dist. Category UC-11,41,60,63,
63a,b,c,e,64,66e,95f,97c

# Satellite Power System

## Concept Development and Evaluation Program

### Reference System Report

October 1978
(Published January 1979)

**U.S. Department of Energy**
Office of Energy Research
Washington, D.C. 20545
and the
**National Aeronautics and Space Administration**

# F O R E W O R D

The possibility of generating large quantities of electrical power in space and transmitting it to earth using satellites was first suggested in 1968. During the following years, several studies of the concept were conducted by the National Aeronautics and Space Administration (NASA) and industry. The energy shortages of 1973 spurred interest in the concept and in early 1976, the Department of Energy (DOE) (then the Energy Research and Development Administration) and NASA initiated an SPS Concept Development and Evaluation Program. This evaluation program is guided by a joint DOE-NASA plan which covers a period from mid-1977 to mid-1980. The key program milestones which guide all substudies and program activities are:

| | |
|---|---|
| Reference System Definition | October 1978 |
| Preliminary Program Recommendations | May 1979 |
| Updated Program Recommendations | January 1980 |
| Final Program Recommendations | June 1980 |

The joint plan states that the Reference System selection milestone "will focus the evaluation effort in what is considered to be at that time the optimal direction." It will particularly emphasize technical and operational information required by DOE to conduct environmental, socioeconomic and comparative studies.

This report is submitted in response to the first major program milestone. It defines a Reference System Concept based on the system definition effort to date. The concept presented is considered to be in the proper "direction," but is not optimum at this time. The system definition studies have, however, indicated technical feasibility of the reference concept and the concept will continue to be analyzed and changed as the results of preceding systems definition and other studies warrant.

## TABLE OF CONTENTS

## LIST OF FIGURES

LIST OF TABLES

## List of Abbreviations

| | |
|---|---|
| AC | ALTERNATING CURRENT |
| ACS | ATTITUDE CONTROL SYSTEM |
| ACSS | ATTITUDE CONTROL AND STATIONKEEPING SUBSYSTEM |
| AMO | AIR MASS ZERO |
| APU | AUXILIARY POWER UNIT |
| Ar | ARGON |
| BOL | BEGINNING OF LIFE |
| CMG | CONTROL MOMENT GYRO |
| CR | CONCENTRATION RATIO |
| CRM | CREW AND RESUPPLY MODULE |
| CW | CONTINUOUS WAVE |
| db | DECIBEL |
| DC | DIRECT CURRENT |
| DDT&E | DESIGN, DEVELOPMENT, TEST AND EVALUATION |
| DOE | DEPARTMENT OF ENERGY |
| EMI | ELECTROMAGNETIC INTERFERENCE |
| EOL | END OF LIFE |
| FET | FIELD EFFECT TRANSISTOR |
| GaAlAs | GALLIUM ALUMINUM ARSENIDE |
| GEO | GEOSYNCHRONOUS EARTH ORBIT |
| GFRTP | GRAPHITE FIBER REINFORCED THERMOPLASTIC |
| GHz | GIGAHERTZ ($10^9$ CYCLES/SECOND) |

| | |
|---|---|
| GW | GIGAWATT ($10^9$ WATTS) |
| GWe | GIGAWATT ELECTRIC |
| HF | HIGH FREQUENCY |
| $H_2$ | HYDROGEN |
| IMPATT | IMPACT AVALANCHE TRANSIT TIME |
| $I_{sp}$ | SPECIFIC IMPULSE |
| JPL | JET PROPULSION LABORATORY |
| JSC | JOHNSON SPACE CENTER |
| KSC | KENNEDY SPACE CENTER |
| kV | KILOVOLT |
| kW | KILOWATT |
| LaRC | LANGLEY RESEARCH CENTER |
| LBF | POUNDS OF FORCE |
| LEO | LOW EARTH ORBIT |
| LeRC | LEWIS RESEARCH CENTER |
| $\mu m$ | MICROMETER |
| MPD | MAGNETOPLASMADYNAMICS |
| MPTS | MICROWAVE POWER TRANSMISSION SYSTEM |
| MSFC | MARSHALL SPACE FLIGHT CENTER |
| MTBF | MEAN TIME BETWEEN FAILURE |
| MT | METRIC TON |
| MW | MEGAWATT ($10^6$ WATTS) |
| N | NEWTON |
| NASA | NATIONAL AERONAUTICS AND SPACE ADMINISTRATION |
| NM | NAUTICAL MILES |

| | |
|---|---|
| NS | NORTH-SOUTH |
| O&M | OPERATING AND MAINTENANCE |
| $O_2$ | OXYGEN |
| POP | PERPENDICULAR TO THE ORBIT PLAN |
| psi | POUNDS PER SQUARE INCH |
| RP | ROCKET PROPELLANT |
| RPC | RECTENNA POWER COLLECTION |
| RF | RADIO FREQUENCY |
| RFI | RADIO FREQUENCY INTERFERENCE |
| SCB | SATELLITE CONSTRUCTION BASE |
| SECS | SOLAR ENERGY COLLECTION SYSTEM |
| SE&I | SYSTEMS ENGINEERING AND INTEGRATION |
| SG | SWITCHGEAR |
| Si | SILICON |
| SPS | SATELLITE POWER SYSTEM |
| VAB | VERTICAL ASSEMBLY BUILDING (AT KSC) |
| VHF | VERY HIGH FREQUENCY |
| VLF | VERY LOW FREQUENCY |

## Transportation Systems

| | |
|---|---|
| BLOW | BOOSTER LIFT OFF WEIGHT |
| $CH_4$ | METHANE |
| COTV | CARGO ORBITAL TRANSFER VEHICLE |
| EOTV | ELECTRIC ORBITAL TRANSFER VEHICLE |
| ET | EXTERNAL TANK |
| GCR | GAS CORE REACTOR |
| GLOW | GROSS LIFT OFF WEIGHT |
| HLLV | HEAVY LIFT LAUNCH VEHICLE |
| HTO | HORIZONTAL TAKEOFF |
| IOTV | INTRA-ORBIT TRANSFER VEHICLE |
| $LCH_4$ | LIQUID METHANE |
| $LH_2$ | LIQUID HYDROGEN |
| LOX | LIQUID OXYGEN |
| MOTV | MANNED ORBITAL TRANSFER VEHICLE |
| OTV | ORBITAL TRANSFER VEHICLE |
| PLV | PERSONNEL LAUNCH VEHICLE |
| POTV | PERSONNEL ORBITAL TRANSFER VEHICLE |
| SRB | SOLID ROCKET BOOSTER |
| SSBE | SPACE SHUTTLE BOOSTER ENGINE |
| SSME | SPACE SHUTTLE MAIN ENGINE |
| SSTO | SINGLE STAGE TO ORBIT |
| T/W | THRUST TO WEIGHT |
| ULOW | UPPER STAGE LIFT OFF WEIGHT |
| $\Delta V$ | DELTA V - CHANGE IN VELOCITY |

## I. SUMMARY

The SPS Reference System concept as defined herein, is largely a product of system definition studies conducted by the Boeing Aerospace Company under contract to the Johnson Space Center (JSC) from December 1976 to December 1977, and Rockwell International under contract to the Marshall Space Flight Center (MSFC) from March 1977 to March 1978. The results of these two system definition studies combined with in-house efforts at both NASA Centers and several smaller contracted studies provided the data from which the Reference System was developed.

The two parallel, but independent, system definition studies resulted in well-integrated system concepts in which some major elements were very similar, but others were markedly different. To meet the Reference System milestone with essentially a single concept, a third system was developed by the selection of system elements of the two individual concepts.

Part III of this report describes the Reference System. Appendix A describes the various systems analyses that have been conducted. Appendix B describes the independent system definitions developed by Boeing and Rockwell.

The Reference System description emphasizes technical and operational information required in support of environmental, socioeconomic, and comparative assessment studies. Supporting information has been developed according to a guideline of implementing two 5 GW SPS systems per year for 30 years beginning with an initial operational date of 2000 and with SPS's being added at the rate of two per year (10 GW/year) until 2030.

Figure 1 illustrates the Reference System concept, which features gallium-aluminum-arsenide (GaAlAs) and silicon solar cell options. The concept utilizes a planar solar array (about 55 $km^2$) built on a graphite fiber reinforced thermoplastic structure. The silicon array uses a concentration ratio of one (no concentration), whereas the GaAlAs array uses a concentration ratio of two. A one-kilometer diameter phased array microwave antenna is mounted on one end. The antenna uses klystrons as power amplifiers with slotted waveguides as radiating elements. The satellite is constructed in geosynchronous orbit in a six-month period. The ground receiving stations (rectenna) are completed during the same time period.

The other two major components of an SPS program are (1) the construction bases in space and launch and mission control bases on earth and (2) fleets of various transportation vehicles that support the construction and maintenance operations of the satellites. These transportation vehicles include Heavy Lift Launch Vehicles (HLLV), Personnel Launch Vehicles (PLV), Cargo Orbit Transfer Vehicles (COTV), and Personnel Orbit Transfer Vehicles (POTV). The earth launch site chosen is the Kennedy Space Center, pending further study.

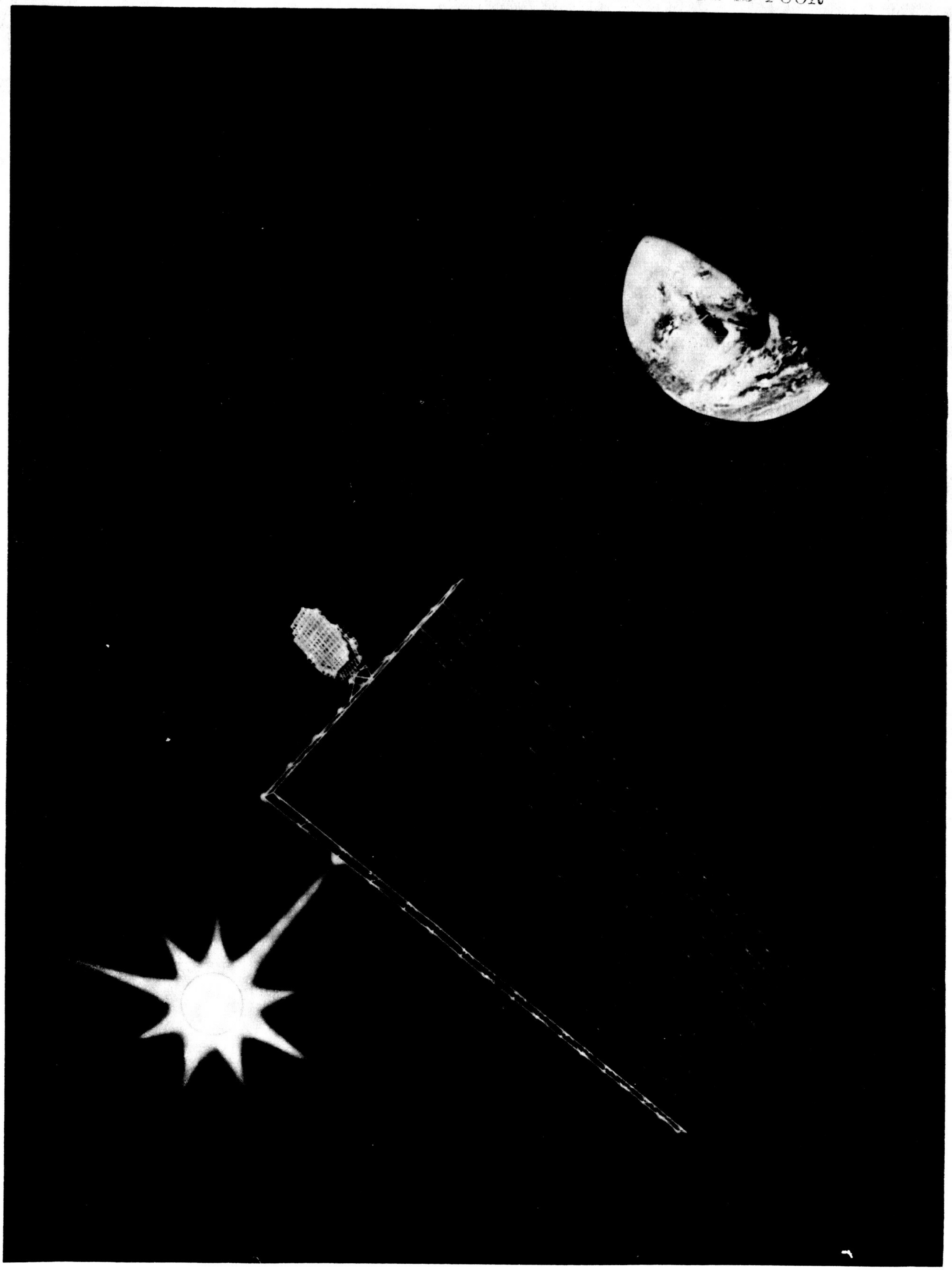

Figure 1. SPS Reference System Concept

## II. INTRODUCTION

The DOE and NASA have initiated a joint program which is described in the document entitled SPS Concept Development and Evaluation Program Plan (July 1977 - August 1980), DOE/ET-0034, dated February 1978. The objective of the program is to generate information from which a rational decision can be made regarding the direction of the SPS program after fiscal year 1980. Briefly, the plan states that NASA will conduct systems definition of the SPS and the DOE will evaluate health, safety, and environmental factors and will study SPS economic, international, and institutional issues. In addition, DOE will make comparative assessments of the concept relative to alternative power sources for the future.

Figure 2 shows a simplified diagram of the development and evaluation methodology. As indicated, the major milestones of the plan are baseline concept(s) selection - October 1978; preliminary program recommendations - May 1979; updated program recommendations - January 1980; and final program recommendations - June 1980. In this report, the term Reference System is used instead of baseline concept(s) as being more appropriate for the current level of definition and understanding. Using the results of this evaluation program as a basis and considering other pertinent factors, it will be possible for the Administration to either recommend continuation of the program in accordance with a defined option or terminate the program.

The purpose of this document is to present a description of the Reference System. It is submitted in response to the Baseline Concept(s) Definition program milestone (October 1978) established in the DOE/NASA plan as indicated above.

Section III of the report presents a description of the Reference System with emphasis on technical and operational information required by DOE to conduct environmental, socioeconomic, and comparative assessment studies. It is recognized that the Reference System lacks maturity as reported herein. Definition work is continuing to develop further understanding of the system.

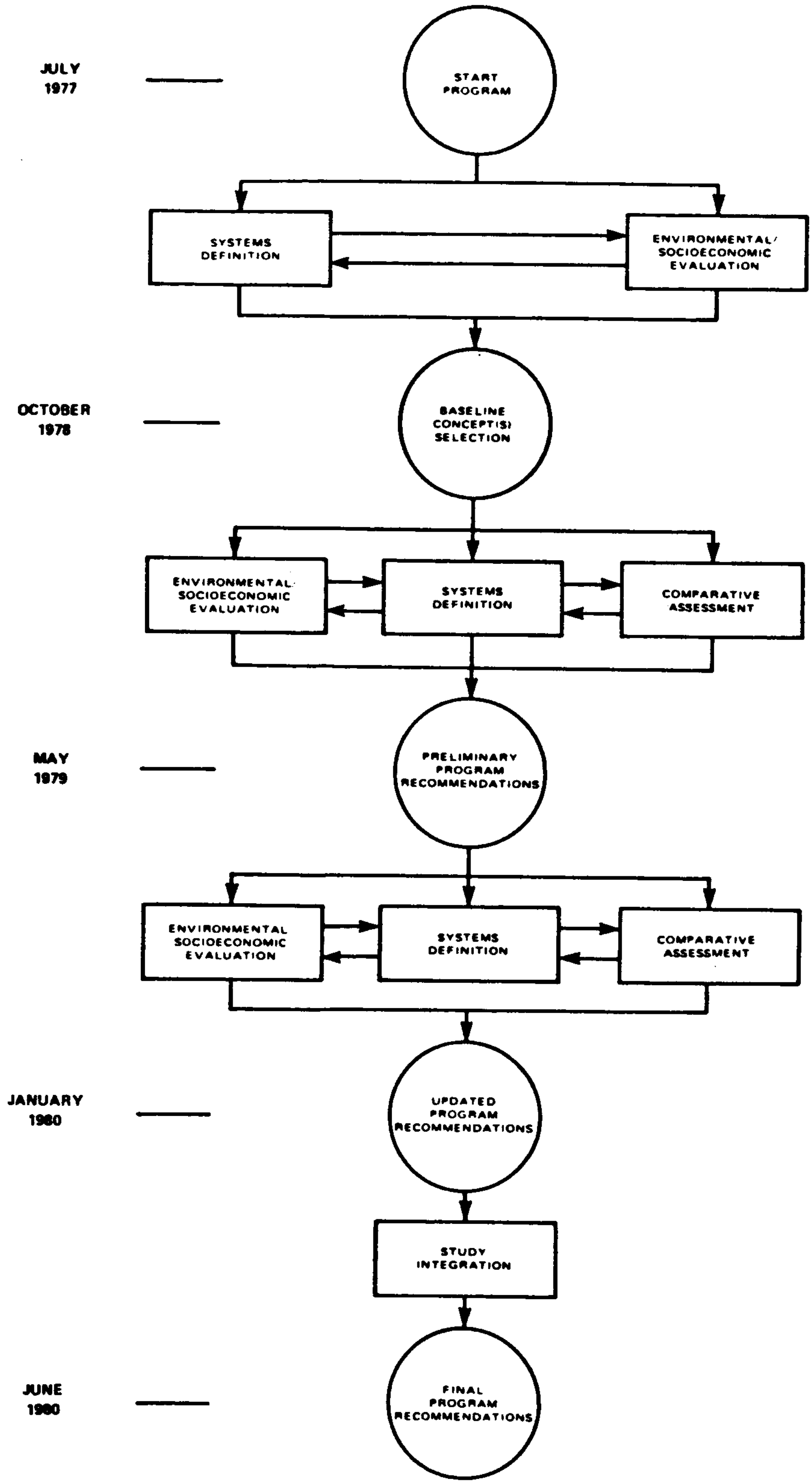


Figure 2. Simplified Diagram of SPS Concept Development and Evaluation Methodology

Section IV provides a discussion of technology advancement requirements which focuses on critical questions to be resolved that affect SPS feasibility. Also, alternate technologies which are delineated in the summary of study results section, are reviewed.

A summary of SPS documentation is provided in Section V to assist the reader in locating reference documents and following the flow of study results that has occurred over the past several years. This documentation summary serves as a list of references for this report.

Appendix A provides a summary of systems analysis results. The information presented is based on results of the key design and operational trade-off studies conducted to date in the major areas of investigation. The data base for the analysis summaries consists of study reports and other documents from current studies as well as those prepared in the late 1960's and early 1970's. Much of the early work was performed by A. D. Little, Raytheon Corporation, Spectrolab, Inc., Grumman Aerospace Corporation and the NASA Lewis Research Center. The Jet Propulsion Laboratory also made significant contributions to the SPS data bank, particularly in the area of microwave power transmission. The primary sources of information for the Reference System description are the systems definition reports published by Rockwell International and Boeing Aerospace Company under contract to MSFC and JSC, respectively.

Appendix B provides systems descriptions resulting from the studies conducted by the Boeing Aerospace Company and Rockwell International.

Background

This document deals with the solar power satellite concept as illustrated in figure 3. It is a primary electrical power source that involves generating electrical power (from solar energy) in geosynchronous orbit, transmitting the power to earth via focused microwave beams, and collecting and converting the microwave beams into useful electricity on the earth's surface. This concept was suggested in 1968 ("Power frcm the Sun: Its Future," Dr. Peter E. Glaser, Science, Vol. 162, November 22, 1968, pp 857-861).

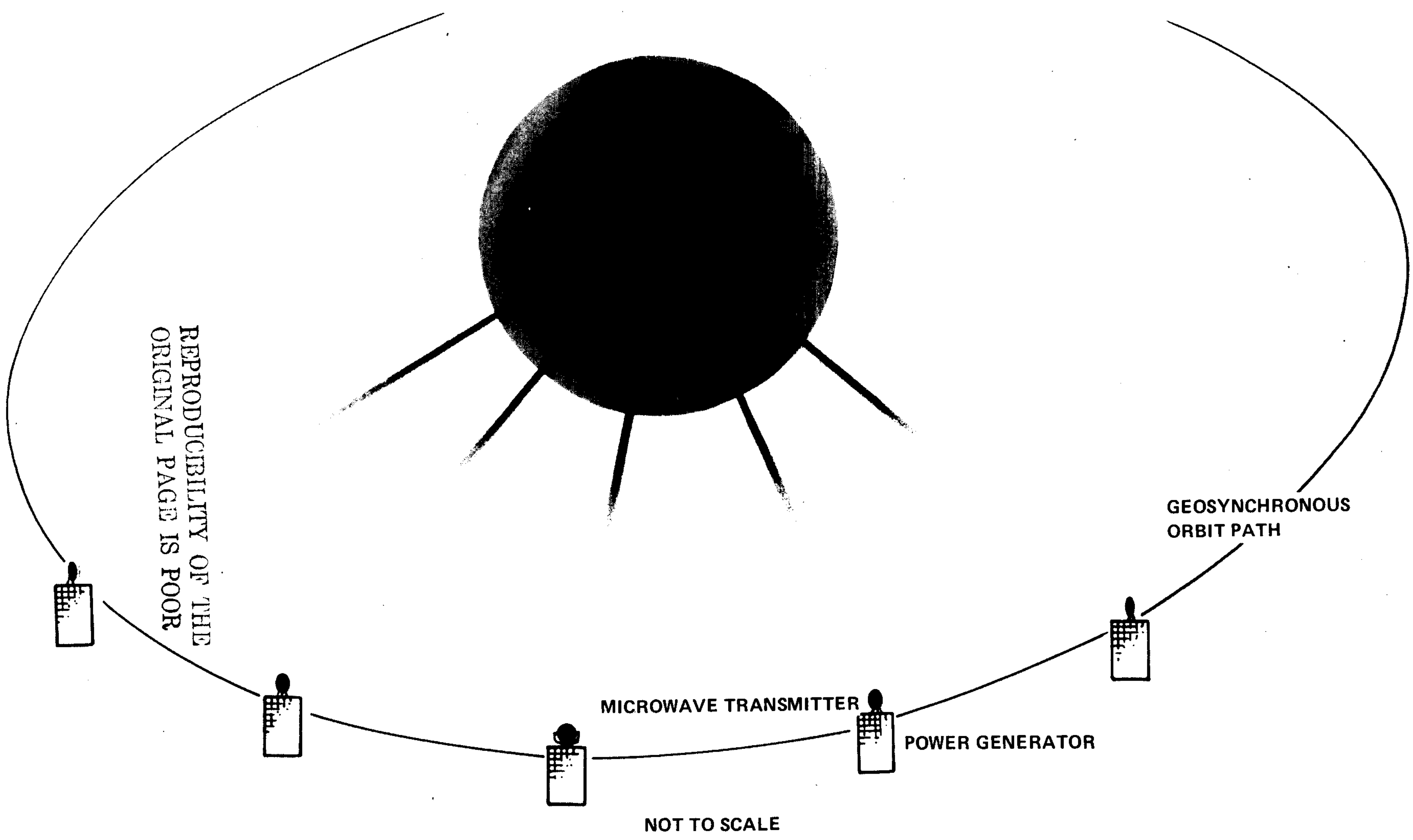


Figure 3. Solar Power Satellites

A number of other potential energy system concept involving the use of space satellites have also been suggested:

1. Orbiting nuclear reactor power systems (in lieu of solar collector/converters) with microwave transmission of power to earth.

2. The power relay satellite concept (Reference 12) in which power systems on the earth's surface or in low orbit transmit power by microwave to geostationary satellites. These geosynchronous satellites then relay (reflect) the microwave energy to ground stations placed at desired locations on earth.

3. Solar reflecting satellites (mirrors) in earth orbit which reflect solar energy directly to earth to augment ground-based solar power plants, allowing night operation or increased output.

4. Laser power transmission (in lieu of microwave) from the satellite.

The orbiting nuclear reactor concept has been evaluated to a limited extent. While it might offer the advantage of compactness relative to solar powered systems, its mass and complexity are significantly greater than solar powered systems. Significant safety and environmental questions remain to be addressed.

The power relay satellite is a long distance power transmission concept rather than a primary electrical energy source; consequently, it is not viewed as a basic alternative to the SPS concept.

The idea of placing large mirrors in earth orbit has been evaluated (Reference 14). Analysis indicates that with a mirror in geosynchronous orbit, the smallest illuminated "spot" on the earth would be about 330 km (205 miles) in diameter, governed by optical geometric considerations. If continuously illuminated at an average level of one sun, this large area would tend to rise in temperature to approximately 150°F, posing severe environmental problems. Placing large mirrors in lower altitude orbit reduces the size of the illuminated "spot." However, the mirrors would not be stationary with respect to a point on the earth. Thus, to achieve continuous illumination at a given location, numerous mirrors would have to be placed in low orbit. In addition, cloud cover and weather conditions would have an adverse effect on solar insolation precluding consideration of this concept as a primary, baseload electrical power source.

Laser power transmission has a significantly lower efficiency for long-distance power transmission than is estimated for microwave power transmission. Atmospheric attenuation is substantial compared to microwave frequency transmission. Therefore, this concept is presently less attractive than the microwave concept for transmitting power from geosynchronous orbit. Alternate system concepts such as solar collectors and laser transmitters in low earth orbit with relays in geosynchronous orbit have received preliminary consideration.

Another SPS concept is being evaluated that makes use of materials derived from the moon to construct the SPS. The moon's lower gravitational force (one-sixth of earth's) would allow much less propulsion energy to move payload to geosynchronous earth orbit. This idea appears to have merit in terms of conserving earth resources and possibly reducing the cost of space transportation; however, it would require development of moon-based mining, manufacturing and launch facilities. Consequently, the research and development requirements for such an approach would be greatly increased.

While the above options offer interesting possibilities, the present DOE/NASA program focuses evaluation on the SPS concept using terrestrial materials and deployed in geosynchronous orbit as illustrated in figure 3. This evaluation does not exclude the possibility of future consideration of the alternatives and options such as identified above.

## III. REFERENCE SYSTEM DESCRIPTION

The purpose of this section is to describe the SPS Reference System which has evolved primarily from system definition studies conducted by Boeing Aerospace Company and Rockwell International. The system concept presented herein is the result of numerous trade-off studies and engineering analyses, which are summarized in Appendix A of this report. It should be emphasized that the system described herein is preliminary and incomplete in detail in some areas. Evaluation by both DOE and NASA will continue to progress with the Reference System evolving and maturing as further details are developed.

### A. Guidelines and Assumptions

The guidelines and assumptions utilized in the Reference System definition are listed below.

- SPS operational date is year 2000.
- Rate of implementation is two 5 GW systems per year; 300 GW total capacity for costing purposes.
- All ground rectennas sized for 5 GW.
- SPS operation in geosynchronous orbit.
- Systems operating frequency is 2.45 GHz.
- Microwave power density not to exceed 23 and 1 $mW/cm^2$ at center and edge, respectively, of rectenna.
- All materials derived from earth resources.
- System life is 30 years with no salvage value or disposition costs.
- Zero launch rate failure assumed.
- Technology availability date is 1990.
- No cost margins will be used.
- Cost estimates in 1977 dollars.
- System weight growth factor (25%) to be reflected in costs.

### B. System Overview

The Reference System is sized for 5 GW DC power output into a conventional power grid. The satellite has one end-mounted antenna which transmits to a rectenna on the ground. This concept is illustrated in Figure 4.

The configuration of the satellite consists of a planar solar array structure built from a graphite composite material. Two conversion options are presented. One is the single-crystal gallium-aluminum-arsenide (GaAlAs) solar cells with a concentration ratio of 2 as illustrated in figure 4. The other energy conversion option is the use of single-crystal silicon (Si) solar cells with no concentration.

The size of the solar array is dictated primarily by the efficiency chain of the various elements in the system. Figure 5 shows the end-to-end efficiency chain for the GaAlAs and silicon solar cell options. With the satellite designed to provide 5 GW of DC power to the utility busbar and an overall efficiency of approximately 7%, it is necessary to size the solar arrays to intercept approximately 70 GW of solar energy as indicated in figure 5. The quoted efficiency is the minimum efficiency, including the worst-case summer solstice factor (0.9675), the seasonal variation (.91), and the end-of-life (30 year) solar cell efficiency assuming annealing. For the GaAlAs case, the end-of-life (30 year) concentrator reflectivity is 0.83. Since only half of the intercepted solar energy is reflected by the concentrators, the equivalent overall efficiency is 0.915.

The GaAlAs option is a five-trough configuration with a solar blanket area of 26.52 $km^2$, a reflector area of 53.04 $km^2$ and an overall planform area of 55.13 $km^2$. The silicon option has the solar blanket with no concentration resulting in a blanket area of 52.34 $km^2$ and a planform area of 54.08 $km^2$.

The satellite in either option is oriented so that the antenna main rotational axis remains perpendicular to the orbital plane.

The end-mounted microwave antenna is a one kilometer diameter phased-array transmitter. The phase control system utilizes an active, retrodirective array with a pilot beam reference for phase conjugation. Klystrons are used as the baseline power amplifier with slotted waveguides as the radiating element. The ground rectenna has subarray panels with an active element area of 78.5 $km^2$.

The satellite is constructed in geosynchronous orbit with construction time being six months. The initial estimates of construction crew size are 555

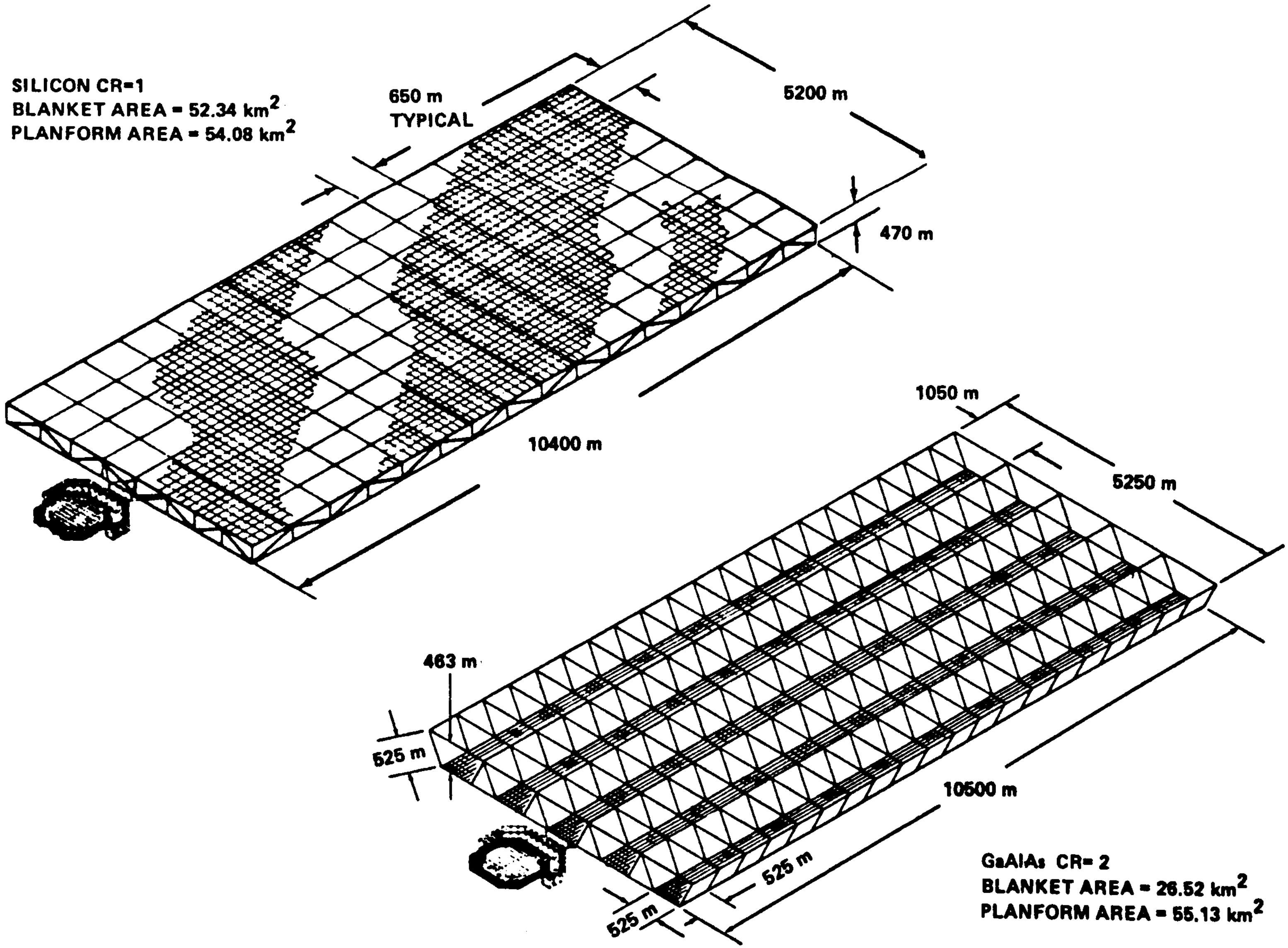


Figure 4. SPS Reference System - Satellite Configuration

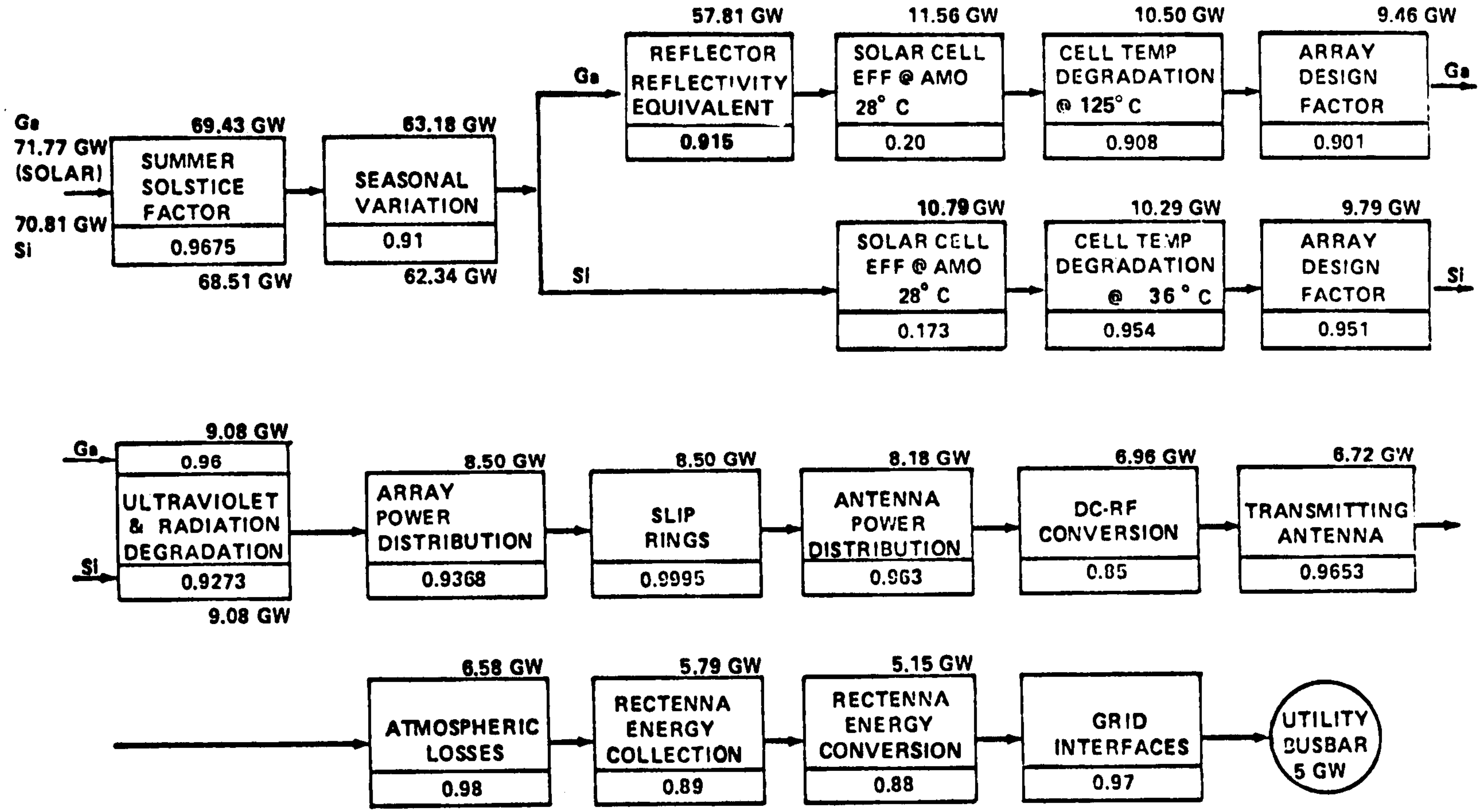


OVERALL EFFICIENCY = 6.97% Ga
7.06% Si

MPTS EFFICIENCY = 63.0%

Figure 5. SPS Efficiency Chain (GaAlAs CR2 and Si CR1)

for the silicon option (480 in GEO and 75 in LEO) and 715 for the GaAlAs option (680 in GEO and 35 in LEO).

The transportation system is made up of four major items. These include: (1) the Heavy Lift Launch Vehicle (HLLV), the Cargo Orbit Transfer Vehicle (COTV), the Personnel Launch Vehicle (PLV), and the Personnel Orbit Transfer Vehicle (POTV). The HLLV is a two-stage, vertical launch, winged, horizontal land-landing, reusable vehicle with 424 metric ton payload to low earth orbit. The earth launch site was chosen as Kennedy Space Center pending further study. The COTV is an independent, reusable electric engine-powered vehicle which transports cargo from the HLLV delivery site in low earth orbit (LEO) to the geosynchronous earth orbit (GEO). For the GaAlAs SPS option, the COTV is powered by GaAlAs solar cells, whereas a silicon solar cell power supply is used for the silicon SPS option.

Personnel for the orbital construction and support functions are transported to LEO via the PLV which is a modified space Shuttle Orbiter with a passenger module. The POTV, a two-stage reusable, chemical fuel vehicle is used to transfer personnel from LEO to GEO and return to LEO.

The satellite construction scenario for the Reference System is illustrated in figure 6. The HLLV is shown transporting cargo to LEO while the COTV and the POTV are illustrated transporting cargo and personnel,respectively, from LEO to GEO. A LEO operations base is used for temporary storage of supplies and propellant. One satellite is shown in GEO during the construction phase while another satellite is shown in the conventional operational phase transmitting energy to ground rectenna. Figure 7 summarizes the characteristics of the Reference System.

## C. Solar Cells and Blankets

Both GaAlAs and single-crystal silicon solar cells are considered reference energy conversion devices. Figure 8 shows a cross-section of the GaAlAs and Si solar cells and blankets. The basic GaAlAs solar cell consists of a 5 $\mu$m thick GaAs-P-N cell with a 0.03 to 0.05 $\mu$m thick GaAlAs front-side window. The solar cell efficiency is 20% at AMO, 28°C. The design operating


Figure 6. SPS Operations

| | | |
|---|---|---|
| SPS generation capability (utility interface) | 5 GW | |
| Overall dimensions (Km) | 5.3 x 10.4 | |
| Power conversion-photovoltaic | GaAlAs (CR=2) | Silicon (CR=1) |
| Satellite Mass (Kg) | 34 X $10^6$ | 51 X $10^6$ |
| Structure material | Graphite composite | |
| Construction location | GEO | |
| **Transportation** | | |
| • Earth-to-LEO -Cargo (payload) | Vertical take-off, winged 2-stage (424,000Kg) | |
| -Personnel (Number) | Modified shuttle (75) | |
| • LEO-to-GEO -Cargo | Dedicated elect. OTV | |
| -Personnel (Number) | 2-stage LOX/$LN_2$ (75) | |
| **Microwave power transmission** | | |
| • No. of antennas | 1 | |
| • DC-RF converter | Klystron | |
| • Frequency (GHZ) | 2.45 | |
| • Rectenna dimensions (Km) | 10 x 13 | |
| • Rectenna power density (mw/$cm^2$) | | |
| Center | 23 | |
| Edge | 1 | |

Figure 7. Reference System Characteristics

temperature is 125°C, which produces an 18.2% cell efficiency. At 125°C, self-annealing of radiation-induced damage occurs in the GaAlAs cells. As indicated in figure 8, the solar cell blanket material is Kapton (25 μm thick). The 20 μm synthetic sapphire ($Al_2O_3$) substrate, used in an inverse orientation, also acts as the cell cover. The blanket weight is 0.252 kg/m$^2$. The projected cost of the GaAs solar cell blanket is \$71/m$^2$.

Solar reflectors for the GaAlAs CR2 concept consist of thin reflective membranes (12.5 μm) of aluminized Kapton mounted in a 60° Vee trough configuration. The reflector membrane has a reflectivity of 0.9 BOL and 0.83 EOL. The effective end-of-life efficiency is 0.915 as previously stated. The membrane mass is 0.018 kg/m$^2$.

The silicon solar blanket consists of 50 μm thick single crystal silicon solar cells with borosilicate cover glass electrostatically bonded to the cells front and back. The cells are designed with both P and N terminals brought to the back of the cells. This feature makes it possible to use 12.5 μm silver-plated copper interconnections which are formed on the substrate glass. Complete panels are assembled electrically by welding together the module-to-module interconnections. The cell efficiency is 17.3% (AMO, 28°C) at beginning of life. At design operating temperature of 36.5°C, the efficiency is 16.5%. A key feature of the blanket design is the ability to perform in-situ annealing of the solar cells using a laser annealing concept. The laser annealing concept utilizes gimbal-mounted $CO_2$ lasers. The gimbals would be mounted on an overhead gantry structure to permit transversing of the entire solar array by several lasers as illustrated in figure 9. The laser beam heats the solar cells to annealing temperature (500°C) without damaging cell interconnect and substrate materials. Annealing is required to recover radiation induced degradation of the cells. The projected cost of the silicon solar blankets is \$35/m$^2$.

### D. Solar Array and Structure

The solar array consists of the deployed solar cell blankets attached to solar array structure. In the case of the CR2 GaAlAs option, the array includes the solar reflectors mounted on each side of the solar cell blankets. The solar cell blankets would be transported to orbit in modular packages in

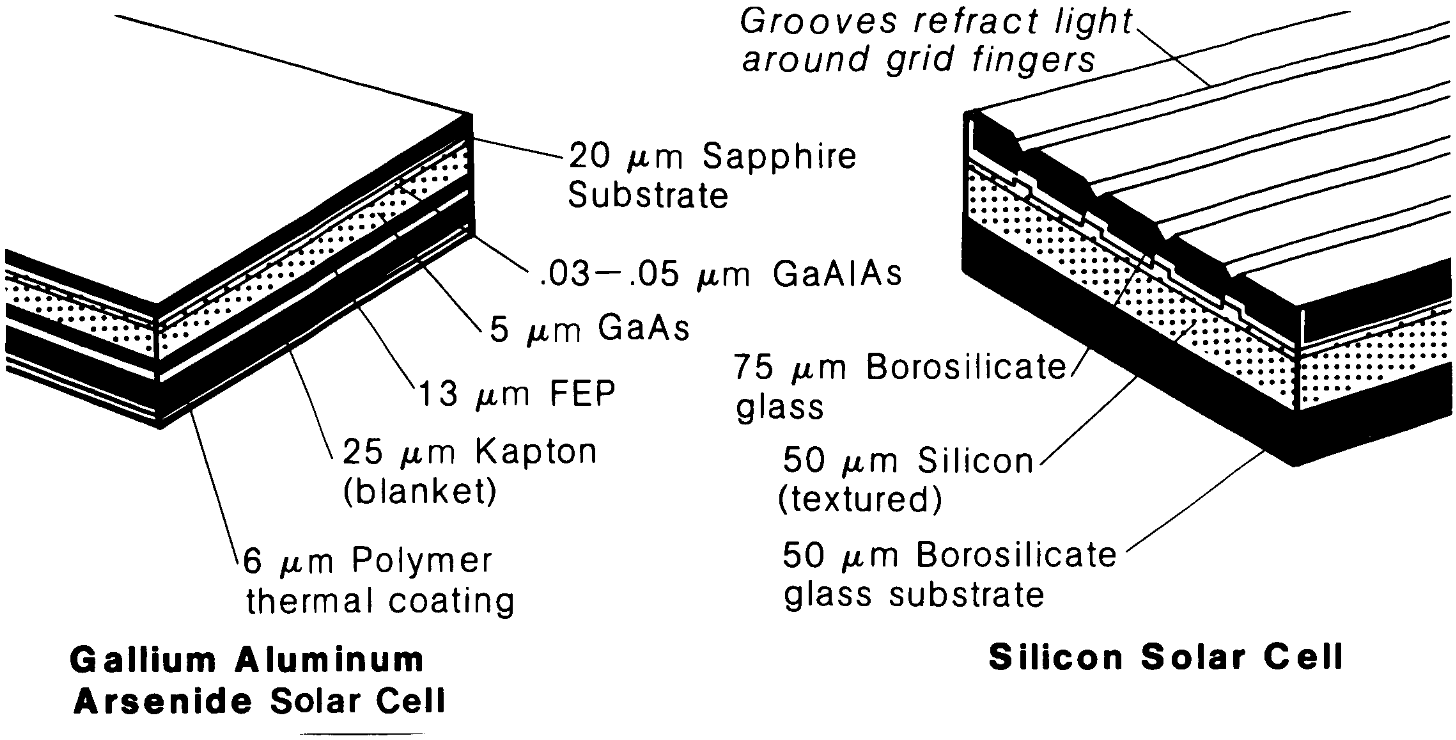


Figure 8. Solar Cell Options for SPS

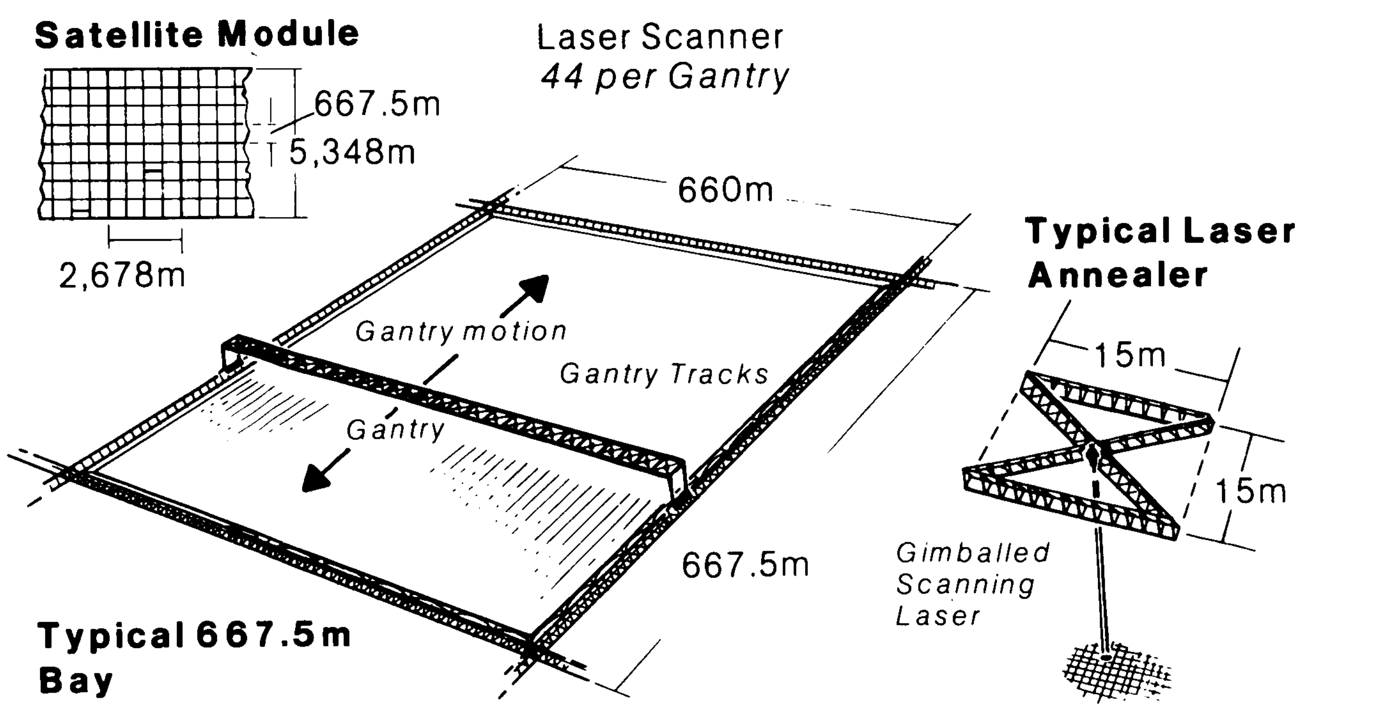


Figure 9. Laser Annealing Concept

either a rolled or folded configuration. The blanket modules would be connected together in a parallel/series arrangement to obtain the desired voltage output of 40 to 45 kv. Figure 10 illustrates the method of attaching the silicon solar cell blankets to the support structure. The GaAlAs blankets would be attached in a similar fashion. The reflector panels for the GaAlAs option are pleated at intervals to produce an accordian fold and then rolled for storage and shipment to orbit. The reflector panels would be attached to the primary structure by cables (catenaries).

The primary structure for solar array and microwave transmitting antenna is an open truss-type design. The structure material is a graphite-fiber reinforced thermoplastic composite. The basic elements (beams) are designed for automatic fabrication in space. The CR1 silicon cell option would utilize a rectangular configuration constructed with truss-type beams. The CR2 GaAlAs option utilizes similar construction elements for the solar array structure, but would include additional elements to form the structure for attaching solar reflectors.

## E. Power Distribution

The prime function of the power distribution system is to accumulate and control prime power from the solar cell panels; control, condition, and regulate the quantity and quality of the electrical power generated for the microwave generators; provide for the required energy storage during solar energy occulation or system maintenance shutdown; and provide for monitoring fault detection, and fault isolation disconnects.

Figure 11 shows a schematic diagram of the solar array power collection and distribution system. The solar array is divided into power sectors. Each power sector is switchable and can be isolated from the main power bus, facilitating solar cell annealing operations (for silicon cells) and/or other servicing.

Solar array power is controlled by high voltage circuit breakers near the buses. Voltage is controlled by turning groups of strings on or off, depending on load requirements. Two sections of the array provide the required voltage at the sliprings using the sheet conductor voltage drop to achieve the required voltage at the sliprings.

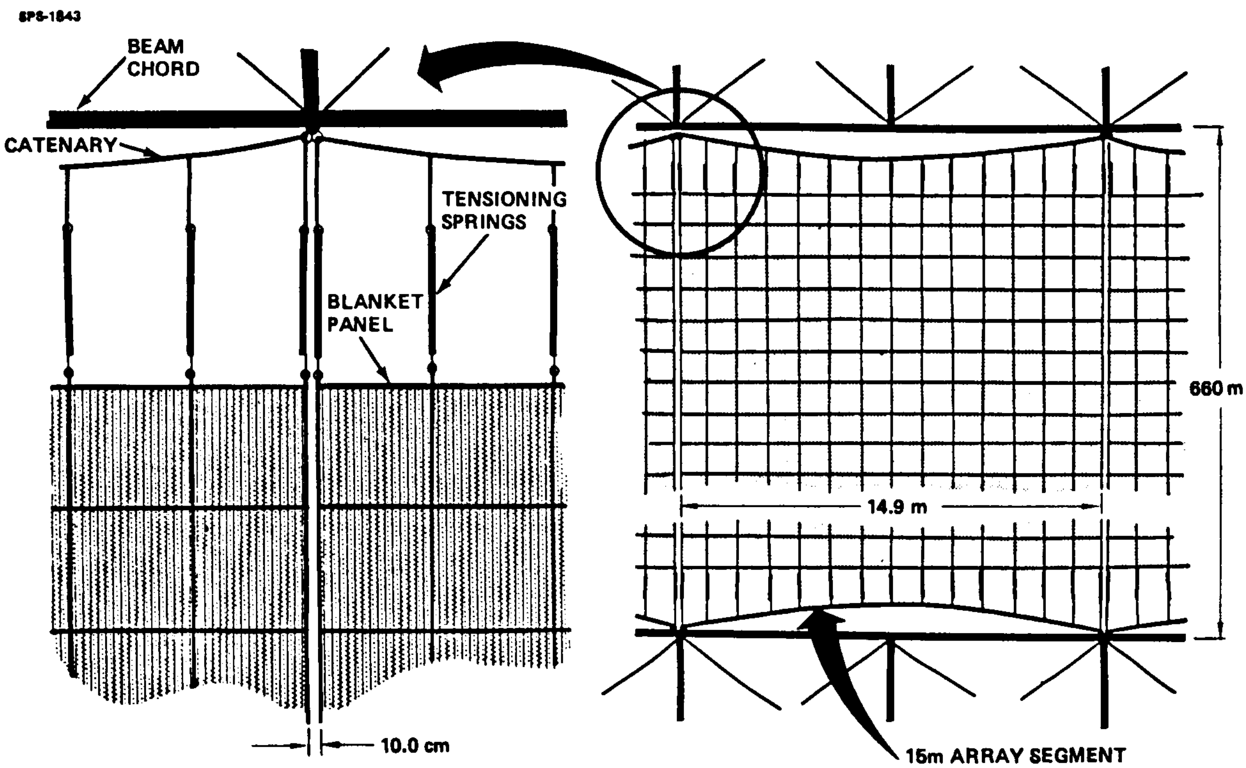


Figure 10. Solar Cell Blanket Support

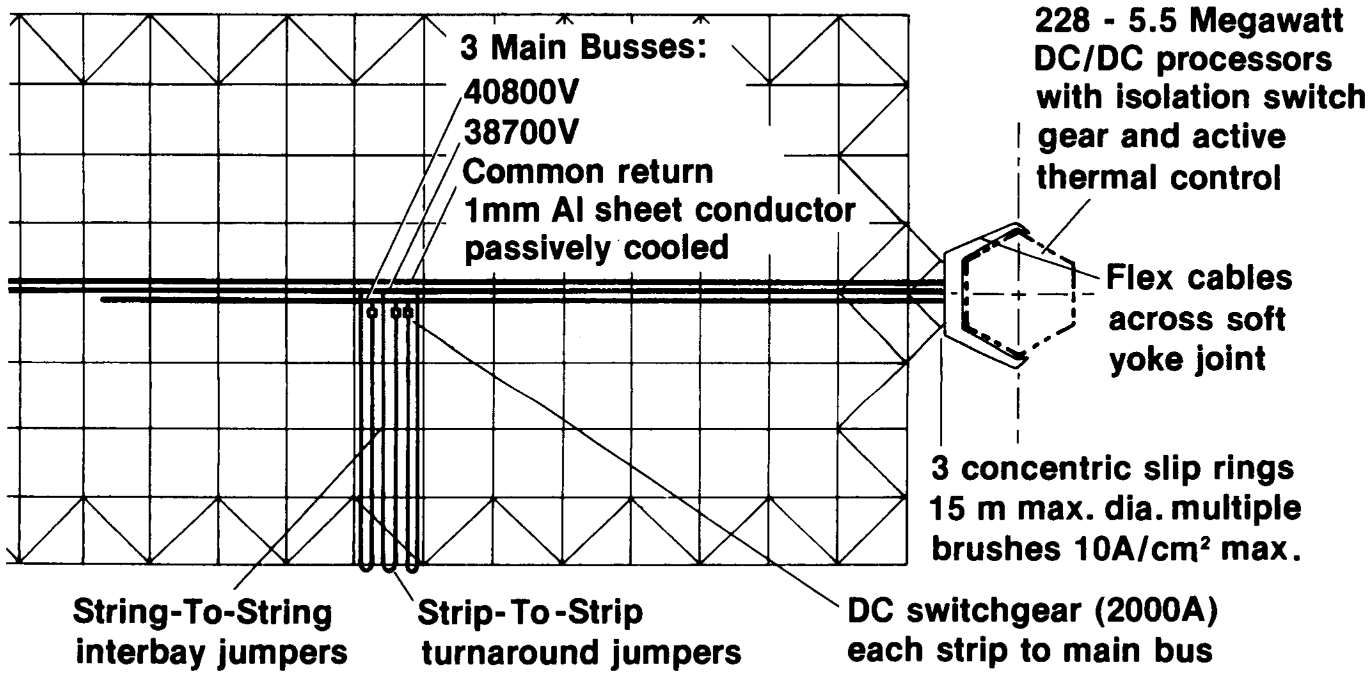


Figure 11. SPS Power Distribution

The microwave power transmitting antenna includes a power distribution system which transmits DC power from the slipring system to the DC-RF generators. Conductors from the slipring brushes are tied to DC/DC converters through switchgear tc allow isolation when performing maintenance. Conductors are then tied between voltage summing buses through other switchgear for transmitting the required power to the klystrons.

An electrical energy storage power system is located on the antenna structure with a bus routed along the regular network for operation during powered-down periods such as may occur during solar eclipse periods. A battery energy storage system would be utilized for storage of about 12 MW-hours of electrical energy.

F. Rotary Joint

Power transfer from the solar array section to the microwave antenna is accomplished via a rotary joint (figure 12) using a slipring/brush assembly. Mechanical rotation and drive is provided by a mechnical turntable 350 m in diameter. The antenna is suspended in the yoke by a compliant mechanical joint to isolate the antenna from turntable vibrations. The antenna is mechanically aimed by control moment gyroscopes (CMG's) installed on its structure. A positive feedback with a low frequency band-pass allows the mechanical turntable to drive the yoke to follow the antenna and also provide sufficient torque through the joint to keep the CMG's desaturated.

G. Attitude Control System (ACS)

The attitude control system for the reference 5 GW system is described for a CR2 GaAlAs option. The ACS for the CR1 Si option will be similar, although the number of thrusters and propellant requirements will differ.

Preliminary Baseline ACS Description - GaAlAs-CR2 - The baseline ACS features an argon ion bombartment thruster reaction control system (RCS) whose characteristics are given in figure 13. A total of 64 thrusters is included in the system to provide the required redundancy assuming: an annual maintenance interval, 5000 hour thruster grid lifetime and a 5-year thruster MTBF. Approxi-

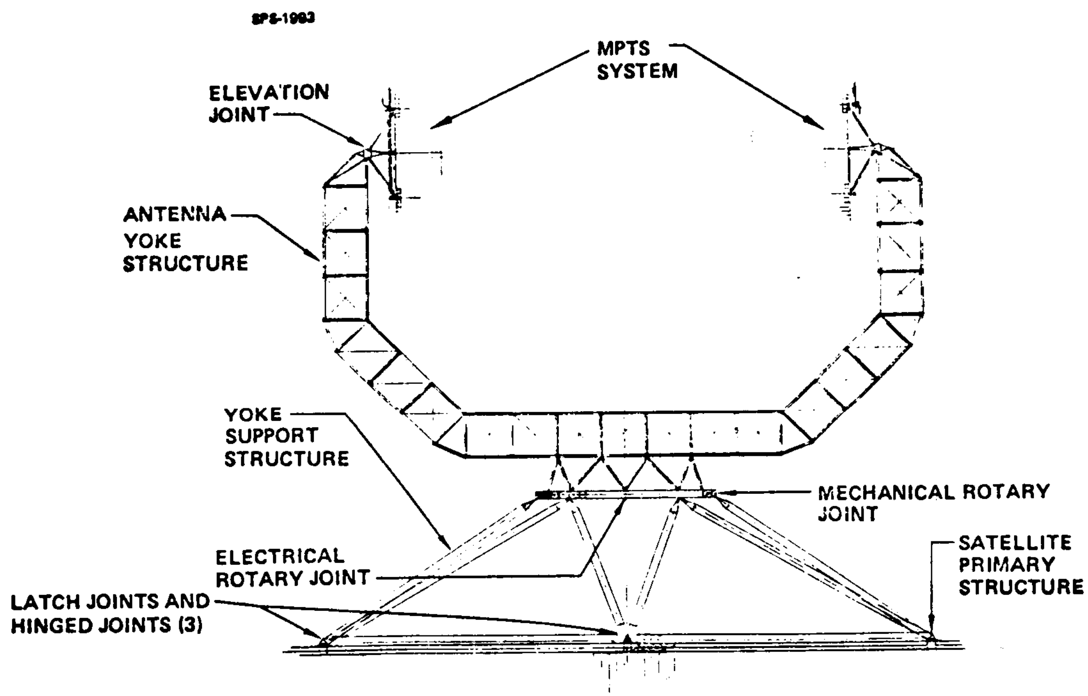


Figure 12. Antenna Yoke and Turntables

ATTITUDE REFERENCE DETERMINATION (7 LOCATIONS)

- CCD SUN SENSOR (1 PER SYSTEM)
- CCD STAR SENSORS (2 PER SYSTEM)
- ELECTROSTATIC OR LASER GYROS (3 PER SYSTEM)
- DEDICATED MINIPROCESSOR

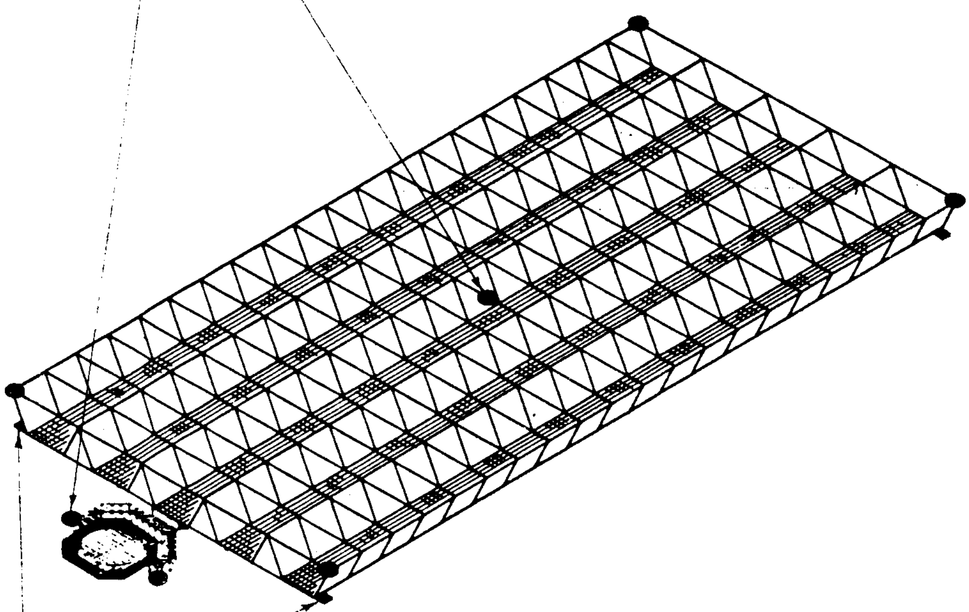

REACTION CONTROL SYSTEM (4 LOCATIONS)

- ARGON ION BOMBARDMENT THRUSTERS
- CRYOGENIC PROPELLANT STORAGE - ELECTRIC REFRIGERATION FOR HEAT LOSS MAKEUP
- HEMISPHERICAL PLUME CLEARANCE
- SERVICEABLE IN-PLACE

THRUSTER CHARACTERISTICS: EACH

- THRUST - 13N
- SPECIFIC IMPULSE - 13,000 SEC.
- POWER - 1,275 kW
- APERTURE - 1M
- MASS (INCL. SUPPORTS & CABLING) - 120 kg
- RESTART TIME - 15 SEC.
- OPERATING LIFE (GRIDS & CATHODES) - >5000 HR.

Figure 13. Attitude Control System Characteristics

mately 36 operating thrusters are required. Sixteen thrusters are located on the lower portion of each corner of the collector. Each thruster is gimballed individually to facilitate thruster servicing using a servicing cab, to permit operation of adjacent thrusters during servicing, and to provide redundancy.

The system is nominally designed for X-POP operation (long axis perpendicular-to-orbit-plane). The pertinent features and locations of the Attitude Reference Determination System (ARDS) are also given in figure 13. The average power required for the system is 34 megawatts.

H. Microwave Power Transmission System

The reference microwave power transmission system was developed considering environmental effects, antenna size tradeoffs, antenna thermal heating limitations, and ionospheric heating effects. The present microwave system has DC-RF power converters feeding a 1 km diameter phased array antenna with a 10-decibel (dB) Gaussian taper illumination across the array surface. This antenna shown in figure 14, is composed of 7220 subarrays, approximately 10 meters X 10 meters on a side, having slotted waveguides as the radiating surface with DC-RF power tubes mounted upon the backside of the subarrays. The antenna structure is a graphite composite material while the slotted waveguides are aluminum.

Each subarray has its own RF receiver and phasing electronics to process a pilot beam phasing signal from the ground. The subarrays are phased together to form a single coherent beam focused at the center of the ground antenna/rectifying system (rectenna). This power beam has approximately 88% of its energy within a 5 km radius perpendicular to boresight, with a resultant beam width of 1.2 arc-minutes.

Microwave System Parameters and Sizing Considerations - Some of the key parameters of the SPS microwave system are presented in figure 15. The power capability of the SPS system was sized by: (1) thermal limitations of 22 $kW/m^2$ in the transmit array due to waste heat from the DC to RF power converter tubes; (2) a peak power density limitation in the ionosphere of 23 $mW/cm^2$

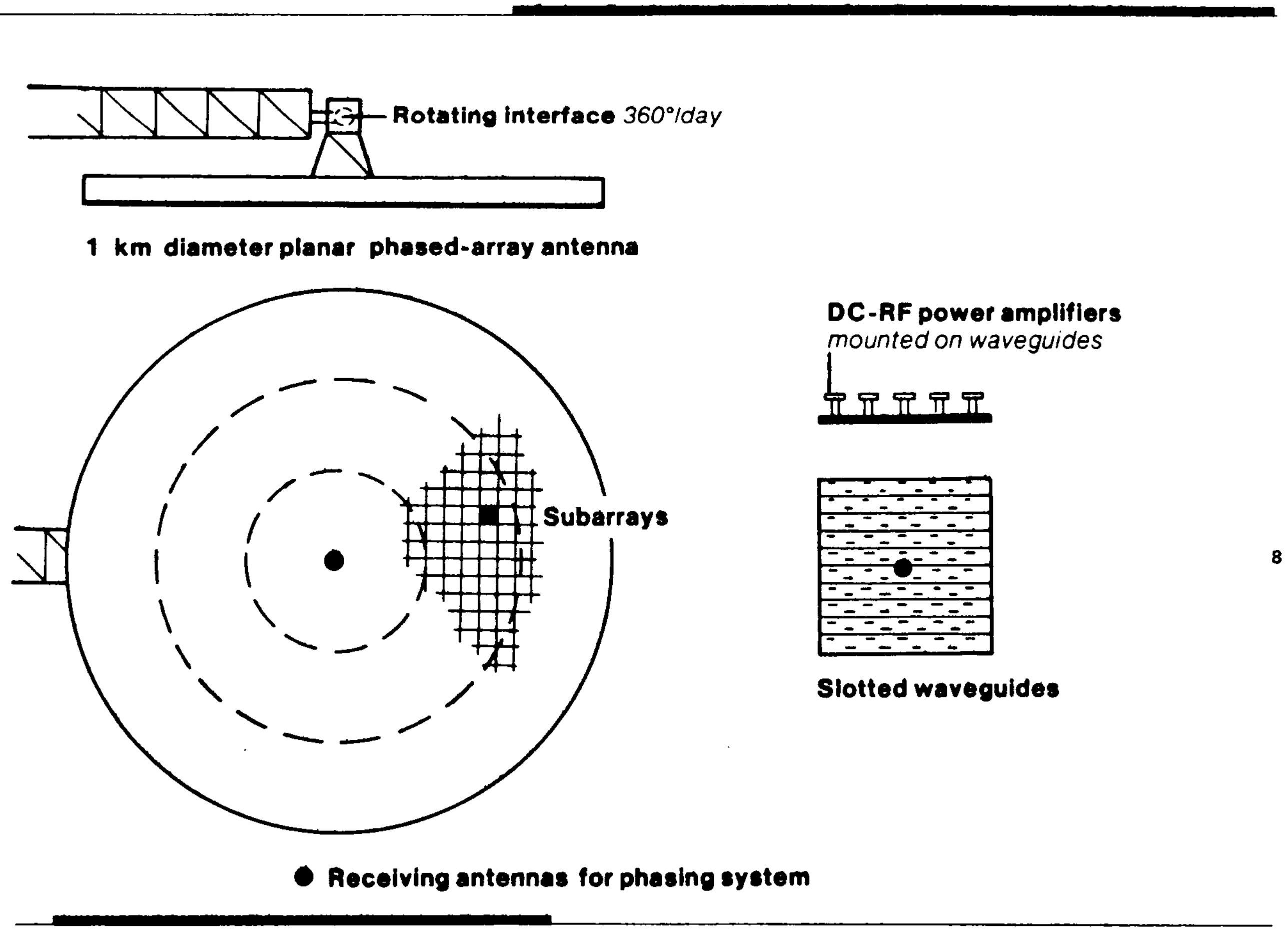


Figure 14. Transmitting Antenna Functional Description

- FREQUENCY 2.45 $GH_z$
- OUTPUT POWER TO POWER GRID 5 GW
- TRANSMIT ARRAY SIZE 1 KM IN DIAMETER
- POWER RADIATED FROM TRANSMIT ARRAY 6.72 GW
- MPTS EFFICIENCY 63%
- ARRAY APERATURE ILLUMINATION – A 10-STEP, TRUNCATED GAUSSIAN AMPLITUDE DISTRIBUTION WITH 10 dB EDGE TAPER
- ERROR BUDGET:
  - TOTAL RMS PHASE ERROR FOR EACH SUBARRAY = 10°
  - MAXIMUM MEAN PHASE ERROR AT EDGE OF TRANSMIT ARRAY = 2°
  - AMPLITUDE TOLERANCE ACROSS SUBARRAY = ±1 DECIBEL
  - FAILURE RATE OF DC-RF POWER CONVERTER TUBES = 2% (A MAXIMUM OF 2% HAVE FAILED AT ANY ONE TIME)
- ANTENNA/SUBARRAY MECHANICAL ALIGNMENT:

  ±3 ARC-MINUTES, WITH THE GRATING LOBES CONSTRAINED TO $\leqslant$.01 mW/cm$^2$ FOR A 108 m$^2$ SUBARRAY
- SUBARRAY SIZE: 108m$^2$
- NUMBER OF SUBARRAYS: 7220

Figure 15. Microwave Power Transmission System Parameters

- POWER DENSITY LEVELS
  - CENTER OF TANSMIT ANTENNA = 22 $kW/m^2$
  - EDGE OF TRANSMIT ANTENNA = 2.4 $kW/m^2$
  - CENTER OF RECTENNA = 23 $mW/cm^2$
  - EDGE OF RECTENNA = 1 $mW/cm^2$
  - FIRST SIDE LOBE LEVEL = .08 $mW/cm^2$ (APPROXIMATELY 9 Km FROM CENTER OF RECTENNA)
- GRATING LOBE LEVELS = $\leqslant$.01 $mW/cm^2$ AT SPACINGS OF 440 Km
- OUT-OF-BAND NOISE LEVELS = $\leqslant$CCIR REQUIREMENT OF -180 $dBW/m^2/H_z$ FOR ARRIVAL ANGLES GREATER THAN 25°
- ANTENNA PATTERN AT RECTENNA USING BASELINE ERROR PARAMETER: SEE FIGURE 18
- BEAM POINTING (ELECTRONIC): (TBD METERS)

  DIFFERENTIAL PHASE DELAYS IN IONOSPHERE AND TROPOSPHERE: MEAN-PHASE BUILDUP AND RMS PHASE JITTER IN TRANSMIT ARRAY; OTHER SOURCES:
- DC-RF POWER CONVERTER: KLYSTRON
- RF RADIATORS: SLOTTED WAVEGUIDE
- RF RADIATOR MATERIAL: ALUMINUM

Figure 15. Microwave Power Transmission System Parameters (Continued)

to prevent non-linear heating interactions between the ionosphere and the microwave beam; and (3) microwave transmission efficiency considerations (particularly the RF levels into the rectenna).

Studies into the microwave beam/ionosphere interactions indicate that non-linear thermal self-focusing instabilities in the F-region (200 to 300 kilometers altitude) and thermal runaway conditions in the D-region (100 kilometers) may limit the maximum power density at the center of the beam to approximately 23 $mW/cm^2$ at the 2450 MHz operating frequency (references 26, 29, 30 and 31). Above this threshold power density level (which is a theoretical number, not yet verified by experiments), non-linear interactions between the power beam and the ionosphere begin to occur. These non-linear heating interactions are of concern because of possible degradations to existing HF and VHF communication and VLF navigation systems due to RFI effects and multipath degradations. The heated ionosphere may also introduce phase jitter and/or differential phase delays on the uplink pilot beam signal. These ionosphere/microwave beam interactions are now being studied, both theoretically and experimentally.

Antenna Characteristics - The microwave antenna has both a primary and a secondary structure composed of a graphite composite material. The primary structure is an open truss, 130 meters deep, with an octagonal shape over 1000 meters in width and length. The secondary structure is a deployable cubic truss, 9.93 meters in depth, which provides support for installation of the microwave subarrays.

The aperture illumination function across the 1-kilometer transmit array was optimized to provide the maximum amount of RF power intercepted by the ground rectenna and to minimize the sidelobe levels. A number of different illumination functions, operating in the presence of phase and amplitude errors and element (subarray) failures, have been studied (see Appendix A). The 10-decibel Gaussian taper has the best overall performance of the optimized illumination functions after considering the maximum power density constraints in the transmit array and rectenna.

A 10 step, 10 dB Gaussian taper for the transmit array is given in figure 16. There are 36 DC-RF power converter tubes per subarray at the center of the antenna, decreasing in quantized steps down to four tubes per subarray at the edge to provide the 10 dB Gaussian taper. There will be a total of 101,552 tubes in the antenna, integrated into the subarrays as shown in figure 17. This particular configuration uses a 70 kw klystron tube; an alternative concept has a 50 kw klystron, which requires approximately 140,000 tubes. The number of tubes per subarray would then vary from 50 tubes at the center of the antenna to six tubes at the edge in order to provide the 10 dB illumination taper.

The radiation pattern for the 10 dB taper, 1 km array (and $\sigma = 10°$ RMS phase error, $\pm 1$ dB amplitude error, and 2% random failures) at the ground rectenna is shown in figure 18. The effect of the antenna errors is to produce a wider, lower intensity main beam with higher sidelobes. For the SPS sytem concept, only a portion of the main lobe will be collected; the sidelobe energy occupies a very large area at very low density levels and is not economically feasible to collect.

The peak power densities are 23 milliwatts per square centimeter at the rectenna boresight, 1 milliwatt per square centimeter at the edge of the rectenna, and 0.08 milliwatt per square centimeter for the first sidelobe, which is two orders of magnitude below the U.S. radiation standard of 10 $mW/cm^2$.

If there is a total failure within the phase control system (for example, the uplink pilot beam transmitter is shut off), the subarrays will no longer be phased together and the total beam will be defocused. As shown in figure 18, the peak intensity of the beam drops to 0.003 $mW/cm^2$ and the beam width greatly increases. This peak power density is significantly less than the USSR guideline indicated on figure 18. Consequently, this is a fail-safe feature of the phasing system. In addition, there are sensors near the rectenna to detect any large changes in incident power density; this information would immediately be transmitted to the antenna to cease operations.

In addition to the sidelobe patterns near the rectenna, the far-sidelobe patterns have been calculated. There had been some concern about the radio

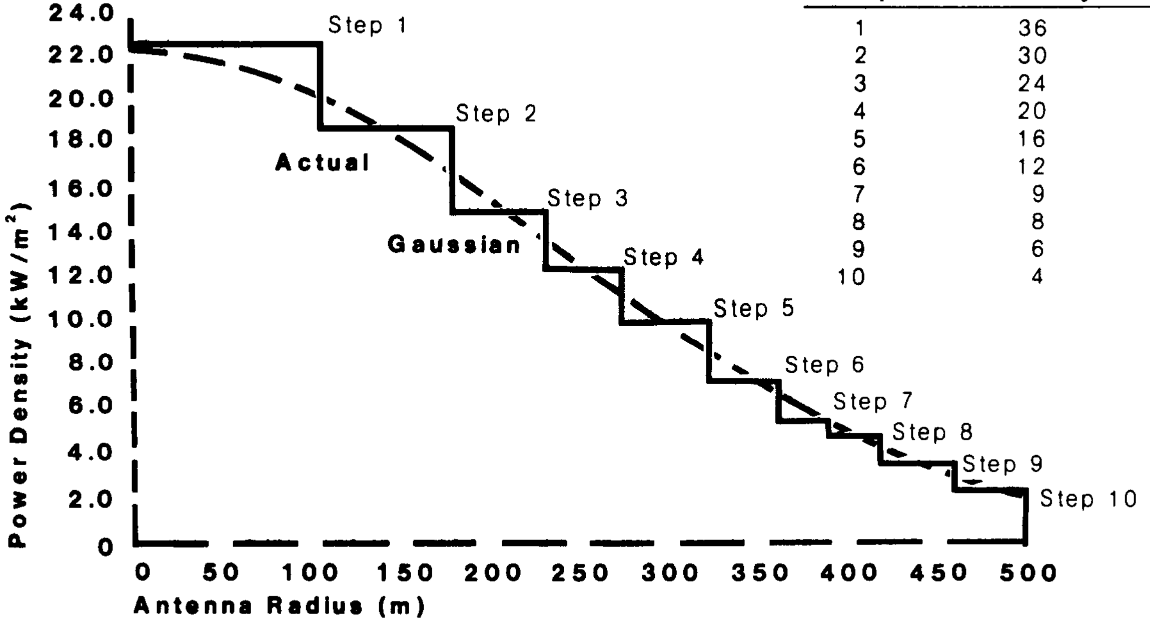


| Step | Elements/ Subarray | Power Density $kW/m^2$ |
|---|---|---|
| 1 | 36 | 22.14 |
| 2 | 30 | 18.45 |
| 3 | 24 | 14.76 |
| 4 | 20 | 12.30 |
| 5 | 16 | 9.84 |
| 6 | 12 | 7.38 |
| 7 | 9 | 5.54 |
| 8 | 8 | 4.92 |
| 9 | 6 | 3.69 |
| 10 | 4 | 2.46 |

Figure 16. Microwave Power Transmission System
10 dB taper

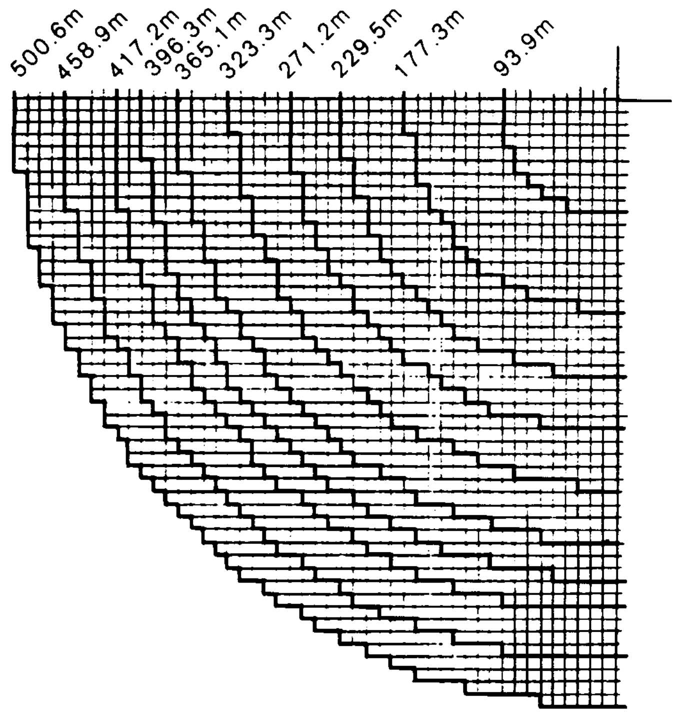


| Step | Number Subarrays | Number Klystrons/ Subarrays | Number Klystrons |
|---|---|---|---|
| 1 | 276 | 36 | 9,936 |
| 2 | 632 | 30 | 18,960 |
| 3 | 644 | 24 | 15,458 |
| 4 | 628 | 20 | 12,560 |
| 5 | 784 | 18 | 12,544 |
| 6 | 900 | 12 | 10,800 |
| 7 | 664 | 9 | 5,976 |
| 8. | 612 | 8 | 4,896 |
| 9 | 1,052 | 6 | 6,312 |
| 10 | 1,028 | 4 | 4,112 |
| **Totals** | **7,220** | | **101,552** |

Figure 17. Microwave Array Power Distribution

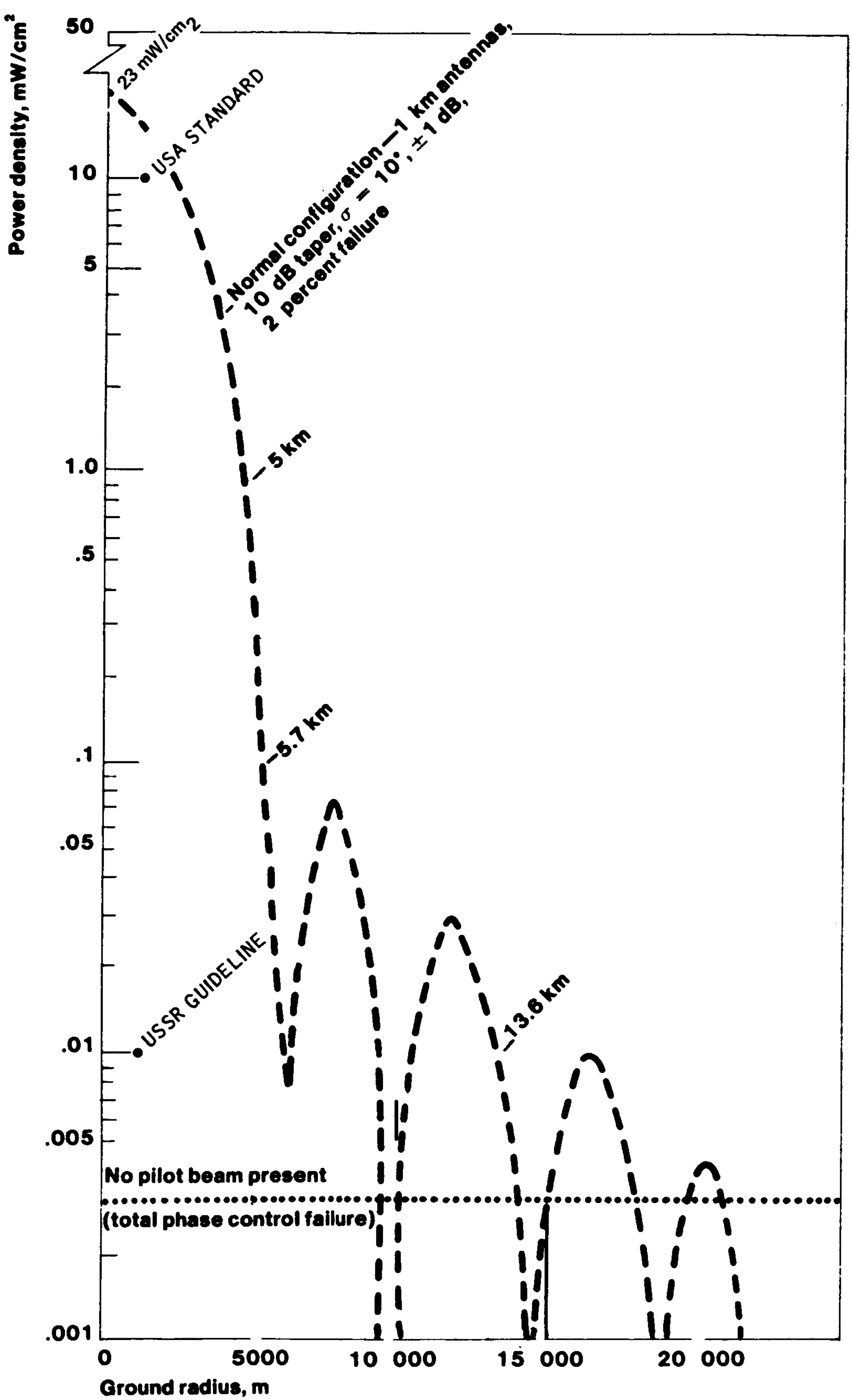


Figure 18. Power Density at Rectenna as a Function of Distance from Boresight

interference levels at large distances from any given rectenna because of frequency allocation problems. The SPS downlink power beam lies in the 2400-2500 MHz frequency band which has been reserved for Government and non-Government industrial, medical, and scientific (IMS) usage. By definition, anyone operating in an IMS band must accept interference from any other user within this band. However, this 100 MHz band is not recognized by some of the eastern European countries which reserve 2375 MHz $\pm$ 50 MHz for the IMS band. The far sidelobe levels as shown in figure 19 indicate the peak levels for one 5 gigawatt SPS system are three to four orders of magnitude below 0.01 mW/cm$^2$. For simultaneous operation of 200, 5 gigawatt SPS systems, the average peak level is still one to two orders of magnitude lower than 0.01 mW/cm$^2$.

Grating lobes, which occur at 440 km intervals from the rectenna, are functions of subarray size and mechanical misalinement of the subarrays within the 1 km phase array. The grating lobes occur at spatial distances corresponding to angular directions off axis of the antenna array where the signals from each of the subarrays add in-phase.

When the boresights of the subarrays are not alined with the uplink pilot beam transmitter at the rectenna, the unwanted contributions of the array factor of the antenna do not lie in the null-points of the subarray pattern as shown in figure 20. Even though the phase control system will still point the composite beam at the rectenna, some energy will be transformed from the main beam into the grating lobes. The amount of energy in the grating lobes depends upon the misalinement (or how far the array factor is displaced from the null points of the subarray pattern). These grating lobes are somewhat unique in that they do not spatially move with misalinement changes, rather they are stationary with an amplitude dependence upon the mechanical misalinements. This behavior is due to the operating characteristics of the retrodirective phasing system. Based on environmental considerations, the grating lobes are constrained to be less than 0.01 mW/cm$^2$. The total mechanical alinement requirements for both the subarrays and the total array can be determined from this constraint. The 10.4 meter X 10.4 meter subarray which is considered

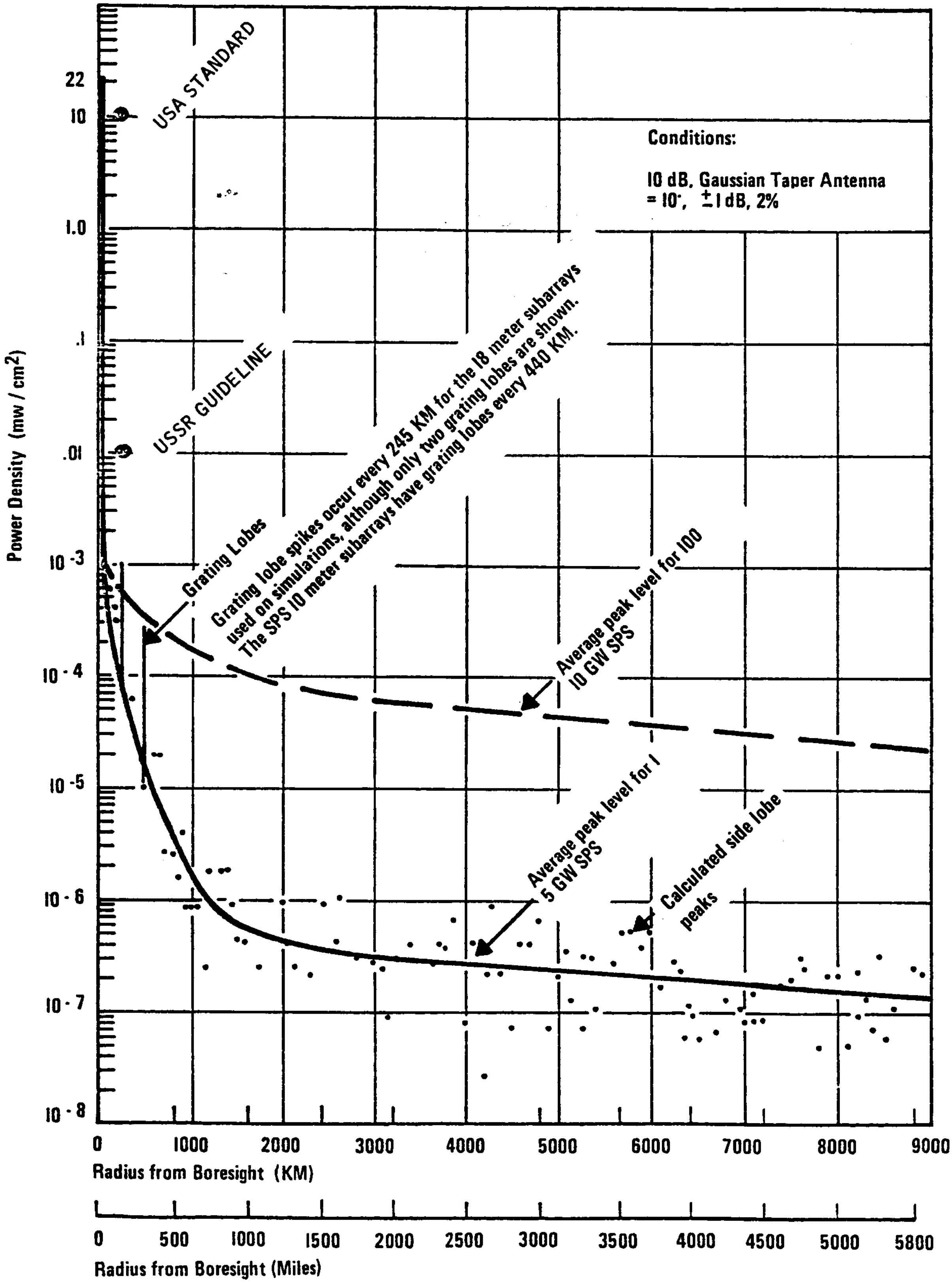


Figure 19. Peak Power Density Levels as a Function of Range From Rectenna

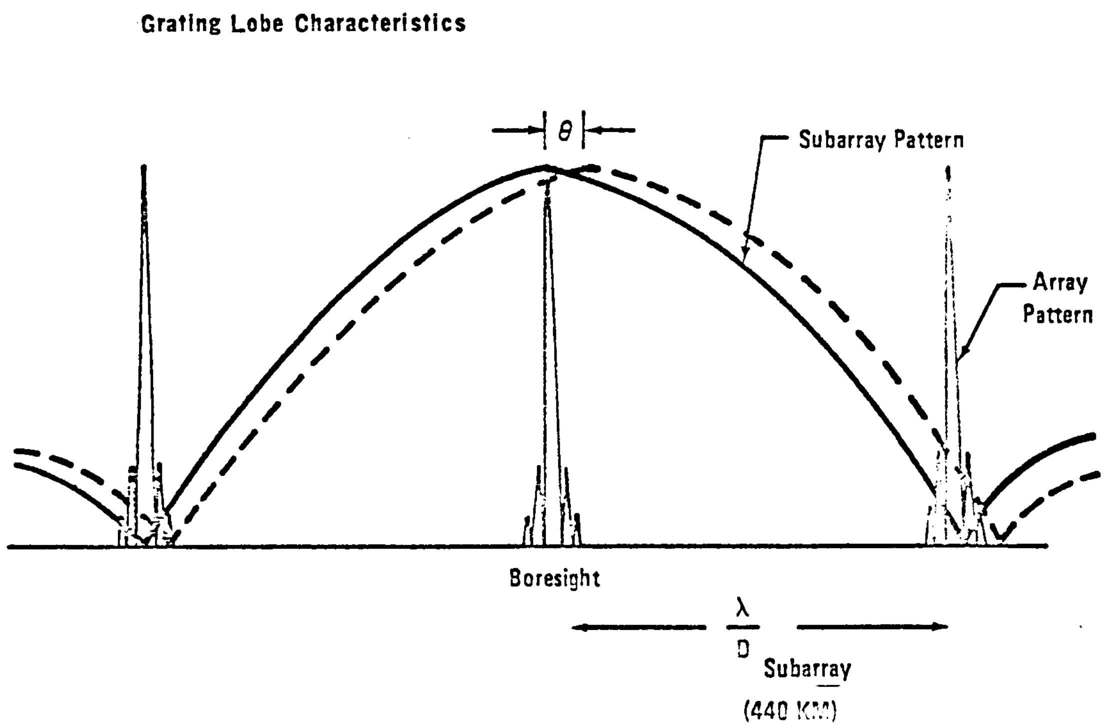


Figure 20. Grating Lobe Characteristics

to be the smallest entity for phase control, has the peaks of the grating lobe patterns at the ground as shown in figure 21. Since the distance between maxima for the grating lobes is inversely proportional to the spacings between subarrays, a 10.4 meter square subarray has peaks every 440 km. If the phase control system is extended down to the power module level, the grating lobes will be spatially smeared and the peaks greatly reduced in amplitude. This improvement in grating lobe pattern would be due to differences in spacings between the power tubes within the antenna. There are two types of mechanical misalinements: (1) a systematic tilt of the entire antenna structure, and (2) a random tilt of the individual subarrays. The systematic tilts have a greater impact than the random subarray tilts on the grating lobe peaks. An example of the first grating lobe peak for a total antenna/subarray tilt of 3.0 arc-minutes is shown in figure 22. Other simulations have established mechanical alinement requirements of less than 1 arc-minute for the antenna tilt and less than 3-arc-minutes for the random subarray tilts.

The near-field antenna pattern for distances close to the transmit array is shown in figure 23. A peak density of approximately 32 kW/m$^2$ occurs at a distance of 1600 km.

Rectenna Characteristics - The present ground receiving antenna (rectenna) configuration, which receives and rectifies the downlink power beam, has half-wave dipoles feeding Schottky barrier diodes. Two-stage low-pass filters between the dipoles and diodes suppress harmonic generation and provide impedance matching. For economic reasons, the rectenna is a series of serrated panels perpendicular to the incident beam rather than a continuous structure. Each panel has a steel mesh ground plane with 75-80% optical transparency. This mesh is mounted on a steel framing structure, supported by steel columns in concrete footings. Aluminum conductors are used for the electrical power collection system.

The rectenna will produce RFI effects due to rescattered incident radiation and harmonic generation within the diodes. There will also be a small amount of RF energy leakage through the ground screen as well as knife edge diffraction patterns at the top edge of each rectenna section. The general

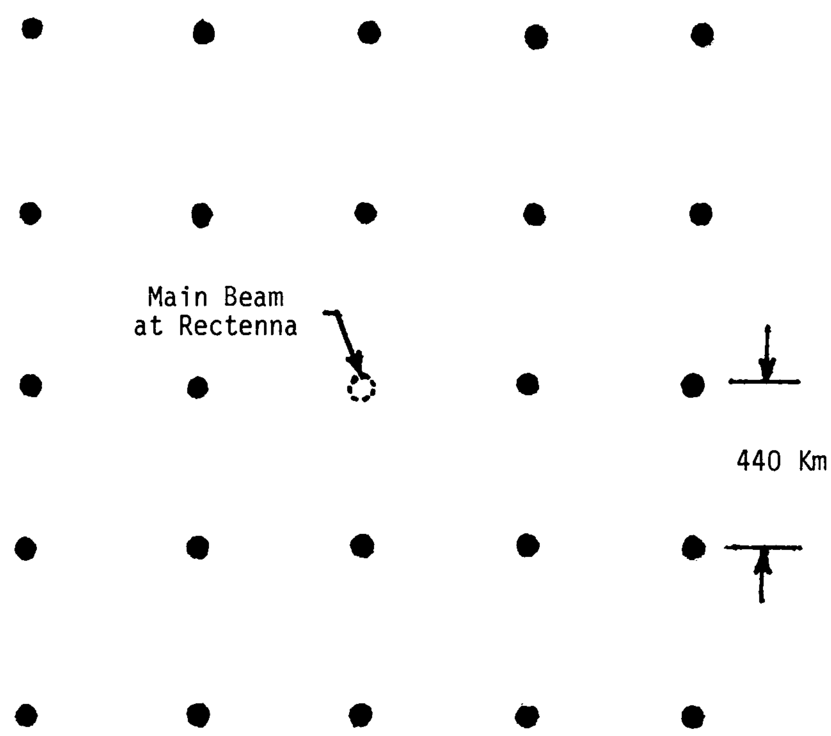


Figure 21. Grating Lobe Maxima

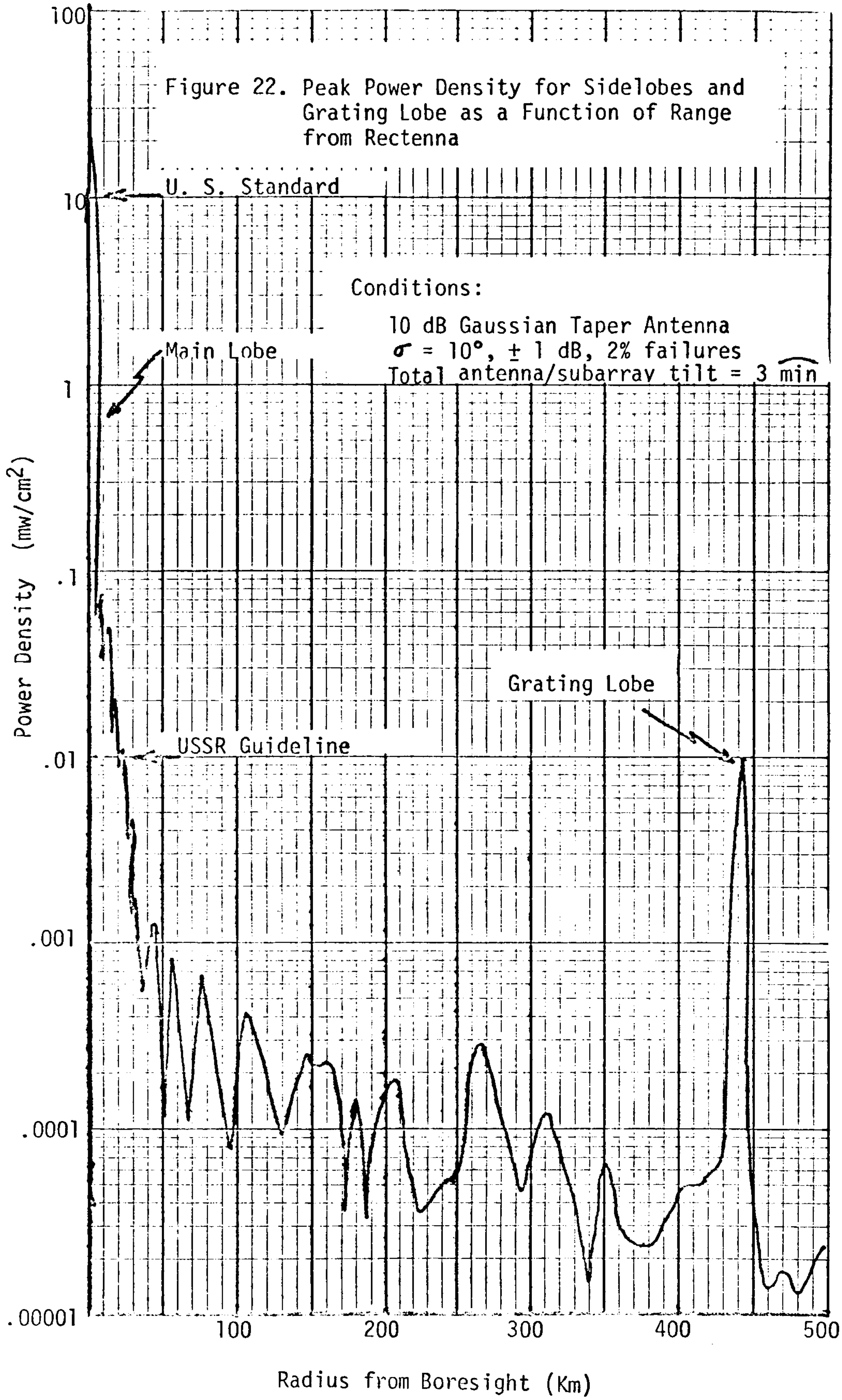
Figure 22. Peak Power Density for Sidelobes and Grating Lobe as a Function of Range from Rectenna
U. S. Standard
Conditions:
10 dB Gaussian Taper Antenna
σ = 10°, ± 1 dB, 2% failures
Total antenna/subarray tilt = 3 min
Main Lobe
Grating Lobe
USSR Guideline
100
10
1
.1
.01
.001
.0001
.00001
Power Density (mw/cm²)
100
200
300
400
500
Radius from Boresight (Km)

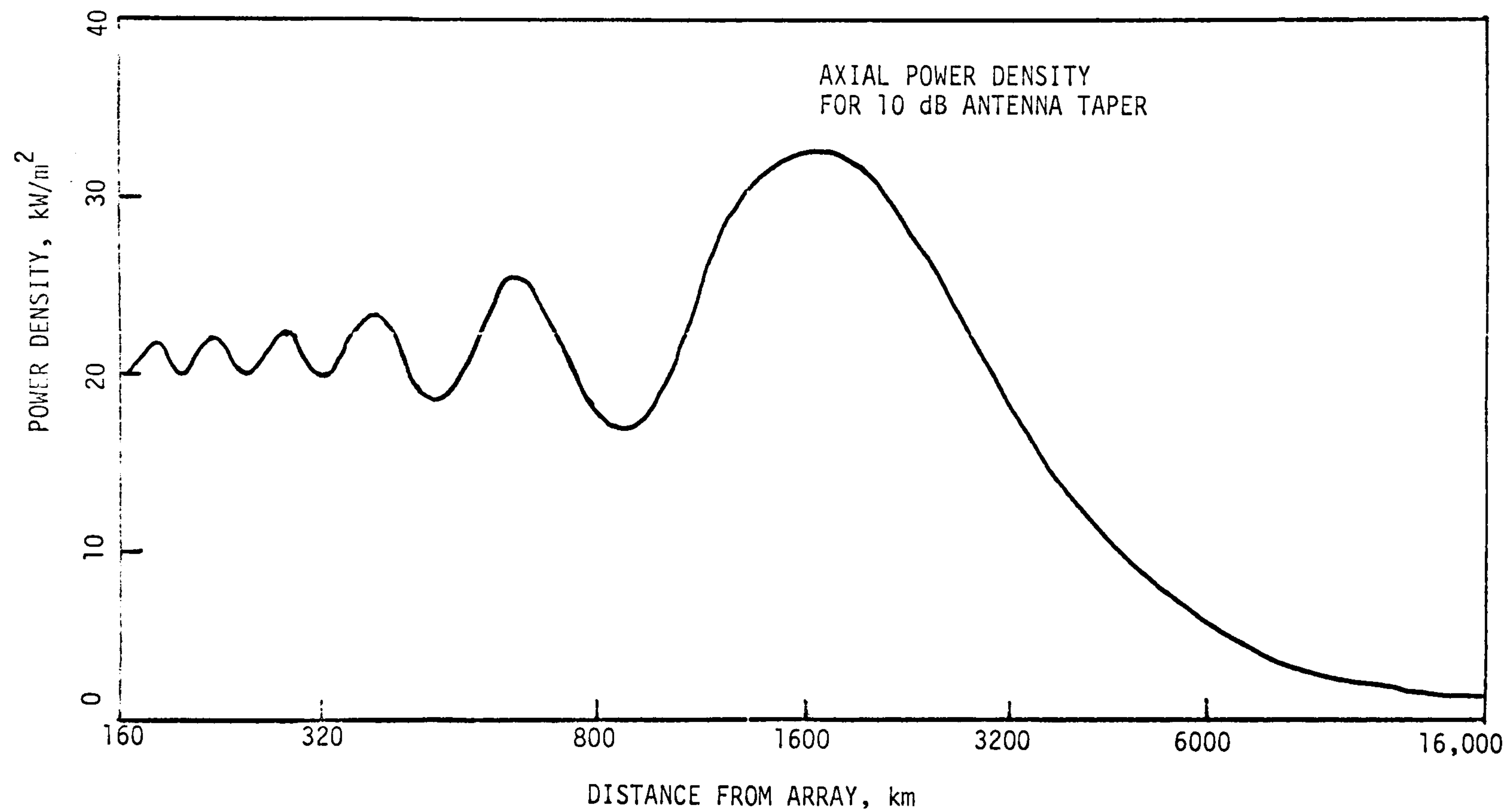


Figure 23. Near-Field Antenna Patterns

rectenna parameters may be summarized as follows:

| | |
|---|---|
| Total Active Panel Area: | 78.5 $km^2$ |
| Configuration: | Panels (multiple antenna elements feeding a single diode. Panels should be open-faced to reduce wind loading, with a maximum of 1% leakage energy. |
| Receive Elements: | Half-wave rectifying diodes. |

To provide an estimate of the power levels around the rectenna, studies indicate that the dipoles have 98% collection efficiency under normal loading conditions (reference 9). The 2% reflected microwave power is directed upward and towards the southern horizon. This reflected energy at 2.45 GHz is only partially coherent since the regions of coherence for the incident beam are limited due to phase irregularities in the heated ionosphere and atmosphere.

Harmonics of 2.45 GHz will be generated within the half-wave rectifying diodes and will be reradiated back through the low-pass filters and dipoles. Initial measurements of the harmonic levels relative to the fundamental indicate the second, third, and fourth harmonics are down by -25 dB, -40 dB, and <70 dB, respectively, for the normal dipole/diode rectifier configuration (reference 9).

There will also be leakage power through the rectenna. For a ground plane transparency of 80%, approximately 1% of the incident power appears as leakage through the wire mesh.

Since the rectenna's receiving surface appears serrated with individual panels perpendicular to the incident radiation, there will be diffraction losses at the top edge of each section. An analysis of the knife edge diffraction pattern has been made to determine the variation in power density incident upon the adjacent rectenna section (reference 9). The power density will vary in the shadow region (area behind the rectenna section) as shown in figure 24. It may be necessary to extend the size of the rectenna section to intercept part of the shadow region. There will also be energy lost as heat in the rectenna due to

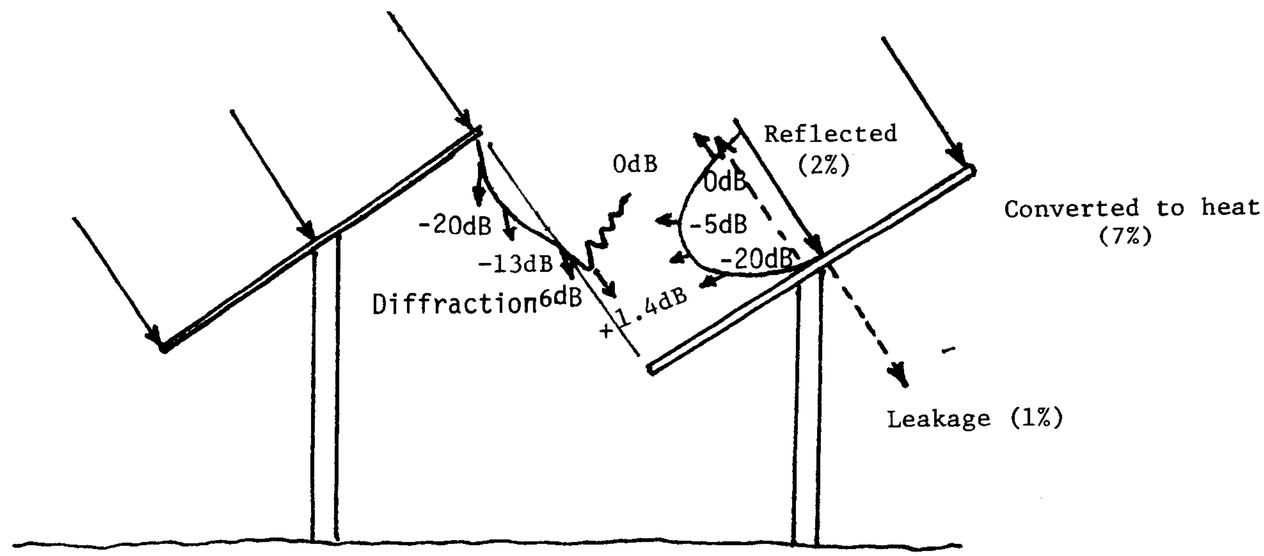


| | Power Densities Center (Boresight) | Edge of Rectenna |
|---|---|---|
| Incident Energy | $23 mw/cm^2$ | $.9 mw/cm^2$ |
| Leakage Energy | $.23 mw/cm^2$ | $.009 mw/cm^2$ |
| Reflected Energy | $.46 mw/cm^2$ | $.18 mw/cm^2$ |
| Scattered Energy | $.046$ to $.0046 mw/cm^2$ | $.0018$ to $.00018 mw/cm^2$ |
| Heat | $1.6 mw/cm^2$ | $.053 mw/cm^2$ |
| Diffracted Energy | | |
| (at edge of section) | $5 mw/cm^2$ | $.25 mw/cm^2$ |
| (at 1/6 of distance behind section) | $1 mw/cm^2$ | $.045 mw/cm^2$ |

Figure 24. Rectenna Patterns and Power Levels

$I^2R$ losses in the receiving elements and in the diodes. Approximately 7% of the incident energy is expected to be lost as heat.

The expected power levels around the rectenna for reflected energy, leakage energy, harmonics, diffractions, and heat losses are summarized in figure 24.

Microwave System Efficiency - The total microwave system efficiency from the DC power output at the rotary joint to the collected DC power output of the rectenna is 63%. A breakdown of the efficiencies of the microwave subsystems is given in figure 25.

Phase Control System - The phase control system has an active, retrodirective array with a pilot beam reference for providing phase conjugation. Each subarray or possibly each power module (that portion of a subarray fed by one klystron tube), has its own RF receiver which processes the uplink pilot beam reference and inserts the proper phasing signal to form a single coherent beam at the ground rectenna. Tradeoff studies are now being conducted to determine if the phase conjugation should be at the subarray level or the power module level. Conjugation at the power module level improves main beam efficiency and microwave environmental effects, but increases costs and complexity. The Reference System includes:

(1) phase lock loop around each power tube for phase stability and noise suppression.

(2) double sideband, suppression carrier modulation which is symmetrical about the downlink power beam frequency $f_{dl}$, as shown below.

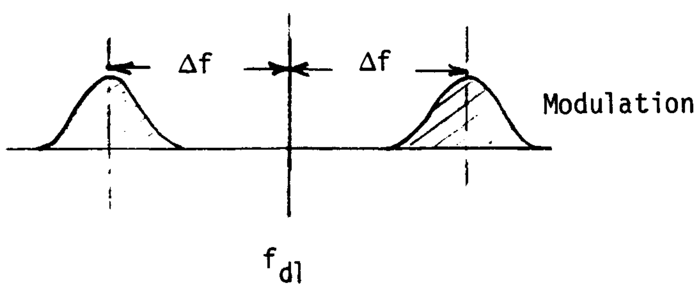

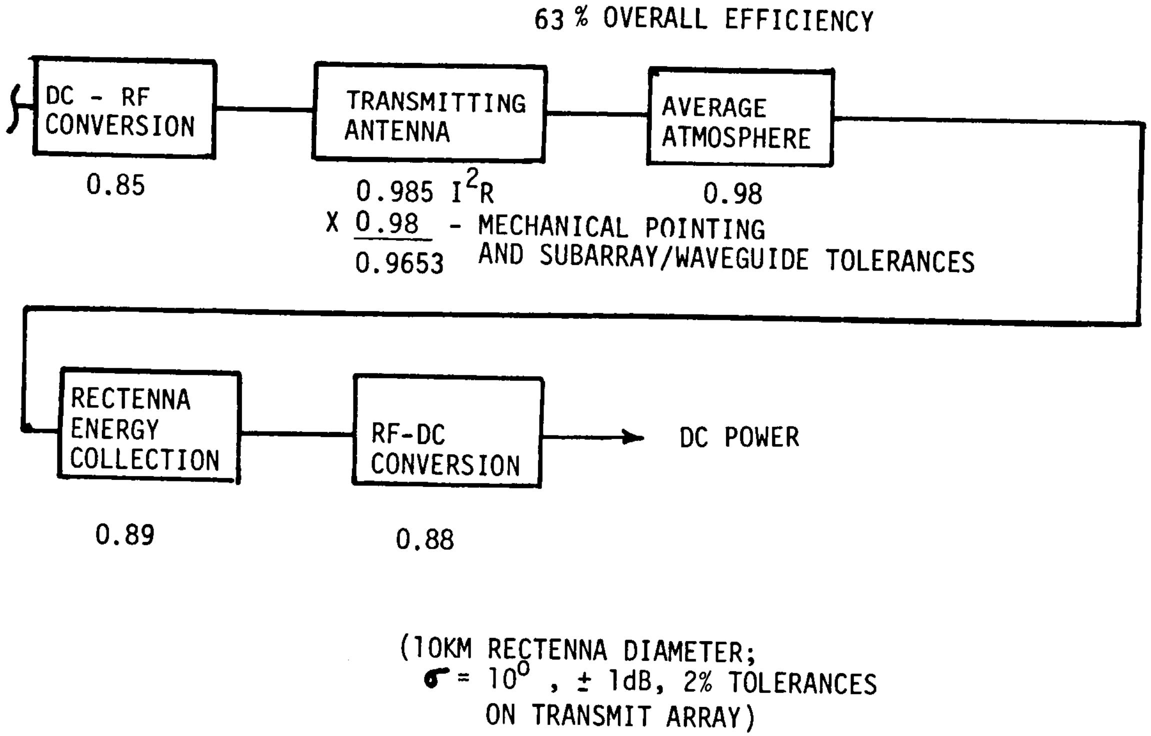


Figure 25. Microwave Transmission Efficiency

The two sidebands are demodulated in the RF receivers in the subarrays (or power modules) and the carrier is reconstructed. This prevents beam squint problems arising from different uplink and downlink frequencies, and it allows the proper phase conjugation to be made. The ionosphere constrains the frequency separation $\Delta f$ between the sidebands and the downlink carrier to be greater than 10 MHz, the maximum plasma resonance frequency. This limitation is to prevent intermodulation products between the uplink pilot beam and the downlink power beam from creating parametric instabilities associated with overdense ionospheric heating.

(3) coding of the pilot beam for security and pilot discrimination. Since multiple SPS satellites will be illuminated by a single pilot beam transmitter, each satellite has to recognize which pilot beam signal it should respond to. In addition, coding will prevent power drain from any intentional interfering signals.

(4) ground safety control system (ground sensors for interpreting beam shape) with a command link capability to the satellite.

RFI Characteristics - The radio frequency interference comes primarily from the DC-RF power converter tubes. This interference can be divided into three main categories: (1) interference from the high power downlink beam due to sidelobe and grating lobe radiations, (2) spurious noise generated near the carrier frequency by the tubes, and (3) harmonic generation within the tubes.

The sidelobe and grating lobe levels were previously examined. Within the phase control system, the phase lock loop around each power tube will reduce the spurious noise close to the carrier frequency. A representative loop might have a 5 MHz bandwidth with a second or third order filter. This loop will not affect the tube noise characteristics outside the 2450 ± 50 MHz band. However, the klystron tubes will have a multiple cavity design which provides additional filtering (24 dB/octave) to reduce the out-of-band noise. The SPS noise density characteristics are summarized in figure 26 (reference 31).

The CCIR (International Radio Consultative Committee) requirement for power flux density at the earth's surface is -180 dBW/m$^2$/Hz for S-band frequencies with an angle of arrival above 25°. As shown in figure 26, the RFI effects due to spurious noise will be below the CCIR requirements, provided the klystron tubes are phase-locked for noise reduction and a multiple cavity design is used.

CRITICAL RADIO ASTRONOMY FREQUENCIES

1400-1427 MHz (Hydrogen Resonance Line)

1660-1670 MHz (Hydroxyl Resonance Line)

2690-2700 MHz } Astronomy Bands
4990-5000 MHz }

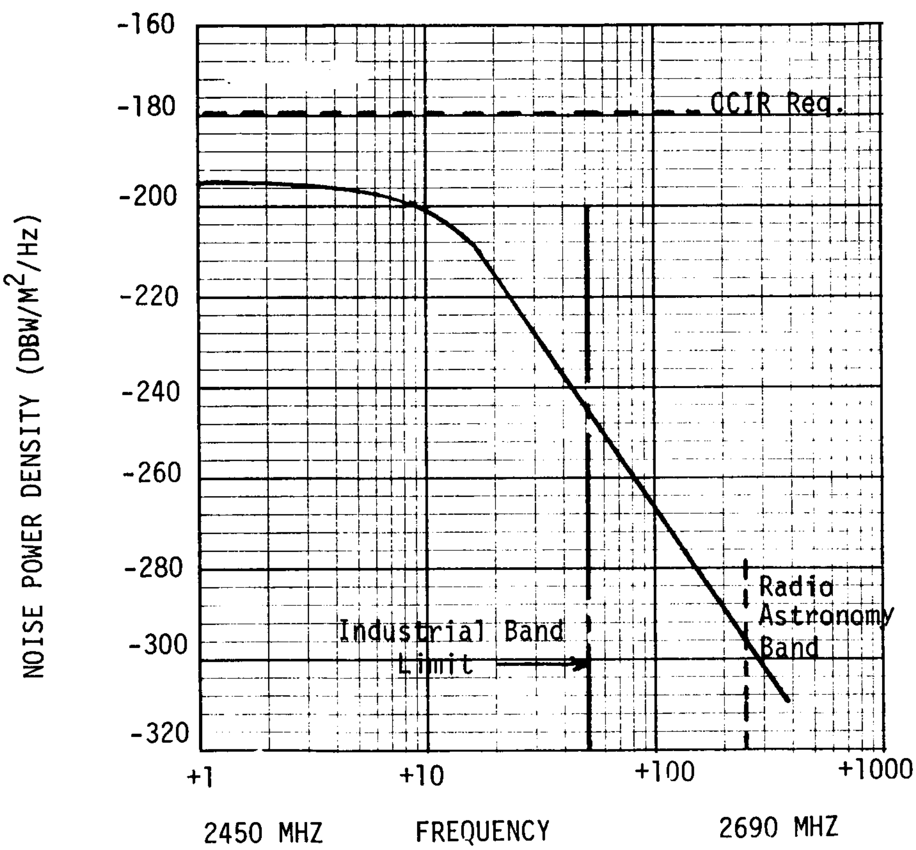


NOTE: CCIR REQUIREMENTS ARE - 180 dBW/m$^2$/Hz FOR ARRIVAL ANGLES GREATER THAN 25$^{\circ}$.

Figure 26. Noise Power Density at Ground for a 1 km, 5 GW SPS Antenna

### I. Mass Statement

A summary of the satellite mass properties is presented in Table 1. The masses are separated into three major segments: solar array, microwave antenna, and array antenna interfaces (the section of satellite between the array and antenna which includes the rotary joint, sliprings, and antenna yoke).

The GaAlAs configuration utilizes a concentration ratio of 2 which reduces the required blanket area and in turn the blanket mass.

The antenna section mass properties are the same for both options. The antenna mass is dominated by the transmitter subarray which includes the klystrons and waveguides. The other large items are the power distribution system and the thermal control system for the klystrons and DC/DC converters.

The total mass for the two options, including a 25% contingency factor, is 34 and 51 million kilograms for the GaAlAs and silicon options, respectively.

### J. Space Transportation

This section provides descriptions of the reference space transportation system vehicles. The alternative concepts from which the Reference System was selected are described in Appendix A. The vehicles are distinguished by their primary payload, either cargo or personnel, and their area of operations between earth and low earth orbit (LEO) or between LEO and geosynchronous earth orbit (GEO). Cargo is transported from the earth's surface to LEO by the HLLV and personnel (and priority cargo) are transported from earth to LEO and back by the PLV. Transportation between LEO and GEO is provided by the COTV and the POTV.

The general groundrules followed in the development and evaluation of the transportation system are:

- The SPS transportation system elements, with the possible exception of shuttle derived PLV's, are dedicated and optimized for the installation, operation, and maintenance of the SPS.

- The SPS transportation system will be designed for minimum total program cost.

Table 1. SPS Mass Statement - Millions of KGs

| SUBSYSTEM | GaAlAs CR = 2 OPTION | | SILICON CR = 1 OPTION | |
|---|---|---|---|---|
| SOLAR ARRAY | | 13.798 | | 27.258 |
| PRIMARY STRUCTURE | 4.172 | | 3.388 | |
| SECONDARY STRUCTURE | 0.581 | | 0.436 | |
| SOLAR BLANKETS | 6.696 | | 22.051 | |
| CONCENTRATORS | 0.955 | | – | |
| POWER DISTRIBUTION & CONDITIONING | 1.144 | | 1.134 | |
| INFORMATION MANAGEMENT & CONTROL | 0.050 | | 0.050 | |
| ATTITUDE CONTROL & STATIONKEEPING | 0.200 | | 0.200 | |
| ANTENNA | | 13.382 | | 13.382 |
| PRIMARY STRUCTURE | 0.250 | | 0.250 | |
| SECONDARY STRUCTURE | 0.786 | | 0.786 | |
| TRANSMITTER SUBARRAYS | 7.178 | | 7.178 | |
| POWER DISTRIBUTION & CONDITIONING | 2.189 | | 2.189 | |
| THERMAL CONTROL | 2.222 | | 2.222 | |
| INFORMATION MANAGEMENT & CONTROL | 0.630 | | 0.630 | |
| ATTITUDE CONTROL | 0.128 | | 0.128 | |
| ARRAY/ANTENNA INTERFACES * | | 0.147 | | 0.147 |
| PRIMARY STRUCTURE | 0.094 | | 0.094 | |
| SECONDARY STRUCTURE | 0.003 | | 0.003 | |
| MECHANISMS | 0.033 | | 0.033 | |
| POWER DISTRIBUTION | 0.017 | | 0.017 | |
| SUB TOTAL | | 27.327 | | 40.787 |
| CONTINGENCY (25%) | | 6.832 | | 10.197 |
| TOTAL | | 34.159 | | 50.984 |

* Rotary joint, slip rings, antenna yoke

- Energy requirements will be minimized consistent with minimum cost.

- Environmental impact will be minimized and, so far as possible, protective measures needed will be factored into cost analyses.

- The use of critical materials will be minimized consistent with cost, energy and environmental impact requirements.

Heavy Lift Launch Vehicle (HLLV) - The reference HLLV is a two-stage, vertical take-off, horizontal landing (VTOHL), fully reusable winged launch vehicle. The launch configuration and overall geometry are detailed in figure 27 and the launch/erector concept is illustrated in figure 28. The vehicle uses 16 $CH_4/O_2$ engines on the booster (first stage) and 14 standard SSME's on the orbiter (second stage). The booster engines employ a gas generator cycle and provide a vacuum thrust of $9.79 \times 10^6$ newtons each. The orbiter SSME's provide a vacuum thrust of $2.09 \times 10^6$ newtons each at 100% power level. The gross lift-off weight of the HLLV is 11,040 metric tons with a payload to LEO of 424 metric tons.

An airbreather propulsion system (aircraft jet engine) is provided on the booster to provide flyback capability and simplify the booster operations. Its landing weight is 934 metric tons. The orbiter deorbits and performs a glide-back landing maneuver. Its landing weight is 453 metric tons which includes an assumed returned payload of 63.5 metric tons or 15% of the payload delivered to LEO.

The HLLV trajectory and exhaust products data are provided in figure 29. This figure shows the propellant expended and the exhaust product components by weight for intervals of altitude versus range from lift-off to orbiter engine cut-off.

Personnel Launch Vehicle (PLV) - The PLV provides for the transportation of personnel and priority cargo between earth and low earth orbit. The reference vehicle is derived from the current space shuttle system. It incorporates a winged liquid propellant fly-back booster instead of the Solid Rocket Boosters and has a personnel compartment in the Orbiter payload bay capable of transporting

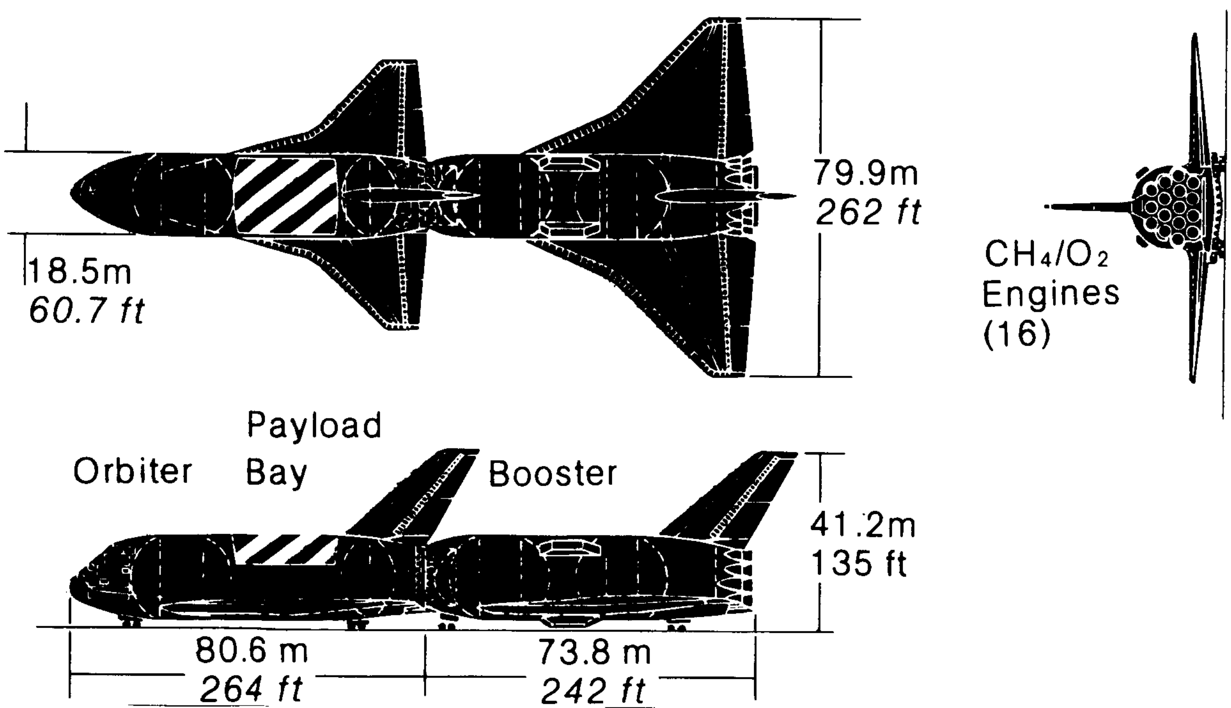


Figure 27. Heavy Lift Launch Vehicle

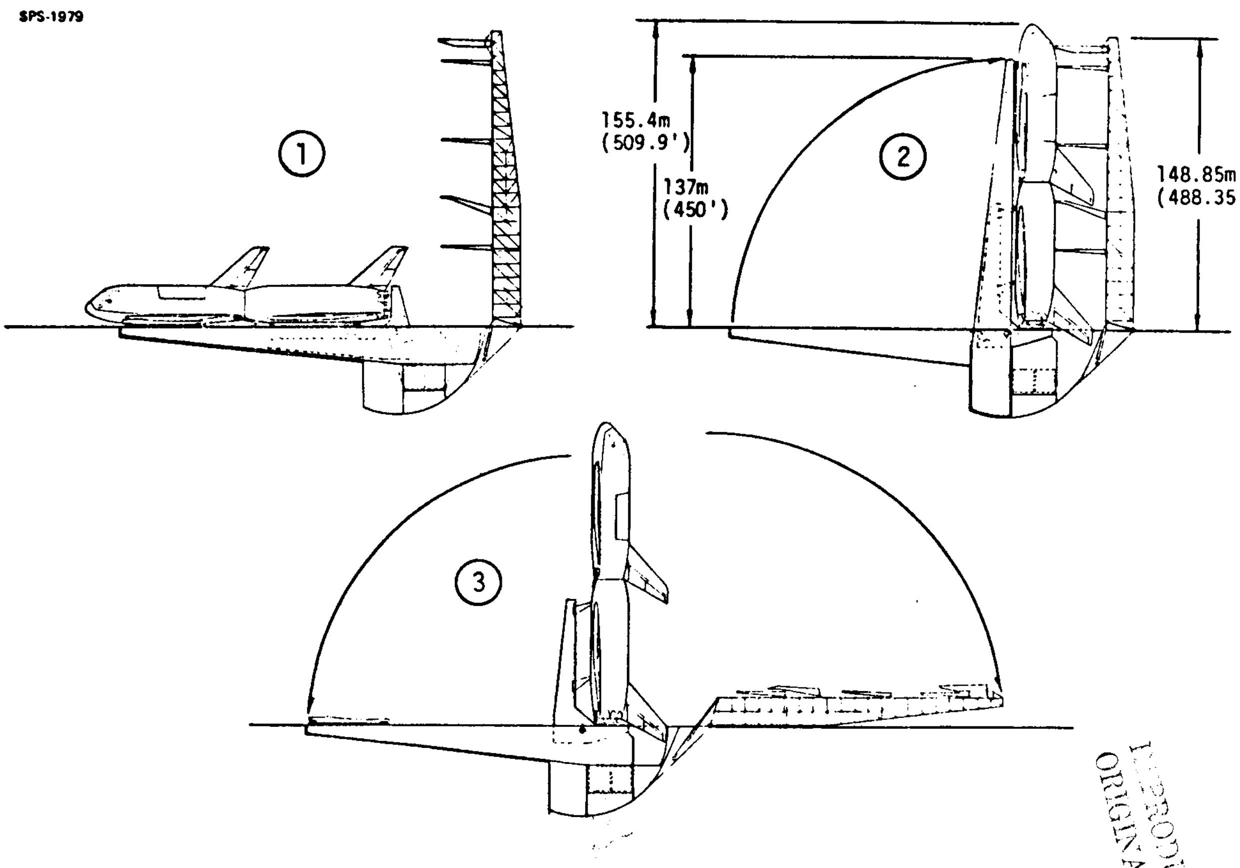


Figure 28. Launcher/Erector Concept

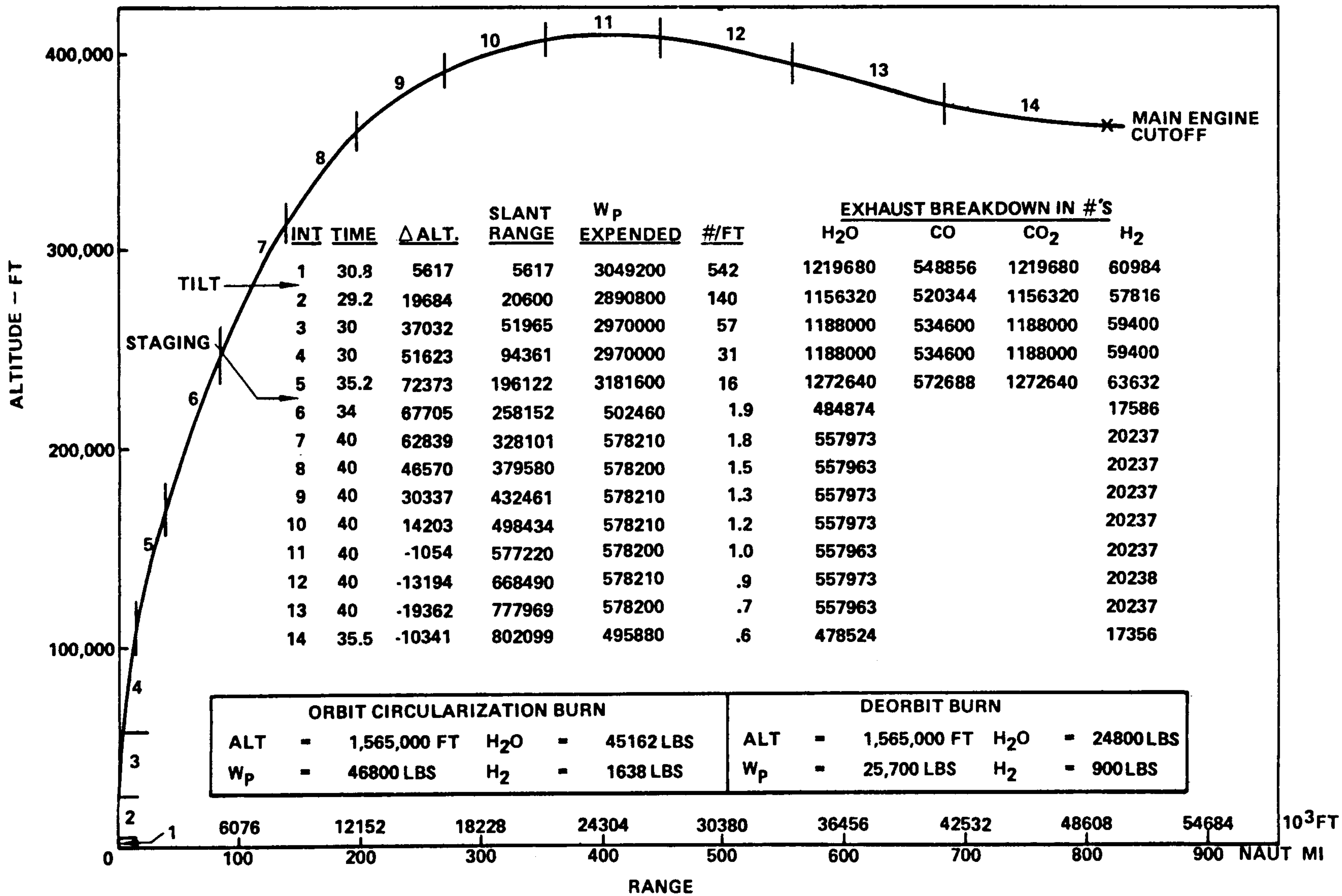


| INT | TIME | ΔALT. | SLANT RANGE | $W_P$ EXPENDED | #/FT | EXHAUST BREAKDOWN IN #'S $H_2O$ | CO | $CO_2$ | $H_2$ |
|---|---|---|---|---|---|---|---|---|---|
| 1 | 30.8 | 5617 | 5617 | 3049200 | 542 | 1219680 | 548856 | 1219680 | 60984 |
| 2 | 29.2 | 19684 | 20600 | 2890800 | 140 | 1156320 | 520344 | 1156320 | 57816 |
| 3 | 30 | 37032 | 51965 | 2970000 | 57 | 1188000 | 534600 | 1188000 | 59400 |
| 4 | 30 | 51623 | 94361 | 2970000 | 31 | 1188000 | 534600 | 1188000 | 59400 |
| 5 | 35.2 | 72373 | 196122 | 3181600 | 16 | 1272640 | 572688 | 1272640 | 63632 |
| 6 | 34 | 67705 | 258152 | 502460 | 1.9 | 484874 | | | 17586 |
| 7 | 40 | 62839 | 328101 | 578210 | 1.8 | 557973 | | | 20237 |
| 8 | 40 | 46570 | 379580 | 578200 | 1.5 | 557963 | | | 20237 |
| 9 | 40 | 30337 | 432461 | 578210 | 1.3 | 557973 | | | 20237 |
| 10 | 40 | 14203 | 498434 | 578210 | 1.2 | 557973 | | | 20237 |
| 11 | 40 | -1054 | 577220 | 578200 | 1.0 | 557963 | | | 20237 |
| 12 | 40 | -13194 | 668490 | 578210 | .9 | 557973 | | | 20238 |
| 13 | 40 | -19362 | 777969 | 578200 | .7 | 557963 | | | 20237 |
| 14 | 35.5 | -10341 | 802099 | 495880 | .6 | 478524 | | | 17356 |

| ORBIT CIRCULARIZATION BURN | | | | DEORBIT BURN | | | |
|---|---|---|---|---|---|---|---|
| ALT | = 1,565,000 FT | $H_2O$ | = 45162 LBS | ALT | = 1,565,000 FT | $H_2O$ | = 24800 LBS |
| $W_P$ | = 46800 LBS | $H_2$ | = 1638 LBS | $W_P$ | = 25,700 LBS | $H_2$ | = 900 LBS |

ALTERNATE TRAJECTORIES CAN BE CONSIDERED WITH LOWER INSERTION ALTITUDES IF ENVIRONMENTAL CONSIDERATIONS DEEM NECESSARY

Figure 29. SPS Heavy Lift Launch Vehicle Trajectory and Exhaust Products Data

75 passengers. The overall configuration and vehicle characteristics are shown in figure 30. The passenger module is illustrated in figure 30 also.

The booster employs four $O_2/CH_4$ engines similar to those on the HLLV booster. A series burn ascent mode is utilized and the external tank (ET) is a resized, smaller version of the space shuttle tank, carrying 546 metric tons of propellant versus 715 metric tons for the current STS.

Personnel Orbital Transfer Vehicle (POTV) - The functions of the POTV are to deliver personnel and priority cargo from LEO to GEO and to return personnel from GEO to LEO.

The reference vehicle is a two-stage (common stage) $LO_2/LH_2$ configuration as illustrated in figure 31.

The start burn weight is 890 tons with an up payload of 151 tons and a down payload of 55 tons. The up payload consists of 160 personnel in a passenger module, 480 man-months of consumables in a resupply module, and a flight control module piloted by a crew of two. The down payload is identical except the resupply module returns empty to LEO.

Cargo Orbital Transfer Vehicle (COTV) - The function of the COTV is to deliver SPS cargo to GEO from the LEO staging area. The basic concept involves the construction of a fleet of reusable electric powered round trip vehicles and their dedicated solar array in LEO. The vehicle uses ion bombardment thrusters with cryogenic argon as the propellant. The ion thruster propellant was selected on the basis of availability, storability, absence of serious environmental impacts, cost, demonstrated performance, and technical suitability. Power conversion options are GaAlAs and Si photovoltaic array systems illustrated in figure 32.

The first option utilizes a self-annealing GaAlAs array with a concentration ratio of 2 and provides a LEO-GEO trip time of 133 days and a total round trip time of less than 180 days. Ion bombardment thrusters of 100 cm diameter are used with an Isp of 13,000 seconds and argon as the working fluid. The primary

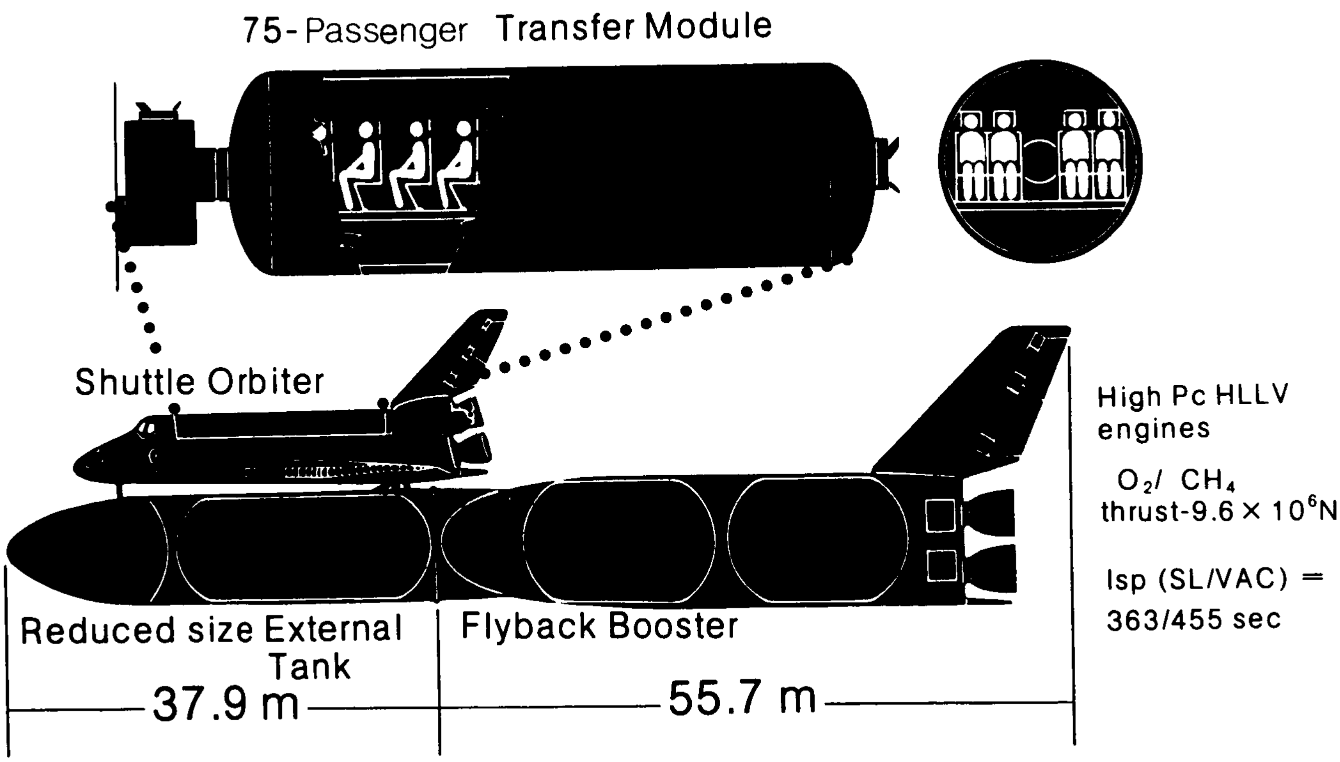


Figure 30. Personnel Launch Vehicle

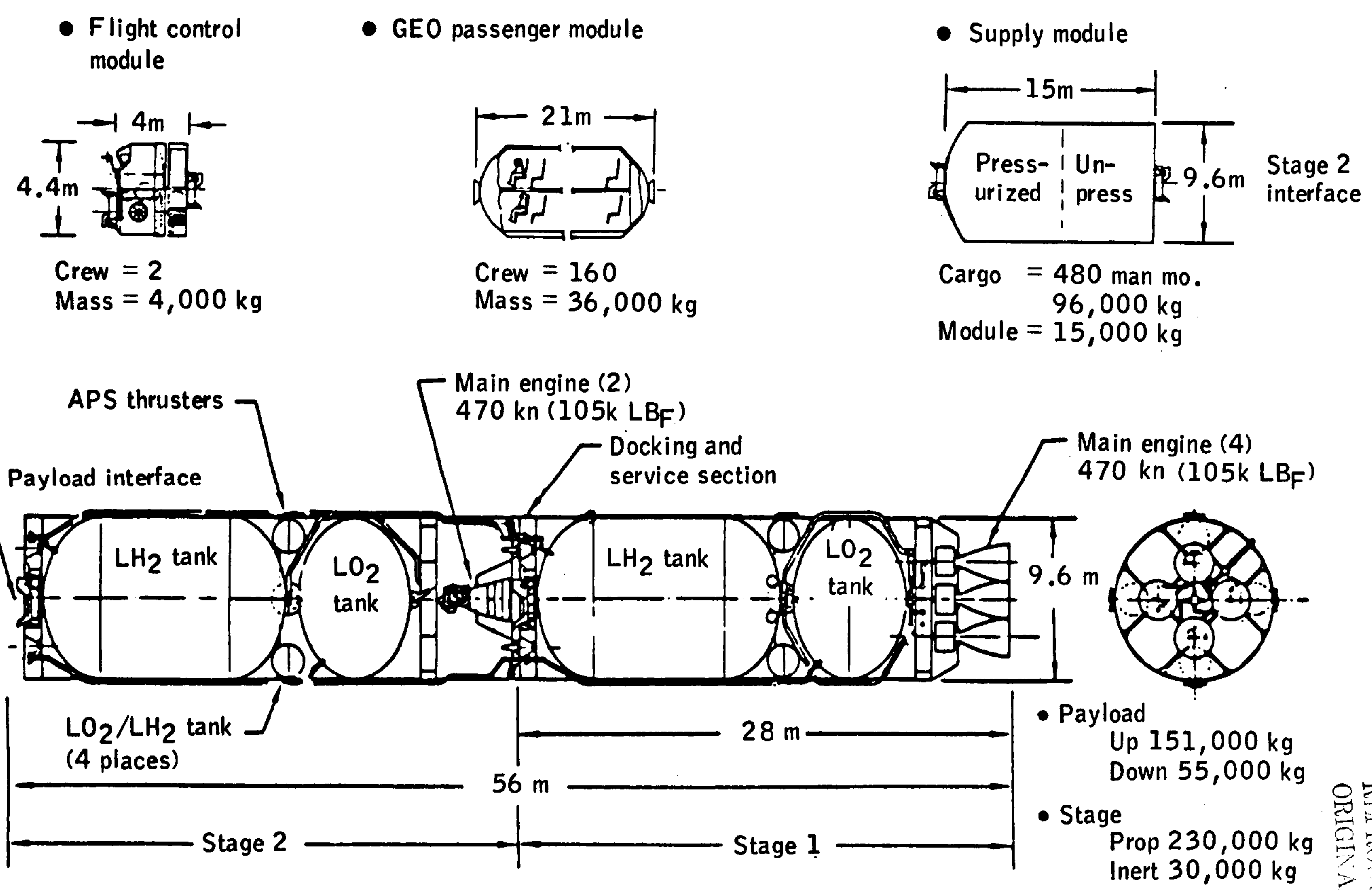


Figure 31. $LO_2/LH_2$ Common Stage POTV

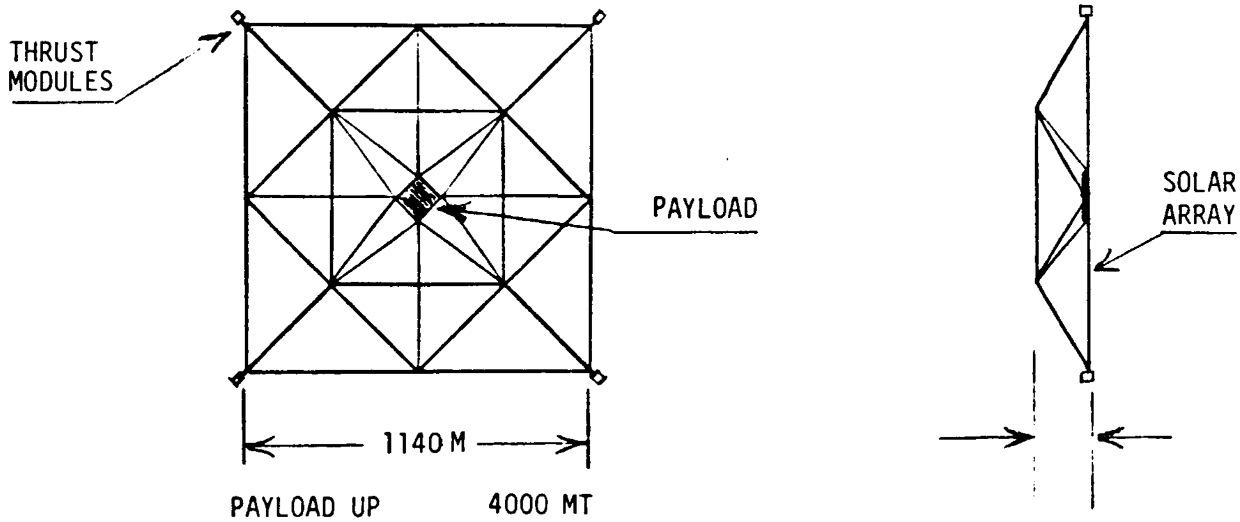


PAYLOAD UP 4000 MT
VEHICLE DRY MASS 1206 MT
PROPELLANT UP 835 MT
PROPELLANT DOWN 150 MT

Silicon Solar Cells

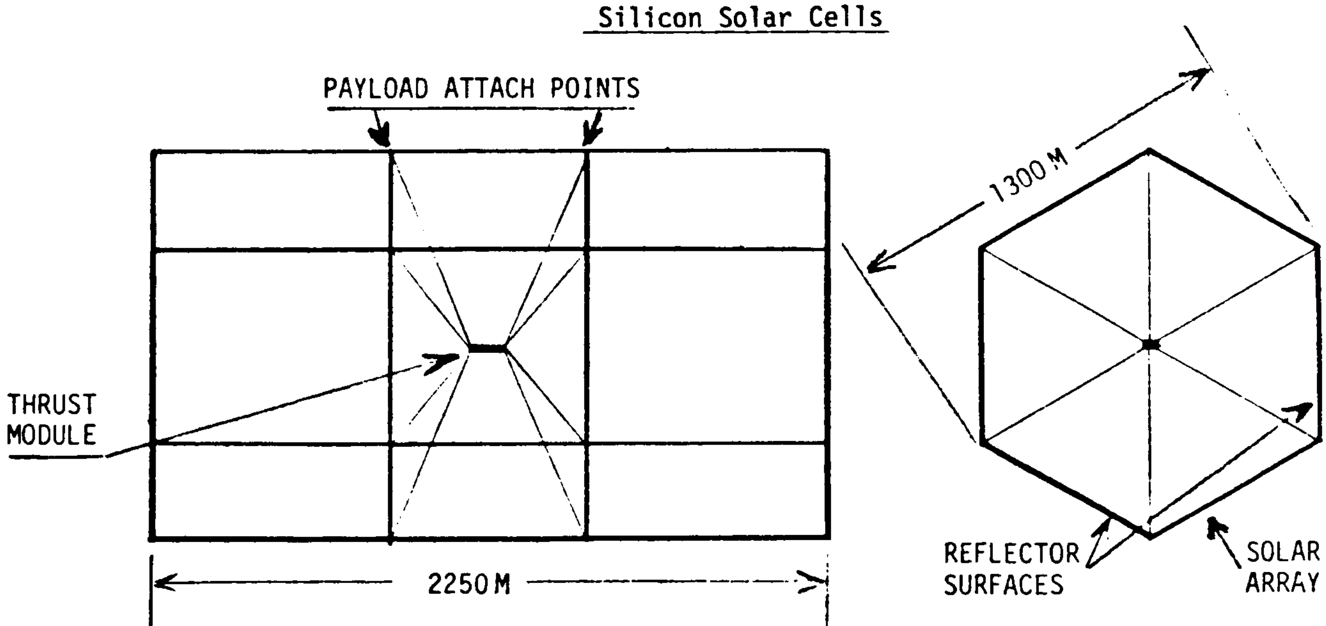


PAYLOAD UP 3,469 MT
VEHICLE DRY MASS 715 MT
PROPELLANT UP 185 MT
PROPELLANT DOWN 27 MT

GaAlAs Solar Cells

Figure 32. Cargo Orbit Transfer Vehicles Options

thruster array of 259 thrusters is suspended by cables and located at the vehicle center of gravity. Additional attitude thruster control packages are located at the structural extremities. The component mass breakdown is given in Table 2.

The second option utilizes a silicon photovoltaic solar array in a planar configuration with no concentration reflectors. Round trip time from LEO-GEO-LEO is approximately 160 days which also allows two trips per year for each COTV. Ion bombardment thrusters of 120 cm diameter are used with an $I_{SP}$ of 7000 seconds and argon as the working fluid. Thruster modules of 296 electric thrusters each and an appropriate number of chemical thrusters are located at the four corners of the COTV. The component mass breakdown is given in Table 3.

Transportation Fleet Requirements - Section L of this report provides a summary of the total transportation requirements for the installation of the orbital bases and of two 5 GW SPS. Requirements are expressed in terms of flights per year for each vehicle and fleet size for both the GaAlAs SPS and silicon SPS.

Table 2 GaAlAs Independent Electric COTV Mass Breakdown

| Vehicle (Dry) | (MT) |
|---|---|
| Power Generation/Distribution | 249 |
| Thrusters | 26 |
| Propellant Tanks and Lines | 39 |
| Structure/Thermal Control | 229 |
| Rotary Joint | 7 |
| Attitude Control/IMS | 22 |
| Primary Power Unit | - |
| Total (Dry) | 572 |
| 25% Growth Margin | 143 |
| Payload | 3469 |
| Propellant Up | 185 |
| Propellant Down | 27 |
| Total in LEO | 4396 |

Table 3 Si Independent Electric COTV Mass Breakdown

| Vehicle (Dry) | (MT) |
|---|---|
| Power Generation/Distribution | 570 |
| Thrusters | 70 |
| Propellant Tanks and Lines | 60 |
| Structure/Thermal Control | 80 |
| Rotary Joint | - |
| Attitude Control/IMS | - |
| Primary Power Unit | 185 |
| Total (Dry) | 965 |
| 25% Growth Margin | 241 |
| Payload | 4000 |
| Propellant Up | 835 |
| Propellant Down | 150 |
| Total in LEO | 6191 |

## K. Natural Resources

The materials for the Reference System are listed in Table 4. The specific materials are identified in column 1 under individual program components such as the satellite, rectenna and various transport vehicles. The second column indicates the mass of each material in metric tons for each component specific to a silicon solar cell satellite program. In those instances where components can be used in both the silicon and gallium arsenide solar cell programs such as several transport vehicles, the masses are listed in the third column. Finally, the masses of those materials for components specific to the gallium arsenide program are listed in the fourth and last column. In the case of the low earth orbit staging and orbital transfer vehicle construction platform and the geosynchronous orbital construction base for the gallium arsenide system only, the estimated total mass is given. These components are being studied in depth at this time to identify the materials and better estimate component mass.

Table 5 compares the total materials masses for all components of the program through the first satellite in columns 2 and 3 and for each year

Table 4 Materials List for Reference System

RESOURCE REQUIREMENTS (METRIC TONS)

| | Silicon System Concentration Ratio Ratio of 1 | Common Satellite Construction Materials | Gallium Arsenide System Concentration Ratio of 2 |
|---|---|---|---|
| 5 GIGAWATT SATELLITE MASS | 50,618 | | 34,159 |
| GFRTP[1] | 6,359 | | 7,680 |
| Stainless Steel | 5,723 | | 5,305 |
| Copper | 6,873 | | 4,834 |
| Sapphire | 0 | | 3,376 |
| Aluminum | 2,204 | | 4,122 |
| GaAs | 0 | | 1,354 |
| Teflon | 0 | | 1,152 |
| Kapton | 0 | | 2,719 |
| Silver | 37 | | 928 |
| Mercury | 89 | | 89 |
| Tungsten | 646 | | 646 |
| Glass | 19,271 | | 0 |
| Silicon | 7,903 | | 0 |
| Misc. and Organics | 1,880 | | 1,947 |
| LOW EARTH ORBIT STAGING AND OTV CONSTRUCTION | 2,405 | | 110[2] |
| GFRTP | 640 | | |
| Aluminum | 1,433 | | |
| Stainless Steel | 108 | | |
| Copper | 26 | | |
| Glass | 20 | | |
| Silicon | 9 | | |

NOTES: (1) GFRTP (Graphite Fiber Reinforced Thermoplastic)

(2) Total mass estimate only is available at this time.

(continuation) Table 4 Materials List for Reference System

| | RESOURCE REQUIREMENTS (METRIC TONS) | | |
|---|---|---|---|
| | Silicon System Concentration Ratio Ratio of 1 | Common Satellite Construction Materials | Gallium Arsenide System Concentration Ratio of 2 |
| GEOSYNCHRONOUS ORBIT CONSTRUCTION | 8,353 | | 6,000(2) |
| GFRTP | 2,551 | | |
| Aluminum | 4,694 | | |
| Stainless Steel | 390 | | |
| Copper | 110 | | |
| Glass | 30 | | |
| Silicon | 13 | | |
| Misc. and Organics | 565 | | |
| HEAVY LIFT LAUNCH VEHICLE (HLLV) | | 1,170 | |
| Aluminum | | 470 | |
| Titanium | | 248 | |
| Stainless Steel | | 232 | |
| Ceramic | | 103 | |
| Copper | | 17 | |
| Misc. and Organics | | 100 | |
| PERSONNEL LAUNCH VEHICLE (PLV) | | 264 | |
| Aluminum | | 106 | |
| Titanium | | 56 | |
| Stainless Steel | | 52 | |
| Ceramic | | 23 | |
| Copper | | 4 | |
| Misc.and Organics | | 23 | |
| PERSONNEL ORBITAL TRANSFER VEHICLE (PORTV) | | 116 | |
| Aluminum | | 81 | |
| Stainless Steel | | 23 | |
| Copper | | 2 | |
| Misc. and Organics | | 10 | |

(continuation)

Table 4 Materials List for Reference System

RESOURCE REQUIREMENTS (METRIC TONS)

| | Silicon System Concentration Ratio Ratio of 1 | Common Satellite Construction Materials | Gallium Arsenide System Concentration Ratio of 2 |
|---|---|---|---|
| CARGO ORBITAL TRANSFER VEHICLE (COTV) | 1,100 | | 679 |
| Aluminum | 3 | | 369 |
| GaAs | 0 | | 38 |
| Teflon | 0 | | 32 |
| Sapphire | 0 | | 93 |
| Kapton | 0 | | 66 |
| GFRTP | 126 | | 0 |
| Copper | 67 | | 15 |
| Silicon | 256 | | 17 |
| Stainless Steel | 14 | | 40 |
| Glass | 623 | | 0 |
| Misc. and Organics | 11 | | 9 |
| RECTENNA | | | |
| Steel | | 1,492,000 | |
| Concrete | | 1,330,000 | |
| Aluminum | | 140,000 | |
| GaAs | | 9 | |

Table 5 Materials for Initial 5 GW SPS and Subsequent Systems

(UNITS IN METRIC TONS)

| SATELLITE PROGRAM MATERIALS | Through First 5 GW SPS | | Two 5 GW Satellite/Year | |
|---|---|---|---|---|
| | Si | Ga | Si | Ga |
| GFRTP | 12,447 | 7,680 | 12,716 | 15,360 |
| Stainless Steel | 7,621 | 6,511 | 11,446 | 10,610 |
| Glass | 33,650 | 0 | 38,542 | 0 |
| Silicon | 13,813 | 0 | 15,806 | 0 |
| Copper | 8,630 | 5,030 | 13,746 | 9,668 |
| Aluminum | 150,654 | 149,227 | 284,408 | 288,244 |
| Silver | 37 | 928 | 74 | 1,856 |
| Molybdenum | 2 | 0 | 4 | 0 |
| Mercury | 89 | 89 | 178 | 178 |
| Tungsten | 646 | 646 | 1,292 | 1,292 |
| Steel | 1,492,000 | 1,492,000 | 2,984,000 | 2,984,000 |
| Concrete | 1,330,000 | 1,330,000 | 2,660,000 | 2,660,000 |
| Gallium Arsenide | 7 | 1,696 | 14 | 2,708 |
| Titanium | 1,104 | 856 | 248 | 124 |
| Ceramics | 458 | 355 | 103 | 52 |
| Misc. and Organics | 3,084 | 8,663 | 3,700 | 3,984 |
| Argon | 20,559 | 4,876 | 18,690 | 4,664 |
| $H_2$ | 107,406 | 61,227 | 128,547 | 80,920 |

(Table 5 continued)

| | Through First 5 GW SPS | | Two 5 GW Satellite/Year | |
|---|---|---|---|---|
| | Si | Ga | Si | Ga |
| $O_2$ | 2,268,033 | 1,164,528 | 2,728,506 | 1,680,710 |
| $CH_4$ | 540,572 | 265,539 | 651,599 | 379,930 |
| Sapphire | 0 | 4,213 | 0 | 6,752 |
| Teflon | 0 | 1,441 | 0 | 2,306 |
| Kapton | 0 | 3,313 | 0 | 5,438 |

Note 1. Material masses through the first 5 GW SPS include:

a. Three Heavy Lift Launch Vehicles
b. Two Personnel Launch Vehicles
c. Two Personnel Orbital Transfer Vehicles
d. Twenty-three Cargo Orbital Transfer Vehicles for silicon satellite

or

e. Nine Cargo Orbital Transfer Vehicles for gallium arsenide satellite
f. One geosynchronous orbit construction base
g. One low earth orbit staging and OTV construction base
h. Fuel for all required flights

Note 2. Material masses for two 5 GW satellite/year columns includes only the two satellites, rectennas and fuel required for all flights necessary for both satellites to become operational.

thereafter with two satellites launched each year in columns 4 and 5. The first satellite includes not only transportation and rectenna, but also the orbital staging and construction bases, plus the construction of the cargo orbital vehicles. It should be noted that because the gallium arsenide system has both construction bases as total mass estimates at this time, (see Table 5) the mass of those components is indicated under miscellaneous and organics heading.

## L. Operations

SPS operations include those activities required to build SPS's and then to operate and maintain them. This requires a wide variety of activities as illustrated by figure 33. Because studies of most of these activities are not yet complete, this section will briefly outline the overall SPS operation as it appears at this time.

### 1. Construction Operations

Construction of an SPS starts with two supporting operations. First the necessary raw materials are mined and manufactured into launch-ready components and propellants. A significant mass production capability will need to be developed to produce the high number of components needed per satellite (e.g., about $10^{11}$ solar cells, $10^5$ klystrons, $10^{10}$ dipoles). Similarly, requirements for large amounts of propellants (oxygen, hydrogen, argon) demand expanded processing capabilities.

The other supporting function involves ground transportation of raw materials, fabricated components, and assemblies to the launch site. Also, about $10^6$ MT of hydrocarbon propellants are used per year. Among the possibilities for propellants under investigation are processing coal at mines and using a gas transmission system, transporting coal to the launch site, using rectenna-supplied electricity to electrolyze water, and others.

At the launch site, principal activities involve receiving, storing, and processing of material and propellants; launching vehicles; and refurbishing and checking out returning vehicles.

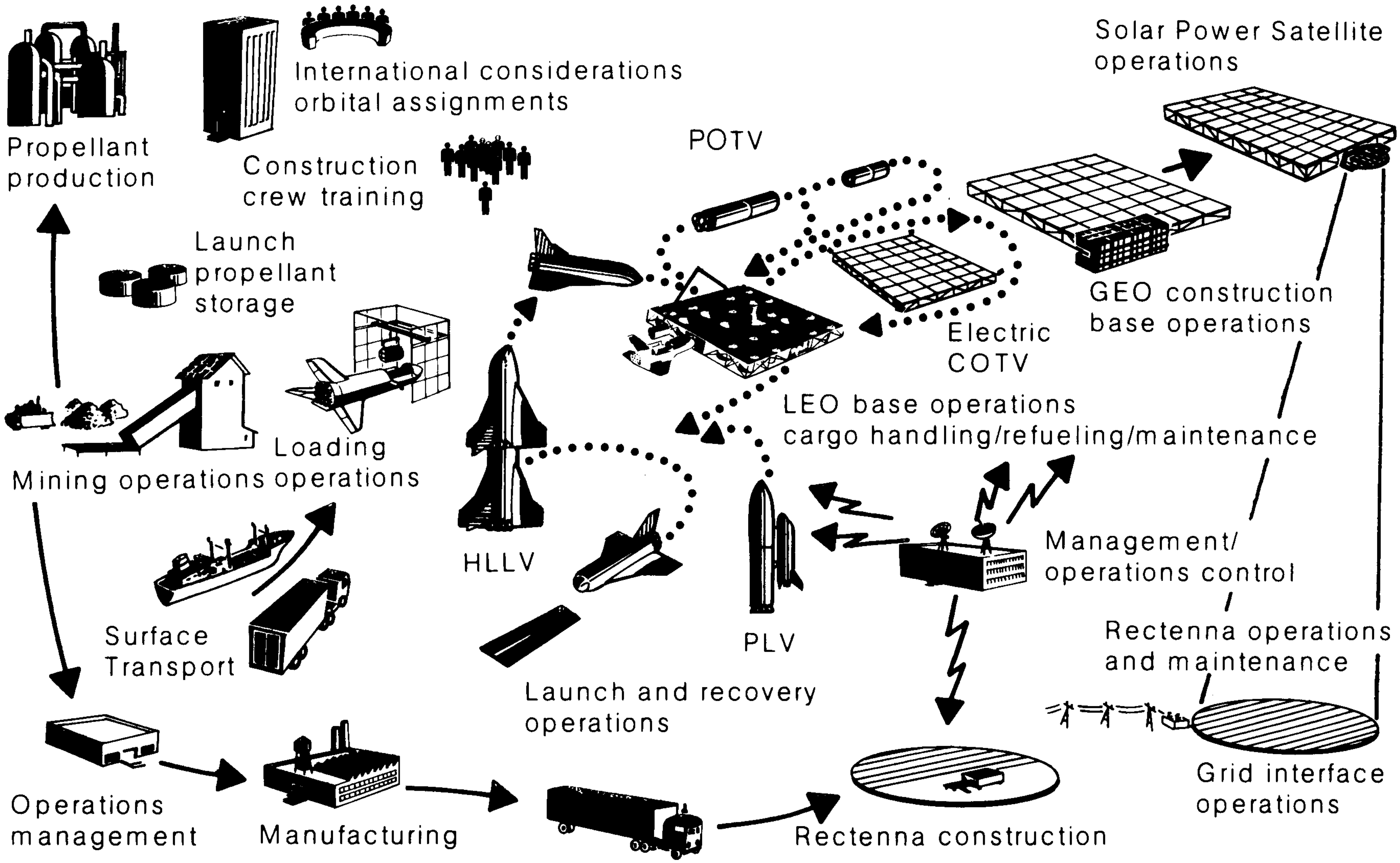


Figure 33. SPS Construction and Commercial Operations

Incoming material (via rail, air, etc.) is off-loaded, inspected, inventoried, and stored in warehouses. Component packaging (for construction material, consumables, spares) is very significant for construction as well as space transportation. Packages must meet dimensional and weight constraints of the launch vehicle and have appropriate mass density for cost effective space transportation. Figure 34 illustrates the dimensions, density and part counts of various SPS components. As indicated, densities vary from a low of 12 $kg/m^3$ for antenna subarray elements to about 2500 $kg/m^3$ for power conductors. To obtain desired densities, components must be packaged in appropriate mixes as indicated in figure 35. Such packaging minimizes the number of launches, thereby reducing transportation costs.

The silicon option requires 375 HLLV flights and the GaAlAs option requires 225 HLLV flights to transport construction material for 10 GW (two 5 GW units) capability. Construction personnel are launched in an updated shuttle Personnel Launch Vehicle.

Operations in LEO include COTV construction and maintenance, payload transfers between HLLV's and COTV's, POTV stage mating, crew transfers, vehicle and base maintenance, and propellant storage and transfer.

After payload transfers, COTV's travel to GEO over a period of several months. At GEO, a small interorbital transfer vehicle docks to and moves the cargo to the construction base. After off-loading, the COTV returns to LEO with packing materials, damaged or defective equipment, and parts and consumables containers. At LEO, argon tanks and thruster grids are replaced, the vehicles refurbished and readied for the next transit.

Personnel arriving at LEO from earth, transfer to POTV's for the trip to GEO, which takes a few hours. Personnel returning from GEO transfer to Personnel Launch Vehicles for the trip back to earth.

Because detailed construction techniques, both for COTV's and SPS's, for the Reference System have not yet been developed, the reader is referred to the Appendices. Appendix A discusses construction issues while Appendix B presents techniques that were developed for the Rockwell and Boeing independent systems. The techniques for the Reference System would be similar in general concept.

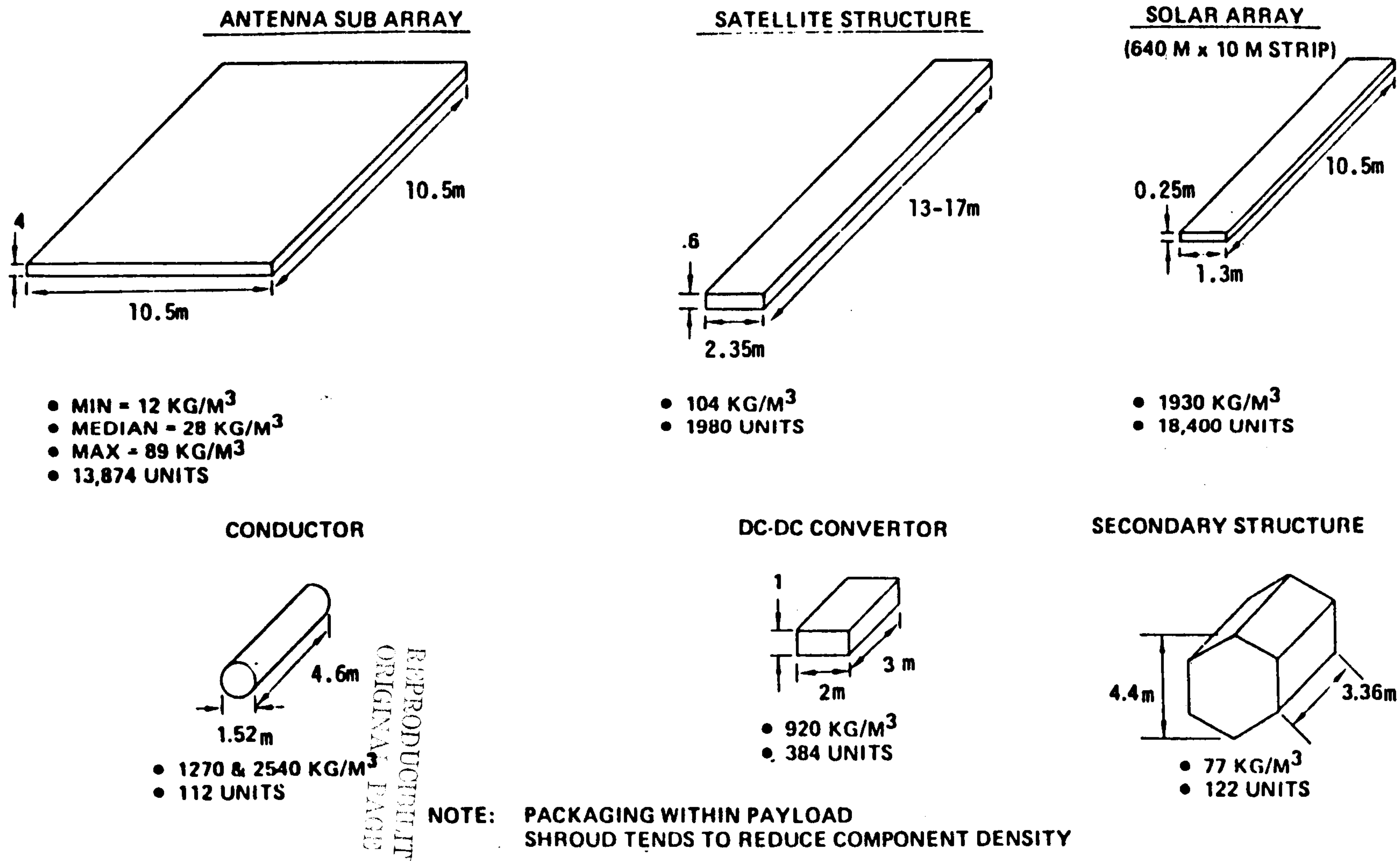


Figure 34. Component Packaging Characteristics

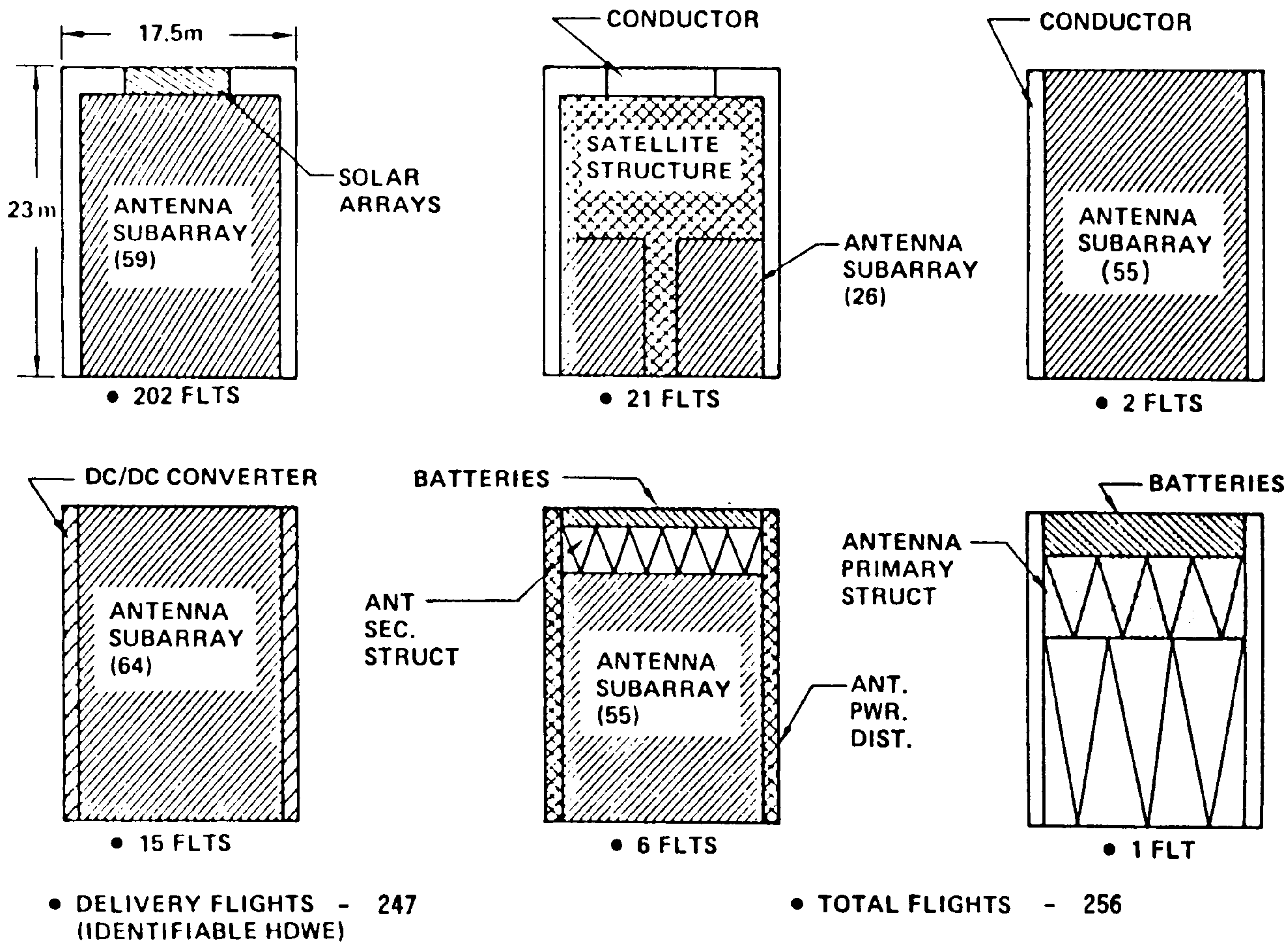


Figure 35. Typical Component Mixing

Figure 36 presents a typical timeline for the silicon option for constructing the initial LEO and GEO bases and the COTV's required to then construct SPS's. Six months are required to construct the LEO base. Three months are required to then construct the first COTV, three additional months to construct the second and third COTV's, and a year to complete the rest of the fleet needed to transport SPS materials from LEO to GEO at the rate of 10 GW per year. Once the first COTV is completed, it begins to transport materials to GEO needed for the GEO construction base. The second and third COTV's transport the remainder of this material. Nine months are required to construct the GEO base. After two years, all of the major elements are available to begin production of the first SPS.

For the gallium option, it has been assumed that the GEO base would be built first in LEO where it would construct the COTV's. Then two COTV's would transfer the base to GEO and leave only staging facilities in LEO.

Figure 37 shows estimates of the number of flights required, payload characteristics, launch vehicle packaging factors assumed, and numbers of people associated with building the LEO base, the COTV's and the GEO base over the initial two-year period. Data is presented for both silicon and GaAlAs options.

Figure 38 presents a typical timeline for construction of two 5 GW SPS's. All the material for one SPS is taken to LEO by HLLV flights in a six-month period. It is transferred to COTV's for six-month trips to GEO, with all materials arriving at GEO over a six-month period. Construction takes place during this six-month arrival period. While the construction of the first SPS takes place, material for the second is being taken to LEO, transferred to COTV's, and is enroute to GEO. When the first satellite is complete, the initial material for the second begins arriving at GEO. Although the entire sequence to build any two 5 GW SPS's takes 18 months, once the process is underway, two SPS's are being produced every year.

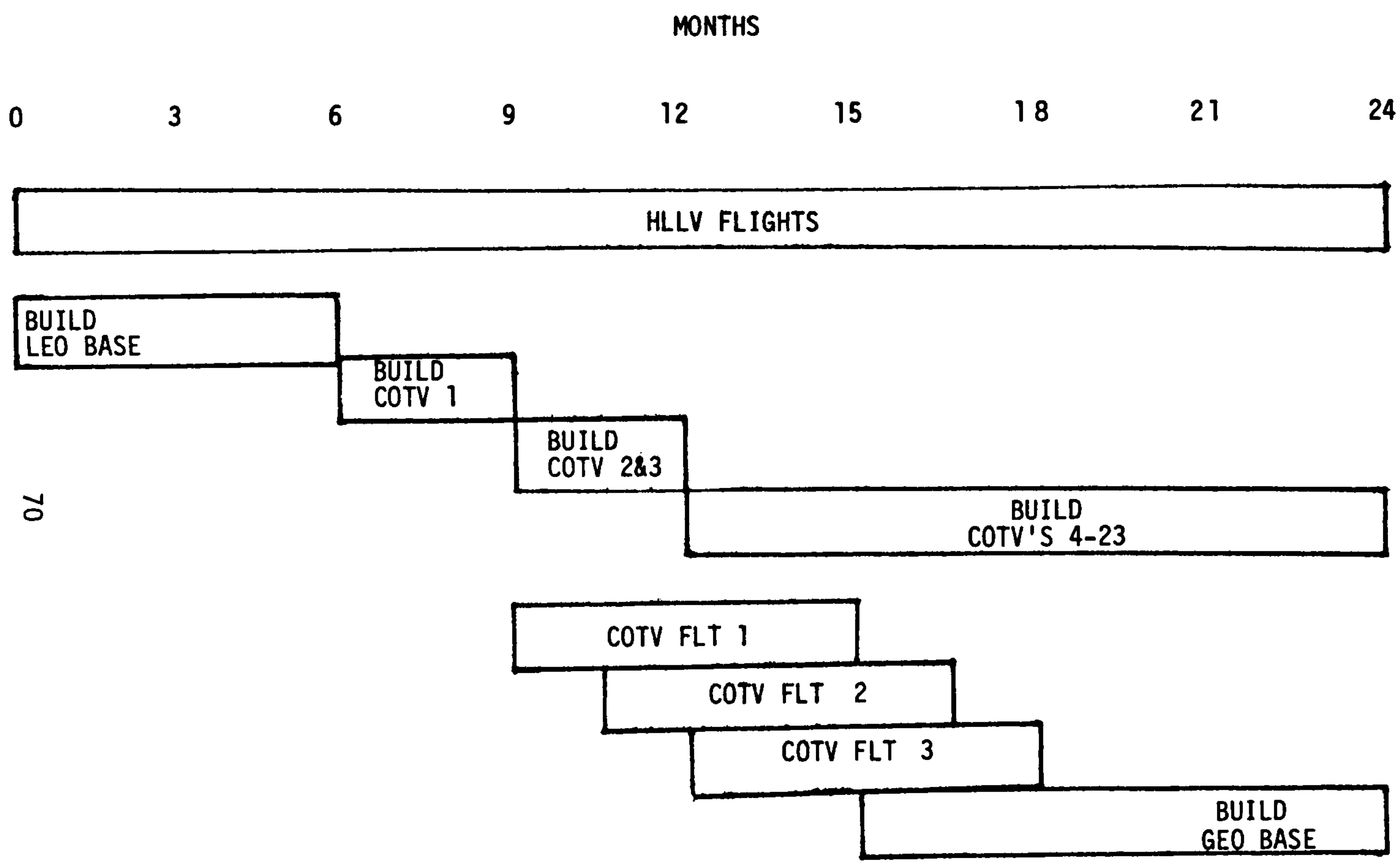


Figure 36. Construction Base Buildup for Silicon System

| | SILICON | GALLIUM |
|---|---|---|
| LEO STAGING | | |
| BASE | | |
| MASS | 2,405 MT | 110 MT |
| PEOPLE | 225 | 35 |
| GEO CONSTR | | |
| BASE | | |
| MASS | 8,353 MT | 6,000 MT |
| PEOPLE | 480 | 680 |
| PAYLOADS | | |
| HLLV | 424 MT | 424 MT |
| PLV | 75 PEOPLE | 75 PEOPLE |
| POTV | 400 MT<br>160 PEOPLE | 400 MT<br>160 PEOPLE |
| COTV | 4,000 MT | 3,500 MT |
| PACKING FACTORS | | |
| HARDWARE | 85% | 95% |
| PROPELLANTS | 95% | 95% |

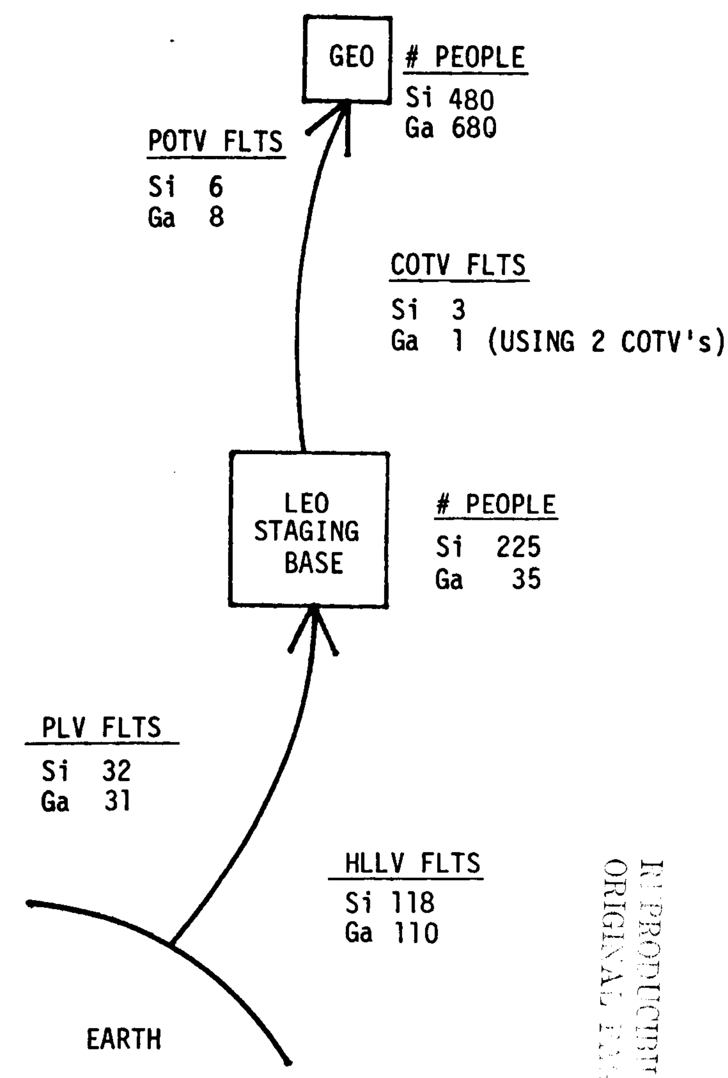


Figure 37. Scenario for Buildup of Construction Bases

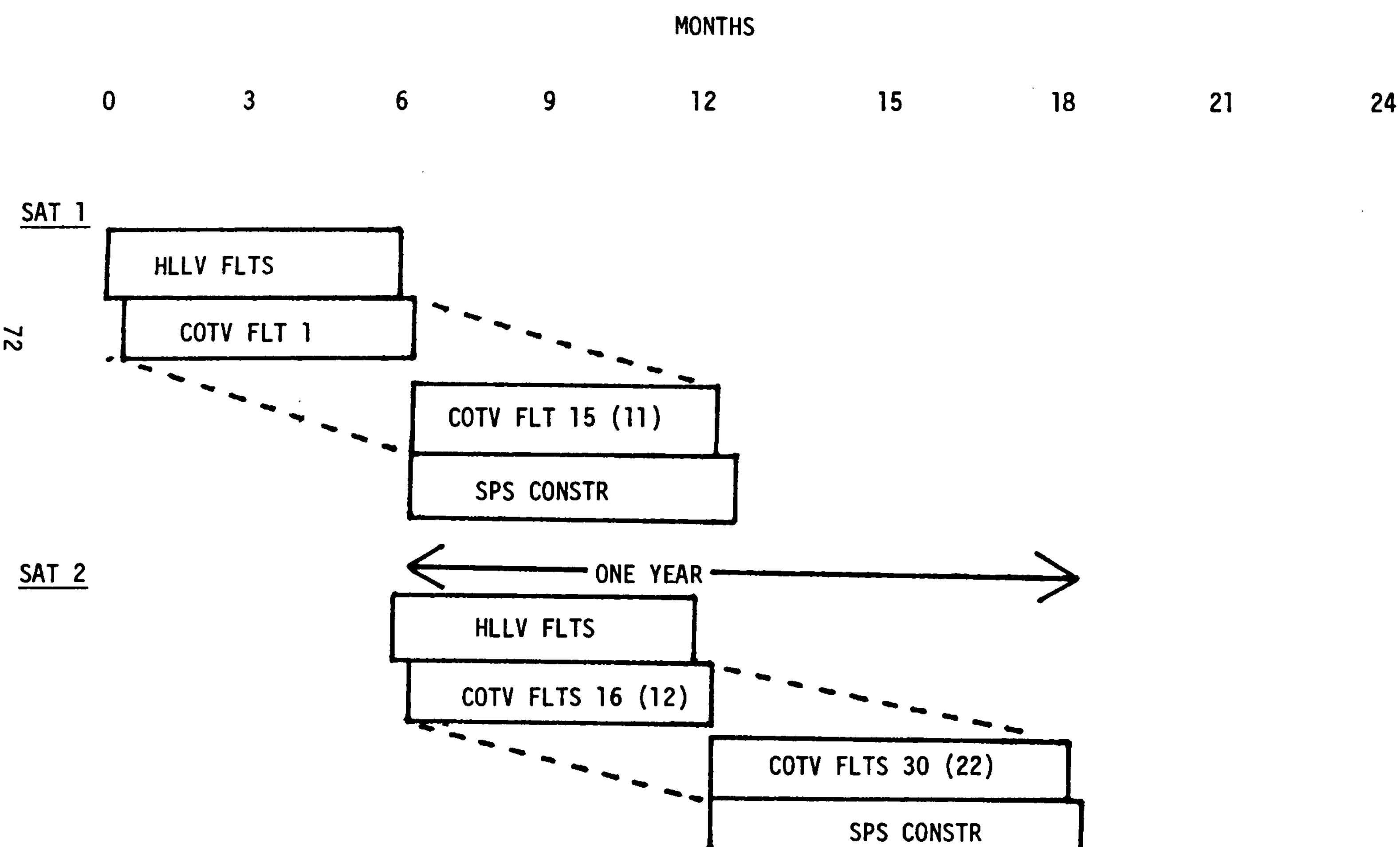


NOTE: Parenthesis () represents flights for Gallium satellite

Figure 38. Construction Timeline for Two 5 GW Satellites/Year

Figure 39 estimates the number of flights required, payload characteristics, packing factors assumed, and numbers of people associated with building two SPS's over a one-year period. Data is presented for both silicon and gallium options.

Table 6 shows the fleet sizes of HLLV's, PLV's, COTV's, and POTV's needed (1) for the buildup period prior to SPS construction and (2) for the construction of two SPS's per year. Data is presented for both silicon and gallium options. Fewer COTV's are needed for the gallium option due to the following combination of factors: different COTV design and flight times, different satellite weights, and different packing factors.

Besides space construction, there is the task of constructing the ground rectenna. Techniques for accomplishing this have not yet been developed; however, some of the relevant issues are present under the construction discussion in Appendix A.

2. Commercial Operations

Once the SPS and rectenna are constructed, the SPS begins to produce commercial power. The main tasks are to operate the interface with the grid and maintain both the SPS and the rectenna.

With regard to the grid interface, it would be ideal if the SPS power would remain uniform at all times. In reality, however, there will be variations from a number of seasonal, daily and orbital path causes. Also, periodic shutdowns due to earth eclipses will occur. Thus, ground-based power generation systems must have a throttling capability to smooth out the demand load.

With regard to maintenance, the large number of components (e.g., $10^5$ klystrons) will result in random failures. Also, it is probable that sections of solar blankets will have to occasionally be replaced due to meteoroid damage or part failures. It is estimated that between 5 and 20 people would be required in GEO per SPS, probably stationed at the construction base. Parts and personnel are transported from LEO to GEO and between SPS's in GEO using OTV stages.

| | SILICON | GALLIUM |
|---|---|---|
| SPS MASS | 50,984 MT | 34,159 MT |
| PAYLOADS | | |
| HLLV | 424 MT | 424 MT |
| PLV | 75 PEOPLE | 75 PEOPLE |
| POTV | 160 PEOPLE<br>400 MT | 160 PEOPLE<br>400 MT |
| COTV | 4,000 MT | 3,500 MT |
| PACKING FACTORS | | |
| HARDWARE | 85% | 95% |
| PROPELLANTS | 95% | 95% |

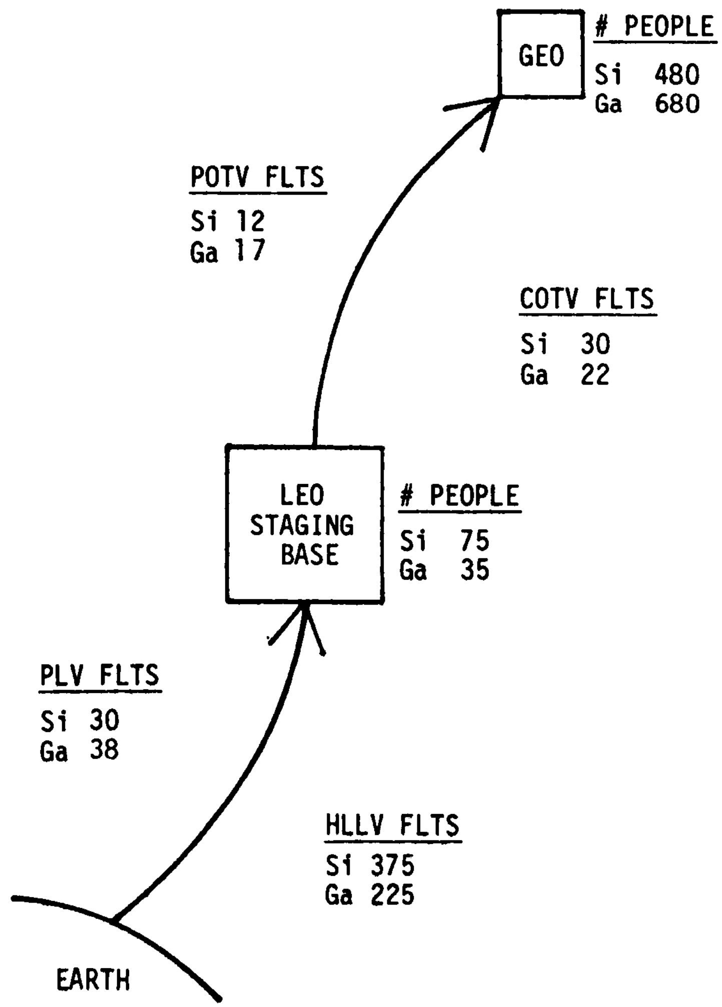


Figure 39. Scenario for Construction of Two 5 GW Satellites/Year

Table 6. SPS Fleet Sizes

| | HLLV | | PLV | COTV | POTV |
|---|---|---|---|---|---|
| | BOOSTERS | ORBITERS | | | |
| STARTUP | 2 (1) | 3 (1) | 2 | 3 (2) | 2 (1) |
| ADDITIONAL REQUIRED FOR CONSTRUCTION OF TWO 5 GW SATELLITE/YEAR | 2 (2) | 2 (2) | - | 20 (8) | - |
| TOTAL REQUIRED FOR CONSTRUCTION OF TWO 5 GW SATELLITE/YEAR | 4 (3) | 5 (3) | 2 | 23 (9) | 2 (1) |

NOTE: PARENTHESIS () IDENTIFIES FLEET REQUIREMENTS FOR GALLIUM SATELLITE AND COTV

### 3. Integrated Operations Management

All of the above construction and commercial operations must occur simultaneously. Thus, there needs to be an integrated operations management scheme that assures they occur in a coordinated manner. Figure 40 illustrates the various functions involved in SPS operations as they have been discussed. Figure 41 illustrates an operations management concept to control, coordinate, and integrate these functions.

The program headquarters function would manage the flow of ground-based resources through manufacturing and transport to the launch site. It would coordinate the communications systems necessary to carrying out SPS operations and, in general, assure that overall SPS operations are conducted satisfactorily.

The launch and landing control function manages the preparation, launch, and landing of cargo and personnel to and from LEO. It maintains and refurbishes launch vehicles.

The LEO and GEO bases manage on-site their respective activities involved with construction, logistics, transportation, checkout, maintenance, etc.

SPS ground control units at each rectenna would operate and control the functioning of their assigned SPS, rectenna and grid interface.

## M. Costs

Cost information has been estimated for the SPS Reference System. This costing information will be included as a part of the Comparative Assessment Study.

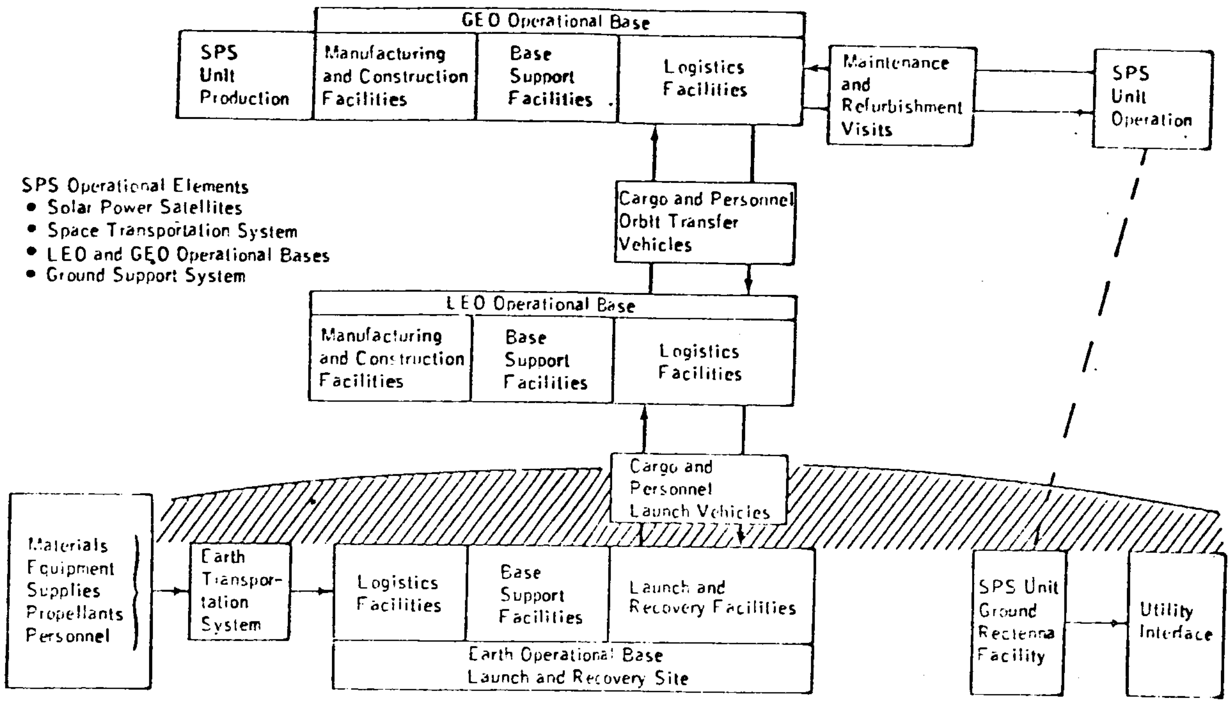


Figure 40. SPS Operational Functions

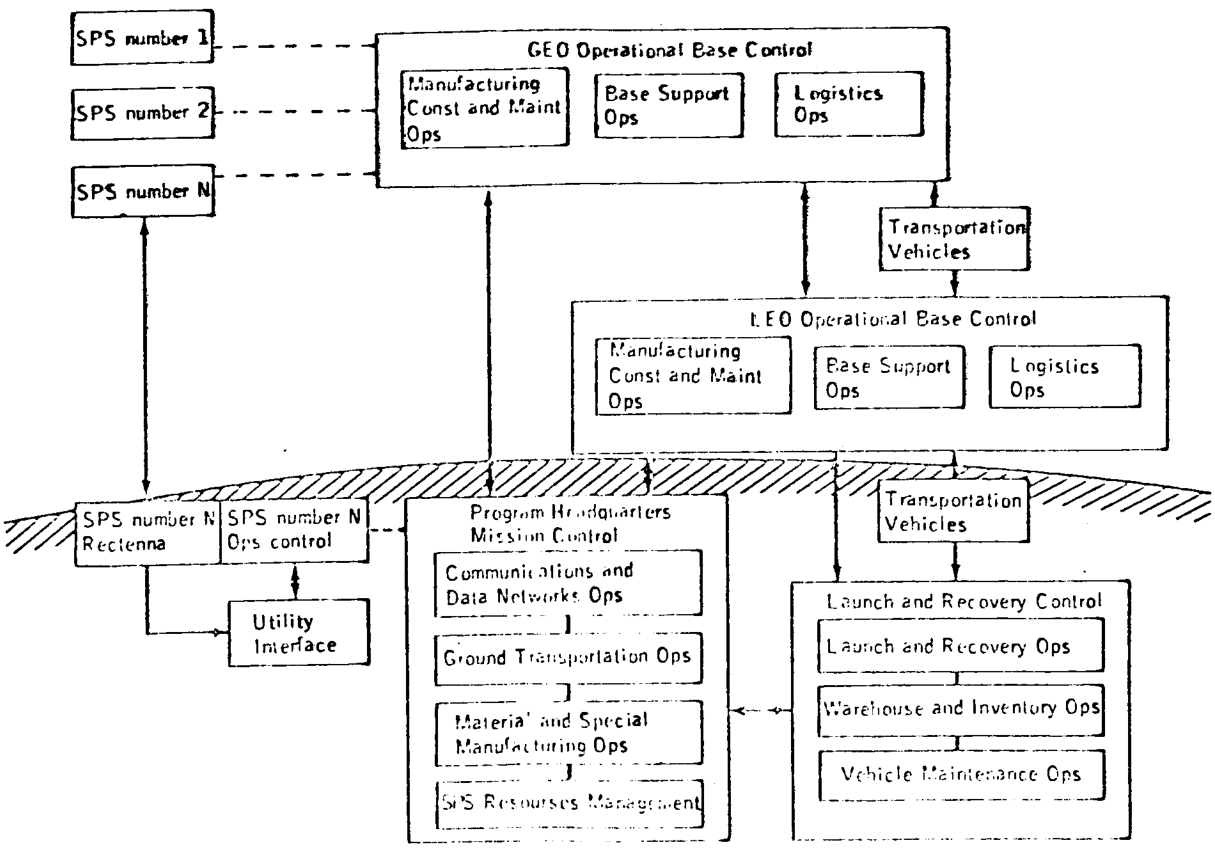


Figure 41. SPS Operations Management Concept

## IV. TECHNOLOGY SUMMARY

### A. Critical Questions

Beginning with the earliest systems definition studies, it has been recognized that SPS will require significant technological advancements in several disciplines. Continued study has indicated that establishment of firm designs, performance levels, cost expectations, development requirements, and environmental acceptability, depends on the resolution of several critical questions. Although overall success of SPS development is possible over a range of performance and design, establishment of specific attainable performance levels is important to establishment of designs and system specifications.

The critical questions involve engineering, economic, and environmental issues, each of which require laboratory test effort to obtain the necessary information for full evaluation of the SPS concept. This summary will confine itself to critical questions primarily related to questions of engineering feasibility. Many of these questions and the required test activity are interlaced with answering critical environmental and economic questions.

The critical questions may be categorized according to the following general subsystem areas.

1. Microwave power transmission
2. Solar arrays
3. Power distribution
4. Structures and control
5. Materials
6. Construction
7. Space transportation

Critical questions under each of the above categories are summarized below.

1. Microwave Power Transmission

o Microwave power amplifier (DC-RF converters) design and development.

o Microwave power transmission phase control system development.

o Microwave power transmitting antenna (subarray) design and development, integrated systems test.

o Rectenna electronic component development.

o Rectenna structures and construction techniques.

2. Solar Arrays

o Solar cell array (blanket) design and materials selection for automated blanket fabrication/production at low cost.

o Long-term environmental effects on candidate solar cell array materials to determine radiation (electron/proton) degradation characteristics, UV susceptibility, and plasma interaction with high voltage arrays.

o Determine thermal annealing characteristics and, where necessary, develop in-situ annealing techniques such as laser heating devices and self-annealing methods.

o Solar reflectors (for concentrated systems).

3. Power Distribution

o Investigate spacecraft charging and high voltage interaction.

o High voltage (40 to 50 kv) DC switchgear development.

o High voltage (40 to 50 kv) electrical cable insulation development.

o Rotary joint/slipring development for 30 year life (electro-mechanical components).

o Power processing technology development for electric propulsion systems.

o Power processing technology development for radiation resistant control electronics, EMI suppression, and long-life, high efficiency transformers with weight constraints.

4. Structures and Controls

o Development of integrated structure/control systems for large lightweight systems.

5. Materials

o Determine outgassing/UV/particle radiation effects on composite materials and coatings.

o Longterm stability of composites and other materials in GEO and LEO environments.

6. Construction

o Space fabrication techniques and equipment (beam builder) development, including the accrual of space operational experience with such equipment.

o Manned remote work station and large-scale crane-manipulator development including docking and berthing techniques.

o Hardware deployment, handling, and installation techniques for solar array blankets, power conductors, structural elements, and antenna subarrays.

7. Space Transportation

o Electric propulsion technology development; thrusters and controls.

o Large liquid-fueled rocket engine development for low cost, long-life HLLV operations.

o Fluids handling and transfer technology for use in orbit.

## B. Alternate Technologies

In consideration of the above technology advancement requirements, it is appropriate to identify alternative technology options available to reduce program risk. The major alternatives and options are summarized below according to system element.

### 1. Microwave Power Transmission

o Use of amplitrons, magnetrons, or solid state RF generators in lieu of klytrons.

### 2. Solar Arrays

o Use of amorphous silicon, high efficiency cadmium sulfide, or other potentially low cost solar cells.

o Development of thermal engine systems such as the potassium Rankine cycle and Brayton cycle for use in lieu of solar photovoltaics. Focus on lightweight radiators and leak-tight joints for fluid system.

### 3. Materials

o Use of aluminum structure with thermal distortion stabilizing design features for transmit antenna and/or solar array.

### 4. Space Transportation

o Single-stage-to-orbit booster in lieu of two-stage vertical booster (HLLV).

## V. DOCUMENTATION SUMMARY

The following is a partial listing of the reports of studies dealing with systems definition of the Solar Power Satellite and related subjects. Reports are grouped by general subject. Listings under each subject heading are chronological.

Most of the reports listed are available through the National Technical Information Service. NTIS numbers are listed in parentheses after each reference if applicable. Where a series of numbers is given, the report consists of more than one volume. An "X" prefix indicates restricted distribution. These restrictions are listed in this document as follows:

N - NASA only
G - Government agencies only
GC - Government agencies and contractors only

### System Definition

1. Glaser, P.E., "Power From the Sun: Its Future," Science, Vol. 162, November 22, 1968.

2. "Initial Technical, Environmental and Economic Evaluation of Space Solar Power Concepts," Johnson Space Center, JSC-11568, August 1976 (N77-16442 and 16443).

3. "Satellite Power System Engineering and Economic Analysis," Marshall Space Flight Center, TMX-73344, November 1976 (N77-15486).

4. "Satellite Power Systems (SPS) Feasibility Study," Rockwell International Corporation, SD76-SA-0239, Contract NAS8-32161, December 1976.

5. "Systems Definition of Space-Based Power Conversion Systems," Boeing Aerospace Corporation, D180-20309, Contract NAS8-31628, February 1977 (X77-10101 and 10102 (GC)).

6. "Space-Based Solar Power Conversion and Delivery Systems," Econ, Inc. and Grumman Aerospace Corporation, Contract NAS8-31308, Second Interim Report, June 1976.

7. "Solar Power Satellite System Definition Study - Part I," Boeing Aerospace Corporation, D180-20689, Contract NAS9-15196, June 1977 (N78-13099 through 13103).

8. "Solar Power Satellite System Definition Study - Part II," Boeing Aerospace Corporation, D180-22876, Contract NAS9-15196, December 1977 (N78-20156 through 20163).

9. "Solar Power Satellite System Definition Study - Part III," Boeing Aerospace Corporation, D180-24071, Contract NAS9-15196, March 1978 (N78-20164).

10. "Solar Power Satellite Concept Evaluation," Johnson Space Center, JSC-12973, July 1977 (N78-12116).

11. "Satellite Power Systems (SPS) Concept Definition Study," Rockwell International Corporation, SD78-AP-0023, Contract NAS8-32475, April 1978.

Other Concepts

12. Ehricke, Krafft A., "The Power Relay Satellite: A Means of Global Energy Transmission Through Space," Rockwell International Corporation, Report E74-3-1, March 1974.

13. "Application of Stationkept Array Concepts to Satellite Solar Power Station Design," Aerospace Corporation, ATR-76(7575)-1, Contract NAS8-31842, November 1976 (X77-10236 through 10238 (GC)).

14. Billman, K. W., W. P. Gilbreath and S. W. Bowen, "Introductory Assessment of Orbiting Reflectors for Terrestrial Power Generation," Ames Research Center, TMX-73230, April 1977 (X77-73872 (N)).

Orbit Characteristics

15. "Orbital Motion of the Solar Power Satellite," Otis F. Graf, Jr., Analytical and Computational Mathematics, Inc., ACM-TR-105, Contract NAS9-15171, May 1977 (N78-15148).

Power Conversion

16. "To Design Variable Orientation Solar Concentrators for Space Applications," University of Georgia, Contract NAS8-31565, October 1975 (X76-72006 through 72009 (N)).

17. "Design of Forward Lighted Solar Concentrators for Space Applications," University of Georgia, Contract NAS8-32149.

18. "Evaluation of Solar Cells for Potential Space Satellite Power Applications," Arthur D. Little, Inc., Contract NAS9-15294, June 1977 (N77-30612).

19. "Development of a Directed Energy Annealable Solar Cell System," Spire Corporation, FR-20066, Subcontract to NAS9-15196, July 1978.

Microwave Power Transmission

20. "Experiments in the Transportation of Energy by Microwave Beams," Brown, W. C., 1964 IEEE Intersociety Conference Record, Vol. 12, Part 2, 1964, pp 8-17.

21. "Free-Space Microwave Power Transmission Study, Combined Phase III and Final Report," W. C. Brown, Raytheon Report No. PT4601, Contract NAS8-25374, September 1975 (N77-16619).

22. "Reception-Conversion Subsystem (RXCV) for Microwave Power Transmission System," Raytheon Report No. ER75-4386, JPL Contract No. 9533968, September 1975 (N76-15598).

23. "Microwave Power Transmission System Studies," Raytheon Company, ER75-4368, Contract NAS3-17835, December 1975 (N76-15594 through 15597).

24. "Electronic and Mechanical Improvement of the Receiving Terminal of a Free-Space Microwave Power Transmission System," W. C. Brown, Raytheon Company, PT-4964, Contract NAS3-19722, August 1977 (N77-31613).

25. "Microwave System Studies Affecting SPS Rectenna Performance," Gutman, Ronald J., Research performed at JSC, August 1977.

26. "Ionosphere/Microwave Beam Interaction Study," L. M. Duncan and W. E. Gordon, Rice University, Contract NAS9-15212, September 1977 (N77-33389).

27. "A Solar Power Satellite Transmission System Incorporating Automatic Beam Forming, Steering and Phase Control," LinCom, Inc., TR-7806-0977, Contract NAS9-15237, June 1978.

28. "Achievable Flatness in a Large Microwave Power Antenna," General Dynamics, Convair Div., Contract NAS9-15423, September 1978.

29. Perkins, F. W. and R. G. Roble, "Ionospheric Heating By Radiowaves: Predictions for Arecibo and the Satellite Power Station," J. Geophysical Research (to be published).

30. Holway, L. H., A. H. Katz, G. Meltz, "Ionospheric Effects of a High Power Space-Borne Microwave Beam," Raytheon Technical Memorandum T-1028, Waltham, M.A., Nov. 1977.

31. Arndt, G. D. and L. Leopold, "Environmental Considerations for the Microwave Beam from a Solar Power Satellite," 13th Intersociety Energy Conversion Engineering Conference, San Diego, CA, August 1978.

Transportation

32. "Future Space Transportation Systems Analysis Study," Boeing Aerospace Corporation, D180-20242, Contract NAS9-14323, December 1976 (Vol. 1: N77-31235; Vol 2: X77-78969 (N); Vol 3: X77-79819 (G)).

33. "Orbital Propellant Handling and Storage Systems for Large Space Programs," General Dynamics Convair Div., CASD-ASP-78-001, Contract NAS9-15305, April 1978.

Orbital Construction

34. "Orbital Assembly and Maintenance Study," Martin Marietta Corporation, MCR-75-319, Contract NAS9-14319, August 1975 (N75-32144).

35. "Orbital Construction Demonstration Study," Grumman Aerospace Corp., NSS-OC-RP-008, Contract NAS9-14916, December 1976 (N77-23136).

36. "Orbital Construction Support Equipment," Martin Marietta Corporation, MCR-77-234, Contract NAS9-15120, June 1977 (N77-27157).

37. "Space Construction Automated Fabrication Experiment Definition Study," General Dynamics Convair Div., CASD-ASP-77-017, Contract NAS9-15310, May 1978 (N78-25111 through 25113).

Rectenna Construction

38. "Feasibility Study for Various Approaches to the Structural Design and Arrangement of the Ground Rectenna for the Proposed Satellite," Bovay Engineers, Inc., Contract NAS9-15280, May 1977.

Technology Advancement

39. "Preliminary Assessment of Technology Advancement Requirements for Space Solar Power," Johnson Space Center, JSC-12702, March 1977.

Economic and Political

40. "An Initial Comparative Assessment of Orbital and Terrestrial Central Power Systems," R. Caputo, Jet Propulsion Lab., JPL-DOC-900-780, March 1977 (N77-22612).

41. "Impacts and Benefits of a Satellite Power System on the Electric Utility Industry," Arthur D. Little, Inc., C-80020, Contract 954639 (JPL), July 1977 (N78-24255).

42. "Political and Legal Implications of Developing and Operating a Satellite Power System," Econ, Inc., ECON-77-195-1, Contract 954652 (JPL), August 1977 (N78-25003).

43. "A Study of Some Economic Factors Relating to Development and Implementation of Satellite Power Systems, ECON, Inc., NASA-CR-150602, Contract NAS2-9655, March 1978.

Biological and Environmental

44. "Research Plan for Study of Biological and Ecological Effects of the Solar Power Satellite Transmission System," Bernard D. Newsom and Associates, Contract NAS2-9655, March 1978.

45. "Compilation and Assessment of Microwave Bioeffects," Pacific Northwest Laboratory, A0-02-01/EA81028, Contract EY-76-C-06-1830 (DOE), May 1978.

46. "Satellite Power System Environmental Impacts - Preliminary Assessment," Floyd R. Livingston, Jet Propulsion Laboratory, 900-822, Rev. A. May 1978.

Work Breakdown Structure

47. "Satellite Power System Work Breakdown Structure Dictionary," Marshall Space Flight Center, TM-78155, January 1978.





C-2

# APPENDIX A

## SYSTEM ANALYSIS RESULTS

This appendix provides discussions of the key trade-off study results and analyses that have been conducted to date. The approach taken in documenting the study results is to describe the evolution of the design work from initial concepts to the present.

The following topics are addressed in this appendix in the order indicated:

A. Design Considerations

B. Solar Energy Collection, Conversion, and Power Distribution

C. Power Transmission, Collection and Conversion

D. Structures and Materials

E. Space Transportation

F. Construction

G. Natural Resources

A. Design Considerations

This section summarizes several trade studies dealing with orbit selection, orientation, system sizing and constructability. These trades have a direct, major influence on the overall configuration of the satellite.

Orbit Selection - Geosynchronous altitude (35800 km) has been used in all studies. Near uninterrupted transmission is possible, antenna steering accelerations are low, and the satellite is stationary with respect to a point on earth.

Three inclinations have been considered (figure A-1). Zero inclination gives a stationary satellite, simplifying the rectenna design. A 7.3° inclination eliminates the lunar and solar perturbation which would otherwise cause the inclination to vary between zero and 15° over a period of years, if uncorrected. A 23.4° inclination places the orbit in the ecliptic plane, permitting the satellite to be oriented simultaneously toward the sun for maximum output and perpendicular to the orbit plane (POP) for minimum gravity gradient torque. Non-zero inclinations cause a daily variation in the angle of incidence on the rectenna of about twice the inclination, increasing the rectenna area required and imposing constraints on the rectenna design for which solutions have not yet been identified. The zero-inclination orbit can be maintained with a relatively small propellant budget, however. All studies have concluded that zero inclination is preferred.

Solar radiation pressure acting on the large, low density solar array induces a small, variable eccentricity in the orbit. This causes a daily oscillation of several degrees of longitude. The design impact of this oscillation is relatively minor: the resulting angular acceleration of the transmitting antenna is manageable and the moderate east-west motion of the microwave beam can be easily accommodated by most proposed rectenna designs. Moreover, the propellant penalty for maintaining zero eccentricity is substantial, amounting to roughly half of the total attitude control and orbit maintenance requirement for typical configurations. Consequently, early studies tended to tolerate the eccentricity in order to reduce propellant resupply requirements. Subsequent

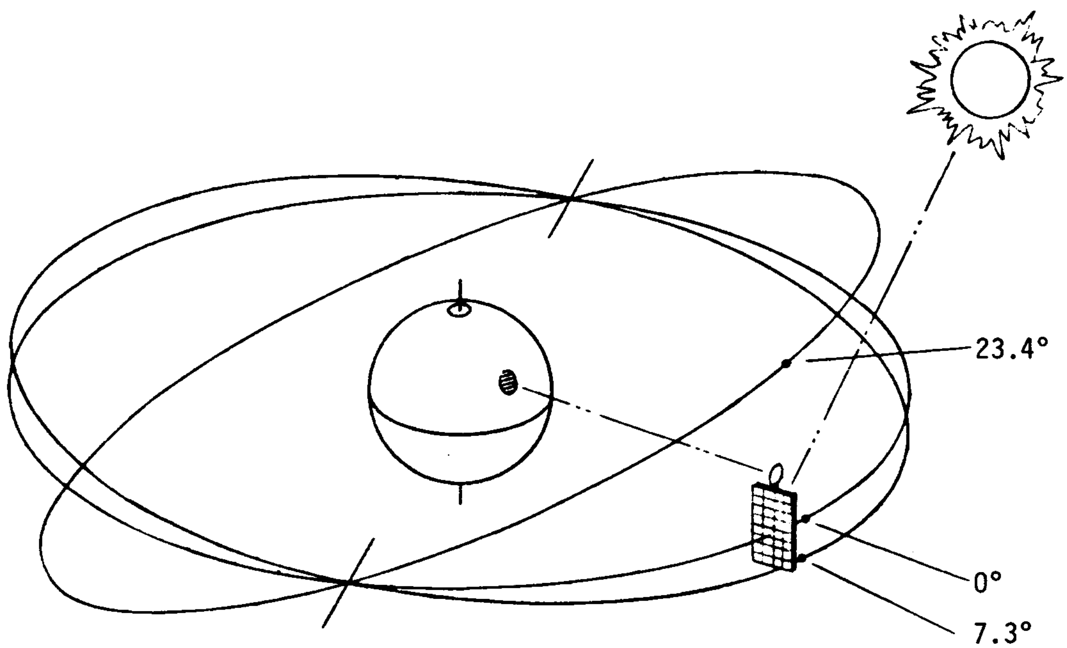


Figure A-1. SPS Orbit Inclinations

results, however, indicate that orbit maintenance can be combined, at least partially, with attitude control to reduce total propellant consumption. In an eccentric orbit (uncorrected for radiation pressure), the large size of the SPS results in an unacceptable probability of collision with other synchronous satellites. Holding the eccentricity to zero will greatly reduce this probability.

In summary, the preferred orbit for the SPS is geosynchronous with zero inclination and eccentricity; i.e., geostationary.

Orientation and Attitude Control - The orientation of the SPS must satisfy two conditions: the solar energy collection system (SECS) must point at the sun and the microwave power transmission system (MPTS) must point at the ground station. The first consequence of this is that the MPTS must rotate continuously at one revolution per day relative to the SECS. This rotation is about an axis perpendicular to the orbit plane (POP), requiring that the MPTS be located at the north or south end of the SECS, mounted centrally on a rotary joint of sufficient size to span the SECS carry-through structure, or mounted centrally on a small rotary joint within dielectric structure for minimum interference with the microwave beam. Early SPS concepts used the last of these. Subsequent studies have avoided this approach in order to eliminate an unnecessary source of interference, the nature of which is not completely understood.

The principal disturbance acting on the SPS is gravity gradient torque. Gravity gradient torque exists whenever the spacecraft principal axes are not orthogonal with the orbit plane and local vertical and the principal moments of inertia are not equal.

An asymmetrical SPS, with the center of pressure offset from the mass center, will also experience torque from solar radiation pressure.

Gravity gradient affects the SPS in two ways. The first occurs when the sun is not in the orbit plane (that is, at all times except at the equinoxes) if the SECS is pointed at the sun (figure A-2). This torque cycles with a period of one year, making momentum storage unattractive. Since the maximum sun angle is 23.4°, however, the SECS can be held in a POP attitude at all times. This eliminates the torque and causes a maximum power loss of only about eight percent.

Because of the large saving in attitude control propellant, all studies have adopted this attitude. The antenna joint can also be simplified in the POP attitude, requiring two axes of rotation (one continuous) instead of three in the solar orientation.

The second gravity gradient effect arises from the continuous attitude change of the SECS relative to the earth (figure A-3). This torque is cyclic with a 12-hour period. Because continous rotation is required, a fixed attitude cannot be used as in the previous case. Consequently, the torque has been minimized in most studies to date by reducing the difference in moments of inertia about the two axes in the orbit plane. This can be done by increasing the length of the SECS (perpendicular to the orbit plane) and reducing the width.

The moment of inertia difference can also be reduced or eliminated by departing from a flat solar energy collector. Several approaches have been proposed for both photovoltaic and thermal conversion, although the geometrical constraints of thermal systems make them less amenable to such treatment. Power distribution paths are generally longer in inertially "balanced" configurations, tending to reduce the total-mass-to-orbit advantage. Most, but not all, inertially balanced configurations appear to be more difficult to construct. Since speed and ease of construction are significant factors in the practicality of the SPS concept, most inertially balanced configurations have not survived evaluation.

Since the gravity gradient torque is cyclic, momentum storage devices such as momentum wheels appear attractive. However, preliminary studies have indicated a cost disadvantage compared to a reaction control system unless the high specific impulse projected cannot be achieved.

Satellite Sizing - For a minimum cost of electricity per kilowatt-hour, the output per antenna should be as large as possible, although studies indicate that the cost per kilowatt-hour increases only slightly for outputs substantially below maximum. Maximum output is constrained by two factors, the power density at the transmitting antenna (heat rejection) and the power density at the ionosphere (ionosphere disruption). The best current definitions of these limits

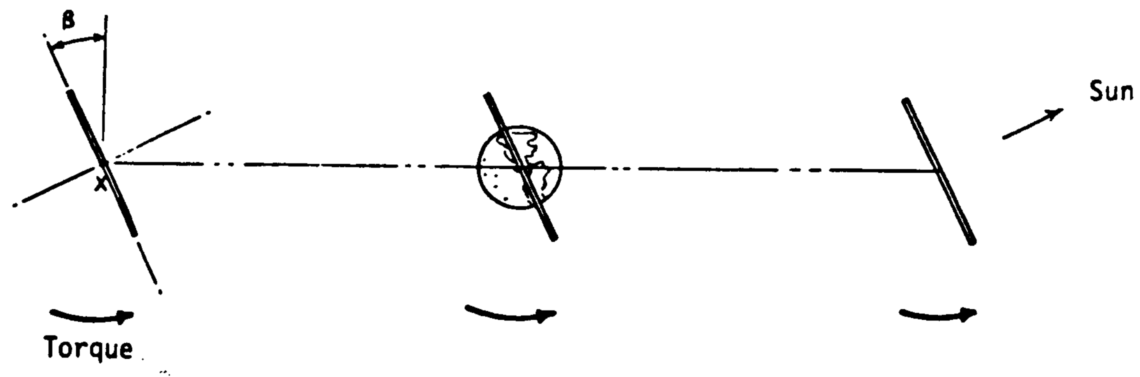


Figure A-2. Long-Period Gravity Gradient Torque

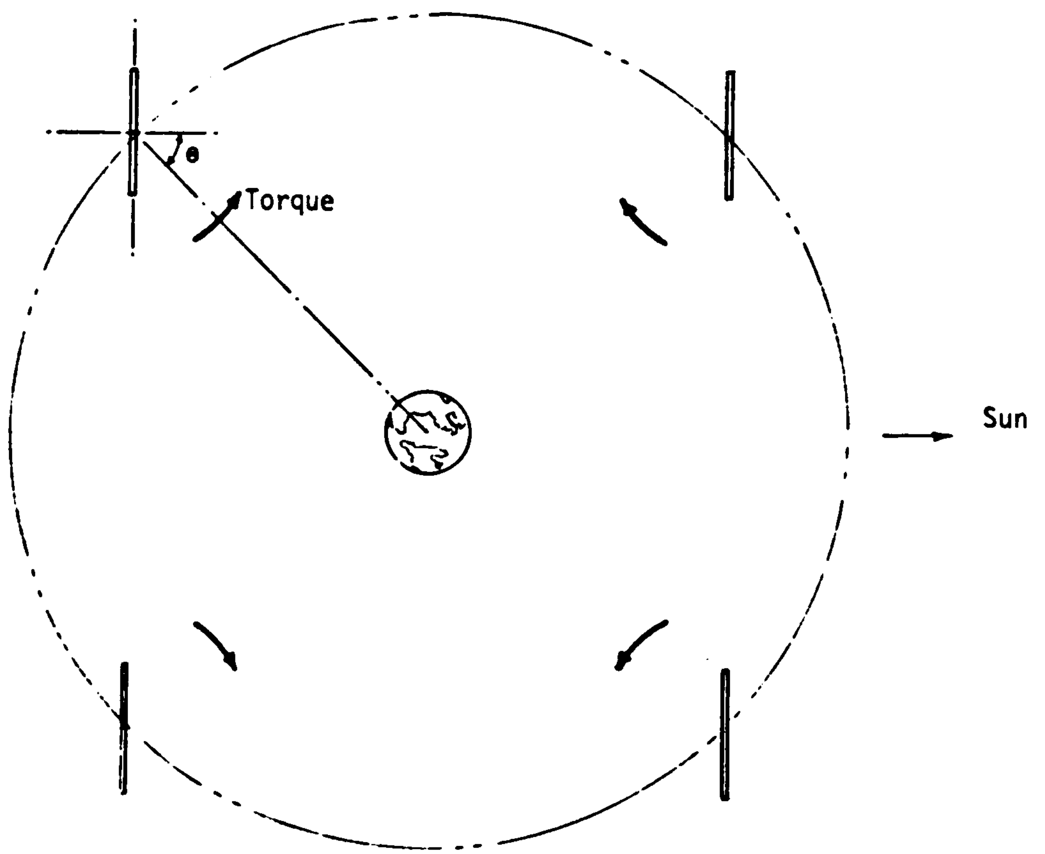


Figure A-3. Short-Period Gravity Gradient Torque are 21 $kW/m^2$ and 23 $mW/cm^2$, respectively, although future tests could indicate revisions. Since the variation of the two factors with antenna size is different, the limits can be used to calculate not only the maximum output, but also antenna and rectenna diameters. Using the microwave system parameters defined elsewhere in this report, maximum output on the ground is approximately 5 GW with an antenna diameter of 1 km and a rectenna diameter of 10 km (figure A-4).

Construction - Construction of the satellite is discussed in Section F of this appendix. However, satellite configuration strongly influences ease of construction, which is probably necessary if the SPS is to be economically competitive. In general, a configuration that permits a high degree of automation in its construction, such as the reference photovoltaic system, can be built more easily. Conversely, a typical thermal cycle configuration requires a large number of different operations. Many of these are performed only a few dozen times. A large number of fluid connections must be made. Even the highly repetitive tasks, such as reflector facet installation, are largely discrete rather than continuous. All of these are comparatively difficult to automate, and as a result the thermal SPS is relatively difficult to construct.

Power Output Variations - Ideally, SPS power output at the rectenna would remain uniform at all times. Actually, however, the power output will depend on the intensity of illumination of the solar collector/converter, its efficiency, and the efficiency of the microwave transmission collection and conversion system. Figure A-5 illustrates the net effect of these variations for a solar photovoltaic solar collection/conversion system. In this case, the 180-day cyclic variation is caused by variation of the sun's declination (angle) with respect to the orbital plane. Superimposed on this variation is a daily cyclic fluctuation resulting from orbit eccentricity. Orbit eccentricity causes a variation in satellite-to-rectenna distance, affecting transmission/collection efficiency.

The power output of a solar array depends on the intensity of illumination at the cells and the temperature of the cells, the power output of cells diminishing as the cells become hotter. In geosynchronous orbit the temperature of the solar cell is related to the intensity of sunlight for any given panel configuration.

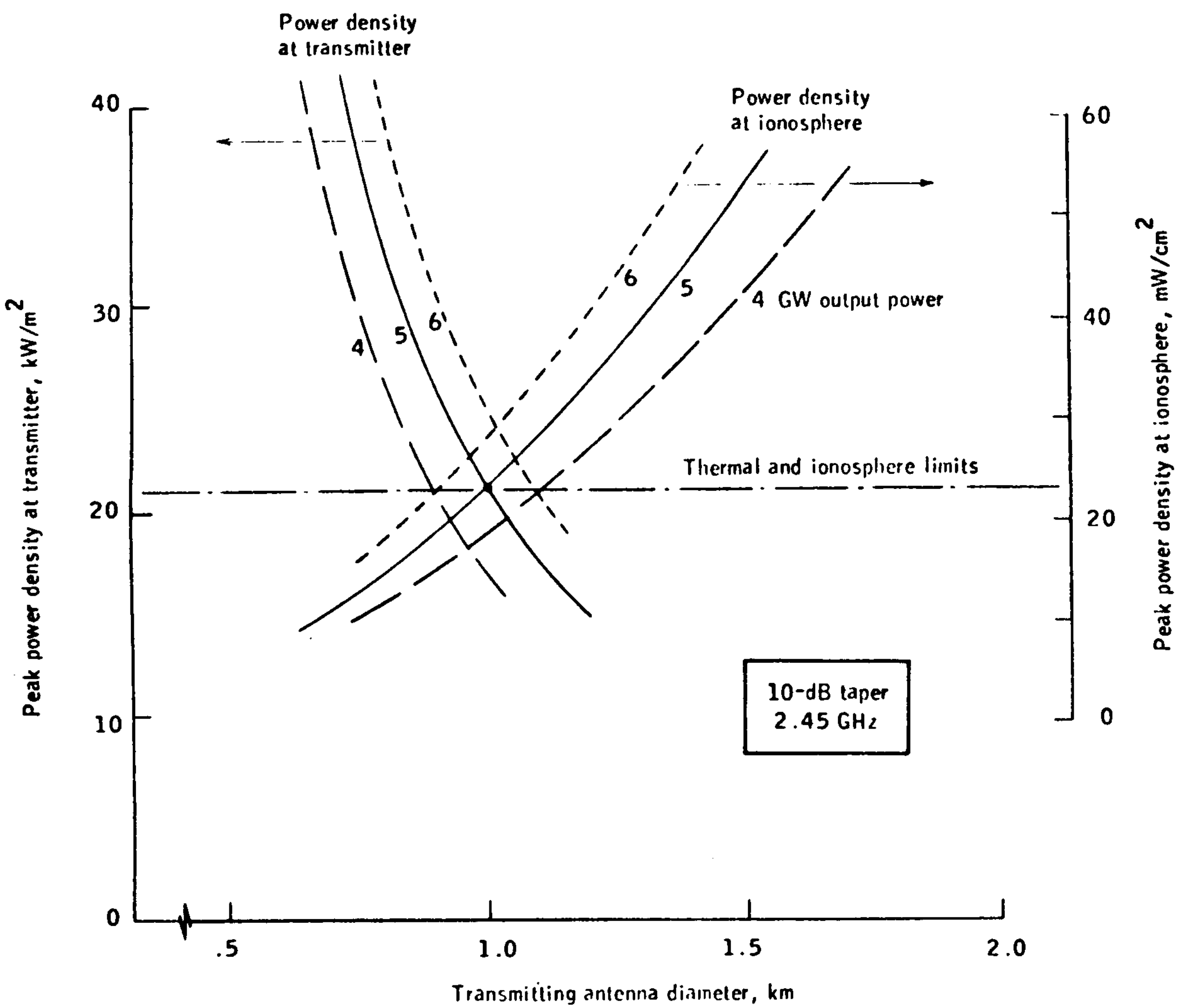


Figure A-4. System Sizing

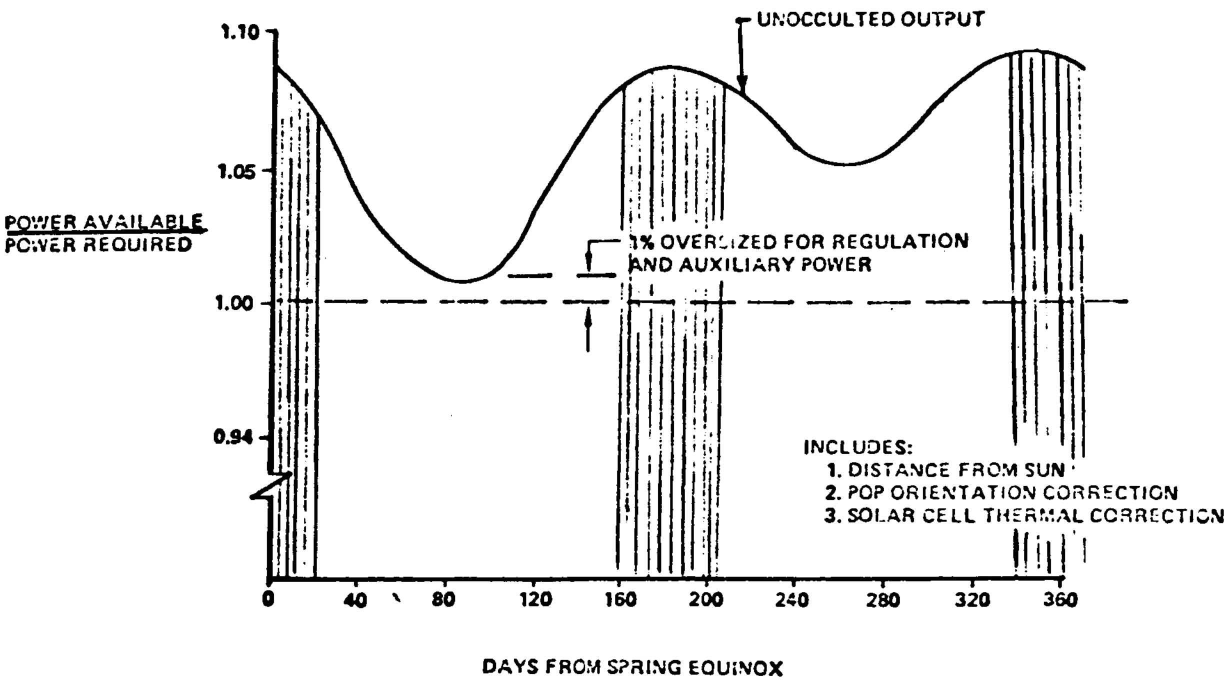


Figure A-5. Seasonal Power Output Variations

The sun is brightest at perihelion, which occurs around winter solstice when the orientation of the array is such that the sun's rays arrive at 23.5° off of normal incidence. The worst-case illumination is at summer solstice where the 23.5° misorientation is accompanied by aphelion where the intensity of sunlight is 0.967° average. However, the solar array temperature is also down, being 36.5°C rather than 46.0°C as at the spring and autumn equinoxes. The net effect of these variations, as shown in figure A-5, is a lower power output during the summer months than during the winter months.

Eclipses by the earth, illustrated in figure A-5 by the close-spaced vertical lines, will cause total shutdowns daily around local midnight for about six weeks in the spring and fall. The maximum duration is about 75 minutes.

## B. Solar Energy Collection, Conversion, and Power Distribution

### 1. Energy Collection and Conversion

The energy collection/conversion system for the SPS has the function of collecting the dispersed solar energy in sufficient quantities for conversion to electrical energy. This electrical energy is then delivered to the power transmission system for beaming to ground-based receiving stations as microwave radiation.

Several major trade studies have been performed on a variety of energy collection/conversion systems to determine the most favorable to the SPS concept. As part of these studies, photovoltaic systems, thermal conversion systems, space nuclear power plants and orbiting solar reflector systems were included. Both NASA JSC and NASA MSFC performed in-house studies (ref. 2,3) on various systems during 1974-1976. During the same period and for the next few years, each center contracted with aerospace companies to perform independent system definition studies. This section summarizes certain of these studies concerning energy collection/conversion systems that have led to the reference system.

The MSFC in-house studies were conducted primarily to obtain a quantitative understanding of the advantages and disadvantages of various schemes rather than to eliminate options. The tradeoffs were performed to minimize mass and costs. The MSFC-Boeing study (ref. 5) evaluated and identified production rates, launch frequencies, facilities, etc., so that electric power cost could be estimated. Satellite size, mass and life cycle cost were established within the limitations of the contract. The JSC in-house study emphasized analysis of the photovoltaic concept and investigated sensitivity of systems to mass, performance, and transportation cost. Also, a thorough review of past system studies involving several thermal energy conversion concepts was accomplished. Most recently, the JSC-Boeing and the MSFC-Rockwell studies both performed a comparative analysis of a variety of systems with the objective of identifying feasible systems. The systems investigated are discussed briefly as follows.

Solar Photovoltaics - Since the SPS concept was first postulated, the passive system advantages of photovoltaics has provided a standard of comparison for other solar collection/conversion systems. The MSFC in-house study (ref. 3) looked at numerous photovoltaic systems to select a solar cell technology suitable for the SPS. The design utilized silicon solar cells although their studies indicated some other compositions showed promise. The MSFC-Boeing (ref. 5) study modeled a silicon photovoltaic and gallium arsenide photovoltaic SPS concept to determine total power generation costs. Although most of the component definitions were extremely preliminary, cost estimates allowed reasonable trade studies. The JSC in-house study (ref. 2) emphasis was on the silicon photovoltaic SPS. The JSC-Boeing study (ref. 7,8,9) included evaluations of several photovoltaic options including single crystal silicon, single crystal gallium arsenide and thin film options and some other less developed thin film approaches such as copper indium selenide. The MSFC-Rockwell study (ref. 11) included silicon and gallium-aluminum-arsenide solar cell evaluations and several concentration ratios. The data base at the beginning of the study was evaluated to determine which SPS approaches should be seriously considered as candidates for further analysis.

In evaluating the various photovoltaics options, a number of factors have been considered including performance (efficiency), mass, materials availability, susceptibility to radiation damage (performance degradation), development status and cost. In addition to the system definition efforts, surveys have been made (ref. 18) to assess materials availability, manufacturing processes requirements, and energy payback of several candidate solar cell designs. This work included an assessment of SPS solar cell requirements with respect to DOE's U.S. Photovoltaic Conversion Program.

In comparing the various photovoltaic options, the single crystal silicon cell and the gallium-aluminum-arsenide cells have emerged as the most promising for SPS application. Other solar cells that have been considered include amorphous silicon, polycrystalline silicon, cadmium sulfide, copper indium selenide and polycrystalline gallium arsenide. These cell types generally have the potential advantage of lower costs; however, at present, the performance (efficiency) is low and mass production methods have not been devised.

Single crystal silicon solar cells are the only solar cell type that has been utilized for spacecraft solar power systems. Research and development has produced continuous improvements in unit mass, efficiency, structural quality and reliability; however, great improvements would still be required for effective SPS application.

Silicon cells have the advantage of more established manufacturing base, lower potential cost per cell, and abundant resource materials. Disadvantages, relative to gallium arsenide, are higher mass per unit solar cell area, greater performance degradation from thermal (temperature) and radiation effects and slightly lower efficiency. The thermal degradation effect can be minimized by designing for low cell operating temperature; i.e., without solar concentration, or by designing so that the concentrator acts as a passive radiator for cell cooling. Performance loss by radiation degradation is projected to be recovered by laser annealing the cells in place.

Gallium arsenide cells have been under investigation for a number of years but significant improvements have been made since 1972. The development of the gallium-aluminum-arsenide "window" which is epitaxially grown on the basic gallium arsenide cell has led to the improvement in cell efficiency. Since most solar radiation is absorbed within 1 μm of the GaAs cell surface, it is possible to construct a very thin cell (~5 μm) with good efficiency. Consequently, the quantity of gallium needed to make the cells is significantly reduced. The advantages of gallium arsenide cells are low mass potential, resistance to degradation by thermal and radiation effects, and good efficiency. Use of solar concentration provides self-annealing of the cells at moderate temperatures. Disadvantages are relatively high cost and less technology base than silicon. Gallium availability is also a consideration.

Table 1 provides an example comparison of gallium arsenide and silicon cells for a specific SPS configuration. Note that with solar concentration (CR=2), the gallium system has a cost advantage over the silicon system, but with CR=1, the silicon system would be either slightly less or competitive with gallium. Because of this close competition, silicon and gallium arsenide are both viable candidates for SPS application. Therefore, they are presented as options in the description of a reference system.

| CASE NO. | SOLAR CELL | CONC. RATIO | ANNEALING | AREA - $KM^2$ | | TOTAL MASS | CELL COST DATA | | COST IN MILLIONS | | | |
|---|---|---|---|---|---|---|---|---|---|---|---|---|
| | | | | CELL | PLANFORM | MILLIONS-KG | SOURCE | $\$/M^2$ | CELLS | TRANS. | OTHER | TOTAL |
| A | GaAlAs | 1 | YES | 44.31 | 46.08 | 15.81 | RI | 71 | 3146 | 632 | 213 | 3991 |
| A | GaAlAs | 1 | YES | 44.31 | 46.08 | 15.81 | ADL | 67 | 2969 | 632 | 213 | 3814 |
| B | GaAlAs | 2 | YES | 26.52 | 55.13 | 13.55 | RI | 71 | 1883 | 542 | 449 | 2874 |
| B | GaAlAs | 2 | YES | 26.52 | 55.13 | 13.55 | ADL | 67 | 1777 | 542 | 449 | 2768 |
| C | SILICON | 1 | YES | 52.33 | 54.08 | 27.06 | BAC | 35 | 1832 | 1082 | 237 | 3151 |
| C | SILICON | 1 | YES | 52.33 | 54.08 | 27.06 | RI | 47 | 2460 | 1082 | 237 | 3779 |
| C | SILICON | 1 | YES | 52.33 | 54.08 | 27.06 | ADL | 53 | 2773 | 1082 | 237 | 4092 |

ASSUMPTIONS

SOLAR CELLS

GaAlAs - 20% EFFICIENCY @ 28°C AMO

Si - 17.3% EFFICIENCY @ 25°C AMO

TOTAL MASS

INCLUDES SOLAR CELLS, REFLECTORS, PRIMARY STRUCTURE, SECONDARY STRUCTURE AND POWER DISTRIBUTION.

INCLUDES NO CONTINGENCY

SOLAR CELL SPECIFIC MASS

GaAlAs - 0.2525 $Kg/M^2$

Si - 0.42133 $Kg/M^2$

COST

SOLAR CELLS

AS SHOWN ABOVE

TRANSPORTATION

$40/Kg TO GEO

OTHER

INCLUDES REFLECTORS, PRIMARY STRUCTURE, SECONDARY STRUCTURE, AND POWER DISTRIBUTION

RI = ROCKWELL INTERNATIONAL
ADL = ARTHUR D. LITTLE
BAC = BOEING AEROSPACE COMPANY

Table 1. Solar Cell Trade-off Comparisons

Solar Brayton Cycle - Figure A-6 shows a schematic diagram of a typical solar Brayton cycle system. Solar energy is collected by a concentrating reflector and is focused into a cavity absorber. The cycle working fluid, usually an inert gas such as helium or argon, passes through the absorber where it is heated to turbine inlet temperature conditions. The hot gas then expands through a turbine which drives a compressor and generator. The generator produces useful electric power. After passing through the turbine, the gas is further cooled in a recuperator heat exchanger where residual heat then preheats the gas passing into the absorber. The working fluid receives final cooling in a cooler heat exchanger where cycle waste heat is transferred to a coolant fluid for rejection to space via a radiator system. The cooled gas then passes through the compressor where its pressure is raised to the turbine inlet pressure level. Typically, the compressor uses about two-thirds of the turbine output work.

The conversion efficiency of a Brayton cycle system ranges from 20 to 35 percent at turbine inlet temperatures in the 1700°F to 2200°F range to greater than 40 percent with turbine inlet temperature in the 2500 to 3000°F range. The higher temperatures require use of more advanced technology ceramic components whereas refractory metal alloys may be used at the lower temperature level.

There are several variations of the basic Brayton cycle including gas (working fluid) radiator systems, alternative working fluids, single versus multiple shaft systems, and dual cycle concepts using thermionics concept at the high temperature end of the cycle or a Rankine cycle at the heat rejection end of the cycle.

The MSFC in-house study (ref. 3) configured a 10 GW satellite with a concentration ratio of 2000:1, a helium working fluid, and a high temperature thermionic generating loop in combination with a Brayton cycle conversion system. The MSFC-Boeing study (ref. 5) investigated a thermionic/Brayton combined cycle system and a closed cycle Brayton system. The JSC in-house study included examination of the closed cycle Brayton concept and investigated several subsystem alternatives. Following the earlier studies, the JSC-Boeing study (ref. 7) probed deeper into many of the apparent problem areas of the closed system

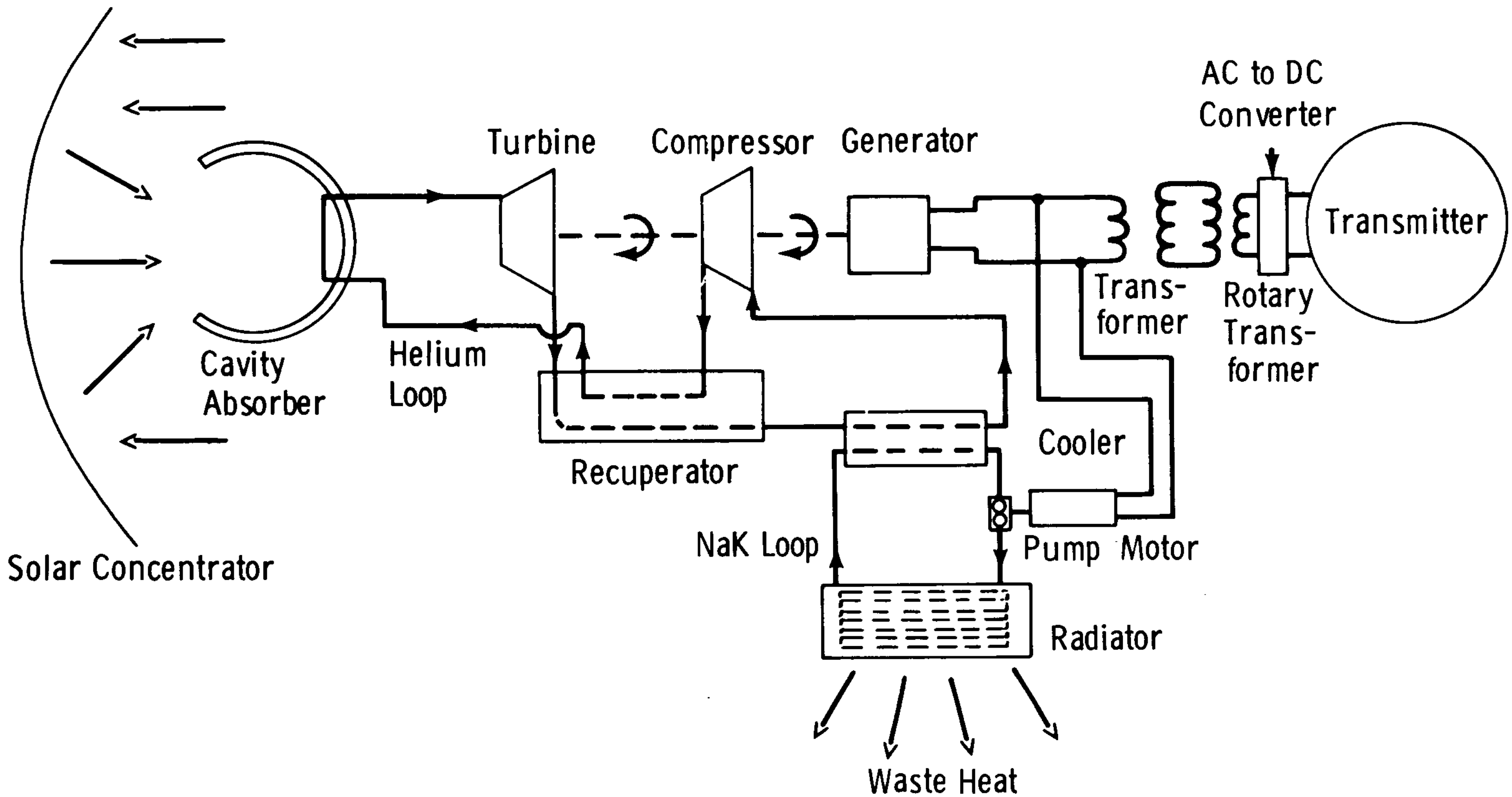


Figure A-6. Solar Brayton Cycle

Brayton cycle design. Reflector degradation was reevaluated resulting in size modifications. The configuration was altered to conform to new construction concepts and geometric improvements. These refinements and more detailed investigation of the construction techniques and materials requirements resulted in determining better cost and mass estimates in the study. This resulted in the determination that the system not only was significantly heavier than photovoltaic and Rankine cycle systems (due primarily to large radiator requirements) but was also more complex to construct. The MSFC-Rockwell concept definition study comparatively analyzed several solar thermal concepts including the closed Brayton cycle and found that, although the technology for the Brayton system was much further advanced than the others, the weight penalties made it less competitive than less developed, but higher performance cascaded Rankine systems.

Solar Rankine Cycle - Like the Brayton cycle, the Rankine cycle utilizes a solar concentrator to collect and focus energy into cavity absorbers (figure A-7); however, instead of an inert gas, a liquid working fluid such as water or potassium is passed into the absorber where it is vaporized (boiled). The hot vapor is then expanded through a turbine which drives a liquid pump (not a compressor as in the Brayton cycle) and a generator which produces electricity. After passing through the turbine the vapor is cooled (condensed to a liquid) either directly in a space radiator or indirectly by an intermediate coolant loop. The liquid then passes through the pump which raises the liquid pressure to boiler inlet conditions. As with the Brayton system, there are several variations of the basic cycle. Typical Rankine cycle conversion efficiencies are 15 to 40 percent depending upon cycle arrangement.

The JSC in-house study (ref. 2) reported on the potential of the solar Rankine cycle to SPS applications. Although the technology was not as advanced as some other thermal systems, the Rankine cycle utilizes higher heat rejection temperatures which results in lower radiator mass. Several working fluids were investigated in the JSC study, but the overall analysis was only a preliminary investigation and no cost and mass estimates were reported. Later, the JSC-Boeing study (ref. 7) developed sufficient detail for comparative analysis

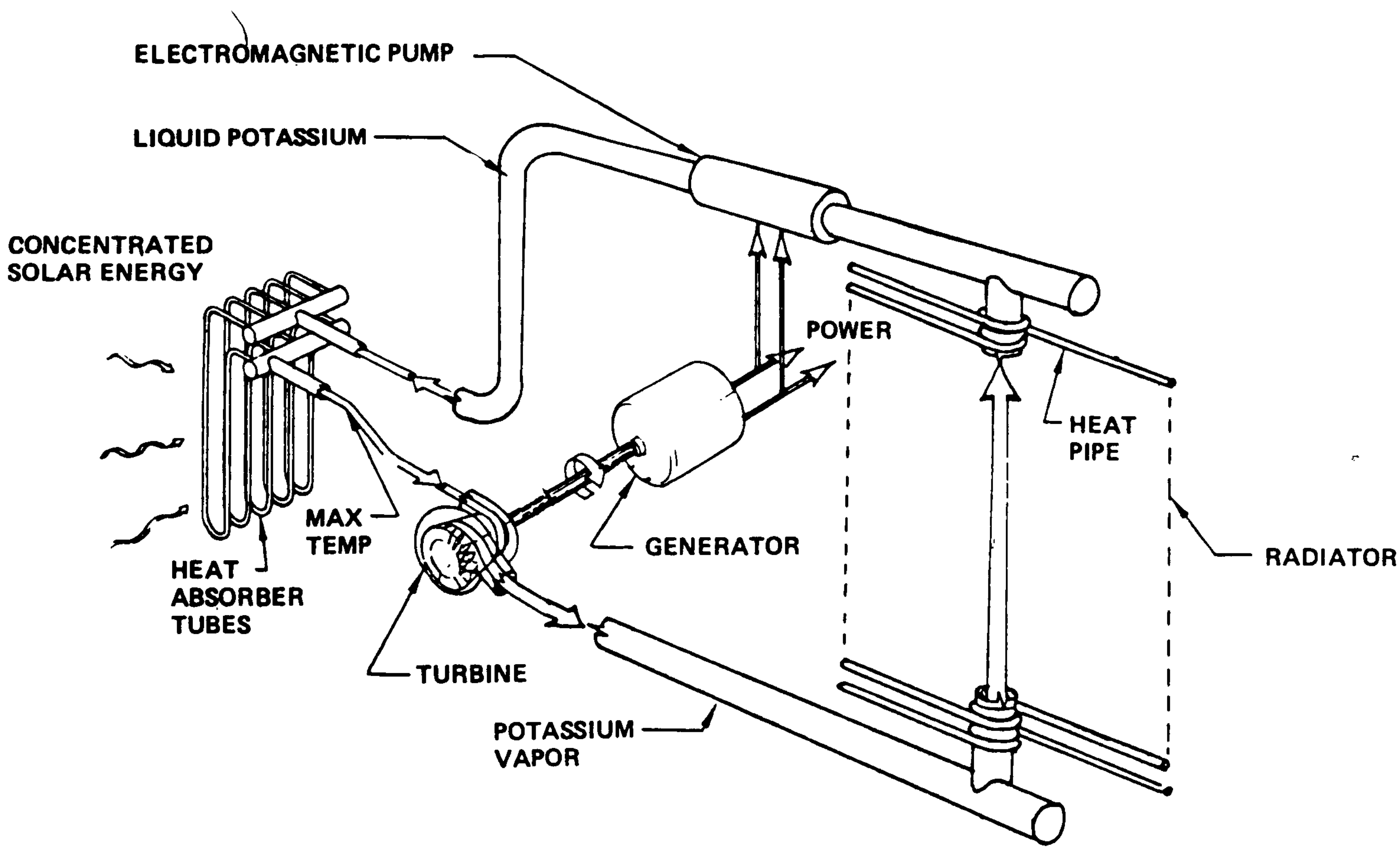


Figure A-7. Rankine Cycle Schematic

with other thermal systems and concluded that the Rankine system has a lower mass and cost potential than the Brayton cycle and other alternative thermal engines investigated. Simultaneously, the MSFC-Rockwell (ref. 11) investigations included the Rankine cycle concept and performed sufficient design definition to determine cost and mass estimates. The configuration selected in the study was a cascaded cesium working fluid/steam bottoming cycle with an open absorber. This arrangement proved to have significantly improved overall efficiency and the lowest specific weight. The report confirmed the Rankine cycle as the solar thermal system offering the potential for least cost.

Solar Thermionics - Thermionic converters provide a potential alternative to energy conversion provided by thermal engines or solar cells. These passive devices use high temperature thermal energy to produce direct current electrical energy. In some studies, the converters were analyzed in combination with other energy systems such as the thermionic/Brayton cycle and a nuclear concept requiring thermionic conversion. Both of these systems were reported in the MSFC-Boeing study (ref.5). The latter study also looked at direct and liquid cooled radiator systems using the thermionic conversion technique. Subsequent studies confined their investigations of thermionics to the singular conversion system. The general conclusion reached in these studies, as well as more recent evaluations by Boeing and Rockwell, is that the thermionic system would be at least 50 percent heavier than other thermal cycle systems. Conversion efficiencies are relatively low (about 20 percent) with peak temperature (emitter) of 3000°F and above, The thermionic system has, therefore, not been further considered in system definition studies.

Other known options have not been included in detailed evaluation for the reasons stated below:

(1) Thermoelectrics - low conversion efficiency, materials resources consumption, and heat rejection considerations.

(2) Magnetoplasmadynamics - rejected on grounds of problems in attaining the necessary working fluid temperature by solar heating.

(3) Direct Thermal Conversion by Electrostatics - Insufficient data available for this recently-proposed thermal engine.

(4) Thermophotovoltaics - rejected on consideration of overall efficiency and problems of waste heat rejection.

In conclusion, the photovoltaic options utilizing either single crystal silicon solar cells or gallium-aluminum-arsenide have evolved as options with the overall lowest cost and mass potential. A concentration ratio of one (no concentration) is preferred for silicon systems, whereas gallium arsenide designs may be more advantageous with a concentration ratio of two. Based on the analysis conducted to date, the results indicate these options would be less complex and would have lower mass than the thermal cycle options. The major disadvantages of the thermal cycle systems are fluid system containment, wear in rotating equipment, construction complexity, and relatively high mass.

It should be noted, however, that the cost advantage of photovoltaics is very sensitive to array blanket costs. To illustrate this point, figure A-8 shows a cost trade-off between silicon photovoltaics and the potassium-Rankine cycle. At the projected solar blanket cost, the silicon system has a 5 to 10 percent cost advantage.

With respect to the thermal cycle options, the recent system definition studies have indicated a preference for the Rankine cycle over the Brayton cycle. The Rankine system would use either a potassium working fluid or a cesium-steam working fluid combined cycle. This preference is not strong because it is based on small mass advantage relative to Brayton systems. Therefore, these systems are regarded as competitive at this time; however, as previously stated, the photovoltaic systems are preferred over the thermal systems.

2. Power Distribution

The purpose of the power distribution systems is to collect, regulate and control power from the power generation system (solar array sections) and transmit this power via power busses and rotary joint/slipring system to microwave generators on the transmitting antenna. This system would also include energy storage as necessary to meet power requirements during the eclipse periods.

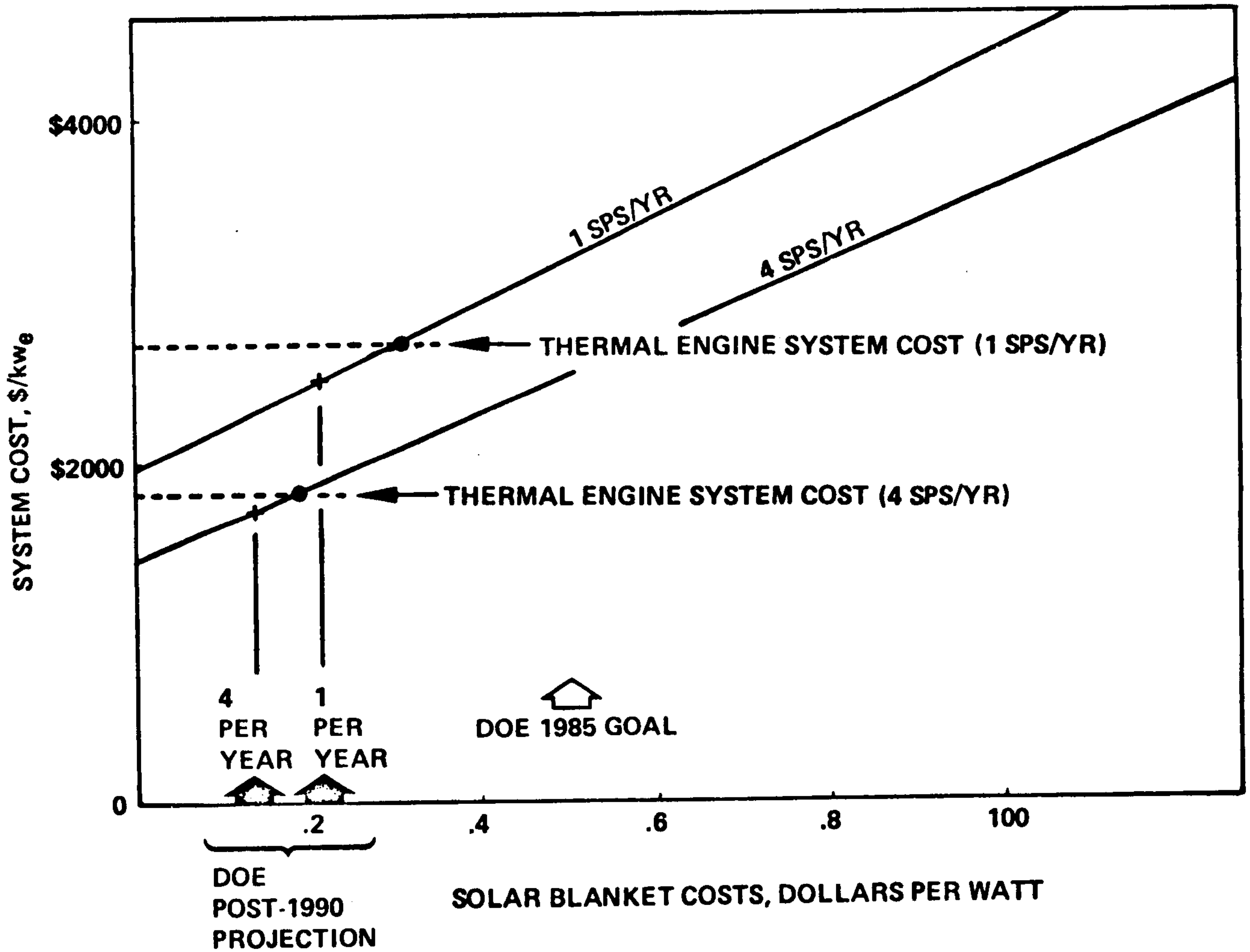


Figure A-8. Sensitivity of Photovoltaic SPS System Cost to Solar Blanket Cost

A number of trade studies on this system have been conducted as listed below:

(1) AC vs. DC Transmission - DC transmission at 40 kV is preferred based on power conductor and conditioning equipment mass considerations.

(2) Central vs. Decentralized Regulation and Control - centralized system preferred for providing regulated power to the transmiting antenna; decentralized system for solar array power control.

(3) Flat (sheet) Conductor vs. Round Cable - flat (sheet) conductor preferred based on mass considerations.

(4) Conductor Material (Copper, Aluminum or Silver) - aluminum preferred based on thermal control and mass considerations.

(5) Use of Structure for Current Return Path vs. Dedicated Conductor - dedicated conductor preferred as a less complex approach.

Even though the above preferences are indicated at this time, continued analysis and optimization may result in changes.

## C. Power Transmission, Collection, and Conversion

The SPS concept for the transfer of energy from geosynchronous orbit to earth is accomplished by means of microwave power transmission. This is basically a 3-step process which has as one of its major requirements high efficiency.

The process consists of:

1. Conversion from DC power to microwave power
2. Focusing and transmission of the microwave power to Earth
3. Collection of the microwave power on Earth and conversion to DC power.

Some of the more significant design and operational trade studies which have been made are summarized below.

Microwave System Frequency - The primary frequency in the SPS microwave system which has been the subject of the majority of the trades thus far is the power beam frequency. (Trade-offs to determine the optimum set of up-link pilot frequencies for the phase control system are still being conducted.) The requirement for high efficiency over the microwave propagation path dictates the band of microwave frequencies which are acceptable; molecular absorption and rain attenuation through the Earth's atmosphere sets an upper limit on frequency selection of not much above 3 GHz. Alternate frequencies have been considered in most of the microwave system studies to date, the most notable being 5.8 GHz. Trades have been made from many points of view such as SPS system sizing of transmit antenna and rectenna, etc., (ref. 2,10,23); propagation effects through the ionosphere (ref. 26); hardware technology projections (ref. 2,10,23), etc. Although higher frequencies offer some advantages (smaller rectenna), the frequency of 2.45 GHz offers many more. This frequency is in the middle of the ISM band (industrial, scientific, and medical) of 100 MHz, there is lower attenuation when propagating through the atmosphere, and the projections for microwave equipment technologies are more promising.

Microwave System Efficiencies - One of the earliest demonstrations that meaningful amounts of power could be transmitted via microwaves was done at Raytheon in May of 1963 (ref. 20). The collection efficiency was 87 percent; however, the RF-DC conversion efficiency was only about 50 percent. Overall efficiency was only 16 percent. As the experiments continued, more attention was devoted to increasing the efficiency of collection and conversion. The concept of a "rectenna" evolved (receiving antenna and rectifier) which exhibited low directionality for the collecting antenna, and high RF-to-DC conversion efficiencies. Early application of the rectenna concept to the SPS resulted in the addition of filters to attenuate the radiation of harmonics and to store energy for rectification. The rectifier was changed from a full-wave bridge using point-contact diodes to a single GaAs Schottky-barrier solid-state diode in a half-wave rectifier configuration. Conversion efficiencies of 80 percent were obtained (ref. 21).

In 1975, the rectenna portion of the microwave system was tested at the JPL Goldstone facility (ref. 22). Microwave power was transmitted from an 85-foot antenna to an array of 270 rectenna dipole-diode elements over a distance of 1.6 km. Of the microwave power impinging upon the rectenna, over 82 percent was converted to DC power. A total of 30 kW was collected and dissipated into a lamp and resistive load. Since that time Raytheon has investigated mechanical and electronic improvements to the rectenna element which has resulted in demonstrated conversion efficiencies of 85 percent at certain power density levels (ref. 24). Current projections, assuming technology advancements, are for conversion efficiencies of approximately 90 percent in the time-frame needed for SPS.

Coupled with this experimental concentration on improving the collection and conversion efficiency at the receiving end, a concept evaluation and technology assessment was being conducted on the transmit antenna. Major contributors toward transmit efficiency in the microwave system are:

1. Microwave power amplifiers (DC to RF converters)
2. Beam focusing and pointing (phase control)

3. $I^2R$ losses in antenna
4. Mechanical tolerances (pointing, subarray/power module misalignment, waveguide/slot tolerances.

These are, of course, dependent on many factors, such as frequency, subarray sizes, phase control concepts, etc. As the microwave system configuration developed and converged into the present concept, system efficiencies became better defined. Some of the differences in estimated efficiencies as they evolved are shown in Figure A-9. The end-to-end efficiency for the current microwave reference system is 61 percent. As an aid to understanding the terminology used in the microwave system, please refer to Figure A-10.

Microwave System Sizing - Sizing and power transfer in the microwave system is dependent on three factors:

1. System end-to-end efficiencies
2. DC power output from rectenna
3. Transmit antenna size.

For a minimum cost of power at the grid, the output of the transmit antenna should be as large as possible. However, this output is constrained by thermal limits on the antenna and power density limits in the ionosphere. Thermal dissipation limits set a heat density value on the transmit antenna of approximately 21 $kW/m^2$. For the operating frequency of 2.45 GHz, studies have indicated that the power density of the SPS beam should not exceed 23 $mW/cm^2$. If the power density exceeds this value, it is postulated that nonlinear interactions may occur between the power beam and the ionosphere. With these two limits, and a desired value of power output at the rectenna, transmit antenna size and rectenna size can be traded. The Raytheon study in 1975 (ref. 25) initially studied overall microwave system sizes. Some of the parameters established were:

1. 5 GW DC output power at rectenna
2. Rectenna size--approximately 10 km diameter (at the equator)
3. Transmit antenna size, 1 km diameter
4. Aperture illumination - 5 step truncated Gaussian with 5 to 10 dB taper.

| | JSC Study | BAC Study | Rock-well Study | Current Reference System |
|---|---|---|---|---|
| DC-RF Conversion | .87 | .85 | .87 | 0.85 |
| Transmit Antenna, $I^2R$ | .98 | .985 | .96* | 0.985 |
| Transmit Antenna Mech-anical Tolerances | * | * | * | 0.98 |
| Average Atmosphere | 0.98 | 0.98 | 0.98 | 0.98 |
| Rectenna Energy Collection | .88* | .85* | .88 | 0.88 |
| RF-DC Conversion | 0.90 | 0.89 | .90 | 0.89 |
| DC Power Interface | 0.99 | 0.97 | .99 | 0.97 |
| 5 GW | | | | |
| *Combined Efficiencies | | | | |
| Overall Efficiency | .655 | .602 | .642 | .611 |

Figure A-9. Microwave System Estimated Efficiencies

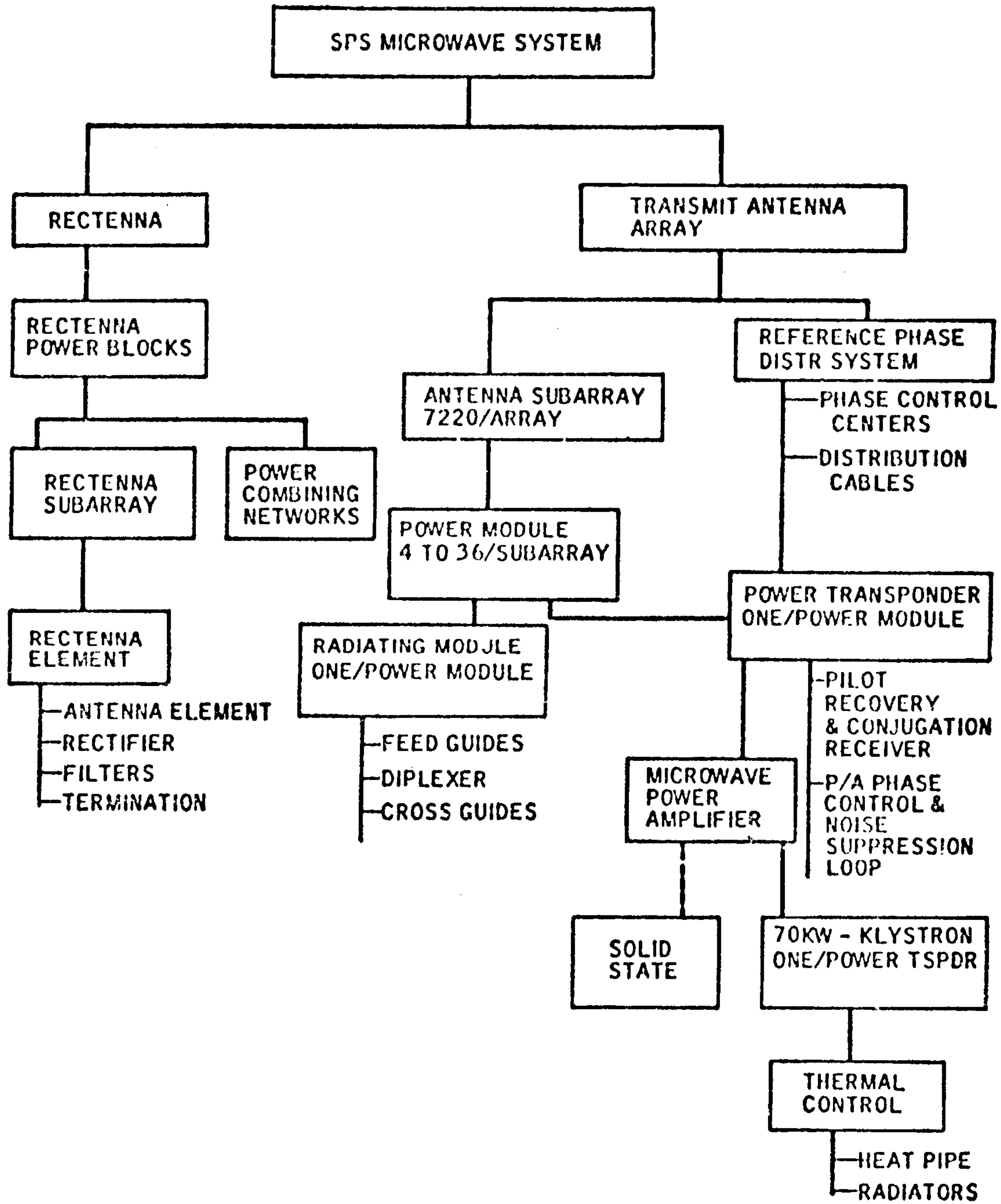


Figure A-10. SPS Microwave System Terminology

The JSC study in August 1976 (ref. 2) expanded on the previous studies, and defined a 10-step truncated Gaussian, 10 dB taper which approximated a continuous taper and provided for side-lobe suppression. Other developments and trades regarding configurations and subsystems are discussed in the following sections.

Transmit Antenna Configuration - The early in-depth study of the SPS microwave system conducted by Raytheon in 1975 (ref. 23) took the system sizing as discussed above and developed a configuration for the transmit antenna with the following characteristics:

The transmit array consisted of 18M X 18M subarrays, with a structure fabricated out of graphite polyimide, based on a 1 percent beam power loss and material coefficients of expansion, and sized to be effectively packed into the Shuttle cargo bay. Because of questions of outgassing of the graphite polyimide, an aluminum configuration was suggested with independent 5M segments within the 18M X 18M subarray. Motor-driven screwjacks were used on each subarray to adjust for subarray deflections and tilt during operation.

The JSC study (ref. 2) investigated 4M X 4M and 10M X 10M subarrays in order to widen the beamwidth and eliminate the requirement for screwjacks. It was determined that the effects of coefficients of expansion on surface tolerances would allow a 10M X 10M subarray, and the larger size (10M X 10M) would reduce the complexity of the phase control problem.

Raytheon also performed a trade-off study of transmit antenna types (including space-fed and cylindrical arrays) and on subarray types, including helical radiators, parabolic dishes, pyramidal horns, and slotted waveguides. The latter was chosen because of its potential for high efficiency and the efficient means of distributing the RF power from the power amplifiers. Thus, as a result of the Raytheon and JSC studies (ref. 23,2) the configuration evolved into:

1. 10M X 10M subarrays (7850 total)
2. Subarray structure - graphite composite

3. Slotted waveguide
4. Waveguide material - aluminum
5. Phase conjugation - to subarray level
6. No mechanical alignment of subarrays.

The subsequent Boeing studies (ref. 5,7,8,9) as part of the overall, indepth trade-offs on the SPS, arrived at basically the same configuration except for the waveguide material. Doubt was expressed that mechanical tolerances such as slot sizes, subarray tilt, waveguide dimensions, etc., could be held tight enough using aluminum waveguide.

As a result of that factor and the weight trade-off, graphite composites (for mechanical stability) together with thin-skin depth aluminum on the waveguide walls (for RF conductivity) was investigated and recommended. Kovar waveguides were also investigated as an alternative.

The MSFC and Rockwell studies (ref. 3,4,11) resulted in basically the same microwave system configuration, with some differences in antenna structure and configuration. The basic building block was a 30M X 30M mechanical module, with approximately 10M X 10M subarrays as an integral part. The radiating portion of the subarrays was defined as a resonant cavity radiator to reduce wall weight of the waveguides.

The reference configuration of the transmit antenna is now as listed in the fourth paragraph of this section, with the following alternate possibilities. Phase conjugation to the power module level may be desirable for more precise control and better focusing. This resulted from the LinCom effort (ref. 27) on the phase control system and will be discussed more later in this section. It may be desirable to go to resonant cavity radiators if efficiency and resonant wave stability show an effective trade-off with weight. Figure A-11 is a pictorial summary showing the transmitter design concept as evolved for the reference configuration.

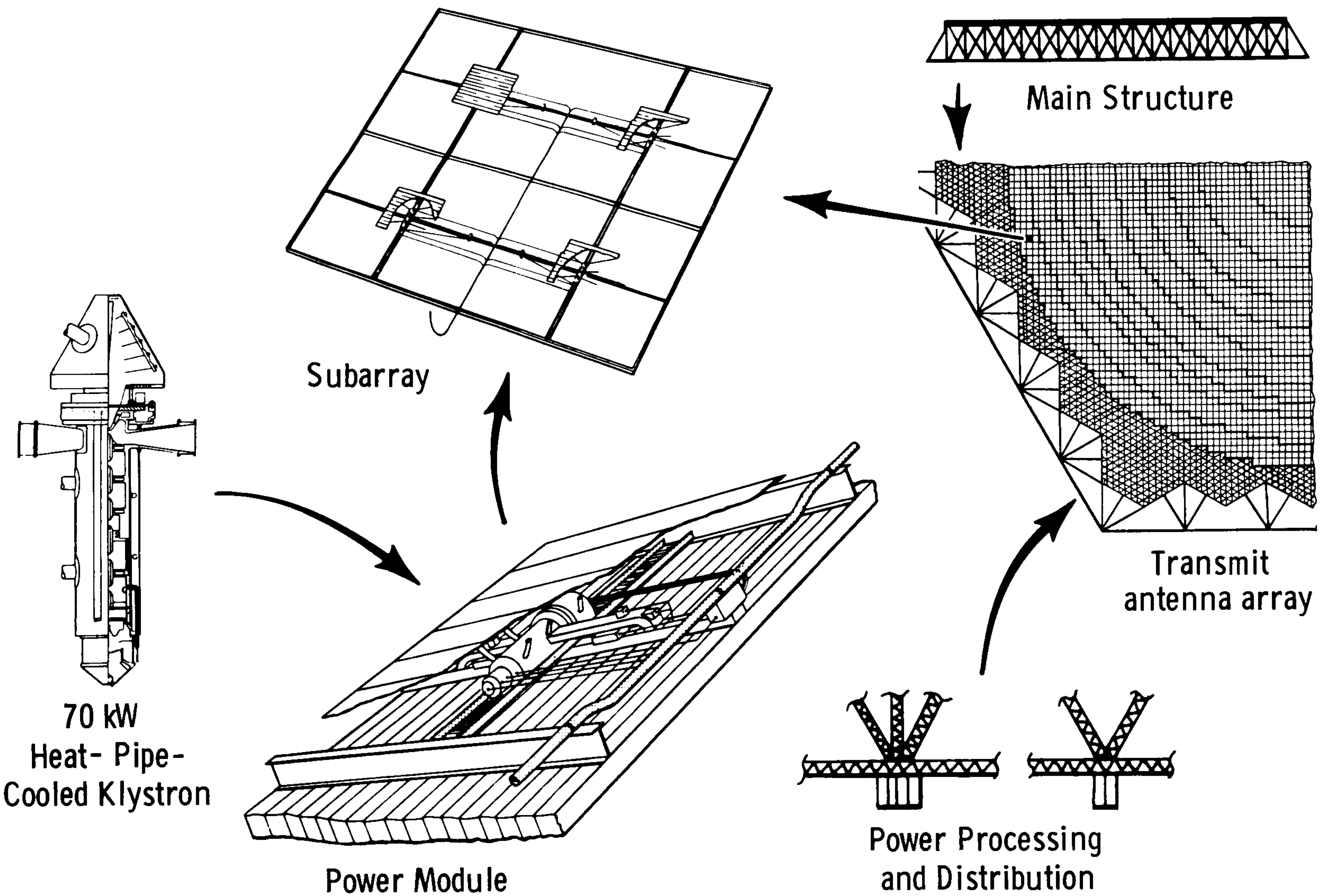


Figure A-11. Microwave Power Transmitter Design Concept

Microwave Power Amplifiers - The in-depth study performed by Raytheon in 1975 (ref. 23) on the microwave system focused on investigation of the amplitron (crossed field amplifier) and the klystron (linear beam amplifier). The amplitron was characterized by high efficiency and low gain, while the klystron was characterized by high gain, low noise levels, and moderately high efficiency. Trade-offs were performed on amplitron versus klystron tube parameters, as well as on integration into the microwave system. The study concluded that either 5 KW amplitrons in series, or 50 KW klystrons in parallel could be used. The MSFC study, concluded in November 1976 (ref. 3) selected the amplitron for initial study because of the possible efficiency and lifetime advantage, and so that electrical operation and mechanical integration into the overall system could be analyzed.

The JSC studies concluding in August 1976, investigated both the amplitron and the klystron. Traveling wave tubes and solid-state amplifiers were also investigated. It was concluded at that time that both the amplitron and the klystron exhibited the best potential for use on the SPS, with the edge being given to the klystron because of system implementation considerations. The major advantages of the klystron were: (a) much higher power per tube, thus simplifying initial assembly and installation operations, and ameliorating the maintainability requirements; (b) higher operating voltage, thus reducing power distribution system weights; (c) much lower phase control drive power; and (d) lower RF noise characteristics.

The Boeing studies (ref. 5,7,8,9) chose the klystron as the amplifier to investigate further, and performed an in-depth, comprehensive study of klystron configurations, integration into the microwave system, maintenance scenarios, manufacturability, cost, weight, etc. The study demonstrated that a klystron can be integrated into an overall SPS and it does have certain advantages. A comparison of features of the amplitron and klystron designs is shown in Table II.

| ITEM | AMPLITRON | | KLYSTRON | |
|---|---|---|---|---|
| POWER | 5 KW with $10^6$ TUBES | | 50-250 KW WITH $<10^5$ TUBES | * |
| EFFICIENCY | 85-90% | * | 80-85% | |
| CATHODE | COLD PURE METAL (AVAIL LIFE DATA – 10,000 HR) | | THERMIONIC OXIDE/MATRIX (AVAIL LIVE DATA ~ 50,000 HRS) | |
| GAIN | 7 db | | 40 db | |
| VOLTAGE | 20 Kv | * | 40-65 Kv | |
| SPURIOUS SIGNAL AM (TYP.) | -100 db/KHz 10 MHz FROM CARRIER | | -125 db/KHz 5 KHz AWAY FROM CARRIER | * |
| TUBE MTBF | COMPARABLE | | COMPARABLE PERHAPS SOMEWHAT LESS | |
| THERMAL DISSIPATION | CONCENTRATED INTERACTION REGION | | DISTRIBUTED, COLLECTOR CAN RUN 500-700°C, REQUIRE HEAT PIPES | * |
| PHASE SHIFT TUBE–TUBE TRACKING | HIGH POWER PHASE SHIFTERS 2° PER % CHANGE IN BEAM CURRENT ±15° PHASE TRACKING | | LOW POWER PHASE SHIFTERS 10°-30° PER % VOLTAGE CHANGE ±20° PHASE TRACKING | * |
| SPECIFIC COST | ~$20/Kw | | $40 TO $20/Kw FOR ABOVE POWER RANGE | |
| SPECIFIC WEIGHT | 0.4 kg/Kw | | 0.8 TO 0.4 kg/Kw FOR ABOVE POWER RANGE | |
| ARRAY INTERFACE | SERIES OPERATION NO FEED WAVEGUIDES | | POWER ADJUSTS TO VOLTAGE CHANGES CORPORATE FEED | |
| TURN-ON | DIRECT FROM BUS BAR ? | | MAY REQUIRE LOGIC SEQUENCE | |
| X-RAY LEVEL (RANGE FOR 5 mR/YEAR) | SAFE @ 1 METER | * | SAFE @ 1-1.8 km FOR 70 kw DESIGN | |

*SIGNIFICANT ADVANTAGE

Table II. Some Features of Amplitron and Klystron Design for SPS

Boeing also surveyed current developments in solid-state amplifiers, and concluded they should definitely be considered, but were not emphasized in the studies. Devices surveyed included bipolar silicon, electron beam devices, GaAs IMPATTS, and silicon FET's. In approximately the same time frame, JSC also independently performed a survey of solid-state devices. Although no particular device surfaced as being an outstanding candidate at that time, subsequent research indicated that GaAs FET's showed significant potential.

Rockwell studies (ref. 11) investigated amplitrons, klystrons, magnetrons, and solid-state power amplifiers. For purposes of performing trade studies on SPS integration issues, the klystron was also chosen. Similarities were evident between the Boeing study results and the Rockwell study results. Basic requirements for the klystron were similar, with some differences evident in implementation into the transmit antenna.

The Boeing study developed a concept for a 70 KW klystron, integrated into a slotted waveguide power module, with 4 to 36 power modules per 10M X 10M subarray. Cooling is accomplished with 300°C body and 500°C collector heat pipes with passive radiators on the backside of each subarray.

The Rockwell study developed a concept for a 50 KW klystron, integrated into a resonant cavity radiator with 6 to 50 klystrons per 10M X 10M subarray. Cooling is accomplished with body heat pipes dissipating heat on the front side of each subarray. Blockage of RF radiating slots is estimated to be approximately 3 percent; however, this was required because of the thermal environment on the backside of the transmit antenna.

Continuing investigations into solid-state power amplifiers provide an increasingly attractive alternative to the power tube amplifiers, especially in the area of low noise and increased reliability. A concentrated technology advancement program is needed for solid-state, coupled with a comprehensive systems integration study.

Phase Control - The phase control system for the SPS must provide high accuracy beam focusing and pointing in the presence of a nonhomogeneous, time-varying ionosphere, thermal distortion of the transmit antenna array and subarrays, and phase variations in the phase reference distribution system, power amplifiers, conjugators, and other electronic components in the system. The subject has been investigated by Raytheon, JPL, Rockwell, Boeing, LinCom, MSFC and JSC. Raytheon studies in 1975 investigated both the command and adaptive (retrodirective) approaches. The command approach relies on (a) phase estimation measurements made over a matrix of sensors covering the received power beam, or (b) a "bit wiggle" examination of each transmit subarray performance by commanding a distinctive phase modulation on the output of each subarray. The retrodirective approach uses a reference pilot beam transmitted from the rectenna to each subarray or power module on the transmit array, where precise phase measurements are made and conjugation of the pilot signal occurs.

To varying degrees, each organization mentioned studied the phase control problem and documented various concepts. In an effort to study the problem on a system level, end-to-end basis JSC awarded a contract to the LinCom Corporation in April 1977. Initial activity consisted of system analysis to evaluate potential techniques for accomplishing phase distribution and beam steering for such large arrays. Basic concepts previously discussed, only superficially, were compared and evaluated on an overall system engineering basis. The techniques considered for beam steering included (a) phase conjugation and open loop phase shift control, (b) ground network monitoring and uplink commanded phase adjustments. The techniques considered for phase distribution included (a) mutually coupled oscillators and (b) electronically compensated distribution system.

This LinCom activity has resulted in a phase control concept which partitions the system into three levels and which has been incorporated into the microwave reference system. The first level consists of a reference phase distribution system or tree which electronically compensates for distribution path length variations to maintain a constant phase reference at each radiating element. The second level consists of a phase conjugation system which receives a uniquely-designed pilot signal allowing reconstruction of a phantom carrier at the same frequency as the power beam, thus avoiding problems of squint due to frequency offsets between the pilot and power beam signals. The pilot signal design also provides for anti-jamming (security) of the pilot receivers, provides additional processing for isolation of the pilot receiver from the power signal, and allows for multiaccess operation (i.e., more than one SPS can be intercepted by the same pilot signal without interference). The third level of control is associated with maintaining an equal and constant phase shift through the microwave power amplifier devices. In addition, this concept of phase locking around the power amplifiers will provide added suppression of transmitted noise and reduce the SPS RFI (radio frequency interference) potential.

As part of the preliminary analysis and system definition activity, an SPS microwave system computer model has been under development which will provide a flexible system engineering tool for evaluation of SPS microwave system performance as parameters which uniquely affect the phase control system are varied.

Efforts thus far have concentrated on modeling and performance trades associated with the reference phase distribution tree. Tentative results show that beam pointing is most sensitive to errors in the first few branches of the distribution tree, while errors in the later branches reduce main beam gain and spread the radiation pattern. These results will be used to continue definition of the reference phase control system.

Rectenna Configuration - As mentioned in Section 3 on microwave system efficiencies, some of the earliest efforts on the SPS were directed toward studies and experiments to improve the power collection and conversion efficiencies. Raytheon pioneered these early efforts and essentially verified the rectenna concept (ref. 20,23,24). The initial studies reviewed several options for the antenna design at the receiving site, including contiguous horns, contiguous reflectors, phased array of small aperture elements with common microwave load, and an array of small aperture elements with independent microwave loads (rectenna concept). A comparison of these approaches is shown in Figure A-12.

It was quickly decided that an array of solid-state diode rectifier elements, each combined with an individual dipole antenna and suitable harmonic filter, was the only option combining both high efficiency and low cost. The combination, receiving antenna and rectifier, came to be known as the rectenna. A simplified schematic of a rectenna element is shown in Figure A-13.

RF-to-DC conversion efficiency has steadily increased from approximately 50 percent in May 1963 (ref. 20) to 82 percent with the JPL Goldstone tests (ref. 22) to 85 percent as a result of Raytheon's investigations into electronic and mechanical improvements in 1977 (ref. 24).

Concepts other than the Raytheon developed concept have been investigated. Renssalaer Polytechnic Institute (RPI) has been investigating other types of receiving elements which have the potential of reducing mass manufacturing costs, as well as reducing the number of rectifying diodes, and in some cases, the number of receiving antenna elements. In addition to a continuing study of the reference system configuration, printed circuit dipoles, printed circuit yagis and conventional construction yagis have been investigated. The most promising to date is the printed circuit yagi which offers both the capability of increased gain and thus fewer elements, as well as a potential for reducing mass manufacturing costs. In addition to this effort RPI has performed an analysis of the sensitivities of series parallel combining the DC outputs from the rectenna elements.

Alternate rectenna concepts were investigated by both Rockwell and Boeing. Rockwell's approach concentrated on stripline and bowtie dipole rectifiers. Analysis indicated that cost and high RF attenuation should be traded against reduced number of elements. The Boeing approach concentrated on (a) increasing the dipole spacing to reduce the total number required; (b) reducing structural cost by trading RF losses versus flat rectenna layout; and (c) increasing the antenna gain (reducing the number of diodes) with a

| Antenna Requirements | Array of Contiguous Horns | Array of Contiguous Reflectors and Feed Horns | Phased Array of Small Elements With Common MW Load | Array of Small Elements with Independent MW Loads (Rectenna) |
|---|---|---|---|---|
| Appropriate power handling capability | yes | yes | yes | yes |
| High reliability | yes | yes | yes | yes |
| Relatively nondirective aperture | no | no | no | yes |
| High absorption efficiency | <70% | <70% | ≈100% | ≈100% |
| Passive radiation of waste heat | no | no | no | yes |
| Low radio frequency interference | yes | yes | yes | yes |
| Capable of large aperture sizes | yes | yes | yes | yes |
| Low mechanical tolerance requirements | no | no | no | yes |
| Low cost | no | no | no | yes |

Figure A-12. Comparison of Antenna Approaches for Reception Of Space-To-Earth Power Transmissions

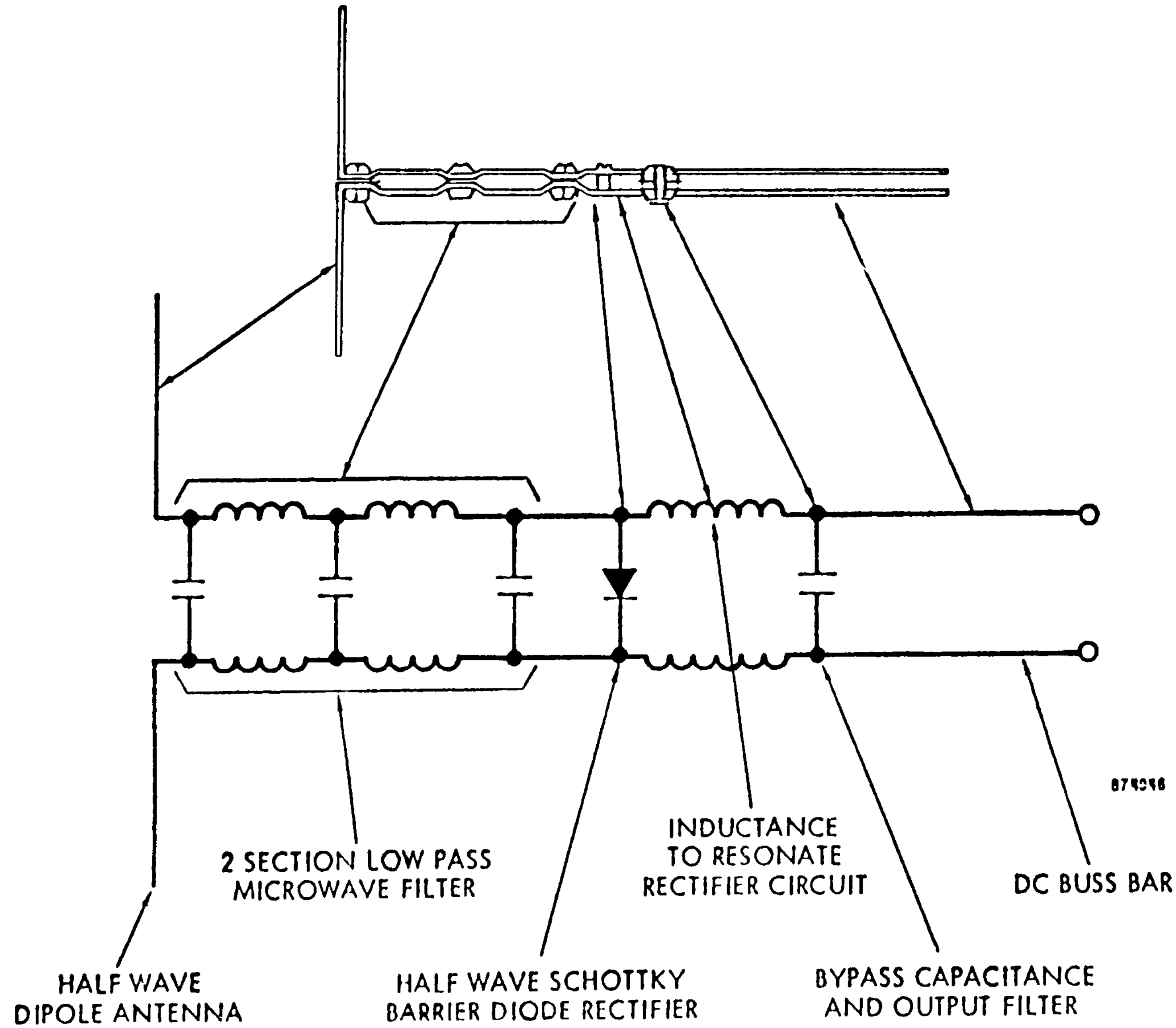


Figure A-13. Simplified Electrical Schematic for the Rectenna Element novel "hogline" antenna concept. The "hogline" combines the characteristics of the hoghorn (horn parabola) and the line-fed cylindrical horn. See Figure A-14 for pictorial concept.

It is recognized by all that additional studies are required to obtain the desirable reduction in the number of rectenna elements. Possibly some combination of the approaches outlined above, based on incoming RF power density levels which are higher in the center and lower at the edge will be shown to be more effective. The other area which requires additional effort is the manufacturing methods area, which has the potential of greatly reducing the cost of each rectenna.

Perhaps the greatest cost reduction will result from developing a novel, low-cost structure and construction technique. The basic area of the rectenna is 78.54 $km^2$ at the equator. This area in itself is sufficient to require a thorough study program to develop methods of lowering the structural and construction costs. In addition, at higher latitudes, the rectenna ground area will increase as much as 35 $km^2$, or a factor of 50 percent. (Even though the rectenna is still only intercepting the circular power beam, since the beam arrives at the Earth at greater angles at the higher latitudes, the ground footprint is changed from a circle to an ellipse.)

The rectenna configuration, although in many respects has had more investigations and experiments than other areas of the SPS, offers the potential for greater change in both electronic and mechanical configurations, and thus greater cost reductions.

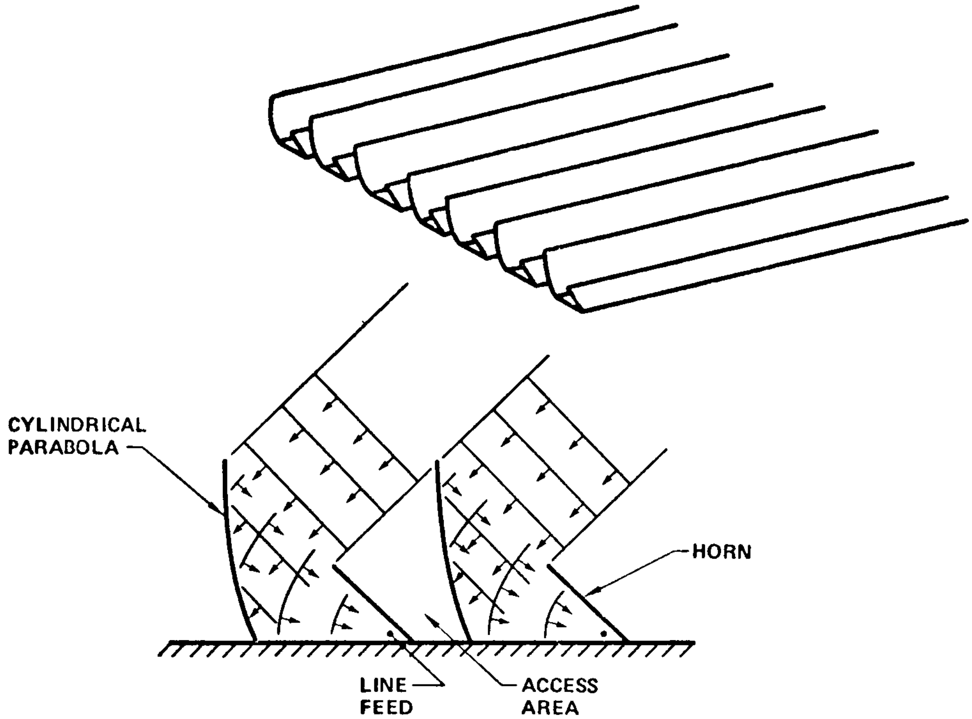


Figure A-14. Hogline Rectenna Concept

D. Structures and Materials

1. Satellite

General Characteristics - A major advantage of the SPS concept for energy is the minimal structural requirements for a very large satellite. Although this has been recognized from the onset (ref. 1), it is not always obvious in conceptual portrayals of the system where the structure may appear as a prominent feature. Studies to date indicate that the entire structural mass is generally less than ten percent and very likely on the order of five percent of the total system mass. The reason is the extremely low load environment of orbiting systems, particularly in geosynchronous orbit. This characteristic is somewhat alien to terrestrial engineering experience where structures can dominate mass and energy investment requirements.

In light of the rather benign load environment, the prime structural function is one of providing adequate stiffness for attitude control and pointing. Feasibility assessments and system studies have focused on passive structures which meet overall system requirements as a result of an underlying philosophy that adequate, simple approaches will be cost effective. This approach is seemingly achievable, even for the stringent dimensional control tolerances of the MPTS (ref. 28). A possible exception is the structural joint between the MPTS and array which might best achieve dynamic isolation through a "smart" structure.

The basic features of a representative SPS structure is one of minimum gauge material operating under low stress, tiered into a truss element of rather large dimensions and sized on the basis of an adequate margin for elastic buckling. The structural design and configuration should reflect the requirements of construction, system operation and the environment. Structural design approaches are evolving with ideas generated as a result of an improving understanding of the relatively novel requirements of the SPS.

Loads - Earth orbit is fundamentally a balance of the body forces associated with gravitational attraction (which is inversely proportional to the square of the distance from the center of the earth) and centrifugal acceleration (which is proportional to the distance from the center of the earth). The finite size of the SPS, therefore, gives rise to a distribution of body forces which, depending on the geometry and orientation, characteristically represents the largest operational applied forces and moments. For a rectangular, 5 GW ground output configuration in the worst orientation, control forces on the order of 300 N at the corners of the array would enable attitude control. The solar radiation pressure of about $5 \times 10^{-6} N/m^2$ acts on illuminated surfaces as a function of the surface solar reflectance and orientation. The greatest influence of this force is a potential daily and six-month periodic perturbation of the orbit. There is also an antenna recoil from the microwave power transmission of about 25 N. Solar and lunar gravity and earth eccentricities give rise to potential orbit perturbation but insignificant structural loads. There is no atmospheric drag at geosynchronous orbit. However, in low earth orbit (~500 Km) this pressure ($\sim 10^{-4} N/m^2$) can give rise to a force which is significant to orbital decay.

Operational system induced loads on the SPS structure must be considered, although they are quite dependent on configuration and system design. Current interaction forces are generally small, although their greatest influence is at the joint where the largest currents and least separation distance between conductors can occur. Depending on the configuration and system operation, centrifugal acceleration about the center of mass can also contribute to structural loading. The applied forces and moments for attitude control and MPTS pointing are significant inputs to the structural loading as discussed above.

Structural loads associated with maintenance, construction, transportation, handling and all relative aspects of the SPS activities must be considered in the structural design. Any governing loads other than operational must, however, be weighed against the impact to the system and, ultimately, to the cost of delivering electricity.

Environment - The normal environmental concerns of terrestrial structures (e.g., wind loading, oxidation and moisture effects, soil mechanics, etc.) are not encountered in earth orbit. However, there are environmental factors in earth orbit which must be considered: heat transfer, vacuum, particulate and ultraviolet radiation and tenuous plasma interactions. Heat transfer is essentially limited to thermal radiation, since conduction and convection effects are generally non-existent.

In normal operation, the MPTS is most affected by the thermal environment due to the waste heat generated and due to the daily cycle of orientation relative to the incident solar flux. Since the waste heat must ultimately be radiated away to space, the characteristic operating temperature levels of a tapered microwave emission profile can range from 550°K at the center to ~300°K at the edge. The centerline temperature imposes a limit to the local power emission and, therefore, the extent of emission tapering. Temperature levels can limit systems designs, material selections and lifetime characteristics. An important aspect to structural design is the distribution of temperatures and the time variations brought about by changes in orientation relative to the sun or shadowing effects (local or system-wide via occultation). Structural temperature levels in space are greatly affected by surface properties, overall geometric configurations and orientation relative to the sun. Temperature differences can give rise to significant local structural distortions, degraded structural performance and overall configuration distortion. These effects are influenced by structural material, structural design and overall configuration. They can be particularly significant to the flatness of the MPTS transmission surface and the dynamic behavior of the entire system.

To illustrate the magnitude of thermal environments, temperature differences across simple structural members can be on the order of 50°K (sun-side to space-side), temperature differences between structural elements can easily be greater than 100°K (due to orientation relative to the sun), and the temperature changes due to an occultation are nominally 200°K and can be 400°K. To accommodate this thermal environment, the structural material must be insensitive to temperature gradients and transients (low coefficient of thermal expansion, $\sim 2 \times 10^{-7}/°K$), or the structure must be active, or the structural design and configuration must be insensitive to thermal effects (environment and/or distortion). The latter is difficult to achieve without compromising other structural requirements.

The significance of the other environmental effects, vacuum, particulate and ultraviolet radiation and plasma interaction, is difficult to assess due to our limited experience with exposure to this environment. The vacuum environment mainly affects the loss of volatile ingredients and surface deposition of effluents. Prime concern with particulate and ultraviolet radiation and plasma interaction is the stability of surface properties such as solar absorptance and infrared emissivity. It is possible that structural properties may be affected particularly for minimum gauge materials. There are spacecraft which have maintained operational performance in this environment for a number of years and there are spacecraft which have suffered degradations of performance which can be correlated to these environmental effects.

System Dynamics - The low structural mass fraction of SPS concepts to date, the stringent pointing and flatness requirements of the MPTS, cyclic disturbances (such as gravity gradient and the configuration kinematics) and the seasonal occultations dictate consideration of the SPS system dynamics and the associated configuration requirements such as structural stiffness. For the array, the most straightforward approach to achieving dynamic stability with a passive structure is to have the natural frequency of the solar blankets be greater than that of the overall array which must in turn be greater than the control frequency which is in turn greater than the disturbance frequency (gravity gradient $\sim 2 \times 10^{-5}$ HZ). The array natural frequency for a given size array and a given structural material is established by the geometry of the structure (e.g., depth), while the solar blanket natural frequency is controlled by the tension level ( $\sim 4$ N/m). This requirement of passive dynamic stability is the source of design structural compression loads (nominally $\sim 10^3$ N). If the array structure material has a high coefficient of thermal expansion (such as aluminum), the dynamic response of the SPS system to occultation would set the stiffness requirements and many of the design loads.

The stiffness requirements for the MPTS are dictated by its pointing requirements ($\sim$arc minute) and a separation of its natural frequency from that of the array. The reference system meets both of these requirements with a frequency margin of more than an order of magnitude.

Materials - Early SPS concepts employed aluminum as an efficient structural material with a wealth of aerospace experience. As the thermal/structural and thermal/structural/dynamic interactions became apparent, however, the desirability of a structural material which was insensitive to the thermal environment also became apparent. Since this insensitivity can be readily obtained by the use of graphite composites (more than two orders of magnitude lower coefficient of thermal expansion than aluminum), this material has been considered as the prime candidate for an SPS structural material. The graphite composite materials have a higher Youngs modulus-to-density ratio than aluminum; however, its raw material costs are an order of magnitude higher than aluminum. The trend of graphite composite material costs is downward due to an expanding market; however, for the raw material cost to approach that of aluminum would require a major market acceptance such as the replacement of steel in the automobile. Energy investment requirements for the production of graphite composites are on the order of one-half to one-quarter that of an equal mass of aluminum.

Raw material costs are only one facet of the structural system costs. The ease by which a material can satisfy overall system requirements or conversely restrict system performance could have a much greater influence on the final cost of electrical energy. For example, the Reference System material is a thermophastic resin which provides ease of forming. It should be emphasized, however, that this is a preliminary selection based on the current level of understanding of the structural material requirements.

Development Features - Our lack of experience with a space structure such as required for an SPS was pointed out in the beginning of this section. There are other unique features which should also be mentioned.

First, there is no known way of testing a full-scale SPS structure, as it is currently envisioned, on the ground. The structural requirement is one of stiffness which requires a zero gravity environment to achieve experimental verification of structural performance. Even component testing would be quite limited since some of the structural concepts would not support their own terrestrial weight. This implies a design predicted on analysis of the performance. A logical way to achieve confidence in this analysis capability is through scale model similitude testing and component testing. If the analysis predicts the data on a scaled system test, confidence would be obtained in the prediction of full-scale system performance.

Second, the design and performance of the SPS structural system is closely coupled to the design and performance of the attitude control and pointing systems. Major load path characteristics and dynamic inputs to the structure depend on the control system design and operation.

Third, the thermal and structural analyses of the SPS can only be decoupled if either a low coefficient of thermal expansion structural material is used or an active structure is employed.

Fourth, the construction of the SPS structure and the assembly of all the systems is a major consideration in the structural design and in the development of the overall system configuration.

Structural Configurations - An initial consideration of a structural configuration for the photovoltaic SPS array used the relatively massive power distribution system as a prime structure "mast", with a solar cell support truss made up of minimum gauge aluminum "venetian blinds" (ref. 11a). This approach afforded adequate structure for the minimal loads and afforded an elastic buckling mechanism to accommodate local off-design loads. An initial MPTS structural configuration (ref. 23) employed a two-tier truss structure. The prime structure afforded overall stiffness, while the secondary structure accommodated the radiating subarray elements. The significance of thermal distortion to achievable flatness was recognized (ref. 23) along with the attractive features of a low coefficient of thermal expansion material such as a graphite composite. Studies of thermal engine concepts led to different structural concepts due to the large concentrated masses in modular units (ref. 11b).

Later studies of photovoltaic systems (ref. 2) achieved symmetry via a dual system of MPTS. This eliminated the need for any interference between the microwave power beam and the structure. Structural configurations were sized for dynamic stability and incorporated tiered triangular trusses with cylindrical or geodetic cylindrical elements. The significance of construction on the system and structural configurations was recognized and attention was directed from structural efficiency to ease of construction. Further studies of the SPS (ref. 5) suggested the incorporation of the modular unit concept for photovoltaic, as well as the thermal system.

More detailed considerations of operational loads and dynamics of a photovoltaic SPS with aluminum triangular trusses made from beam builders are developed in ref. 6. The study of space shuttle orbiter delivered erectable structures resulted in the use of a planar truss based on a tetrahedron. This structure (called a tetratruss) was employed in a two-tiered MPTS antenna (ref. 10). A concept for an efficient space-fabricated, graphite-composite geodetic cylindrical element has also been developed (ref. 10). A first order analysis for a 1/15 scale similitude space test of the SPS structure and its major systems under appropriately scaled loadings and environmental factors has also been performed.

Further studies (ref. 8) of the SPS structure addressed the potential of an erectable structure via an efficiently packaged graphite-composite, "dixie cup" element for establishing firm cost estimates of the structural system. Recent innovative structural concepts for the MPTS and photovoltaic array have been developed (ref. 11). Ref. 11 provides a good discussion of structural element and configuration trades and addresses control/structure trade-offs.

2. Rectenna Structure and Materials

The rectenna is the ground unit of the SPS which receives the beamed microwave power and converts it to grid compatible electric power. The receiving area is elliptical due to the location of the receiving station relative to the equatorial orbit plane of the MPTS antenna. As now envisioned conceptually the rectenna is composed of rows of panels oriented normal to the incoming beam.

The weight of the rectenna structure is a significant part of the total design load and, thus, enters into the material selection process. Environmental loads include wind, rain, snow and ice, etc. Studies (ref. 35) have indicated that steel is the most cost effective material for the rectenna structure. Other materials studied were aluminum and wood. The disadvantages of aluminum are relatively high cost (compared to steel) and electrical energy demand for its production. Wood is projected to have a higher cost and its lifetime is questionable.

## E. Space Transportation

### Systems Considerations

The transportation system is a key element in the overall SPS program. Systems selection is dominated by the need to achieve the lowest cost possible in terms of dollars per mass to orbit.

The mission of the transportation system is to carry personnel and material between earth and the required locations in space. Performance and economic considerations dictate that transportation between earth and low earth orbit (LEO) be accomplished by vehicles designed for the appropriate flight rates, payloads and the loads associated with launch, atmospheric flight, re-entry and landing, whereas transportation between LEO and geosynchronous orbit (GEO) be accomplished by orbital transfer vehicles (OTV's) designed for non-atmospheric loads and high specific impulse (possibly low thrust) propulsion. A single vehicle design suitable for both regimes would be difficult with present technology and would require a compromise design that would not be cost competitive with separate, functionally optimized vehicles. The LEO staging location is at approximately 500 km altitude and at the inclination of the launch site.

The SPS transportation system consists of four basic vehicle types (plus their associated support facilities) which respond to the requirements of their operational regimes and the differing needs of human and material cargo. The Heavy Lift Launch Vehicle (HLLV) and the Personnel Launch Vehicle (PLV) handle material and personnel traffic between earth and LEO while the Cargo Orbital Transfer Vehicle (COTV) and the Personnel Orbital Transfer Vehicle (POTV) satisfy the requirements between LEO and GEO.

Several studies have investigated the vehicle design characteristics that respond most cost effectively to the payload and launch rate requirements of a wide spectrum of potential missions. These studies have provided a data base of design features supporting the SPS study. The Heavy Lift Launch Vehicles Study (NAS 9-14710), contracted to Boeing in July 1975, investigated the effect of payload and annual mass to LEO requirements on vehicle configurations for the most cost effective performance. The Future Space Transportation Systems Analysis Study (NAS 9-14323) contracted to Boeing in September 1974, investigated the transportation system concepts best meeting the requirements of several future program scenarios. These studies, plus several in-house heavy lift launch vehicle studies, provided an initial appraisal of candidate vehicle concepts for SPS requirements.

The Heavy Lift Launch Vehicle (HLLV)

The function of the HLLV is to transport cargo from the earth launch site to LEO. There were five basic vehicle configurations considered:

1. Single Stage to Orbit (SSTO) - Ballistic, VTOVL
2. Two Stage to Orbit - Ballistic - VTOVL
3. Modified SSTO - Winged, VTOHL
4. Two Stage to Orbit - Winged, VTOHL
5. Single Stage to Orbit (SSTO) - Winged, HTOHL

Where: VTOVL = Vertical takeoff, Vertical landing
VTOHL = Vertical takeoff, Horizontal landing
HTOHL = Horizontal takeoff, Horizontal landing

SSTO - Ballistic, VTOVL - This concept was investigated extensively by Boeing in the Heavy Lift Launch Vehicle Study and the SPS Systems Definition Study. Its characteristics are shown in figure A-15. The LOX/RP-1 engines are shut down after 127.4 seconds of flight and the $LOX/LH_2$ engines continue alone until a 92.6 x 500 km orbit is achieved. A small separate stage then circularizes the payload's orbit. After discharging the payload, the vehicle is deorbited and reenters. Final deceleration for landing is accomplished by LOX/RP-1 engines which bring the vehicle to near zero velocity. The vehicle retros into a specially constructed 5 km diameter fresh water pond adjacent to the launch site. The vehicle then undergoes refurbishment and is ready for reuse.

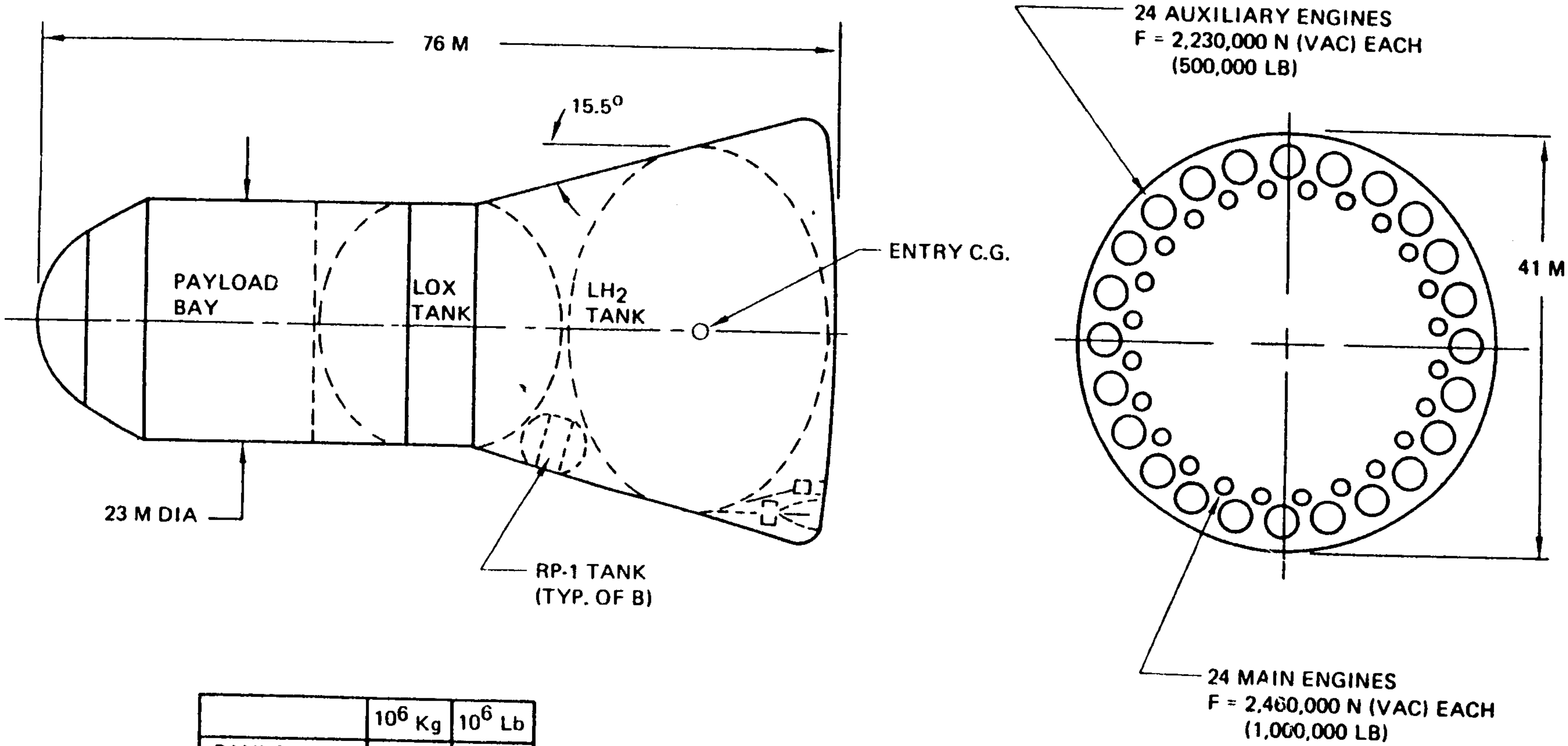


| | $10^6$ Kg | $10^6$ Lb |
|---|---|---|
| PAYLOAD | 0.228 | 0.502 |
| KICK STAGE | 0.007 | 0.016 |
| MAIN STAGE | 10.188 | 22.464 |
| GLOW | 10.423 | 22.982 |

Figure A-15. Reusable Ballistic SSTO

Two Stage Ballistic, VTOVL - This concept was evaluated in considerable detail by Boeing and JSC. JSC utilized computer aided design techniques (EDIN) to evaluate the following four configurations:

| Propellant | | |
|---|---|---|
| 1st Stage | 2nd Stage | Payload |
| $O_2$/RP-1 | LOX/$LH_2$ | 450 MT |
| $O_2$/Propane | " | 450 |
| $O_2$/RP-1 | " | 900 |
| $O_2$/Propane | " | 900 |

The characteristics of these vehicles are shown in figure A-16, with a Saturn V for comparison. Weight estimating relationships developed for Saturn were used for sizing and performance and staging points were optimized on the basis of minimum lift-off weight. Both stages retro to a water landing.

Boeing developed a concept illustrated in figure A-17. The vehicle was designed for simplicity in construction and operation. It is steered by differential throttling and uses no gimbals. The first stage is landed downrange on water and the second stage on a 5 km diameter pond adjacent to the launch pad.

Modified Single Stage to Orbit, VTOHL - This concept was investigated at JSC and utilizes an expendable external hydrogen tank (hence, modified SSTO) and is winged. The vehicle is launched vertically but lands horizontally adjacent to the launch site. Its characteristics and configuration are illustrated in figure A-18.

Two Stage Winged, VTOHL - This configuration was analyzed extensively at JSC utilizing EDIN. Seventeen variations representing different engines, propellants, propellant feed arrangements, payloads and structural material were investigated. These variations included:

| | |
|---|---|
| Payload | 500 to 1000 K lbs |
| Propellant | $LH_2$, $C_3H_8$, $CH_4$ and RP-1 |

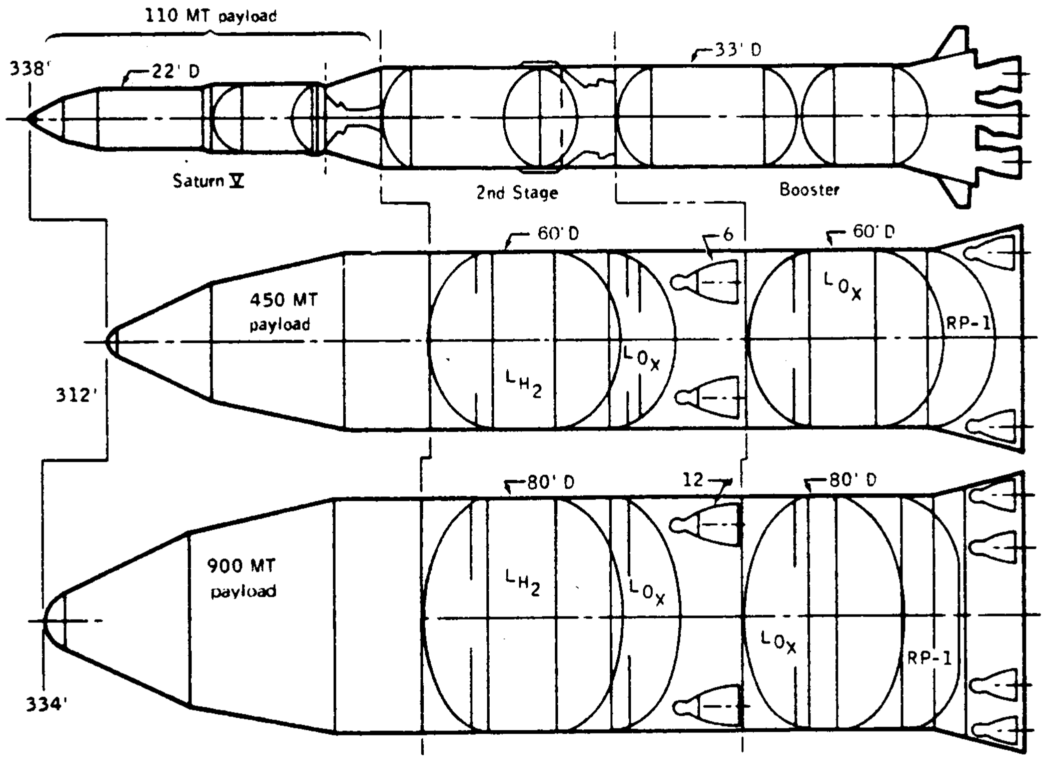


| | $O_2$/RP-1 Booster | | $O_2$/Propane Booster | |
|---|---|---|---|---|
| Payload, tons, 90 x 500 km | 454 | 907 | 454 | 907 |
| Stage 1 inert, tons | 500 | 889 | 485 | 865 |
| Stage 1 propellant, tons | 4441 | 8236 | 4410 | 8177 |
| Stage 2 inert, tons | 233 | 400 | 245 | 421 |
| Stage 2 propellant, tons | 1937 | 3599 | 2065 | 3832 |
| Gross lift-off weight, tons | 7565 | 14031 | 7659 | 14203 |
| Number of engines, stage 1 | 12 | 24 | 12 | 24 |
| Number of engines, stage 2 | 6 | 12 | 6 | 12 |
| Staging altitude, km | 43.4 | 43.5 | 41.3 | 40.6 |
| Staging velocity (REL), km/sec | 1.84 | 1.91 | 1.70 | 1.78 |
| Booster maximum down range | 381 | 396 | 346 | 357 |

Figure A-16. Two-Stage Ballistic Launch Vehicle

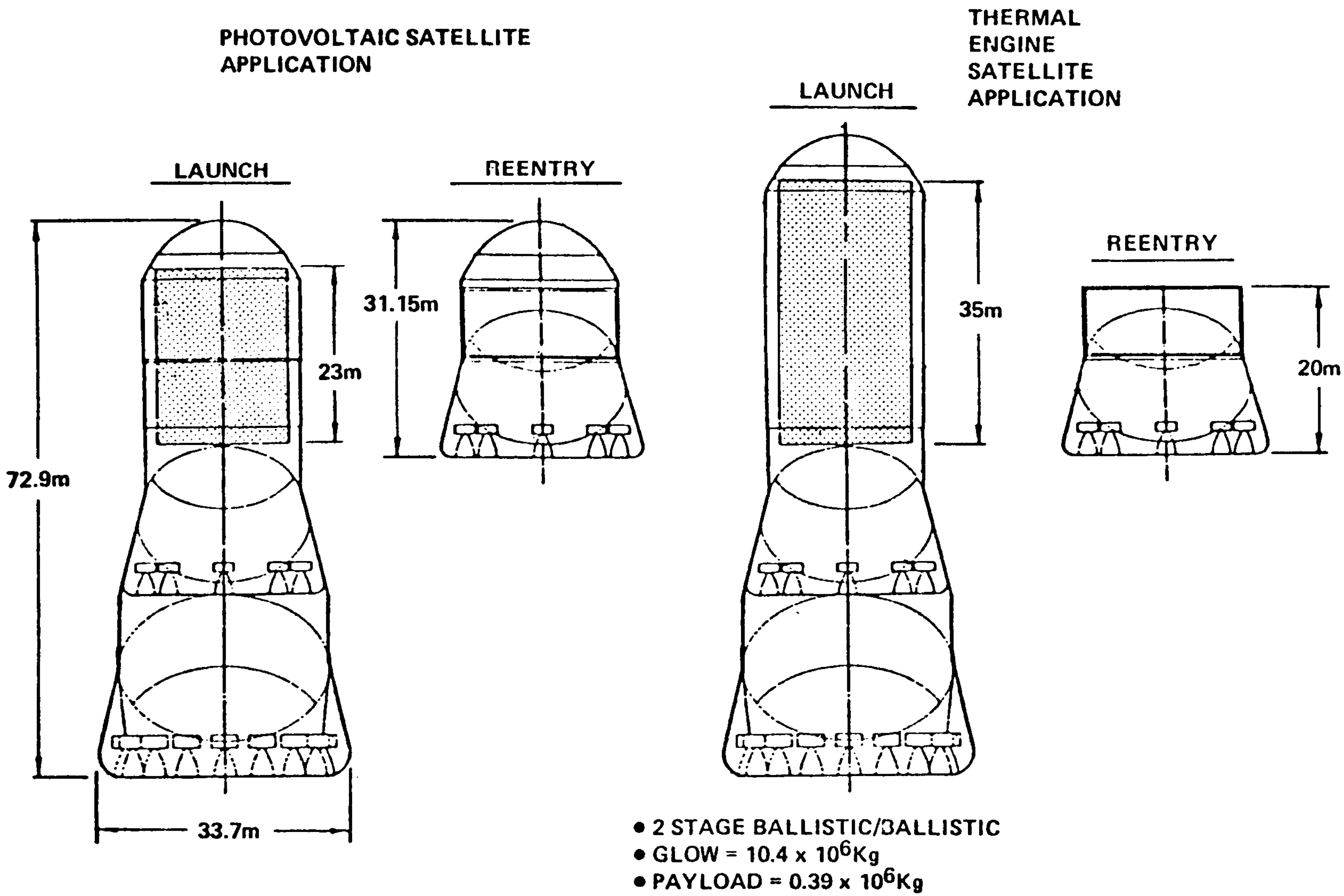


Figure A-17. Boeing Two-Stage Ballistic Concept

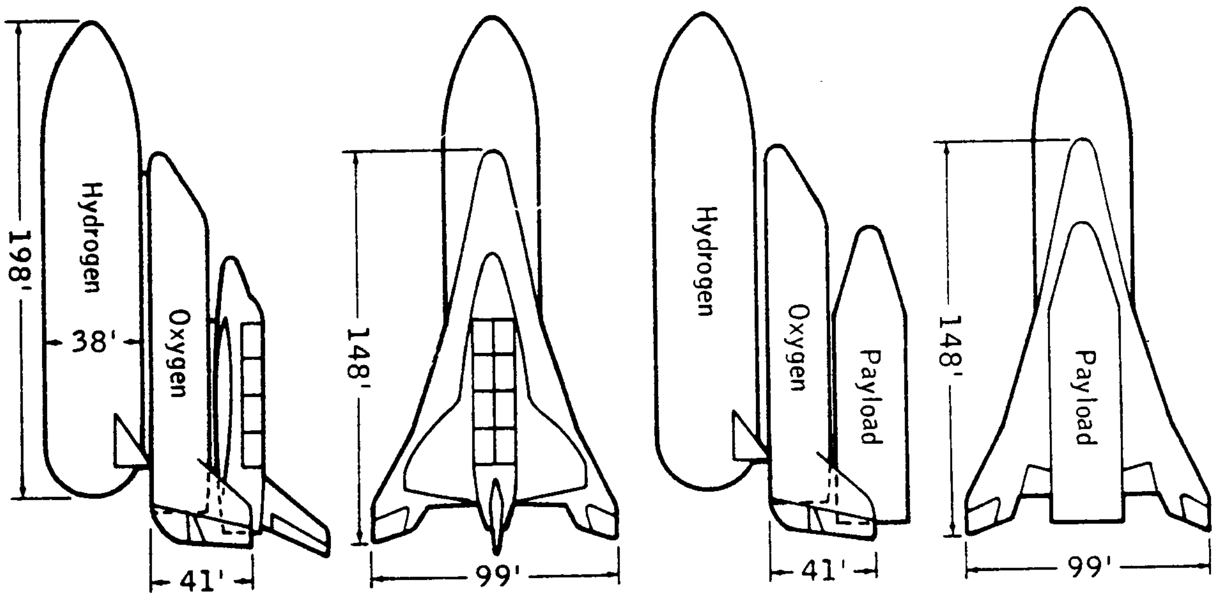


| | |
|---|---|
| Payload, tons, 185 x 185 km, tons | 140 (shroud) - 45 (in Orbiter) |
| Modified Orbiter inert, tons | 61 |
| Stage inert, tons | 166 |
| Stage oxidizer, tons | 2352 |
| External tank inert, tons | 69 |
| External tank fuel, tons | 392 |
| Gross lift-off weight, tons | 3143 |
| Number of engines (uprated SSME's) | 15 |
| Tank staging altitude, km | 111 |
| Tank staging velocity, km/sec | 7.82 |
| Thrust/weight ratio | 1.25 |

Figure A-18. Modified Single-Stage-to-Orbit Launch Vehicle

| | |
|---|---|
| Stages | Tandem and parallel |
| Materials | Aluminum and Composite |
| Payload density | 10 $lbs/ft^3$ and 30 $lbs/ft^3$ |
| Engines | Gas generator, staged combustion, Tripropellant |
| Crossfeed | With crossfeed and without |
| First Stage Return | Flyback and downrange landing |

The current concept is illustrated in Section III of this report. Jet engines provide flyback capability for the first stage and both stages land adjacent to the launch site.

MSFC and Rockwell are currently engaged in the configuration development and preliminary sizing of a two stage winged vehicle, featuring parallel burn with crossfeed.

<u>SSTO - Winged, HTOHL</u> - This concept was investigated by MSFC and Rockwell. The vehicle takes off horizontally, using turbofan jet engines, climbs to optimum altitude for cruise to the equatorial plane. It then dives to achieve transonic flight and accelerates into a supersonic climb. At Mach 3, ramjets operate in parallel with the turbofans up to 130,000 feet where the airbreathing engines shutdown, and the SSME's complete the achievement of a 91 X 550 km orbit. The rocket engines are then shutdown and an auxiliary propulsion system circularizes the payload orbit.

Each of these five options was evaluated for technical and economic feasibility.

Important distinguishing characteristics of each concept are summarized below:

| Vehicle | Propellant | Payload MT | Recovery Area |
|---|---|---|---|
| SSTO-Ballistic | LOX/RP-1, $LH_2$ | 230 | Landing pond at Launch |
| Two Stage Ballistic - Stage 1 | LOX/RP-1 | | Downrange - Water |
| - Stage 2 | $LOX/LH_2$ | 390 | Launch site - Water |
| SSTO - Winged Vertical Takeoff | $LOX/LH_2$ | 455 | Launch site |
| Two Stage Winged - Stage 1 | $LOX/CH_4$ | | Launch site |
| - Stage 2 | $LOX/LH_2$ | 424 | Launch site |
| SSTO - Winged - Horiz. Takeoff | $Air/LH_2$<br>$LOX/LH_2$ | 91 | Launch site |

The following considerations led to the selection of the two-stage winged, vertical takeoff, horizontal landing, configuration as the reference system:

1. In both ballistic and winged concepts a two stage configuration has fewer technology development requirements and is less sensitive to design and operations constraints which result in lower operational costs.

2. Winged vehicles are preferred to ballistic vehicles because of the operational simplicity and reduced recovery time of horizontal land landings adjacent to the launch site compared to vertical water landings and the recovery of first stages downrange in the sea.

3. Hydrocarbon fuel is preferred to hydrogen for first stages because of its lesser volume and cost. The relatively simple production of methane by coal gasification guarantees its availability in the time period involved. For these reasons methane was selected for the first stage

while hydrogen is to be used for the second stage because of its superior performance.

Personnel Launch Vehicle (PLV) - The PLV transports crews and crew supplies to LEO. The vehicles considered for this function were all derivatives of the STS. MSFC and Boeing have investigated various concepts for replacing the STS solid rocket boosters (SRB's) and have, in particular, studied a twin $LOX/LH_2$ strap-on booster configuration. JSC also investigated several alternatives including series and parallel burns, winged and ballistic configurations and the use of $LH_2$, RP-1, and $CH_4$ (methane) as fuels.

Rockwell has proposed a concept for modifying the Orbiter to carry 68 passengers and other concepts have ranged between 50 and 100. Improved booster performance would permit even higher passenger payloads.

The booster configuration actually to be utilized for the SPS program will depend on whether it is designed strictly for the SPS traffic requirements or if a suitably modified STS will be available. The reference system is based on a design for SPS requirements and compatibility with the SPS HLLV technology. It utilizes a methane fueled winged booster, series burn and a resized, smaller external tank. (See figure 19.)

Cargo Orbit Transfer Vehicle (COTV)- The COTV transports cargo from LEO to GEO. Several approaches to meeting this requirement were considered: A conventional chemically fueled high thrust COTV with a short round trip time and a high degree of reusability, a nuclear COTV featuring a propulsion system capable of high thrust and high specific impulse, and an electrical COTV requiring an extended transit time, but deriving the electrical power to run its ion engines from a solar cell array. The electrical approach was subdivided into two options, the self powered option in which part of the SPS solar array is used to power the COTV and the independent option in which the array remains dedicated to the COTV function.

The chemical option is a space-based common stage system with both stages having the same $LOX/LH_2$ capacity and utilizing conventional

**VEHICLE CHARACTERISTICS:**

| | |
|---|---|
| GLOW | 2,714,750 kg |
| BLOW | 1,959,140 kg |
| $W_{P_1}$ | 1,699,820 kg |
| OLOW | 666,880 kg |
| $W_{P_2}$ | 551,720 kg |
| PAYLOAD | 88,730 kg |

| ENGINE CHARACTERISTICS | | | | | |
|---|---|---|---|---|---|
| STAGE | E | NO. | TYPE | $I_{SP}$ (SL/VAC) | THRUST (VAC) |
| 1 | 60 | 4 | HIGH $P_C$ $LO_2/LCH_4$ | 318.5/352 | $2.15 \times 10^6$ LBF<br>$9.564 \times 10^6$ N |
| 2 | 77.5 | 3 | SSME | 363.2/455.2 | $.470 \times 10^6$ LBF<br>$2.091 \times 10^6$ N |

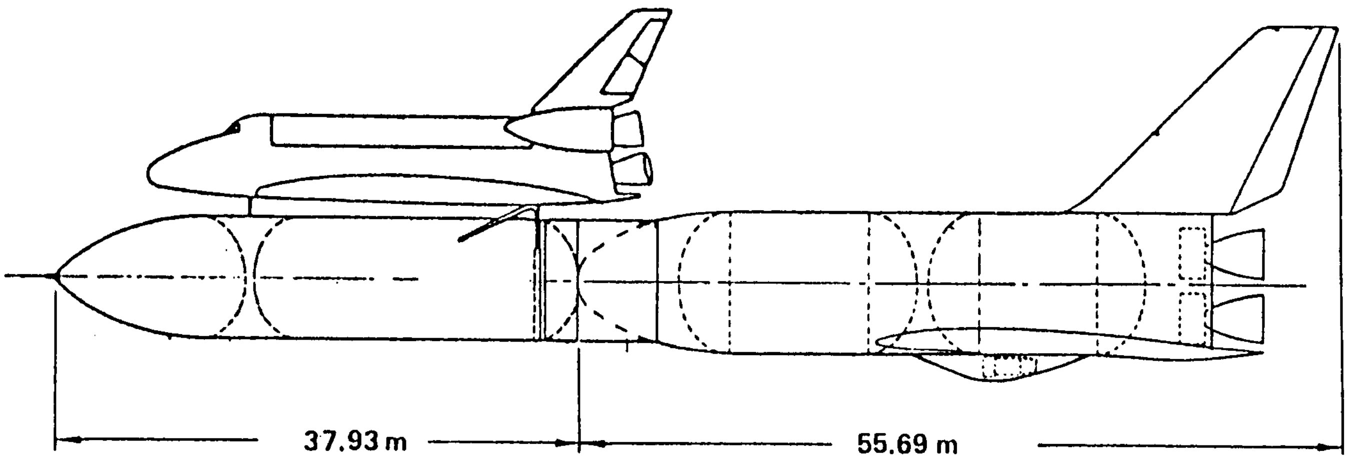


Figure A-19. Shuttle PLV with Winged Flyback Booster types of rocket engines. The first stage supplies approximately 2/3 of the delta-V requirements, after which it is separated and returns to the LEO staging depot. The second stage completes the boost from LEO to GEO and also provides the thrust for returning the stage to the LEO staging depot for reuse. The vehicle gross weight at start burn of 1,290,000 kg of which 400,000 kg is payload and 830,000 kg is propellant (Figure A-20). More than two out of every three HLLV flights would be required to carry fuel for the COTV. The chief advantage of the chemical COTV is the short trip times of 30 hours for the round trip from LEO to GEO and back to LEO.

The nuclear COTV concept analyzed combined the desirable features of the chemical COTV and the electrical COTV - high thrust and high specific impulse, respectively. The stage, shown on Figure A-21, has a nuclear gas core, light bulb-shaped engine with a theoretical specific impulse of 2250 seconds and a thrust level of 890,000 newtons. The component mass breakdown is given in Table A-3. Although such a system could meet the short trip time requirement for personnel transfer and the high performance requirement for cargo transfer, the development risks and the presence of nuclear materials in LEO eliminated this system from further consideration.

The electric approach utilizes low thrust engines with high Isp and round trip time measured in months rather than hours. Studies were conducted to determine the optimum thruster, propellant type, and trip time. Thruster types considered were the nuclear-thermal, resistojet, thermal arc-jet, MPD arcjet and ion bombardment. Fuels considered were mercury, argon, cesium and xenon. Of these, the ion bombardment thruster had the most satisfactory performance in terms of thrust and specific impulse technology readiness. Argon, stored as a cryogenic, appears to be the best propellant because of its ready availability as a by-product of LOX production and its consequent low cost (about $0.50 per kg). Furthermore, experience with the development of 8 and 30 cm diameter mercury ion thrusters is sufficient to analytically predict the performance of argon ion thrusters as large as 120 cm.

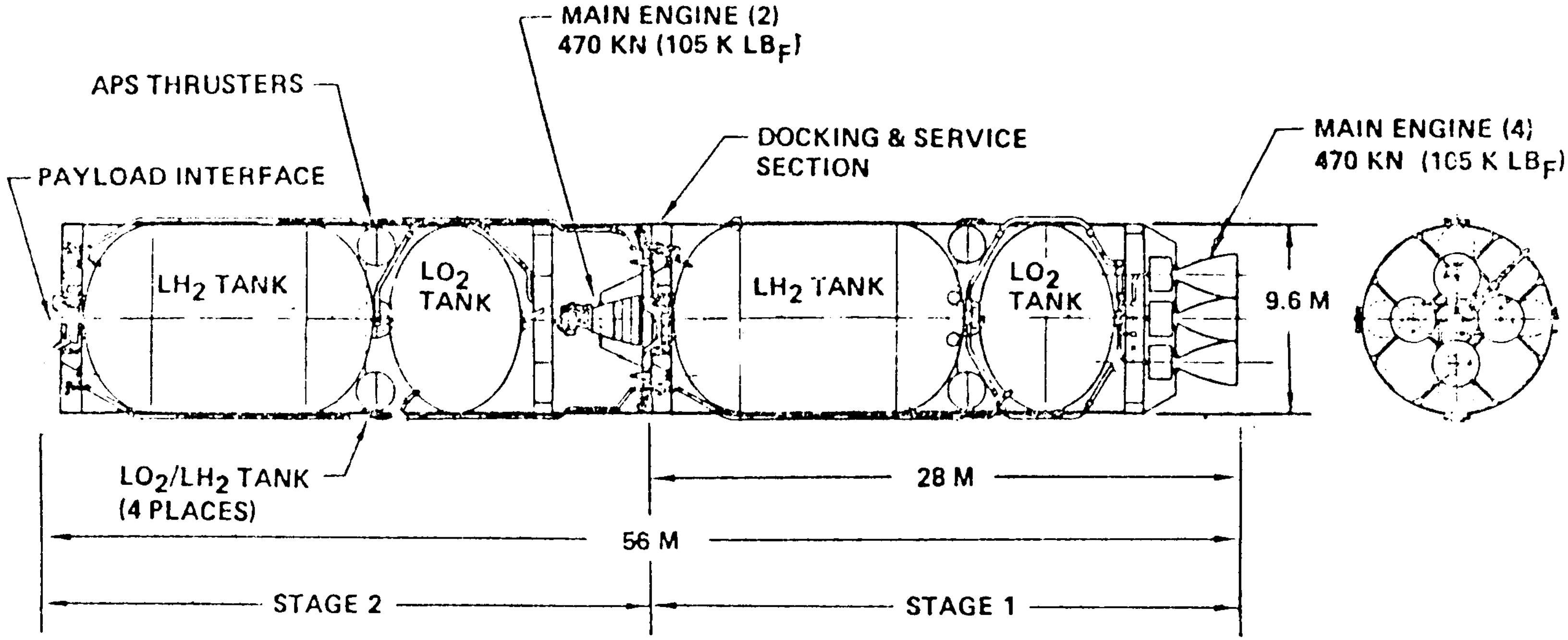


- PAYLOAD CAPABILITY = 400,000 KG
- OTV STARTBURN MASS = 890,000 KG
- STAGE CHARACTERISTICS (EACH
  - PROPELLANT = 415,000 KG
  - INERTS =30,000 KG
    (INCLUDING NONIMPULSE PROPELLANT)
- 280 OTV FLIGHTS PER SATELLITE

Figure A-20. LOX/$LH_2$ Common Stage COTV - GEO Construction

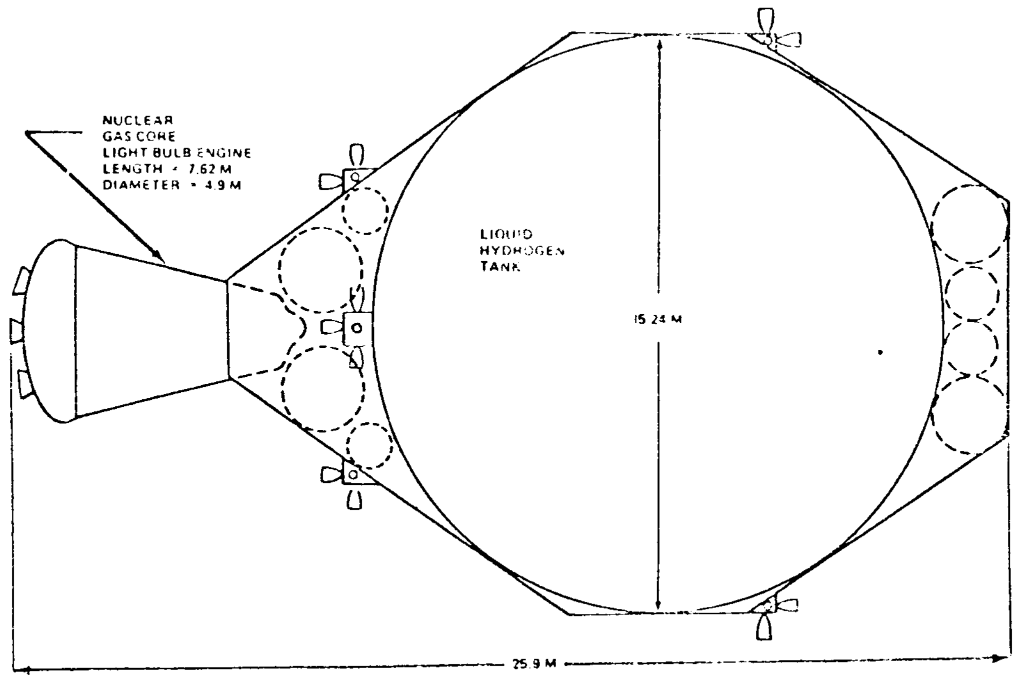


Figure A-21. Nuclear COTV

Table A-3. Nuclear COTV Mass Breakdown

| Stage Element | Weight Kg |
| --- | --- |
| Structures and Mechanics | 18,780 |
| Main Propulsion | 56,850 |
| Auxiliary Propulsion | 600 |
| Avionics | 260 |
| Electric Power | 480 |
| Thermal Control | 1,220 |
| Growth (15%) | 11,730 |
| Dry Weight | 89,920 |
| Other Propellants and Fluids | 2,000 |
| Total Inert Weight | 91,920 |
| Mainstage Propellants | |
| LOX | |
| $LH_2$ | 124,280 |
| Stage Weight | 206,204 |

Once the thruster type and propellant were selected, investigations were conducted to determine optimum trip time, and the desirability of utilizing the SPS array itself to provide power for the ion engines. In the self powered approach, studies were completed of assembling the complete SPS in LEO and self-powering to GEO as well as constructing the SPS in eight modules in LEO and self-powering each to GEO. For the second option, thruster and power processing systems are located at four corners of the satellite module and connected to a gimbal system to enable required pointing (Figure A-22). A joint cost optimization of Isp and trip time resulted in a selection of a 180 day transfer at 7000 seconds electrical Isp. The effective Isp, after accounting for losses for attitude control thrusting and the use of chemical propulsion during transits of the Earth's shadow is about 3000 seconds. This high specific impulse option therefore requires about 0.25 kg of propellant per kg of payload to GEO compared to about 2.1 kg of propellant per kg of payload to GEO for the chemical COTV option.

Approximately one-quarter of the SPS solar blankets on each module are deployed for the transfer from LEO to GEO; the remainder are deployed from their shipping boxes at GEO. The deployed arrays will be degraded by Van Allen belt radiation absorbed during the transfer but will be annealed at GEO to regain most of the lost efficiency during the final checkout and preparation process. The ion thrusters and propellant tanks would remain in GEO as an integral part of the SPS, thus incurring no propellant penalty for returning them to LEO.

A second electric solar array option, called the independent electric OTV, involves the construction of a fleet of reusable electric powered round-trip vehicles and their associated solar array in LEO. These vehicles are used to transport SPS material which is fabricated in GEO. Potentially, this option offers the performance advantages of the LEO construction/self-power concept and the monolithic satellite construction operations associated with the GEO construction/chemical COTV.

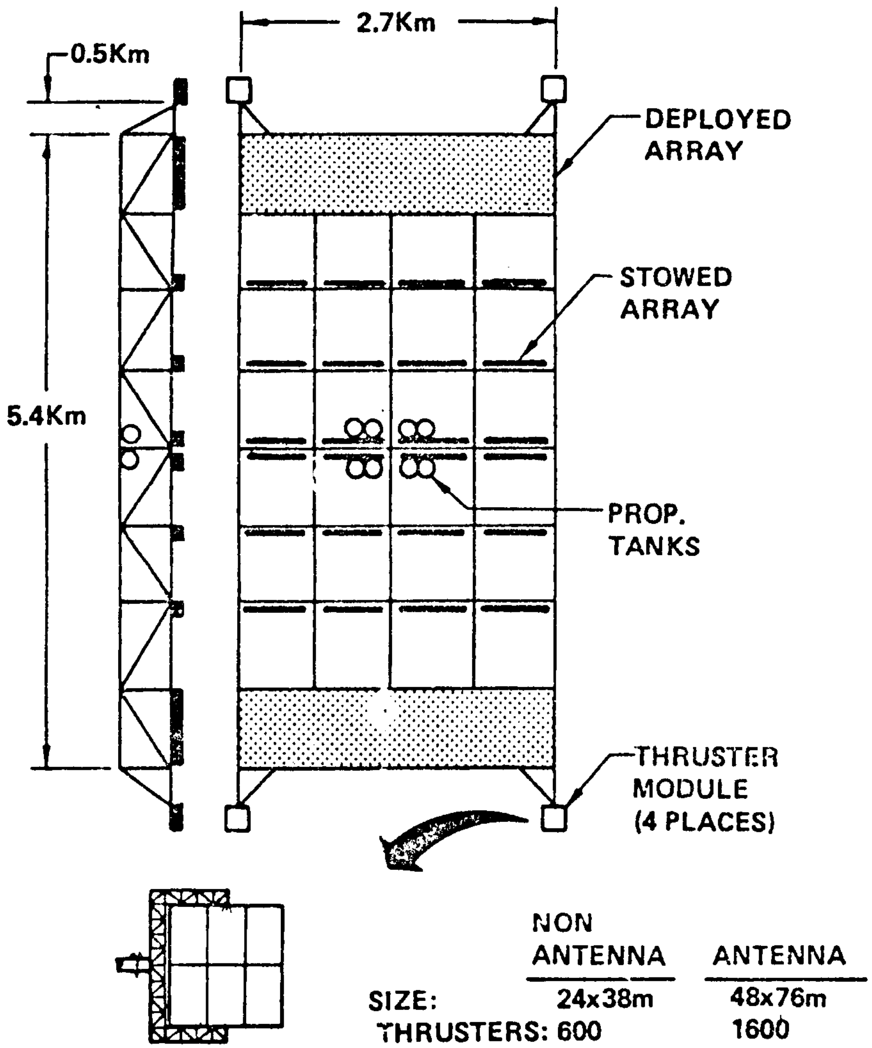


## GENERAL CHARACTERISTICS

- 5% OVERSIZING (RADIATION)
- TRIP TIME = 180 DAYS
- ISP = 7000 SEC

| MODULE CHARACTERISTICS | NON ANTENNA MODULE | ANTENNA MODULE |
|---|---|---|
| • NO. MODULES | 6 | 2 |
| • MODULE MASS ($10^6$KG) | 8.7 | 23.7 |
| • POWER REQ'D ($10^6$Kw) | 0.3 | 0.81 |
| • ARRAY % | 13 | 36 |
| • OTS DRY ($10^6$KG) | 1.1 | 2.9 |
| • ARGON ($10^6$KG) | 2.0 | 5.6 |
| • $LO_2/LH_2$ ($10^6$KG) | 1.0 | 2.8 |
| • ELEC THRUST ($10^3$N) | 4.5 | 12.2 |
| • CHEM THRUST ($10^3$N) | 12.0 | 5.0 |

Figure A-22. Self-Powered Electric COTV - LEO Construction

Two configurations of the independent electric COTV have been synthesized and are currently under investigation. Both COTV configurations are large, lightweight structures constructed in LEO and are associated with an all-GEO SPS construction mode. The first concept utilizes a self-annealing gallium aluminum arsenide array with a concentration ratio of 2 and carries a payload of 4000 MT for a LEO-GEO trip time of 133 days and a total round trip time of less than 180 days. Ion bombardment thrusters of 100 cm diameter are used with an Isp of 13,000 seconds and argon as the working fluid. The concept is shown on Figure A-23. The primary thruster array of 259 thrusters is suspended by cables and located at the vehicle c.g. Additional attitude thruster control packages are located at the structural extremities. The component mass breakdown is given in Table A-4.

The second concept utilizes a silicon photovoltaic solar array in a planar configuration with no concentration reflectors. Round trip time from LEO-GEO-LEO is approximately 160 days which also allows two trips per year for each COTV. Ion bombardment thrusters of 120 cm diameter are used with an Isp of 7,000 seconds and argon as the working fluid. The concept is shown on Figure A-24. Thruster modules of 296 electric thrusters each and an appropriate number of chemical thrusters are located at the four corners of the COTV. The component mass breakdown is given in Table A-5. The COTV start-burn mass is seen as 2085 MT for the second concept as compared to 1442 MT for the first concept of the independent electric COTV. The cost effectiveness of both configurations is quite sensitive to items which have very little data base such as maintenance/refurbishment requirements, design life of various components and unit cost.

Both electric approaches have their advantages--the self-powered requiring less HLLV flights and the independent minimizing the damage to SPS solar cells while traversing the Van Allen belts. The cost comparison of the two approaches is difficult to assess due to the lack of data base. The relative advantages and disadvantages of conducting construction operations in LEO vs GEO have been explored, and GEO construction has been selected for

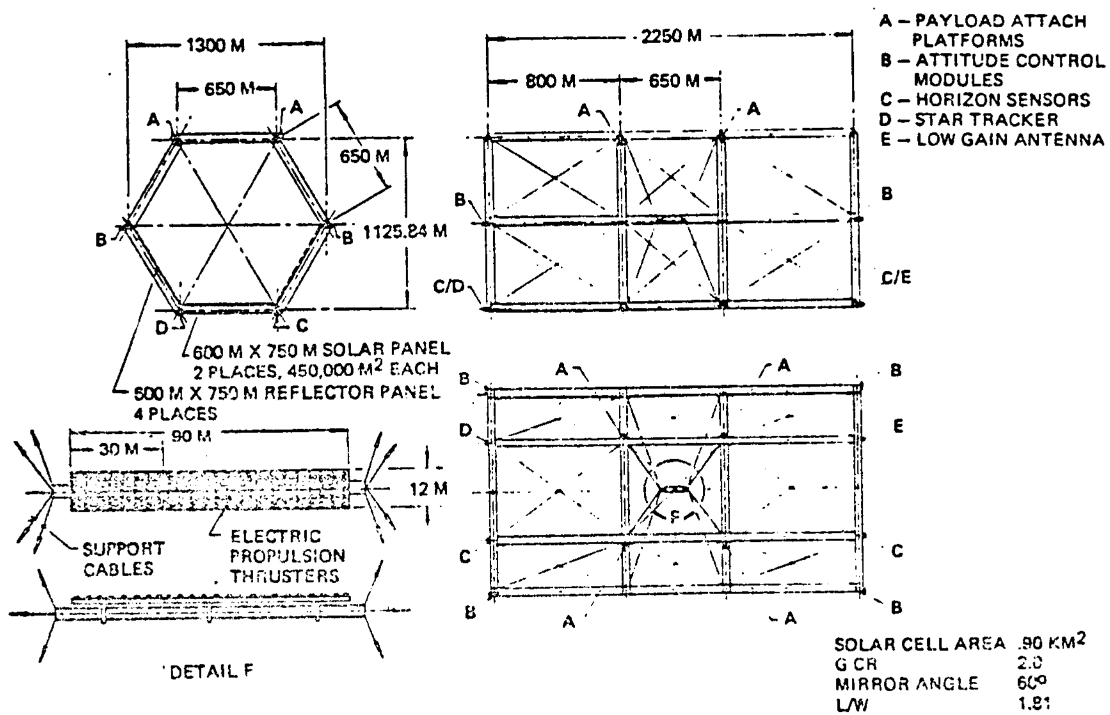


Figure A-23. GaAlAs Independent Electric OTV - GEO Construction

Table A-4 GaAlAs Independent Electric COTV Mass Breakdown

| Vehicle (Dry) | (MT) |
|---|---|
| Power Generation/Distribution | 249 |
| Thrusters | 26 |
| Propellant Tanks and Lines | 39 |
| Structure/Thermal Control | 229 |
| Rotary Joint | 7 |
| Attitude Control/IMS | 22 |
| Primary Power Unit | - |
| Total (Dry) | 572 |
| 25% Growth Margin | 143 |
| Payload | 3469 |
| Propellant Up | 185 |
| Propellant Down | 27 |
| Total in LEO | 4396 |

Table A-5 Si Independent Electric COTV Mass Breakdown

| Vehicle (Dry) | (MT) |
|---|---|
| Power Generation/Distribution | 570 |
| Thrusters | 70 |
| Propellant Tanks and Lines | 60 |
| Structure/Thermal Control | 80 |
| Rotary Joint | - |
| Attitude Control/IMS | - |
| Primary Power Unit | 185 |
| Total (Dry) | 965 |
| 25% Growth Margin | 241 |
| Payload | 4000 |
| Propellant Up | 835 |
| Propellant Down | 150 |
| Total in LEO | 6191 |

- PAYLOAD UP 4000 MT
- PAYLOAD DN 0
- VEHICLE DRY MASS 1100 MT
- PROP. UP 835 MT
- PROP. DN 150 MT

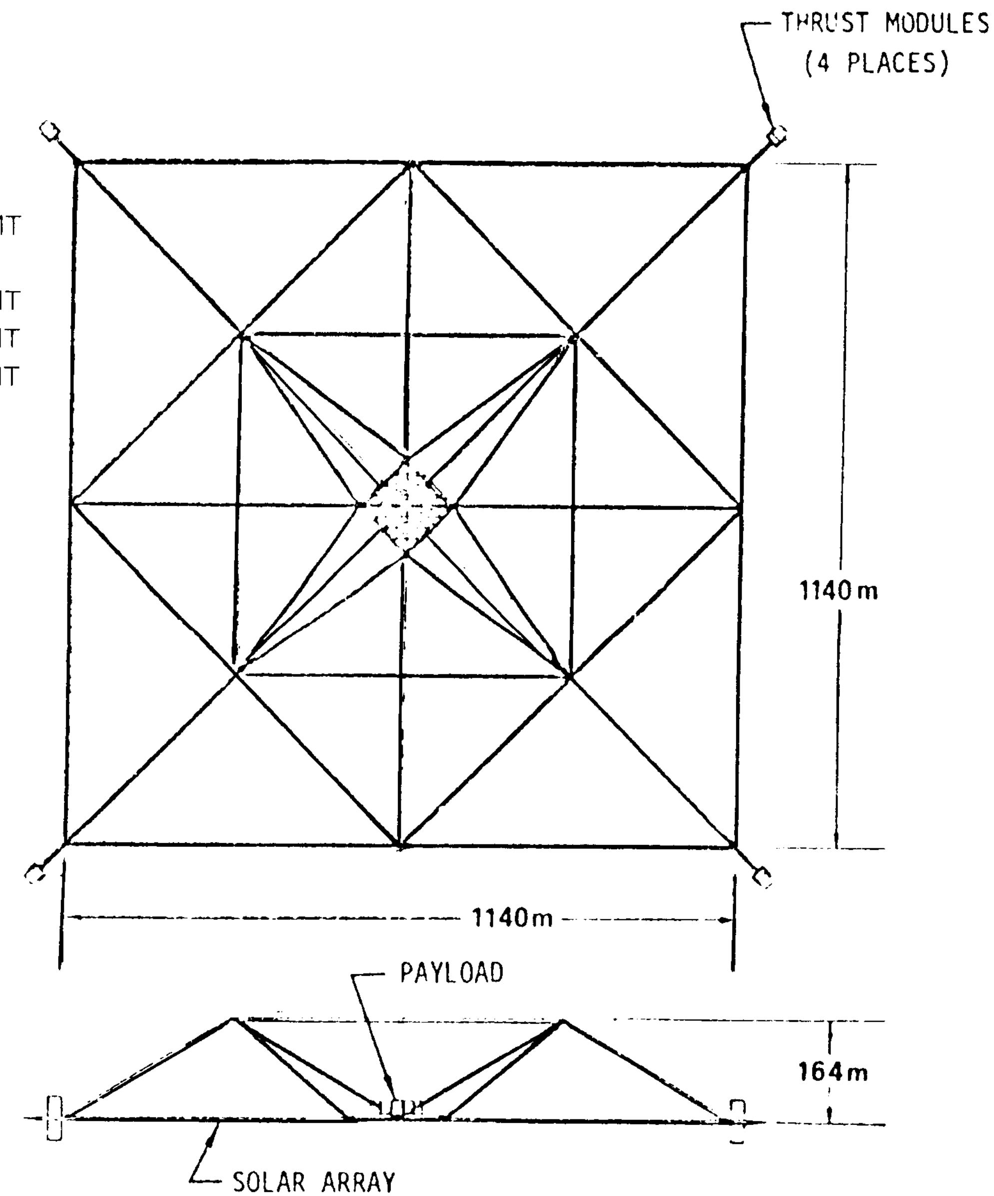




Figure A-24. Silicon Independent Electric OTV - GEO Construction the reference orbit. In the comparison of chemical versus electric COTV options, the chemical option has a shorter trip time and requires significantly less technology development for SPS application; but due to the lower performance, significantly more propellant, i.e., HLLV flights, is required to support the chemical transfer. Consequently, the best approach at this time appears to be an electric propulsion COTV augmented by a chemical propulsion system to overcome gravity gradient torque at low altitude (<2500 km) and to provide attitude control during occultation.

Personnel Orbital Transfer Vehicle (POTV) - The functions of the POTV are to deliver personnel and supplies from LEO to GEO and to return personnel from GEO to LEO at 90-day intervals. For this orbital transfer function, the electrically propelled option is not viable due to its extended trip time. Therefore, a $LOX/LH_2$ fueled vehicle which can make the trip in the order of one day was chosen for the crew rotation function.

For the option of electric propulsion for cargo transfer, a dedicated $LOX/LH_2$ OTV with two common stages is chosen as the most cost effective POTV configuration. The propulsion vehicle with associated modules is shown on Figure A-25. The vehicle transports 160 personnel and crew supplies for 480 man-months from LEO to GEO and returns 160 personnel to LEO for rotation. The propulsion vehicle has a start burn weight of 890 tons and a payload up of 151 tons and a payload down of 55 tons. The payload up consists of 160 personnel in a passenger module, 480 man-months consumables in a resupply module, and a flight control module piloted by a crew of two. The payload down is identical except the resupply module returns empty to LEO.

For the option of chemical propulsion for cargo transfer, only one stage of the two stage $LOX/LH_2$ COTV (Figure A-19) would be required due to the lower mass of the crew rotation module and flight control module as compared to the cargo payload delivered to GEO by the common stage COTV. The use of this approach minimizes the DDT&E expense, as well as maximizing the utilization of the vehicles.

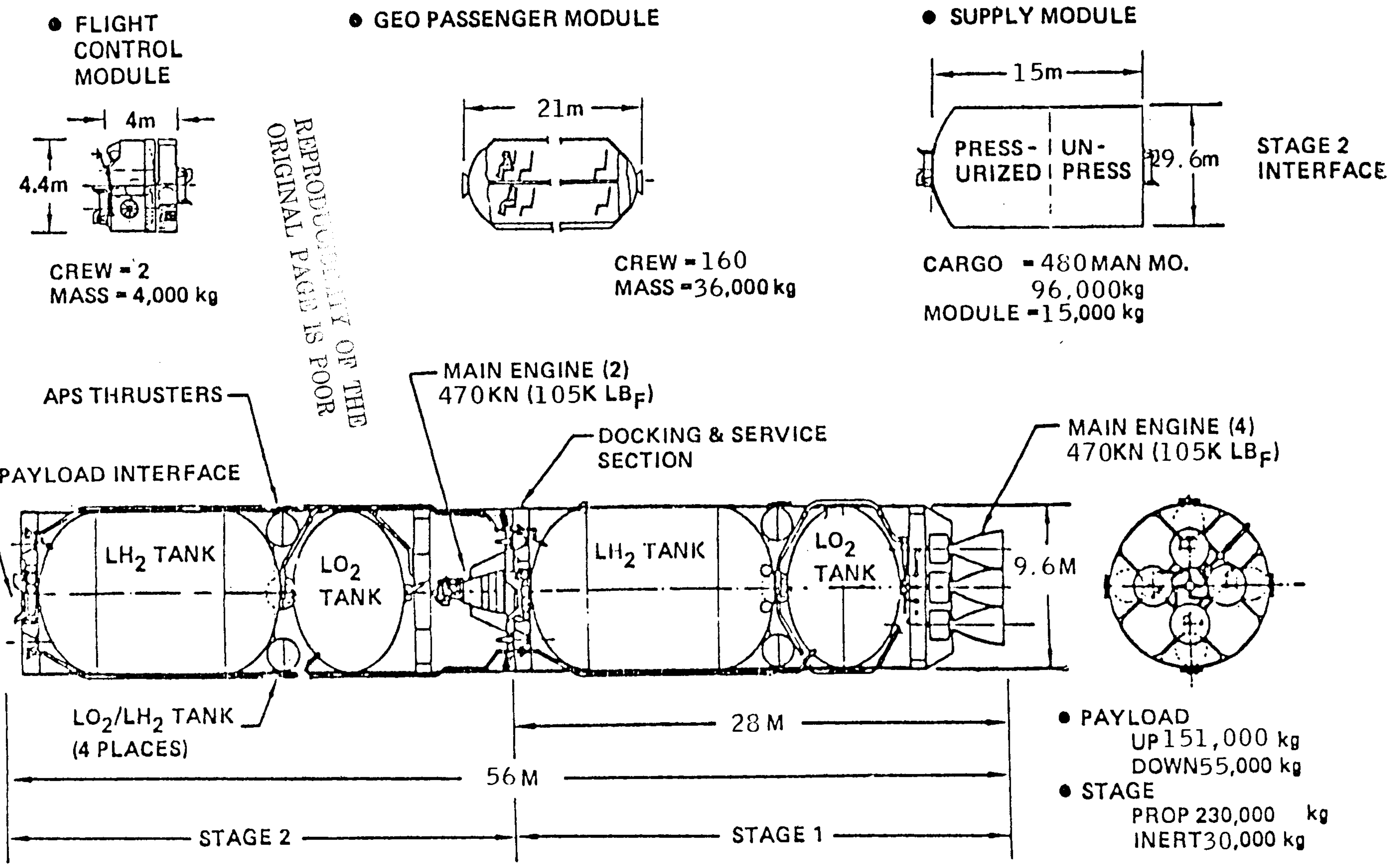


Figure A-25. LOX/$LH_2$ Common Stage POTV

Ground Support Facilities - All launches, both the HLLV and PLV were assumed to take place from Cape Kennedy. Since the PLV is a Shuttle-derived vehicle, a large portion of the facilities and equipment built for shuttle can be used. The launch facilities required for the HLLV are more extensive. Several launch pads will be required to support an SPS implementation rate of 10 GW per year. A preliminary cost estimate of $3.4 billion for the construction of the required facilities and the fabrication of specialized ground support equipment has been made.

Consideration of 28.5 Degree Versus 55 Degree Inclination - A comparison was made by the Marshall Space Flight Center which considered the potential cost impacts of launching SPS construction materials into a 55 degree inclination as opposed to the baseline inclination of 28.5 degrees for low Earth orbit (LEO) assembly. Potential benefits of the higher inclination were elimination of chemical propulsion subsystem requirements by earth shadowing. Such chemical augmentation of the already on-board SPS ion propulsion subsystem would not be necessary at 55 degrees. Eliminating the chemical system was estimated to save about 100 million dollars in development cost and about 500 million per satellite in launch costs associated with the propulsion hardware. These savings were reduced however, by the lower launch vehicle performance into 55 degrees. A number of other factors would have to be considered in more detail before a conclusive decision could be reached regarding the most desirable inclination for a low earth orbit assembly of the SPS. This has not been pursued due to the subsequent selection of geosynchronous orbit construction; however, the trade data does tend to suggest that further analysis is warranted should the LEO assembly option be reconsidered.

## F. Construction

### 1. Satellite Construction

The early SPS configuration studies indicated that construction in space was desirable because fabrication of a large area of lightweight structure in orbit takes advantage of the absence of severe loading conditions. Favorable packaging density requirements for heavy lift launch vehicles can be accomplished with space fabrication. This allows a reduction in the number of flights and greater load capability of satellite components when the components are most efficiently packaged. As concepts for construction have been developed, the concepts have been reflected in various satellite configurations and constructability of a configuration is a major parameter in selecting a design configuration. The difficulty of constructing a configuration is generally related to the concentration ratio, where concentration ratios greater than two begin to become more difficult to construct. With regard to construction location in GEO or LEO, the transportation and operation requirements are the principal drivers in the selection.

A variety of construction and support equipment will be necessary to complete a satellite. Because of the very large scale of the operation, a high degree of automation will be employed to keep the number of personnel to a reasonable level and the total construction time to a minimum. These personnel will principally perform monitoring and repair functions. As SPS systems have been defined, the need for a maintenance capability has become an important operational consideration.

Construction Location - Low Earth Orbit (LEO) vs. Geosynchronous Earth Orbit (GEO) - The issue of where to construct the SPS received considerable study effort. Conclusions varied due to the sensitivity to assumptions and performance parameters.

Construction of the satellite in GEO offers many desirable features. Gravity gradient loads are two orders of magnitude lower than in LEO, aerodynamic drag loads are not significant, thermal effects from passing through the earth's shadow are negligible, collision hazard from other satellites is low, and the construction sequence is simpler. Personnel logistics requirements, on the other hand, are greater than in LEO, but the percentage cost impact of personnel is not significant.

The most effective mode of construction in LEO is to build the satellite in modules sized to be compatible with the thruster requirements for the control of the SPS in GEO operation. The modules are berthed together in GEO. Building the satellite as a complete unit in LEO for transport to GEO is not practical because of control requirements and loads to the structure due to gravity gradients.

LEO construction offers a potential cost saving by using a self-powered mode where the output from the partially deployed SPS solar cells is used to power a LEO-to-GEO propulsion system. The degree of degradation of the deployed solar cells by Van Allen belt radiation is an important parameter in the LEO-GEO trade. For self-powered transfer, the satellite solar array must be oversized to maintain the specified output or the cells subjected to an annealing process to restore efficiency. The use of an electric OTV concept for GEO construction may reduce the cost differential between LEO and GEO sites; however, radiation effects also affect the efficiency of the electric OTV.

Studies to date have indicated that either LEO or GEO construction appears feasible. The GEO construction location is used as the reference.

Configuration Constructability - In the initial phases of the SPS studies, the satellite configurations were generated and then methods were devised to construct the configuration. Relative ease of construction was sometimes used as a parameter in comparison of various power systems. As the understanding of space construction improved and the percentage of satellite weight required for structure was determined to be small, the configurations were modified or originated to improve the ability to rapidly and simply construct them. This may be illustrated by two early configurations, which are the "column-cable configuration" and the "truss configuration".

The "column-cable" concept (figure A-26) emphasized a very efficient use of compression and tension members to minimize structural weight. In the "column-cable configuration", orthogonal central columns were stabilized by cables with the solar cell blankets stretched on the cables also. Construction facilities necessarily were dispersed because the configuration had to grow symmetrically to be structurally stable. Equipment to install solar cell blankets and power distribution had to be supported on the satellite structure and cables.

In order to provide a continuous automatic assembly process, a long narrow geometry was conceived called the "truss configuration" (figure A-27). Structural efficiency was sacrificed to improve construction. Structure was automatically fabricated and the concentrator membranes, solar cell blankets and power distribution were installed from a facility which was the full width of the SPS. In later designs, this approach is exemplified by the Rockwell International extrusion concept (figure A-28). This concept results in a facility with a size and shape similar to the cross section of the SPS. The "extrusion" concept features uniform generation of longitudinal structure with solar cell blankets and power distribution (figure A-29) added as the structure leaves the facility. An alternative concept is the Boeing configuration (figure A-30) which builds a structural bay then steps one bay to build the next bay while solar cell blankets and power distribution are installed in the just completed bay.

Thermal engine satellite configurations are relatively more difficult to construct than photovoltaic system because the geometry is irregular and they require large active systems with fluids systems associated with the heat absorber cavity and thermal radiators (figures A-31 and A-32). The concentrating reflectors must approximate a parabolic segment. Building the concentrator support in a cylindrical shape (figure A-33) was an improvement, but constructability has remained one of several disadvantages of the thermal conversion approach relative to photovoltaic configurations.

Launch Vehicle Packing Density - The capability to handle the construction logistic requirements in a manner that minimizes the impact on the HLLV is an important economic factor. The HLLV payload volume for efficient

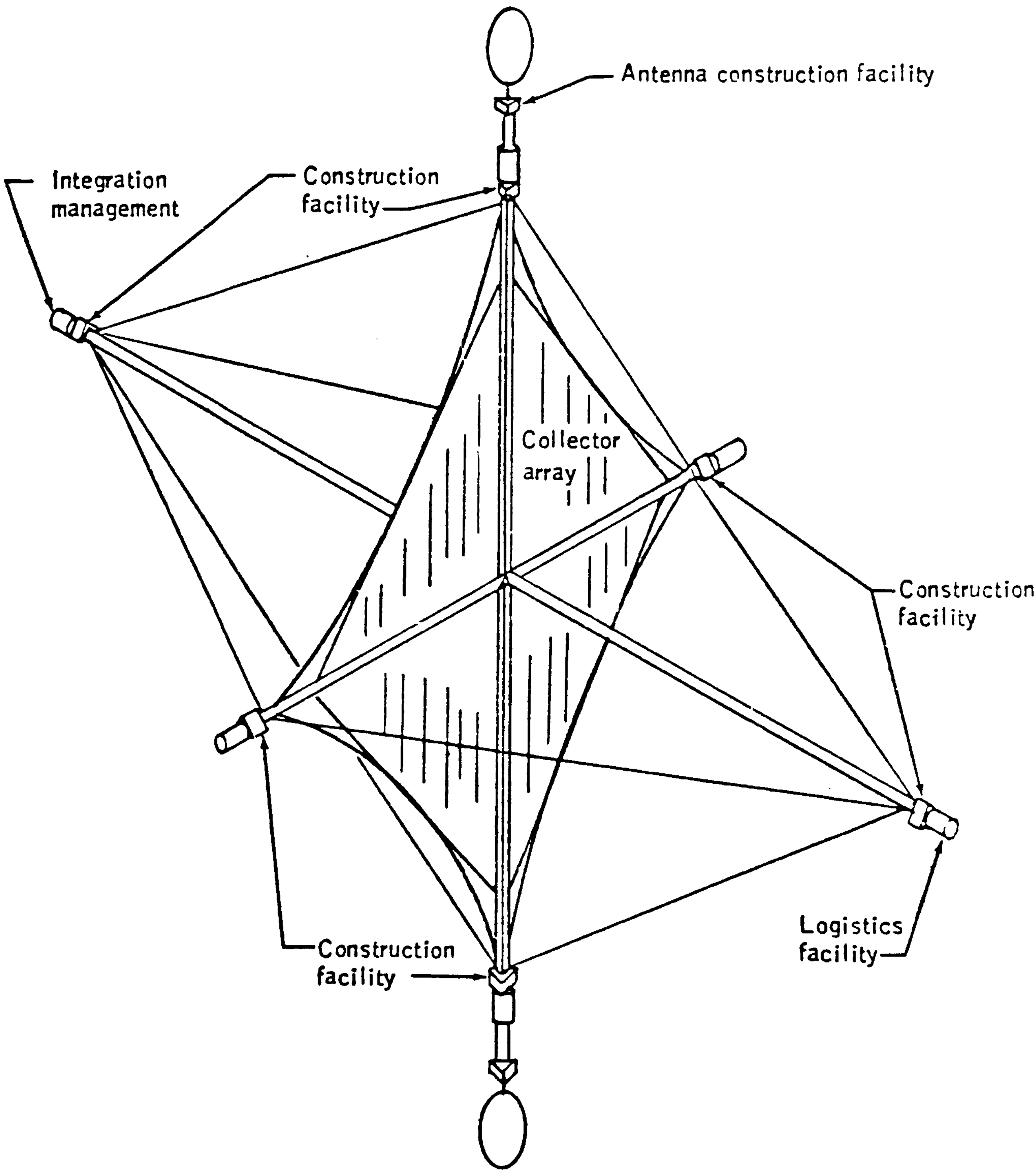


Figure A-26. Construction Base Concept for Column/Cable Configuration

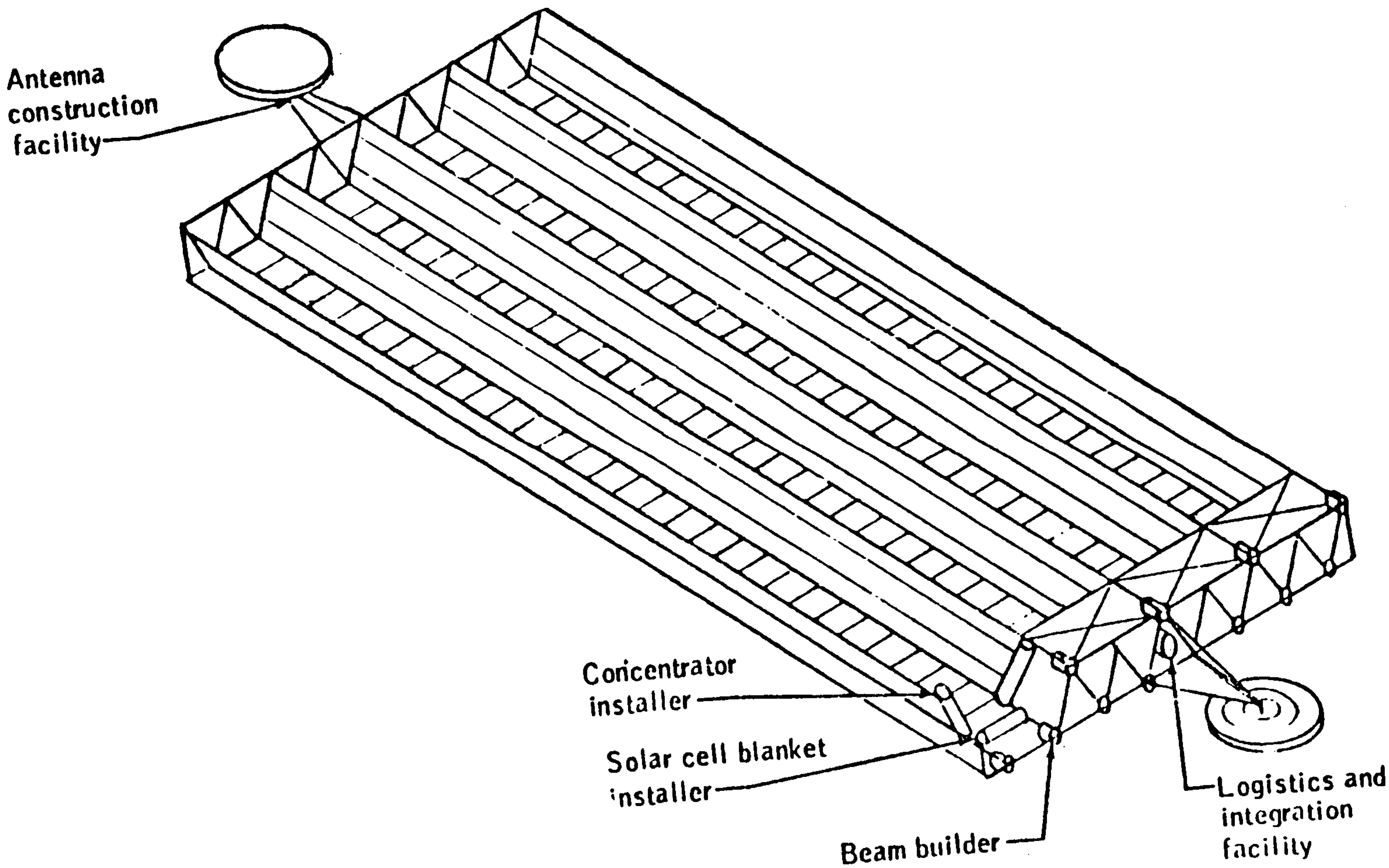


Figure A-27. Construction Base Concept for Truss Configuration

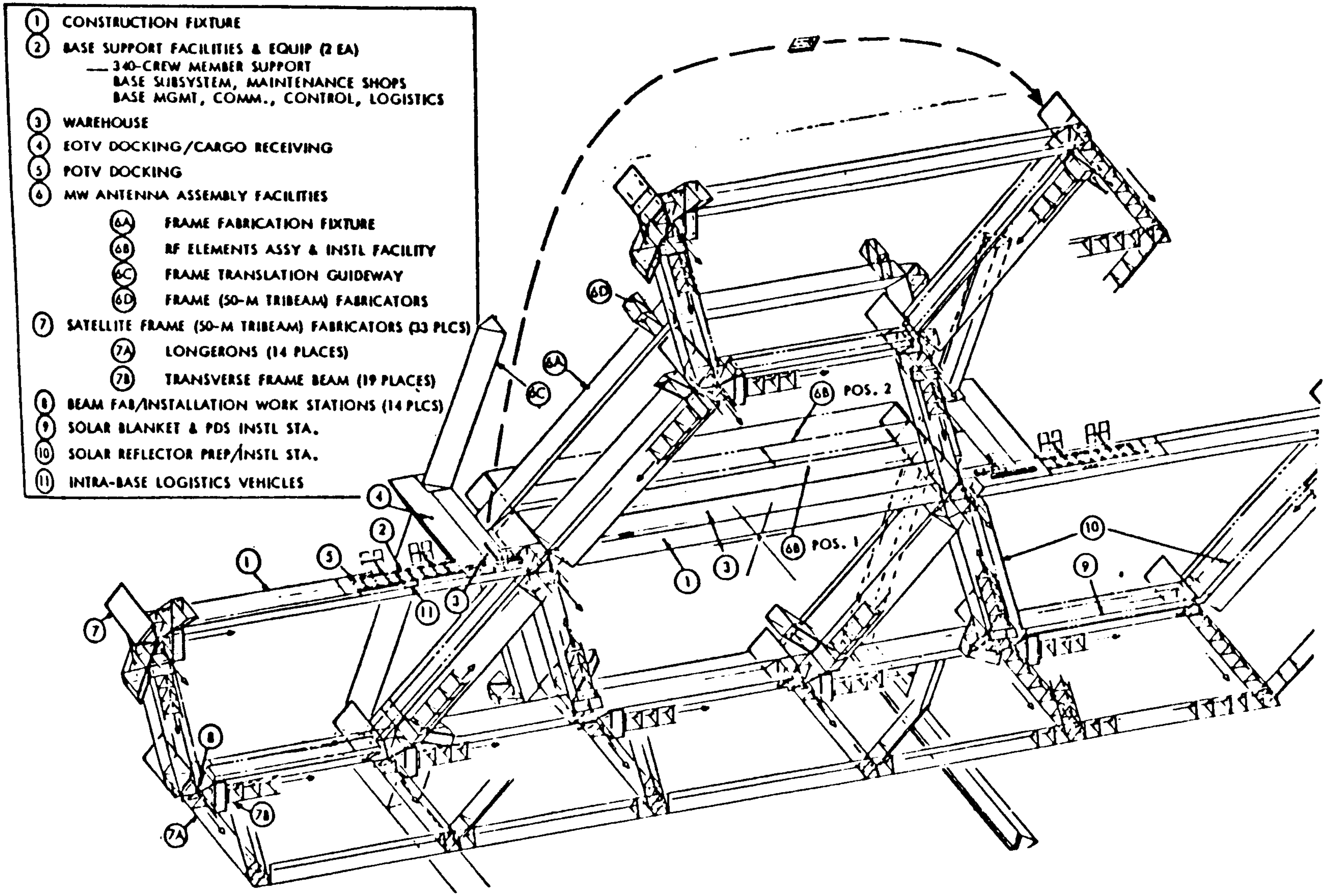


Figure A-28. Satellite Construction Base
(GEO Located)

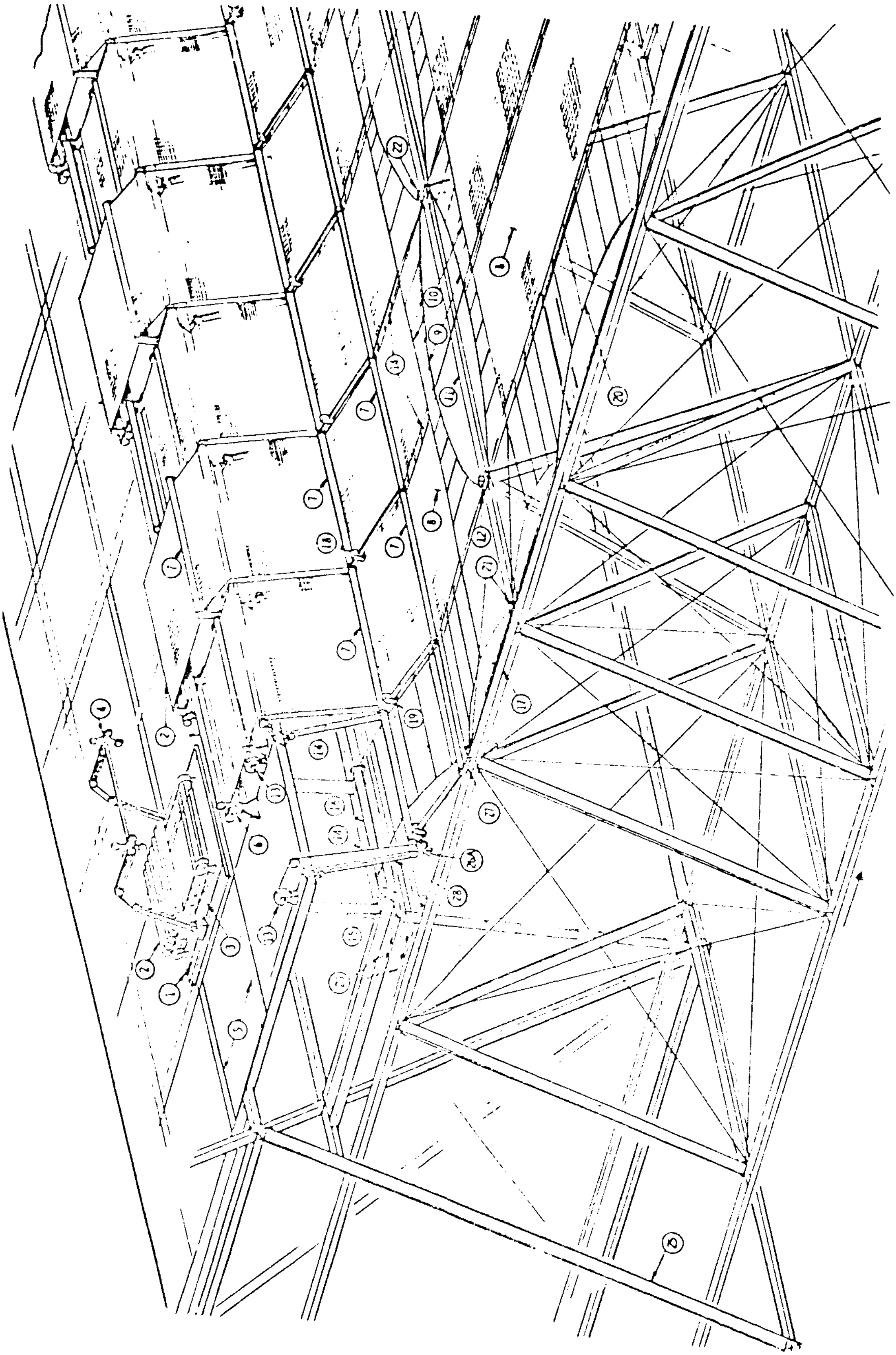

Figure A-29. Solar Cell Blanket Installation Concept

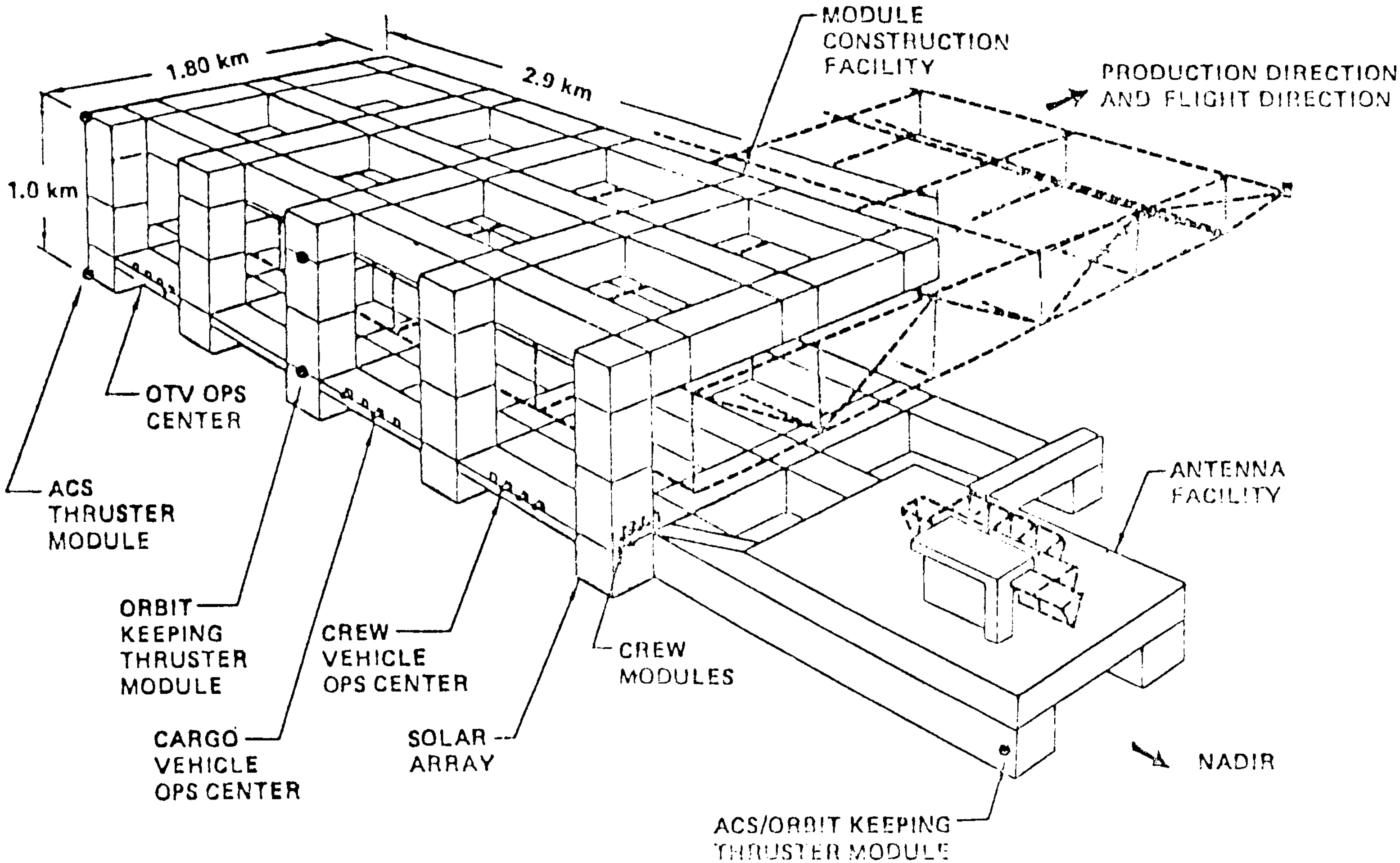


Figure A-30. LEO Construction Base - Photovoltaic Satellite

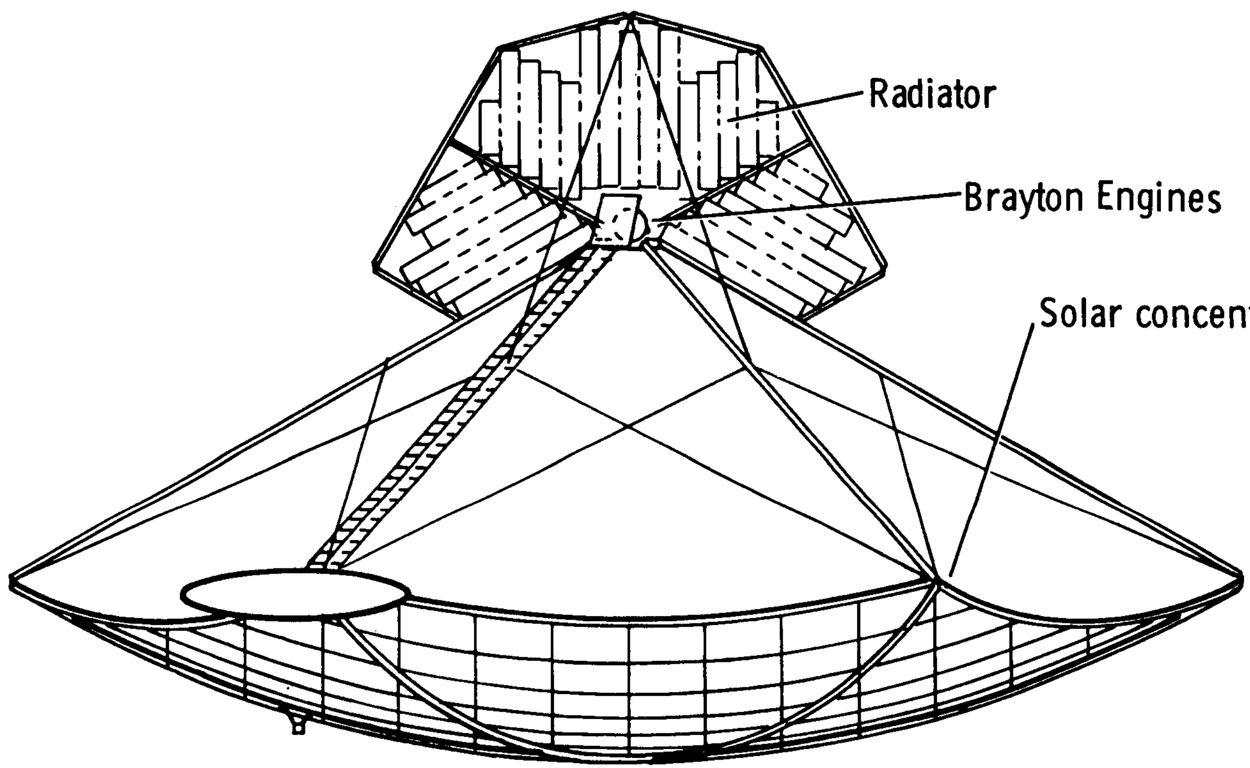


Figure A-31. General Arrangement - Solar Power Satellite - Solar Brayton

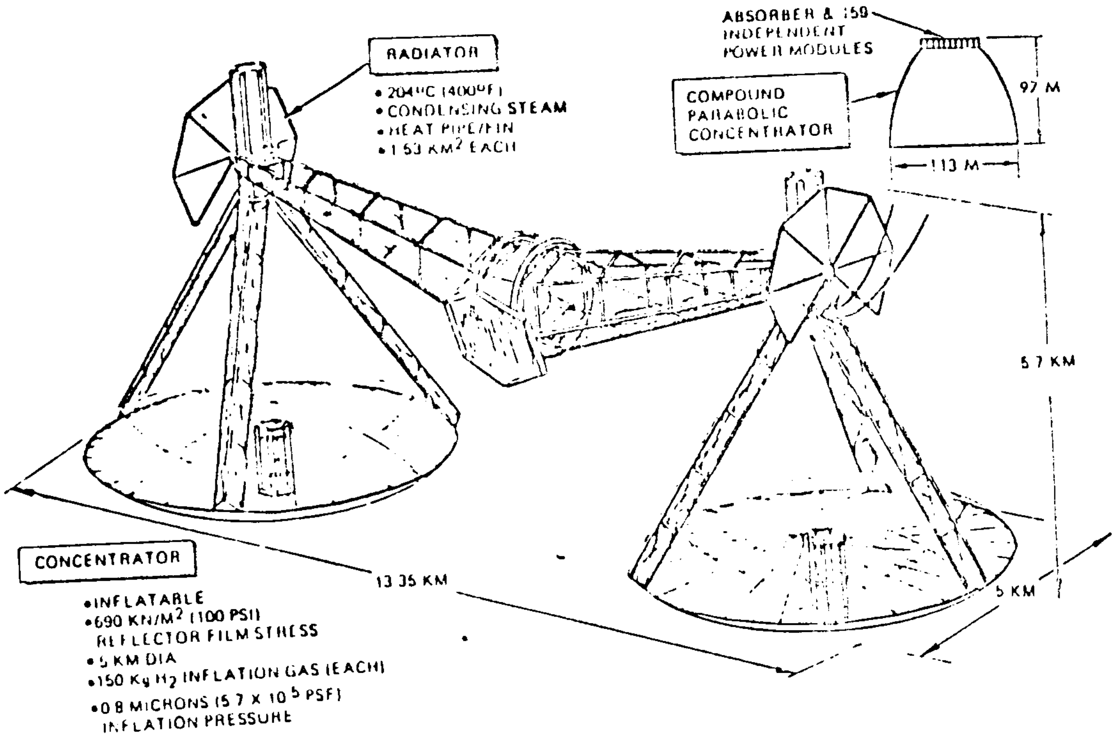


Figure A-32. Solar Thermal Design Concept

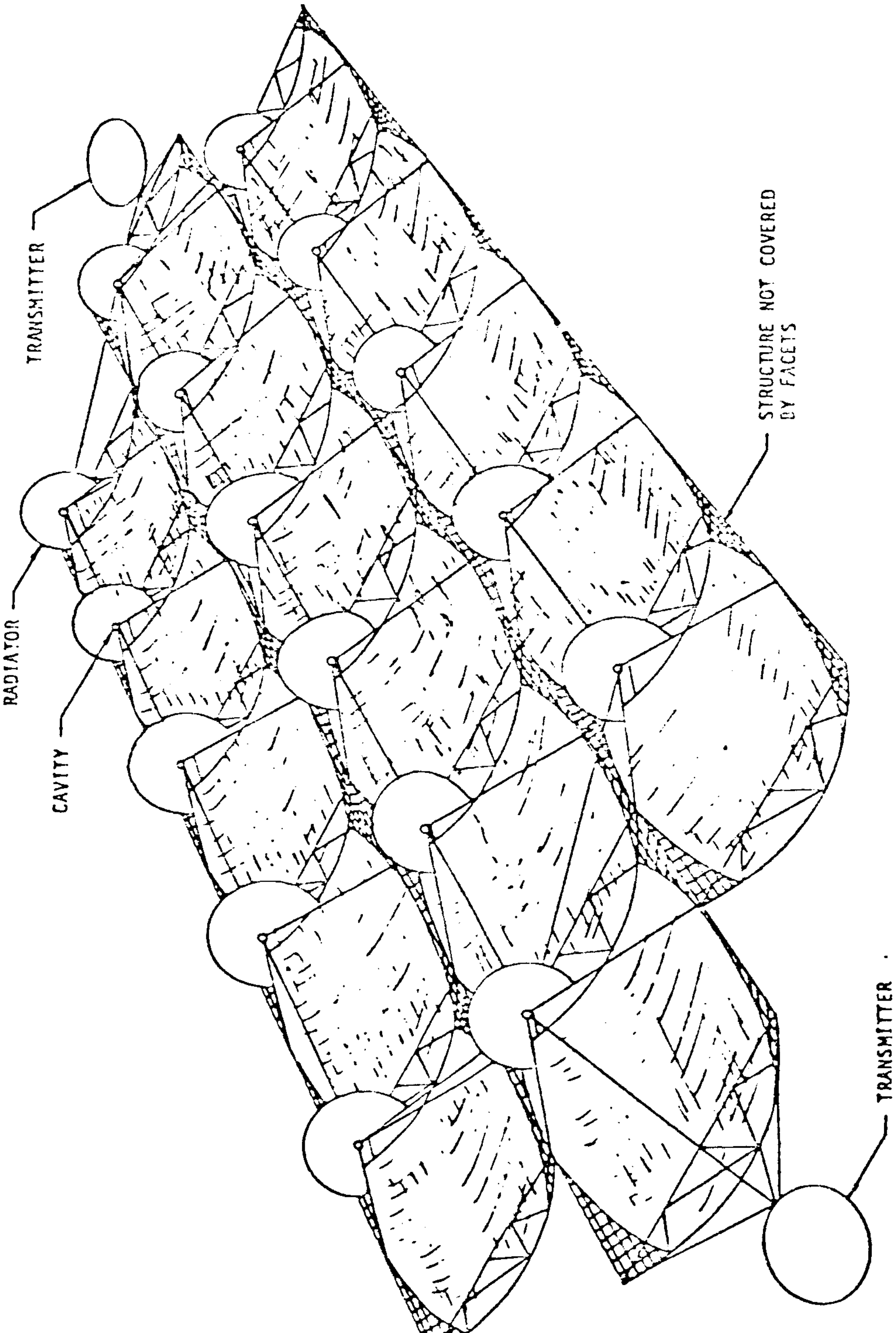


Figure A-33. 16 Module SPS Configuration operation should be as small as possible to enclose the mass to be delivered to orbit. The automatic fabrication of structure in space results in high density packaging. Solar cell blankets, concentrator membranes and power distribution busses also can be densely packaged. The antenna waveguides are lightweight, precision hardware. See figure A-34 for nominal densities of various components. Early concepts tolerated lightly-loaded HLLV's to avoid manufacture of waveguides in orbit. However, more recent studies have shown that by mixing low-density components with high-density components on individual flights, packing densities approaching 100 $kg/m^3$ can be achieved, thereby avoiding a relatively difficult space manufacturing activity for antenna subarrays while maintaining high launch vehicle payload density. Figure A-35 illustrates a typical component mix to reduce the number of launches.

Space Construction Personnel - The number of construction personnel required for building the SPS is a function of the degree of automation, the ratio of direct monitoring of operations to remote monitoring, the rate of construction and the amount of maintenance anticipated on the facility equipment. Once estimates of construction workers are made, the requirements for support personnel are derived. There has been little fluctuation in the construction crew requirements during the SPS studies. Table A-6 provides a chronology of the estimates that have been made.

Construction Equipment and Construction Support Equipment - For the purpose of developing construction concepts and costing, the categories of construction equipment and construction support equipment were established. Generally, the construction equipment is designed for a specific function such as solar cell blanket deployment, fabrication of structural elements, or power distribution system installation. The construction support equipment performs a variety of tasks or more universal function such as the facility proper, logistics vehicles, work stations, or remote manipulators.

A primary requirement in space construction is providing a means of positioning construction equipment so it can perform its function. The construction facility or base is a space frame with support points, guides and

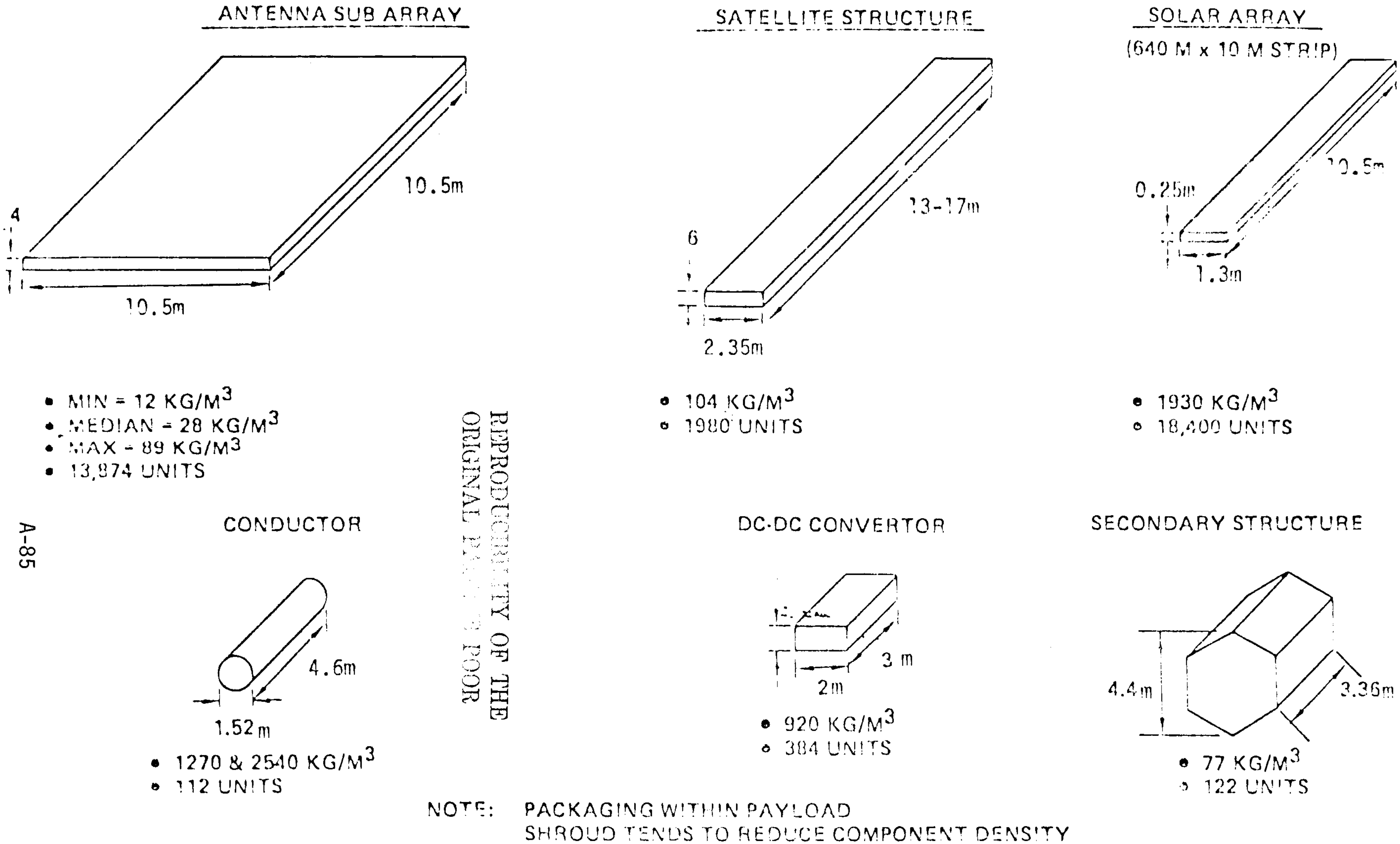




Figure A-34. Component Densities

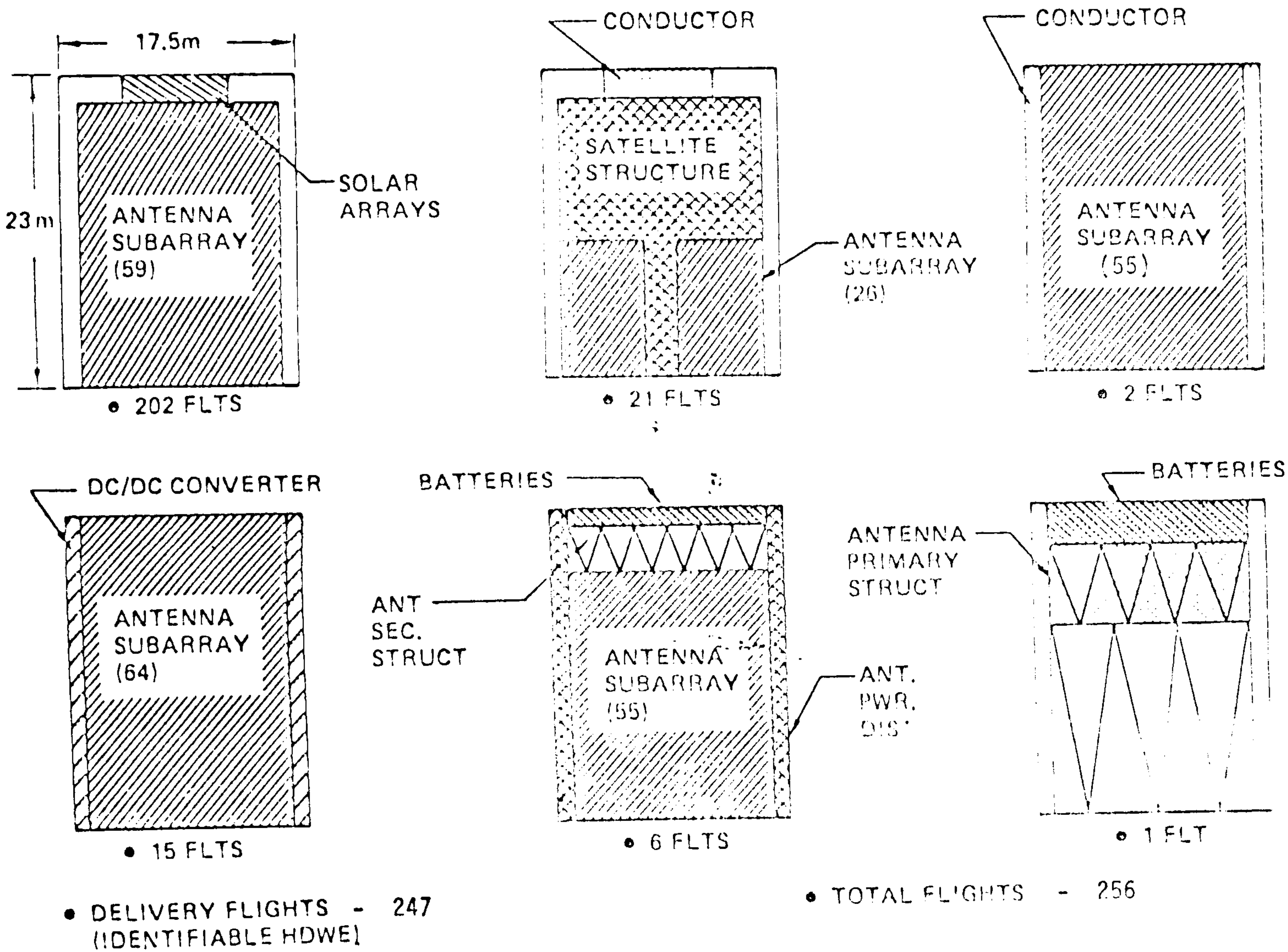


Figure A-35. Component Mix

| SOURCE | DATE | LEO CREW | GEO CREW | TOTAL |
|---|---|---|---|---|
| GAC/ECON (STRUCTURE ONLY) (Ref. 6) | 6-76 | | 117 | |
| JSC GREENBOOK (Ref. 2) | 8-76 | | | |
| - CABLE/COLUMN | | 176 | 474 | 650 |
| - TRUSS GEO | | 176 | 574 | 750 |
| - TRUSS LEO | | 740 | 200 | 940 |
| GAC/ECON (LEO) (Ref. 6) | 3-77 | 700 | | 700 |
| BOEING PART I (Ref. 7) | 6-77 | 477 | 259 | 736 |
| PART III (Ref. 8) | 3-78 | 478 | 67 | 545 |
| ROCKWELL (Ref. 11) | 4-78 | 30 | 640 | 670 |

Table A-6. Construction Personnel Requirements Chronology tracks to position equipment and provide a logistics capability to transport supplies and operating personnel. The base also acts as a receiving depot for OTV traffic and it provides personnel housing.

Also considered as construction support equipment (CSE), are manned remote work stations as illustrated in concept in figure A-36. This concept provides close contact with work to be performed while maintaining the crew in a controlled environment. A variety of remote manipulators will be needed ranging from short precise ones to space cranes to accomplish tasks at over 100 meters from facility supports. Some CSE tasks are the assembly of automatically fabricated beams into the deep trusses needed for the primary structure, servicing deployment machines, and installing equipment modules.

The task of construction of very large lightweight structure resulted in the concept of a "beam builder". This is construction equipment which takes preprocessed flat strip material, forms the strip into a structural shape for the cap member of a triangular truss, and attaches cross members to the cap to complete the structural truss (figure A-37). An alternative approach is a automatic beam assembler which builds the lightweight truss structure from prefabricated structural elements.

The solar cell blankets are to be stretched in membrane fashion between bays of the structural truss. The blankets can be densely packaged in a container which is loaded into construction equipment which performs the deployment.

If concentrating reflectors are used in the configuration, deployment directly from the shipping container by the construction equipment is a conceptual approach. The reflector will require tension support to achieve the required flatness. This requirement complicates the installation by the need to join the packaged strips at the edges and to apply a lateral stretching force within each structural bay.

The power busses are thin flat strips several meters wide to permit

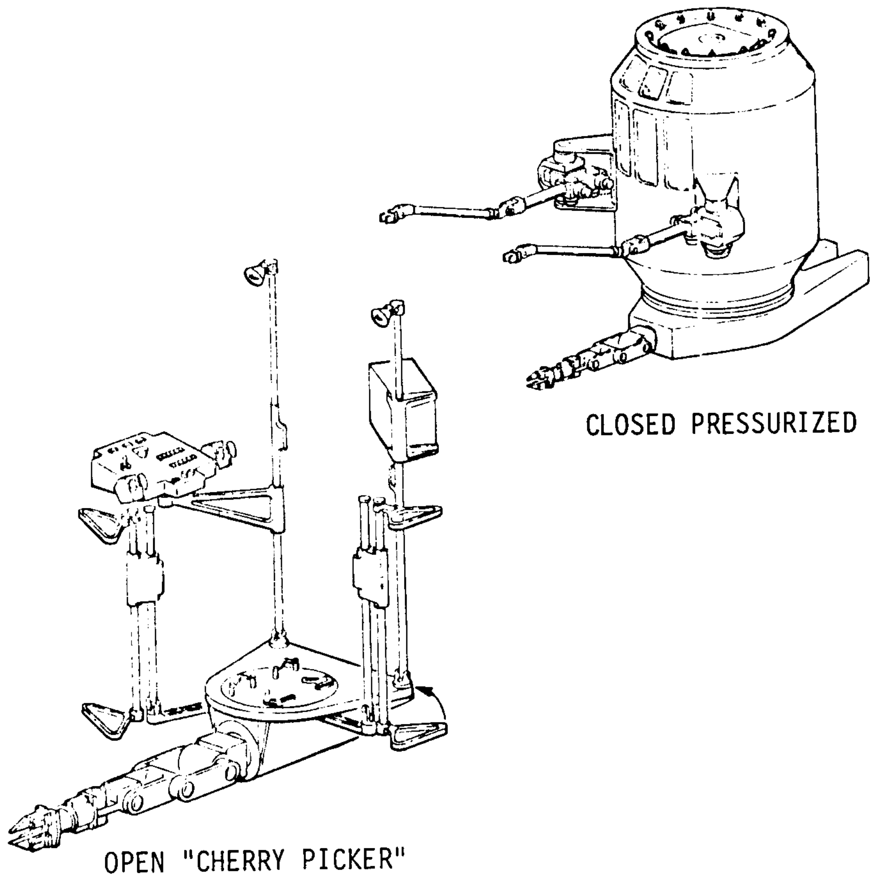


Figure A-36. Manned Remote Station Concept Configurations

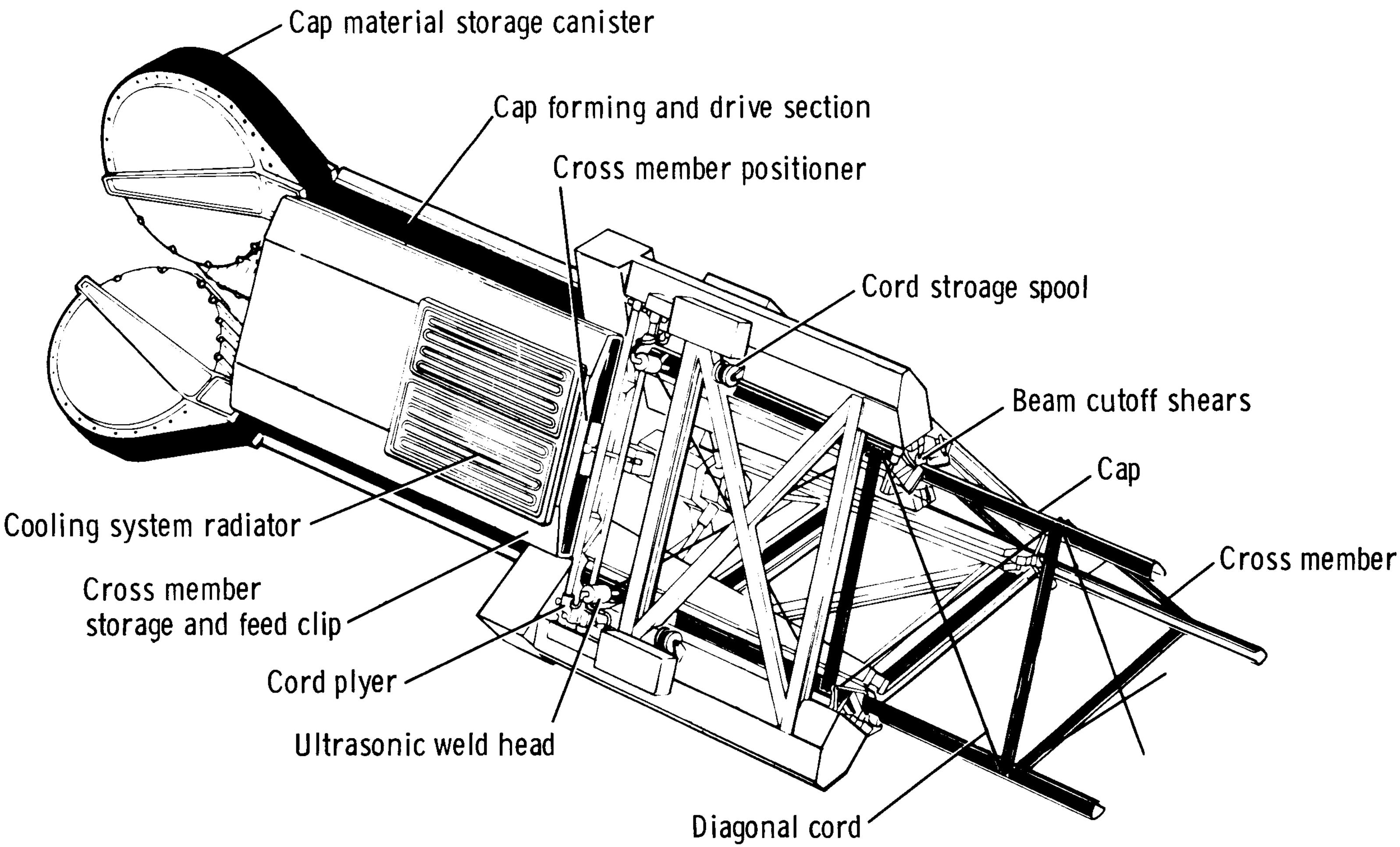


Figure A-37. Beam Builder Concept

effective radiation of waste heat. The strips can be coiled for transport and deployed and installed by construction equipment with little direct labor. Connection of power busses to solar cell blankets is less amenable to automation and may involve more CSE.

In summary, construction of the SPS represents a significant technology challenge because the size and operational location have no valid analogies. The number of parameters and options in developing concepts is almost unlimited. Analysis of construction has been concentrated in defining feasible approaches. A technology base must be developed to establish the credibility of construction techniques and of productivity and cost estimates.

2. Rectenna Construction

The initial concept of an SPS rectenna advanced by Raytheon utilized a 10 km diameter rectenna with its groundplane perpendicular to the microwave beam. This was accomplished by segmenting the groundplane into a series of tilted (relative to the ground) panels.

An in-house study (ref. 2) was conducted at JSC to further define the Raytheon concept so that materials requirements and costs could be analyzed. Primary ground rules for the study were: (1) groundplane must be perpendicular to the microwave beam, (2) maintenance of the entire area is required, (3) land must be available for other purposes, (4) terrain is flat, and (5) location is near the Houston area. The preliminary design selected was a very simple conventional structural concept and no attempt was made to optimize the structure as to concept, weight, constructability, or cost. Material selected for the structure was basically structural aluminum shapes. The unit cost for a 5 GW rectenna system was $0.60/ft$^2$ based on structural materials, construction labor, and site preparation 1975 cost indexes.

The quantities of aluminum required to construct the number of rectennas projected for the year 2000 would result in a 7 percent increase in the projected annual United States aluminum demand for the year 2000. Also, the energy required to produce the aluminum would require a longer payback time than steel. Because of this high aluminum usage, a small study contract was initiated

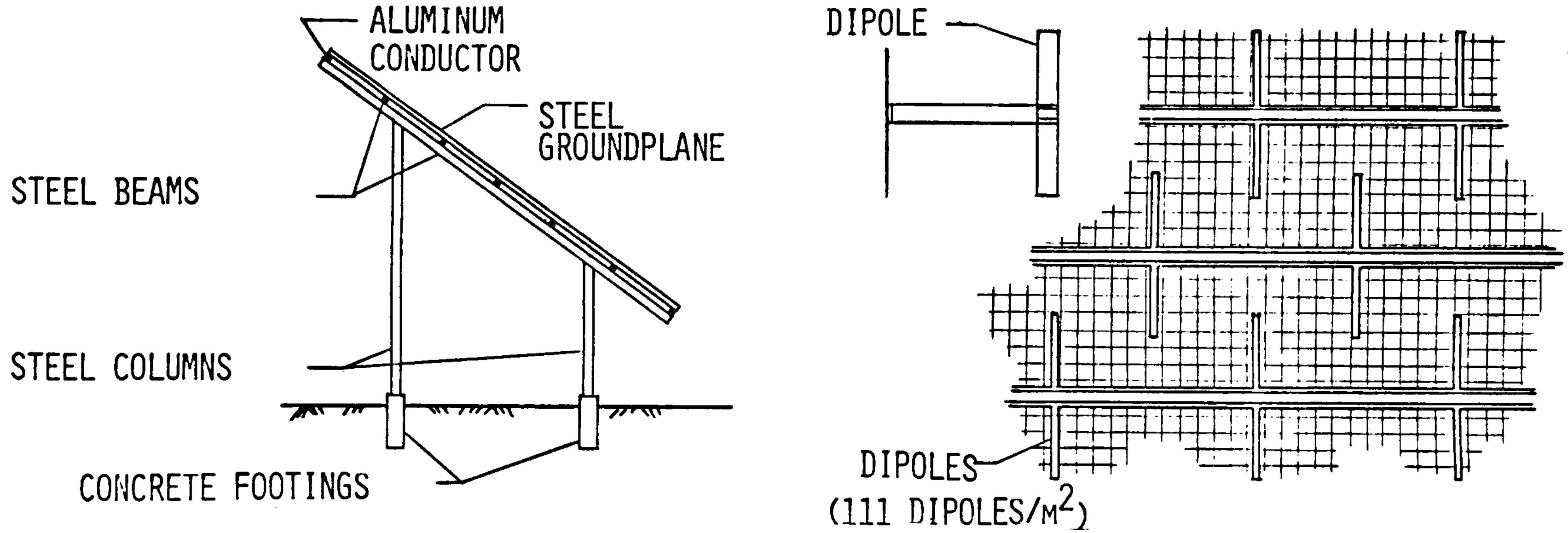


Figure A-38. Typical Rectenna Structure Sections with Bovay Engineers, Inc., of Houston (ref. 38). The basic ground rules for the study were the same as the above in-house study. Several configurations for the support structure were analyzed and materials analysis included steel, aluminum, and concrete. Figure A-38 illustrates a typical configuration. The study concluded that the least expensive material would be a galvanized or weathering steel and the cost would be $\$1.94/ft^2$ for materials and construction labor. Site preparation would add another $\$0.06/ft^2$. This study utilized conventional construction practices for determining the total cost. The only aluminum remaining in the structure is the quantity required to collect and transmit power. This reduced the year 2000 aluminum demand from the 7 percent mentioned above to 2 percent.

The present concept for the rectenna structure is based on the work done by Bovay Engineers, Inc. However, the projected costs for the structure is over 20 percent of the total SPS program. Because of this cost, this area needs further study to determine if costs can be reduced. The area believed to be the best candidate for reducing costs is construction because no automatic fabrication has been investigated for the rectenna. An artist's concept of an automatic fabrication system for the rectenna is shown in figure A-39. This concept was included in the Part III Systems Definition Study by Boeing (ref. 9). This concept (or one similar) requires further definition.

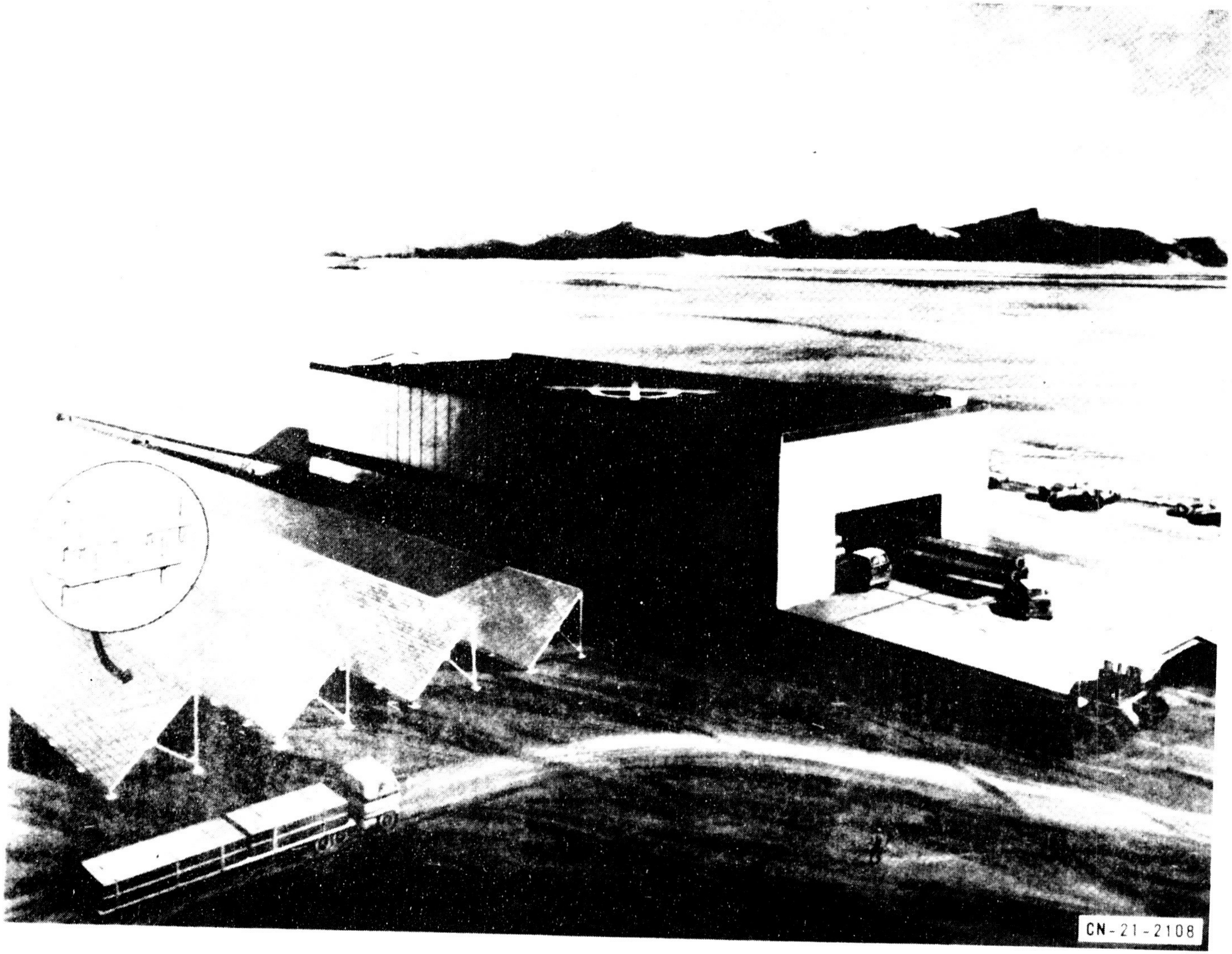


Figure A-39. Artist's Concept of Moving Rectenna Factory

## G. Natural Resources

In a program as large as the solar power satellite program which utilizes advanced technology, the selection of materials is often influenced by availability of a particular material. The material availability may be limited by total natural resource or limited by the amount of yearly production. The first program materials list was published by NASA in 1976 (ref. 2). This list is shown in column 1 table A-7. However, before that time several modifications had been made to informal working materials lists based on design changes required for supply reasons. The following is a list of significant changes prior to 1976.

1. Original concepts for photovoltaic cells utilized gold for electrical contact; however, size and number of cells required for each satellite precluded the use of gold. Designs are now using silver, copper, and aluminum in various amounts.

2. The rotary electrical joint as originally designed contained large amounts of silver. The joint was redesigned to reduce the requirement for this precious metal to less than 40 metric tons per rotary joint.

3. Both klystrons and amplitrons have been considered for use as microwave generators in the satellite. Each has advantages and disadvantages. One disadvantage to the use of amplitrons as presently designed is the 7 to 10 metric tons of platinum required (15 to 20 percent of U.S. production) in the cathode. This demand for platinum would restrict the use of amplitrons for use in the solar power satellite program. Alternative designs to replace platinum with thoriated tungsten are being pursued. Subsequent to the mid-1976 materials lists, two other significant adjustments to design have occurred because of material demand. These are as follows:

1. A redesign of the rectenna structural members eliminated over 75 percent of the aluminum from the rectenna design. The aluminum was replaced by steel--a more abundant natural resource. Further detailed design studies are being pursued to obtain the best minimum resource design for the rectenna.

2. Gallium arsenide photovoltaic cells have certain advantages over the more common silicon cells, especially in orbital applications. Early in the program, gallium arsenide cells were not strongly considered because of limited supply of gallium. This limit arises from the fact that though widely distributed, gallium is generally found in very low concentrations averaging less than 15 parts per million. Gallium is found in higher concentrations in bauxite and can be recovered in association with aluminum production. At this time, gallium recovery from bauxite is the only economically available process. Gallium arsenide cells are being considered because of technical advantages over silicon cells. However to avoid exceeding the projected availability of gallium, the gallium aluminum arsenide solar cell design was driven toward very thin cells (5 micrometers) and synthetic sapphire replaced additional gallium arsenide as the substrate material. In addition, a further demand reduction is achieved by designing a solar concentration of two into the collection system.

Table A-7 shows changes in the estimated materials requirements for the silicon systems between mid-1976 and January 1978 for both the satellite and rectenna in columns 2 and 3. In columns 4 and 5, the estimated materials requirements for the gallium arsenide system as projected in mid-1977 and January 1978 are shown.

| MATERIALS | SILICON CELL SYSTEM (CR-1) | | GALLIUM ARSENIDE CELL SYSTEM (CR-1) | |
|---|---|---|---|---|
| | AUGUST 1976 | JANUARY 1978 | SEPTEMBER 1977 | JANUARY 1978 |
| **Satellite** | | | | |
| GFRTP | 0 | 6,265 | 4,088 | 4,230 |
| Steel | 0 | 3,875 | 1,288 | 2,705 |
| Aluminum | 1,500 | 3,160 | 8,422 | 8,625 |
| Copper | 6,500 | 5,385 | 3,606 | 3,695 |
| Tungsten | 1,250 | 565 | 2 | 5 |
| Glass | 0 | 18,050 | 10 | 10 |
| Silicon | 13,500 | 7,385 | 0 | 25 |
| Gallium Arsenide | 0 | 0 | 2,513 | 2,575 |
| Teflon | 0 | 0 | 2,125 | 2,175 |
| Kapton | 7,750 | 0 | 2,836 | 2,905 |
| Sapphire | 0 | 0 | 6,222 | 6,370 |
| Silver | 0 | 15 | 1,149 | 1,390 |
| Mercury | 0 | 135 | 0 | 0 |
| Ceramics | 0 | 0 | 761 | 780 |
| Misc. & Organics | 11,750 | 3,935 | 2,618 | 400 |
| TOTALS | 42,250 | 48,770 | 35,640 | 35,860 |
| **Rectenna** | | | | |
| Concrete | $1.68 \times 10^6$ | $1.33 \times 10^6$ | -undefined- | |
| Aluminum | $0.62 \times 10^6$ | $0.14 \times 10^6$ | -undefined- | |
| Steel | 0 | $1.49 \times 10^6$ | -undefined- | |

Table A-7. 5 GW Systems (Mass in Metric Tons)

C-3

## REFERENCES

The following is a partial listing of the reports of studies dealing with systems definition of the Solar Power Satellite and related subjects. Reports are grouped by general subject. Listings under each subject heading are chronological.

Most of the reports listed are available through the National Technical Information Service. NTIS numbers are listed in parentheses after each reference if applicable. Where a series of numbers is given, the report consists of more than one volume. An "X" prefix indicates restricted distribution. These restrictions are listed in this document as follows:

N - NASA only
G - Government agencies only
GC - Government agencies and contractors only

System Definition


1. Glaser, P.E., "Power From the Sun: Its Future," Science, Vol. 162, November 22, 1968.

2. "Initial Technical, Environmental and Economic Evaluation of Space Solar Power Concepts," Johnson Space Center, JSC-11568, August 1976 (N77-16442 and 16443).

3. "Satellite Power System Engineering and Economic Analysis," Marshall Space Flight Center, TMX-73344, November 1976 (N77-15486).

4. "Satellite Power Systems (SPS) Feasibility Study," Rockwell International Corporation, SD76-SA-0239, Contract NAS8-32161, December 1976.

5. "Systems Definition of Space-Based Power Conversion Systems," Boeing Aerospace Corporation, D180-20309, Contract NAS8-31628, February 1977 (X77-10101 and 10102 (GC)).

6. "Space-Based Solar Power Conversion and Delivery Systems," Econ, Inc. and Grumman Aerospace Corporation, Contract NAS8-31308, Second Interim Report, June 1976.

7. "Solar Power Satellite System Definition Study - Part I," Boeing Aerospace Corporation, D180-20689, Contract NAS9-15196, June 1977 (N78-13099 through 13103).

8. "Solar Power Satellite System Definition Study - Part II," Boeing Aerospace Corporation, D180-22876, Contract NAS9-15196, December 1977 (N78-20156 through 20163).

9. "Solar Power Satellite System Definition Study - Part III," Boeing Aerospace Corporation, D180-24071, Contract NAS9-15196, March 1978 (N78-20164).

10. "Solar Power Satellite Concept Evaluation," Johnson Space Center, JSC-12973, July 1977 (N78-12116).

11. "Satellite Power Systems (SPS) Concept Definition Study," Rockwell International Corporation, SD78-AP-0023, Contract NAS8-32475, April 1978.

11.a. "Feasibility Study of a Satellite Solar Power Station," NAS3-16809, Arthur D. Little, Inc., NASA CR-2357, February 1974, NTIS N74-17784.

11.b. "Derivation of a Total Satellite Energy System," AIAA Paper 75-640, AIAA/AAS Solar Energy for Earth Conference, Los Angeles, Ca., April 24, 1975.

Other Concepts

12. Ehricke, Krafft A., "The Power Relay Satellite: A Means of Global Energy Transmission Through Space," Rockwell International Corporation, Report E74-3-1, March 1974.

13. "Application of Stationkept Array Concepts to Satellite Solar Power Station Design," Aerospace Corporation, ATR-76(7575)-1, Contract NAS8-31842, November 1976 (X77-10236 through 10238 (GC)).

14. Billman, K. W., W. P. Gilbreath and S. W. Bowen, "Introductory Assessment of Orbiting Reflectors for Terrestrial Power Generation," Ames Research Center, TMX-73230, April 1977 (x77-73872 (N)).

15. "Orbital Motion of the Solar Power Satellite," Otis F. Graf, Jr., Analytical and Computational Mathematics, Inc., ACM-TR-105, Contract NAS9-15171, May 1977 (N78-15148).

Power Conversion

16. "To Design Variable Orientation Solar Concentrators for Space Applications," University of Georgia, Contract NAS8-31565, October 1975 (X76-72006 through 72009 (N)).

17. "Design of Forward Lighted Solar Concentrators for Space Applications," University of Georgia, Contract NAS8-32149.

18. "Evaluation of Solar Cells for Potential Space Satellite Power Applications," Arthur D. Little, Inc., Contract NAS9-15294, June 1977 (N77-30612).

19. "Development of a Directed Energy Annealable Solar Cell System," Spire Corporation, FR-20066, Subcontract to NAS9-15196, July 1978.

Microwave Power Transmission

20. "Experiments in the Transportation of Energy by Microwave Beams," Brown, W. C., 1964 IEEE Intersociety Conference Record, Vol. 12, Part 2, 1964, pp 8-17.

21. "Free-Space Microwave Power Transmission Study, Combined Phase III and Final Report," W. C. Brown, Raytheon Report No. PT4601, Contract NAS8-25374, September 1975 (N77-16619).

22. "Reception-Conversion Subsystem (RXCV) for Microwave Power Transmission System," Raytheon Report No. ER75-4386, JPL Contract NO. 9533968, September 1975 (N76-15598).

23. "Microwave Power Transmission System Studies," Raytheon Company, ER75-4368, Contract NAS3-17835, December 1975 (N76-15594 through 15597).

24. "Electronic and Mechanical Improvement of the Receiving Terminal of a Free-Space Microwave Power Transmission System," W. C. Brown, Raytheon Company, PT-4964, Contract NAS3-19722, August 1977 (N77-31613).

25. "Microwave System Studies Affecting SPS Rectenna Performance," Gutman, Ronald J., Research performed at JSC, August 1977.

26. "Ionosphere/Microwave Beam Interaction Study," L. M. Duncan and W. E. Gordon, Rice University, Contract NAS9-15212, September 1977 (N77-33389).

27. "A Solar Power Satellite Transmission System Incorporating Automatic Beam Forming, Steering and Phase Control," LinCom, Inc., TR-7806-0977, Contract NAS9-15237, June 1978.

28. "Achievable Flatness in a Large Microwave Power Antenna," General Dynamics, Convair Div., Contract NAS9-15423, September 1978.

29. Perkins, F. W. and R. G. Roble, "Ionospheric Heating By Radiowaves: Predictions for Arecibo and the Satellite Power Station," J. Geophysical Research (to be published).

30. Holway, L. H., A. H. Katz, G. Melty, "Ionospheric Effects of a High Power Space-Borne Microwave Beam," Raytheon Technical Memorandum T-1028, Waltham, M.A., Nov. 1977.

31. Arndt, G. D. and L. Leopold, "Environmental Considerations for the Microwave Beam from a Solar Power Satellite," 13th Intersociety Energy Conversion Engineering Conference, San Diego, CA, August 1978.

Transportation

32. "Future Space Transportation Systems Analysis Study," Boeing Aerospace Corporation, D180-20242, Contract NAS9-14323, December 1976 (Vol. 1: N77-31235; Vol 2: X77-78969 (N); Vol 3: X77-79819 (G)).

33. "Orbital Propellant Handling and Storage Systems for Large Space Programs," General Dynamics Convair Div., CASD-ASP-78-001, Contract NAS9-15305, April 1978.

Orbital Construction

34. "Orbital Assembly and Maintenance Study," Martin Marietta Corporation, MCR-75-319, Contract NAS9-14319, August 1975 (N75-32144).

35. "Orbital Construction Demonstration Study," Grumman Aerospace Corp., NSS-OC-RP-008, Contract NAS9-14916, December 1976 (N77-23136).

36. "Orbital Construction Support Equipment," Martin Marietta Corporation, MCR-77-234, Contract NAS9-15120, June 1977 (N77-27157).

37. "Space Construction Automated Fabrication Experiment Definition Study," General Dynamics Convair Div., CASD-ASP-77-017, Contract NAS9-15310, May 1978 (N78-2511 through 25113).

37.a. "Large Space Erectable Structures Study," NAS9-14914, Boeing Aerospace Company, April 1977.

Rectenna Construction

38. "Feasibility Study for Various Approaches to the Structural Design and Arrangement of the Ground Rectenna for the Proposed Satellite," Bovay Engineers, Inc., Contract NAS9-15280, May 1977.

Technology Advancement

39. "Preliminary Assessment of Technology Advancement Requirements for Space Solar Power," Johnson Space Center, JSC-12702, March 1977.

Economic and Political

40. "An Initial Comparative Assessment of Orbital and Terrestrial Central Power System," R. Caputo, Jet Propulsion Lab., JPL-DOC-900-780, March 1977 (N77-22612).

41. "Impacts and Benefits of a Satellite Power System on the Electric Utility Industry," Arthur D. Little, Inc., C-80020, Contract 954639 (JPL), July 1977 (N78-24255).

42. "Political and Legal Implications of Developing and Operating a Satellite Power System," Econ, Inc., ECON-77-195-1, Contract 954625 (JPL), August 1977 (N78-25003).

43. "A Study of Some Economic Factors Relating to Development and Implementation of Satellite Power Systems, NASA-CR-150602, Contract NAS8-32698 (N78-19654).

Biological and Environmental

44. "Research Plan for Study of Biological Effects of the Solar Power Satellite Transmission System," Bernard D. Newsom and Associates, Contract NAS2-9655, March 1978.

45. "Compilation and Assessment of Microwave Bioeffects," Pacific Northwest Laboratory, AO-02-01/EA81028, Contract EY-76-C-06-1830 (DOE), May 1978.

46. "Satellite Power System Environmental Impacts - Preliminary Assessment," Floyd R. Livingston, Jet Propulsion Laboratory, 900-822, Rev. A. May 1978.

Work Breakdown Structure

47. "Satellite Power System Work Breakdown Structure Dictionary," Marshall Space Flight Center, TM-78155, January 1978.

APPENDIX B

CONTRACTED SYSTEM DEFINITION STUDIES

1. ROCKWELL INTERNATIONAL

2. BOEING AEROSPACE COMPANY

## 1. ROCKWELL INTERNATIONAL

The following is a description of the SPS concept produced by Rockwell International under contract to the NASA Marshall Space Flight Center. A documentation roadmap is provided at the conclusion of this section to aid the reader in locating more detailed information from study reports.

### A. Guidelines and Assumptions

The guidelines and assumptions for this study were essentially the same as for the Reference System.

### B. System Overview

The system definition includes satellite, ground and space systems, and transportation and their relationship.

The satellite system concept is illustrated in Figure R-1. Solar energy is converted to electrical energy using solar arrays having reflectors that concentrate the energy onto the solar cells. The solar cells convert the solar energy to dc electrical energy which is conducted to a centrally located microwave antenna. The microwave antenna transforms the dc power to RF microwave. Key features of this design concept include use of concentrators (CR=2), gallium-aluminum-arsenide solar cells, three trough configuration designs, tension web/compression frame antenna structure, klystron dc-RF microwave converters, aluminum structural material, a single, center mounted antenna, GEO construction, 45.5 kV power distribution, and subarray phase control.

Each rectenna is designed to accept power from a single satellite and provide 5 GW of power to the utility interface. A typical rectenna site located at 34°N latitude covers an elliptical area 13 km in the north-south direction by 10 km in the east-west direction. This area provides an active intercept area of 78.2 $km^2$. A phased array comprised of strip line patterns of bow-tie dipoles was selected. This selection was based primarily on the increased efficiency and decreased diode count obtained using this approach. The support structure employs preformed hat sections, standard I-beams, and 3.5 inch diameter tube braces. The I-beams and braces support the structure on concrete piers.

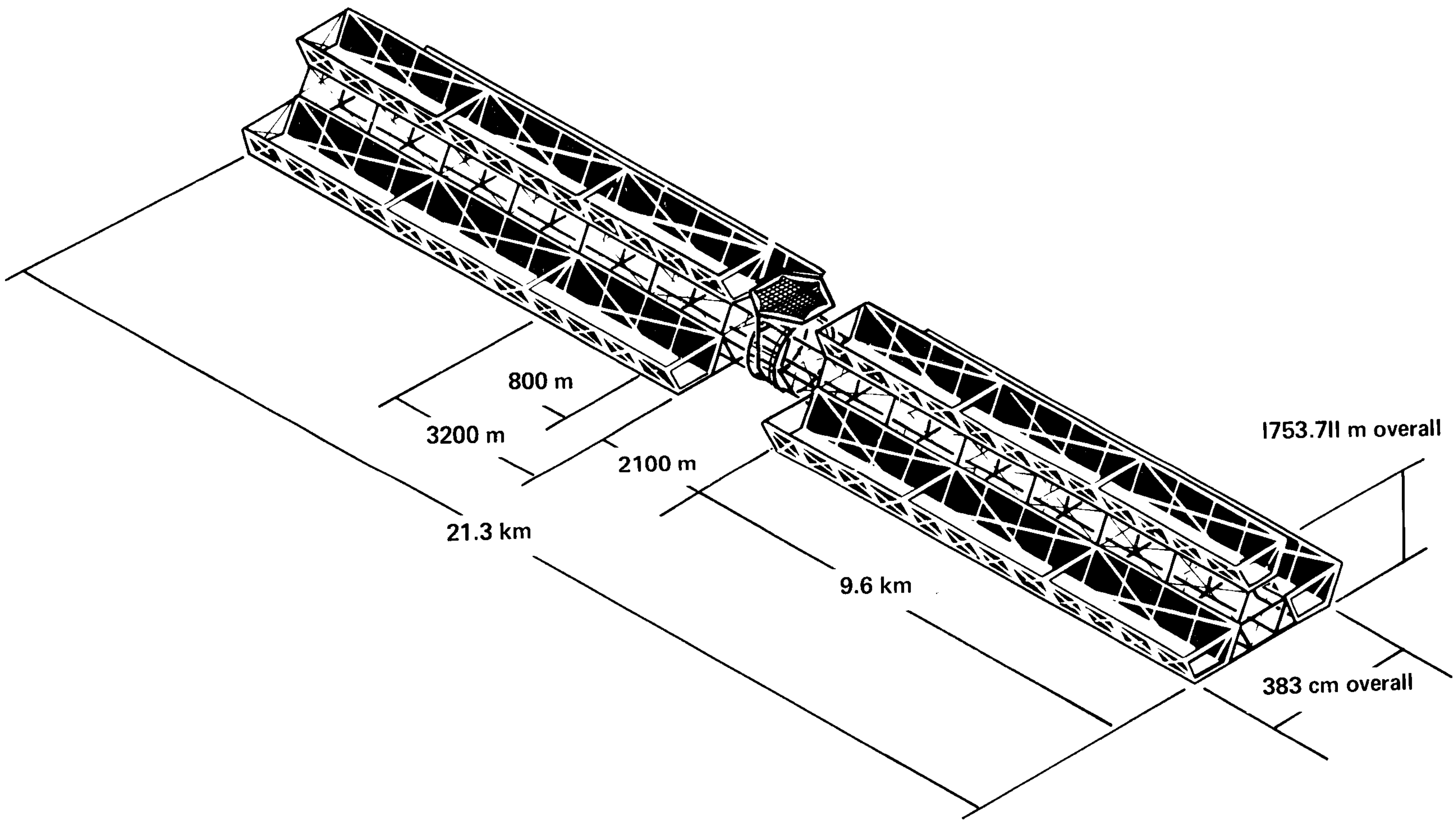


Figure R-1. Photovoltaic Power Design Concept

The transportation system selected for the point design includes: (1) a horizontal takeoff HLLV (one or two stage) for earth to LEO operation; (2) a dedicated electric ion thruster OTV for cargo transport; (3) a two stage $LO_2/LH_2$ OTV for personnel and priority cargo transport; and (4) a single-stage $LO_2/LH_2$ vehicle for orbit transfer (short distance and small $\Delta V$)of personnel and cargo. These elements are illustrated in a low earth orbit scenario in Figure R-2. An alternative 2 stage vertical takeoff earth to LEO operation has also been defined as a viable option for SPS. The electric ion thruster OTV utilizes the satellite solar array design of GaALAs solar cells at a concentration ratio of 2.

The basic approach for satellite construction assumes that the entire satellite is constructed in geosynchronous orbit and that the necessary construction material is transported from low earth orbit to GEO using the OTV's. The OTV's are constructed in LEO.

Three orbital bases have been identified to support GEO construction: (1) satellite construction base; (2) operations and maintenance base; and (3) low earth orbit base.

A crew size of 640 has been established for accomplishing the construction in a scheduled 90 days. An additional crew of 20 has been estimated for satellite maintenance and operations.

A description of the system and subsystems is given in Table R-1.

Figure R-3 shows the end-to-end efficiency chain for the system which has been sized to provide 5 GW of electrical power to the utility busbar. With an overall efficiency of 6.29 percent, it is necessary to size the solar arrays to intercept 79.0 GW of solar energy. The quoted efficiency is the minimum efficiency, including the worst-case seasonal variation (91%), the end-of-life (30-year) concentrator reflectivity (91.5%), and the end-of-life (30-year) solar cell efficiency (15.4%).

C. Solar Cells and Blankets

Figure R-4 shows the solar array blanket description and array characteristics. The point design utilizes a GaAlAs solar cell efficiency of 20-percent

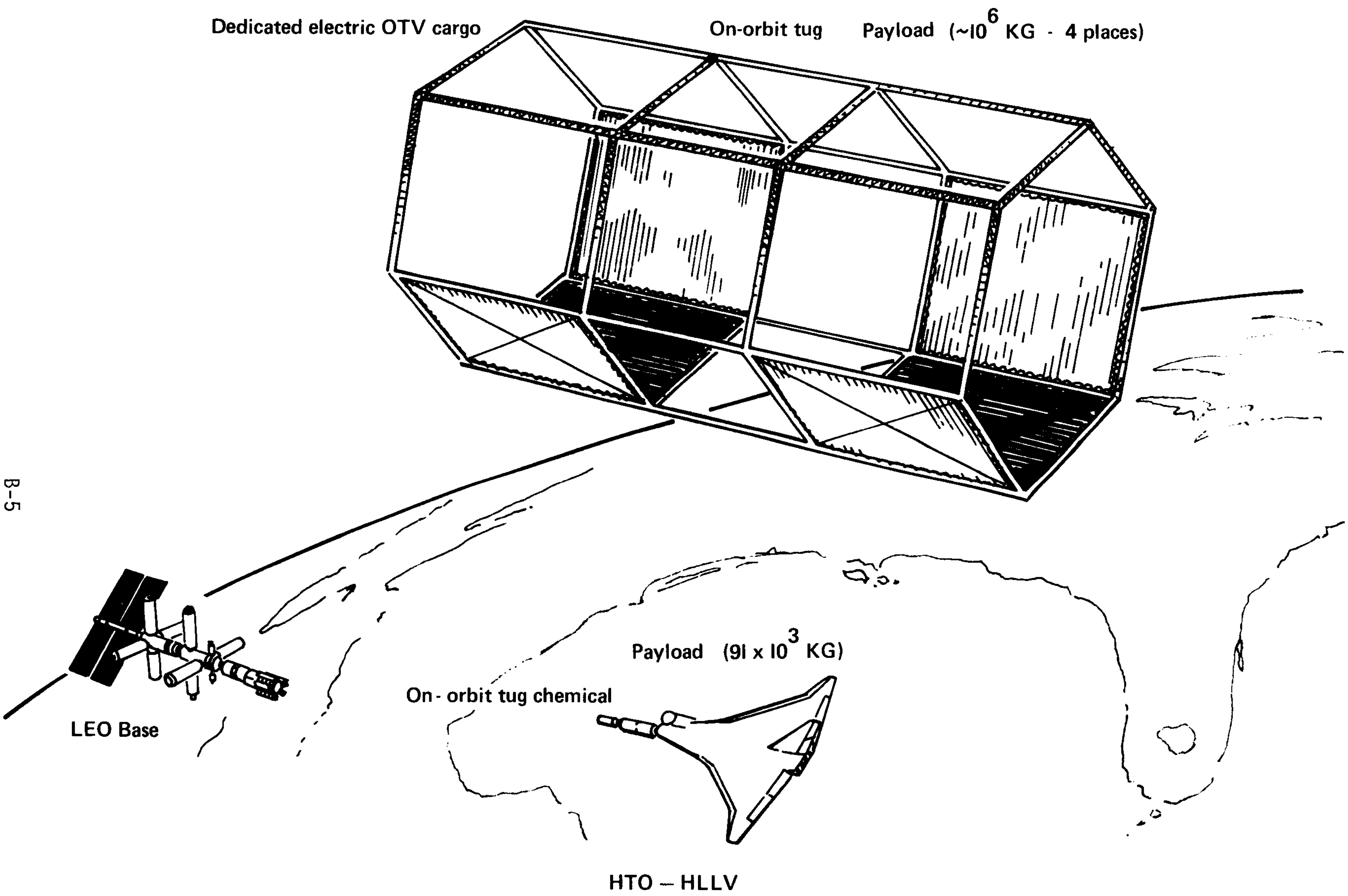


Figure R-2. Selected Transportation System Concept

## Table R-1. Photovoltaic Point Design Characteristics

**Overall Description**

- 5–GW power to utility interface
- Geosynchronous construction location
- Single microwave antenna
- Geosynchronous equatorial operational orbit

**Subsystems**

Power conversion
- GaAlAs solar cells
- Concentration ratio = 2

Attitude control/stationkeeping
- Y – POP, X – IOP
- Argon ion thrusters

Power distribution
- 45.5 KV DC
- Structure/wiring not integrated

Microwave antenna
- Gaussian beam
- 2.45 – GHz frequency
- Subarray phase control
- RCR waveguide panels
- Tension – web, compression frame structure

Structure
- Aluminum (graphite/thermal plastic alternate as needed)
- Beam machine construction

Information management
- Distributed

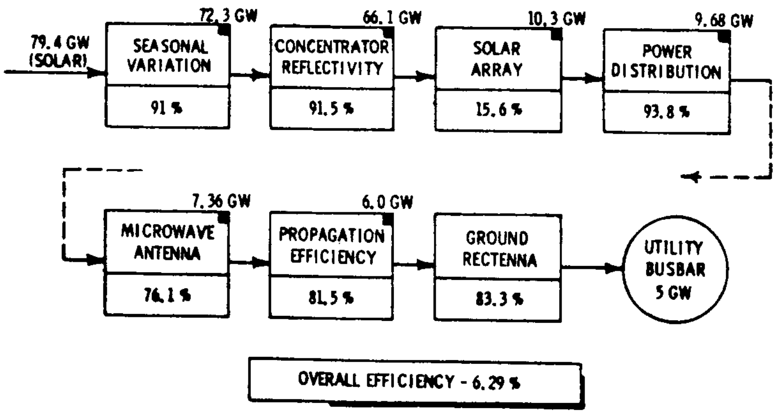


Figure R-3. *Photovoltaic Point Design End-of-Life Efficiency Chain*

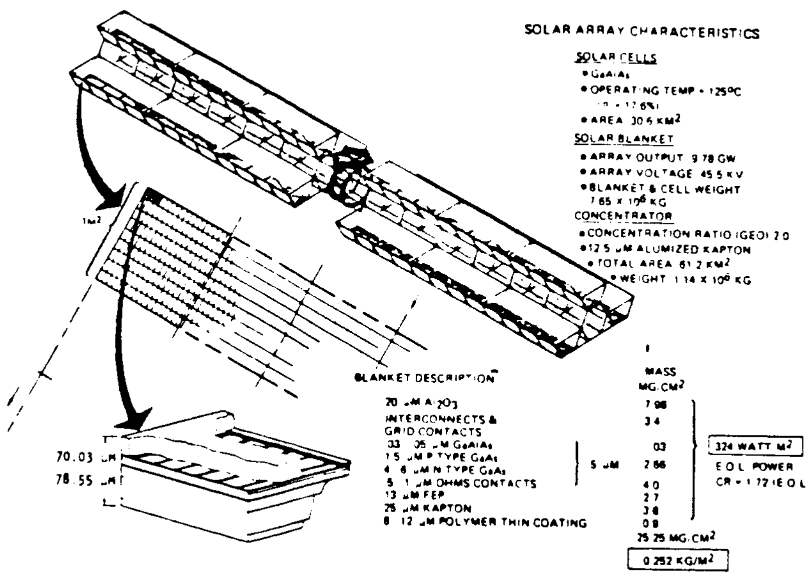


Figure R-4. *Photovoltaic Energy Conversion System*

AMO, 28°C, and the sizing of the array is based on 125°C operating temperature (18.2% cell efficiency). The total output of the array is 10.3 GW with a voltage output of 45.5 kv for each array panel. The solar blanket weight is 7.65 x $10^6$ kg, and the total array weight (including the concentrator) is 8.83 x $10^6$ kg. This weight is based on a specific weight for the blanket of 0.25 kg/$m^2$ and 61.2 x $10^6$ $m^2$ cell area. A cross-section of the solar cell is also shown (Figure R-4). The 20-μm synthetic sapphire ($Al_2O_3$) substrate, used in an inverse orientation, also acts as the cell cover.

The solar blanket layout is shown in Figure R-5. The solar panel in the top trough (effective cell area) measures 600 x 750 m x 2 for 900,000 $m^2$. Twelve panels are required for the top trough. The panels for the two lower troughs are slightly smaller in width and measure 550 x 750 m x 2 for 825,000 $m^2$ (effective cell area). Twenty-four panels are required for the bottom troughs. The total deployed solar area for the SPS is 30.6 x $10^6$ $m^2$ which is comprised of 10.8 x $10^6$ $m^2$ in the top troughs and 19.8 x $10^6$ $m^2$ in the bottom troughs.

The basic building block is a 1 $m^2$ module configuration and the cells are connected together in a series parallel arrangement. The voltage output of each 1 $m^2$ module is 30.3 V with a current of 11.11 amps. The module output is calculated to be 336.6 W/$m^2$ at the end of life.

D. Solar Array and Structure

Reflectors - Thin reflector membranes are used on the SPS to reflect the sun onto the solar cell surfaces and obtain a nominal concentration ratio of 2. The reflector is made of 12.5 μm (0.5 mil) aluminized Kapton. Reflectivity of the reflector was taken at 0.9 BOL and 0.72 EOL. The reflector membrane has a mass of 0.018 kg/$m^2$. The reflective membranes are mounted on the structure using attachments and tensioning devices. Tensioning based on structural limit of the existing beam design (with safety factor of 1.5) indicates that tensioning of up to 75 psi can be used.

The selected design concept is the 60° Vee trough configuration. The point design solar array sizing allows for 20% reflectivity degradation over 30 years. Figure R-6 presents a cross-sectional view of the satellite.

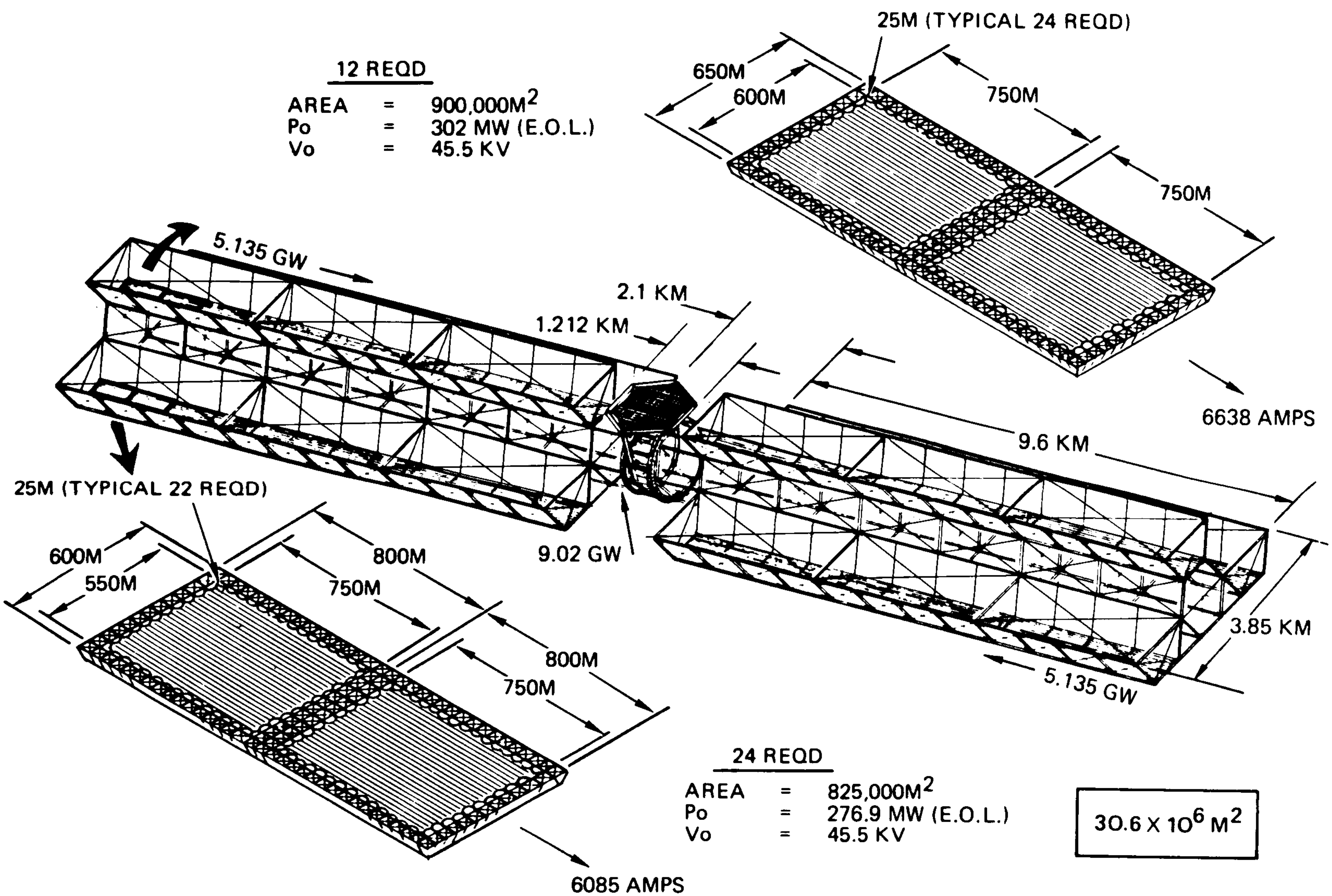


Figure R-5. Solar Blanket Concept

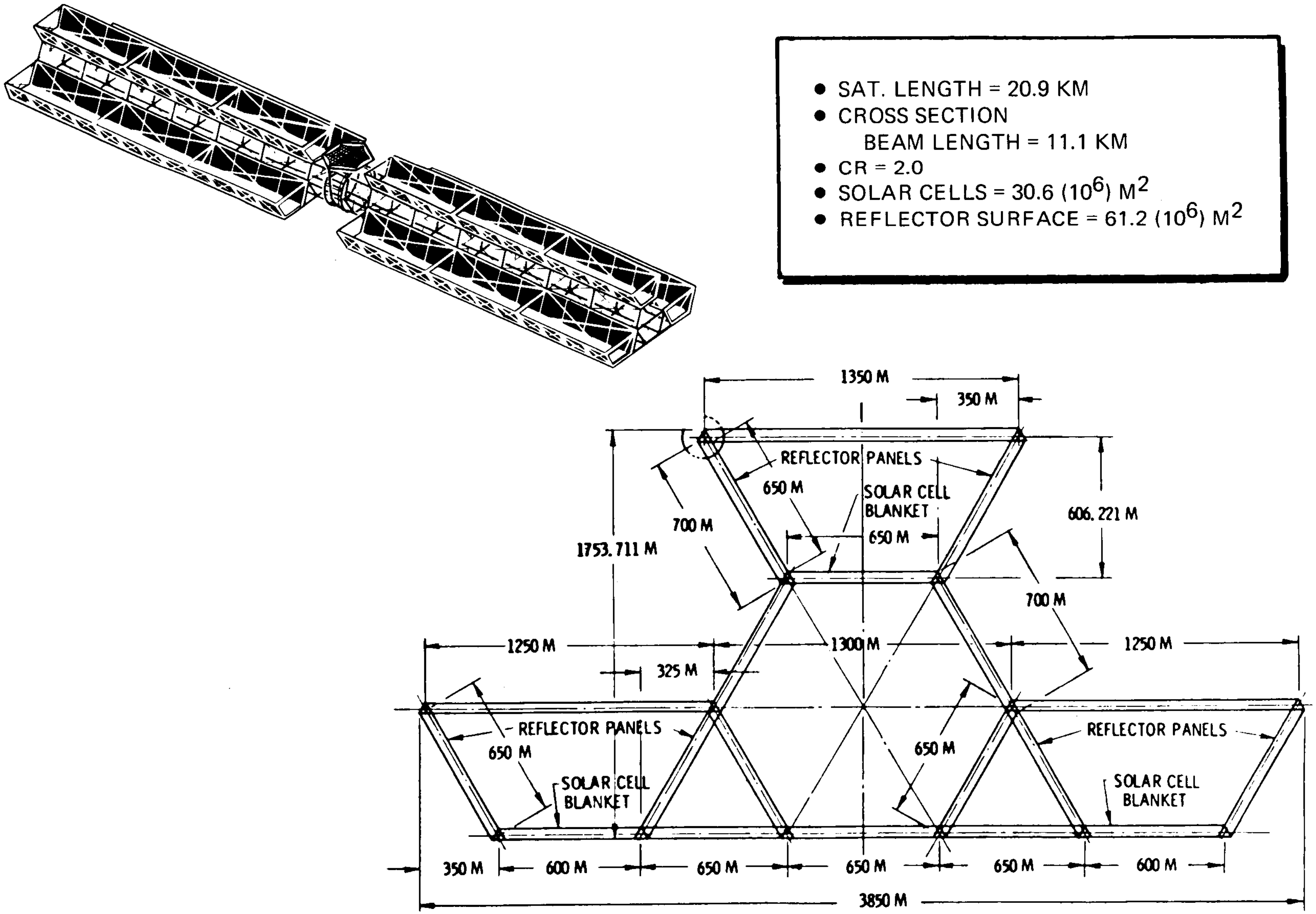


Figure R-6. SPS Structural Cross Section (60°)

Structure - Figure R-7 shows the configuration of the SPS point design solar array wing structure. The concept is a three-trough, two-tier system. The structure is made up of tri-beam girders whose longitudinal members and transverse struts are fabricated on orbit by a beam machine. Shear stabilization of the tri-beam girders and the wing itself is achieved by the use of X-tension cables. Current structure material is structural aluminum. Excessive stresses and/or deflections could drive the material selection to the regime of composites. The dimensions indicated have been verified to be adequate when the vehicle is subjected to operational forces and torques environment in geosynchronous orbit in that they result in an acceptable margin of safety for a basic material thickness of 0.254 mm (0.010 in.), which is considered minimum gauge.

The girder is 50 m on a side, and each bay is 50 m in length, stabilized by X-tension ties. The three longitudinal elements and the transverse struts, are formed by basic beam elements fabricated on orbit by a beam machine. The basic beam element is 2 m on a side with transverse struts every 2 m and modified triangular cap sections at the vertices. The cap sections, transverse struts, and X-tension braces are made from three sheets of 0.254 mm (10 mil) 2000 series aluminum, with approximately 88 percent cutouts, which is roll-formed, flanged, and welded by the beam machine to form a basic beam element 2 m on a side.

E. Power Collection and Distribution

A flow diagram of the overall power distribution subsystem is presented in Figure R-8. Power obtained at the subarray is transferred to a summing bus through a switch gear (SG) and manually operated circuit-breaker. Power is then transferred from the nonrotating member to the rotating member of the rotary joint through slip rings and brushes. On the rotating member, power is conducted through switch gears to dc/dc converters which output the five primary voltages required by the klystrons. Each voltage is conducted to a summing bus through a switch gear. Subsequently, each voltage is conducted from the summing buses to the 135,864 klystrons.

A more detailed schematic block diagram of the power distribution subsystem on the array or nonrotating portion of the satellite is presented in Figure R-9.

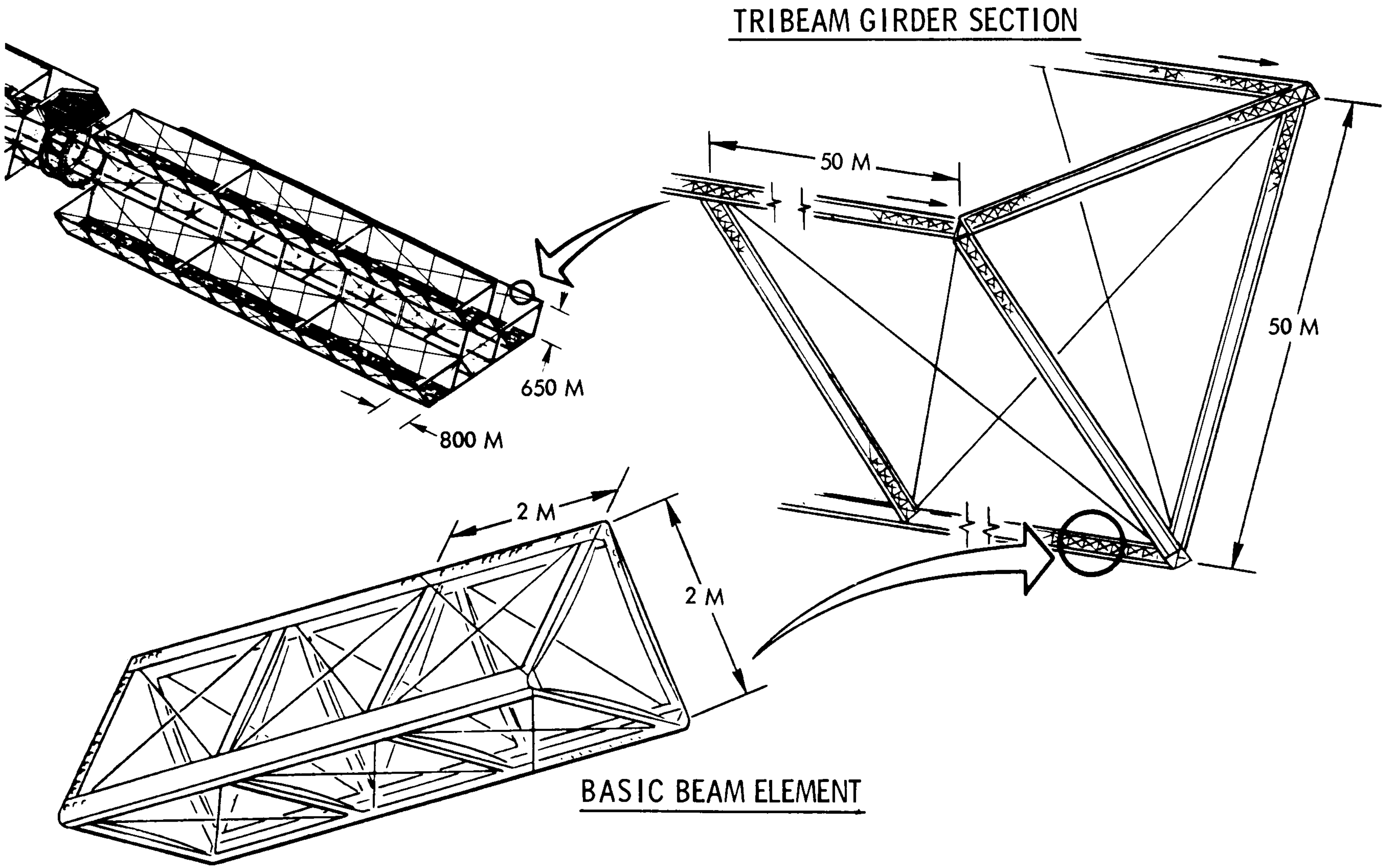


Figure R-7. Photovoltaic Wing Structure

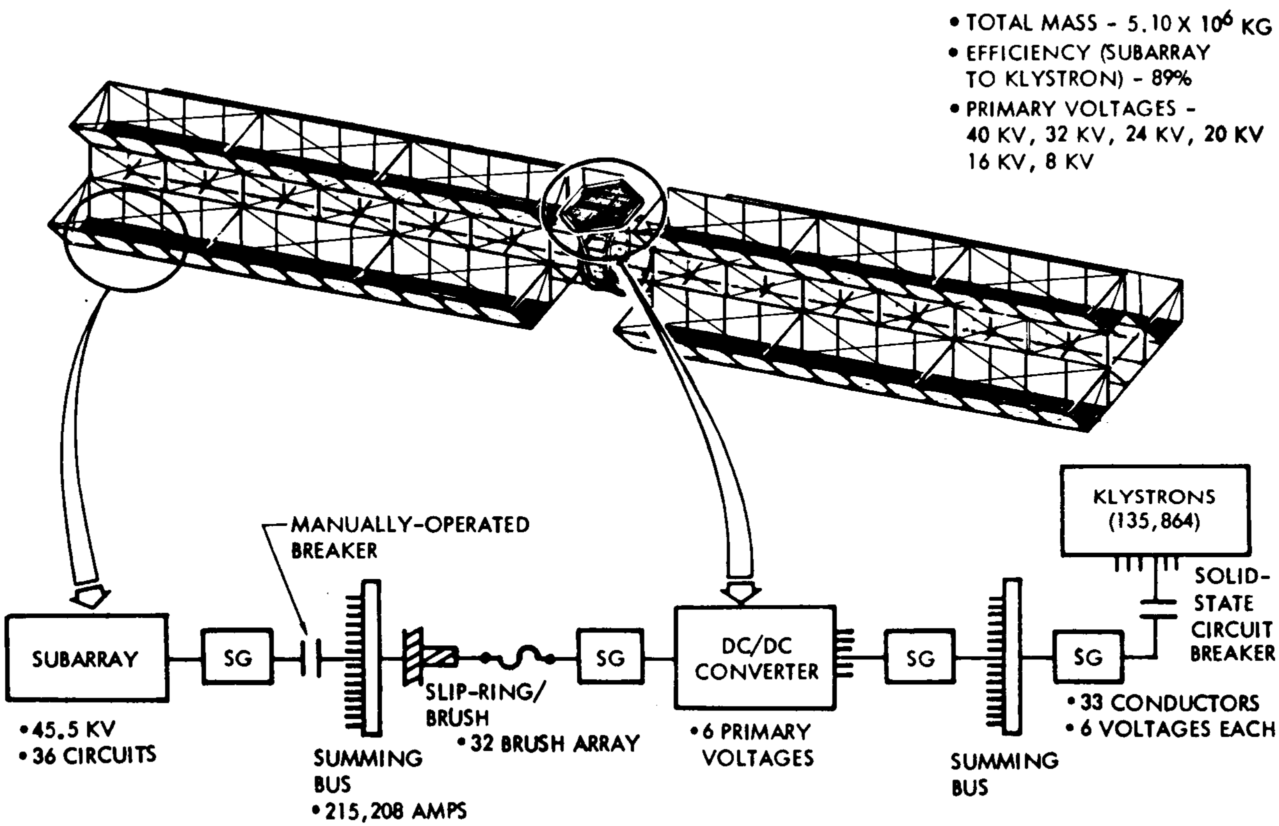


Figure R-8. Overall Photovoltaic Power Distribution Subsystem

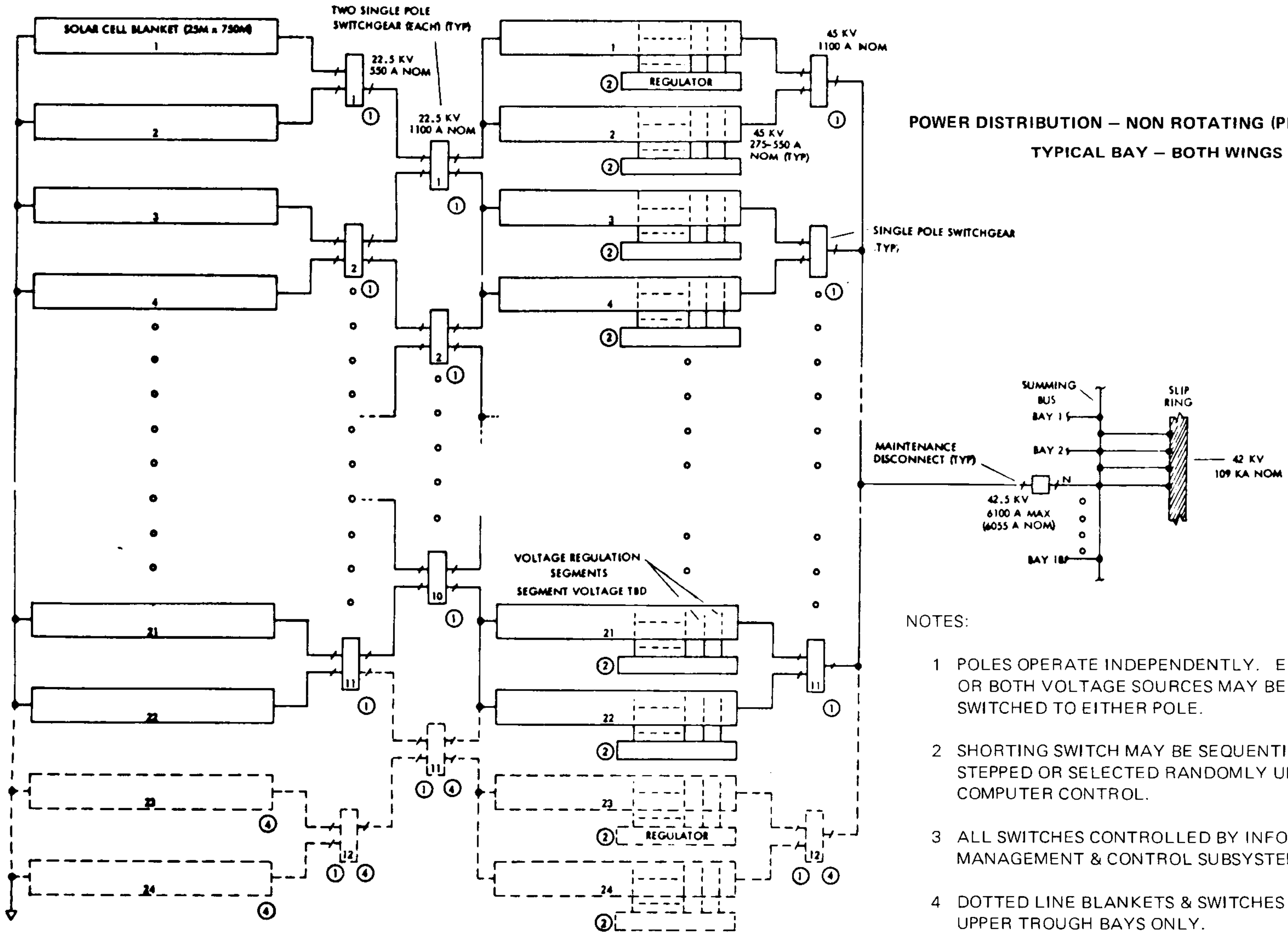


**POWER DISTRIBUTION – NON ROTATING (PRELIMINARY)**

**TYPICAL BAY – BOTH WINGS**

NOTES:

1 POLES OPERATE INDEPENDENTLY. EITHER OR BOTH VOLTAGE SOURCES MAY BE SWITCHED TO EITHER POLE.

2 SHORTING SWITCH MAY BE SEQUENTIALLY STEPPED OR SELECTED RANDOMLY UNDER COMPUTER CONTROL.

3 ALL SWITCHES CONTROLLED BY INFORMATION MANAGEMENT & CONTROL SUBSYSTEM.

4 DOTTED LINE BLANKETS & SWITCHES USED ON UPPER TROUGH BAYS ONLY.

Figure R-9. Power Distribution-Non-Rotating (Preliminary) Typical Bay - Both Wings

Included on the schematic are the switching and regulating switch gear. The latter function being accomplished by selective shorting of the last segments of the 45.5 kV blanket to assure voltage outputs compatible with summing bus voltage characteristics.

F. Rotary Joint

Mechanical - The rotary joint attached to the hexagonal center carry-through structure is illustrated in Figure R-10. The joint consists of a double set of inner stationary and outer rotating rings. The rings are modified 50-m tri-beam girders fabricated on orbit by beam machines. Rotary joint dimensions are noted in the Figure.

Electrical - The rotary joint is utilized to transfer energy through slip rings and brushes from the satellite fixed member to the satellite rotating member upon which the microwave antenna is located. The rotary joint assembly design characteristics are given in Table R-2.

G. Attitude Control System (ACS)

Figure R-11 shows an ACS employing high-performance electric thrusters, and use of the Y-POP, X-IOP orientation and inertia balancing to minimize attitude control propellants. This approach employs eight RCS quads. The total RCS propellant requirements (see table) are low, due primarily to the high specific impulse (13,000 s) which is believed to be feasible with the argon ion bombardment thrusters.

The ACS attitude reference determination system features charge-coupled device (CCD) star and sun sensors as well as electrostatic or laser gyros and dedicated microprocessors. Five attitude reference determination units are at various locations on the spacecraft to sense thermal and dynamic body bending and to desensitize the system to these disturbances. The control algorithms will feature statistical estimators for determining principal aixs orientation, body-bending state observers or estimators, and a quasi-linear RCS thrust command policy to provide precise control and minimize structural bending excitation. The ACS hardware mass is very small relative to the 30-year propellant requirement.

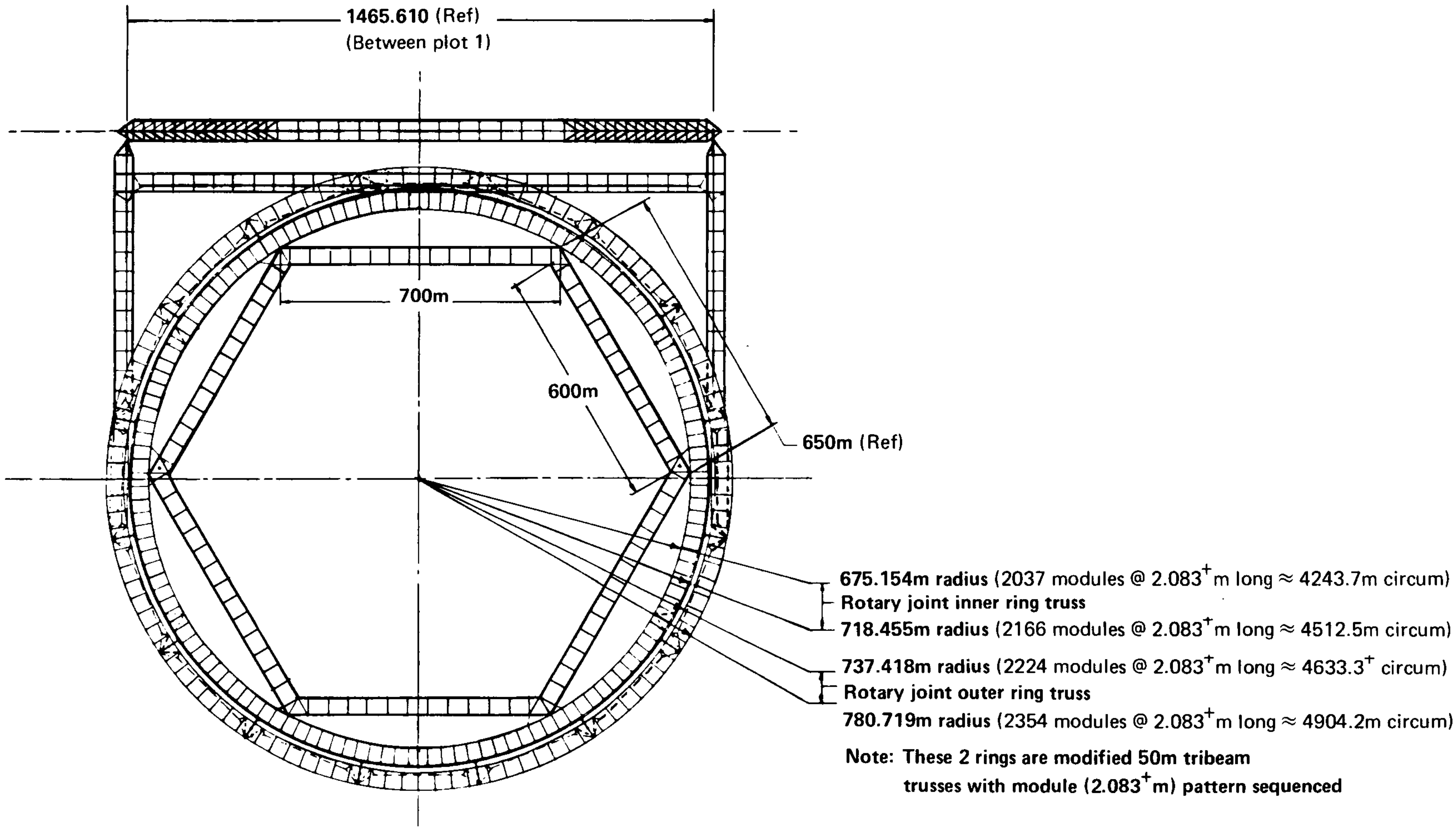


Figure R-10. Rotary Joint Dimensions

Table R-2. *Rotary Joint Design Characteristics*

| | |
|---|---|
| **TOTAL ASSEMBLY** | |
| OPERATING VOLTAGE (kV) | 42.9 |
| AMPS PER RING ASSEMBLY | 113,000 |
| TOTAL MASS (kg) | 173,400 |
| **SLIP RINGS (4)** | |
| CORE | ALUMINUM |
| CLADDING | COIN-SILVER |
| CORE SIZE ($cm^2$) | 41.3 (CROSS SECTION) |
| DIAMETER (km) | 1.13 |
| LENGTH (km) | 3.55 |
| **SHOE BRUSH (16/SLIP RING ASSEMBLY)** | |
| MATERIAL | 75% Mo Sz, 25 Mo + Ta |
| SHOE SIZE | 11.7 cm × 12.7 cm × 3 m |
| CURRENT ($A/cm^2$) | 7.75 |
| CONTACT AREA ($cm^2$) | 8.68 |
| QUANTITY | 64 BRUSHES PER SHOE ASSY |
| **GROUNDING** | |
| SINGLE POINT - COPPER BUS (THERMAL ISOLATED FROM STRUCTURE) | |

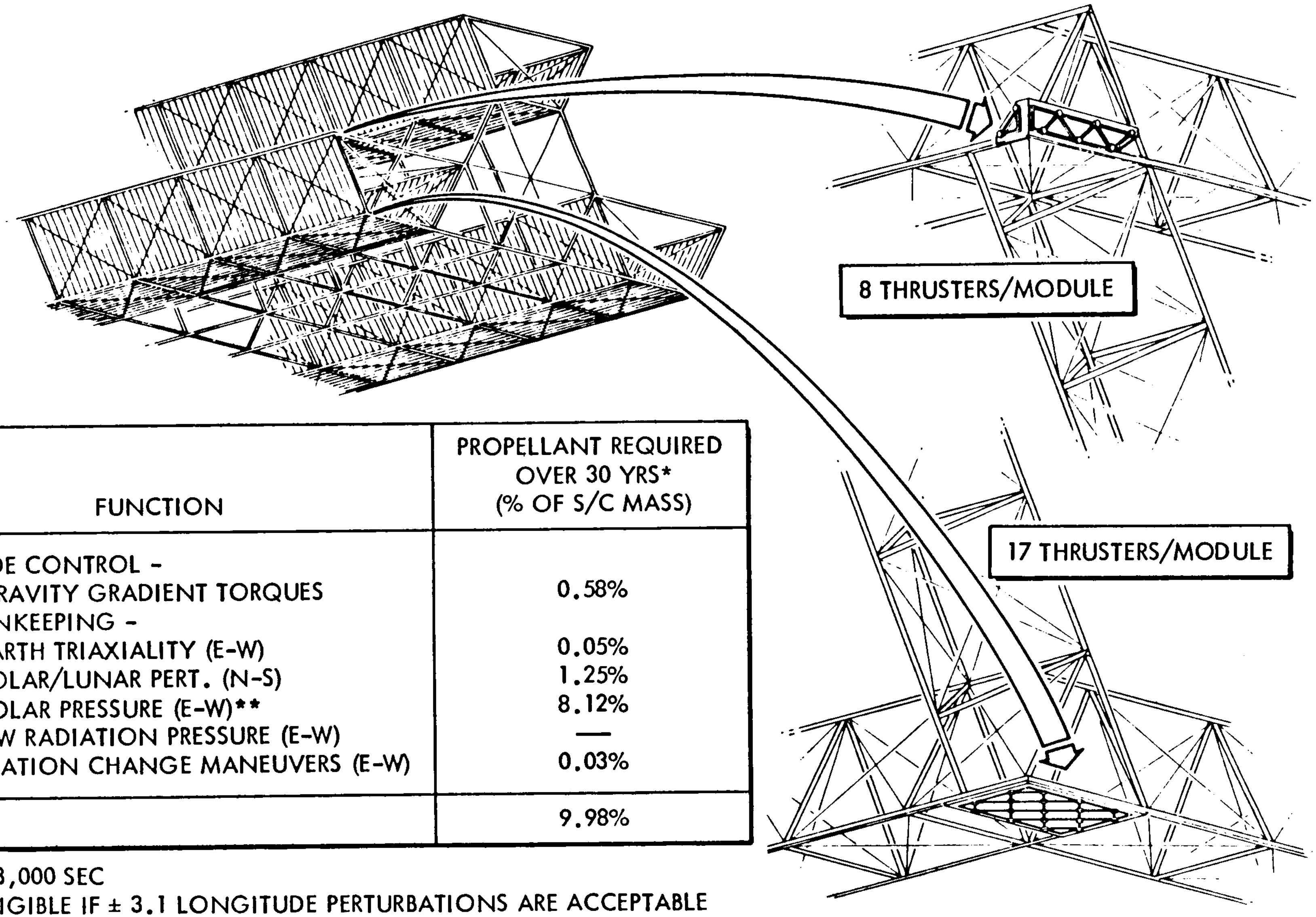


| FUNCTION | PROPELLANT REQUIRED OVER 30 YRS* (% OF S/C MASS) |
|---|---|
| ATTITUDE CONTROL - | |
| • GRAVITY GRADIENT TORQUES | 0.58% |
| STATIONKEEPING - | |
| • EARTH TRIAXIALITY (E-W) | 0.05% |
| • SOLAR/LUNAR PERT. (N-S) | 1.25% |
| • SOLAR PRESSURE (E-W)** | 8.12% |
| • MW RADIATION PRESSURE (E-W) | — |
| • STATION CHANGE MANEUVERS (E-W) | 0.03% |
| TOTAL | 9.98% |

*$I_{sp}$ = 13,000 SEC
** NEGLIGIBLE IF ± 3.1 LONGITUDE PERTURBATIONS ARE ACCEPTABLE

Figure R-11. Photovoltaic Attitude Control and Stationkeeping Subsystem

## H. Microwave Power Transmission System

Satellite Antenna - The basic satellite antenna configuration is shown in Figure R-12. Three main components comprise the structure - a tension web made from composite wires or tapes, a catenary cable that transfers the web tension to the vertices of the third component which is a hexagonal compression frame. Midspan deflections of approximately one meter are acceptable with the resulting misalignment being compensated by electronic beam steering.

The smallest antenna building block is the power module, which varies in size from the one illustrated (which is used at the center portion of the antenna) to 3.40 by 5.82 meters at the periphery of the antenna. Ten different power module sizes are used to comprise the antenna. Each power module has a klystron located in its center. The power modules are arranged into subarrays measuring 10.2 by 11.64 meters. Each subarray has its own phase control electronics. Nine subarrays are connected to form a mechanical module 30.62 by 34.92 meters. The mechanical modules are attached to the tension webs.

Antenna Structure - The tension web compression frame antenna structure concept, shown in Figure R-13, consists of three major elements (1) the tension web to which the dc-to-RF conversion and transmission hardware is attached, (2) a catenary rope system which is attached to the perimeter of the tension web, and (3) a hexagonal compression frame. The tension web resists the lateral pressure loading described in Figure R-14. The loading is transmitted to the vertices of the hexagonal compression frame via the catenary rope system. The compression frame members are loaded in pure compression and can be analyzed as columns. Three of the six catenary-to-compression-frame vertice attachments are fixed. The other three attachments at every other intersection have lateral adjustment jacks. The three fixed attachments describe a plane perpendicular to the desired boresight, and the adjustable attachments maintain the tension web as a flat surface. All six catenary rope/compression frame attachments have in-plane tensioning devices which maintain the tension web flat within the design limits. Antenna elevation (north-south) adjustments are accomplished by gimbals in the trunnion structure which attaches the antenna to the rotary joint. Azimuth adjustments are made by the rotary joint.

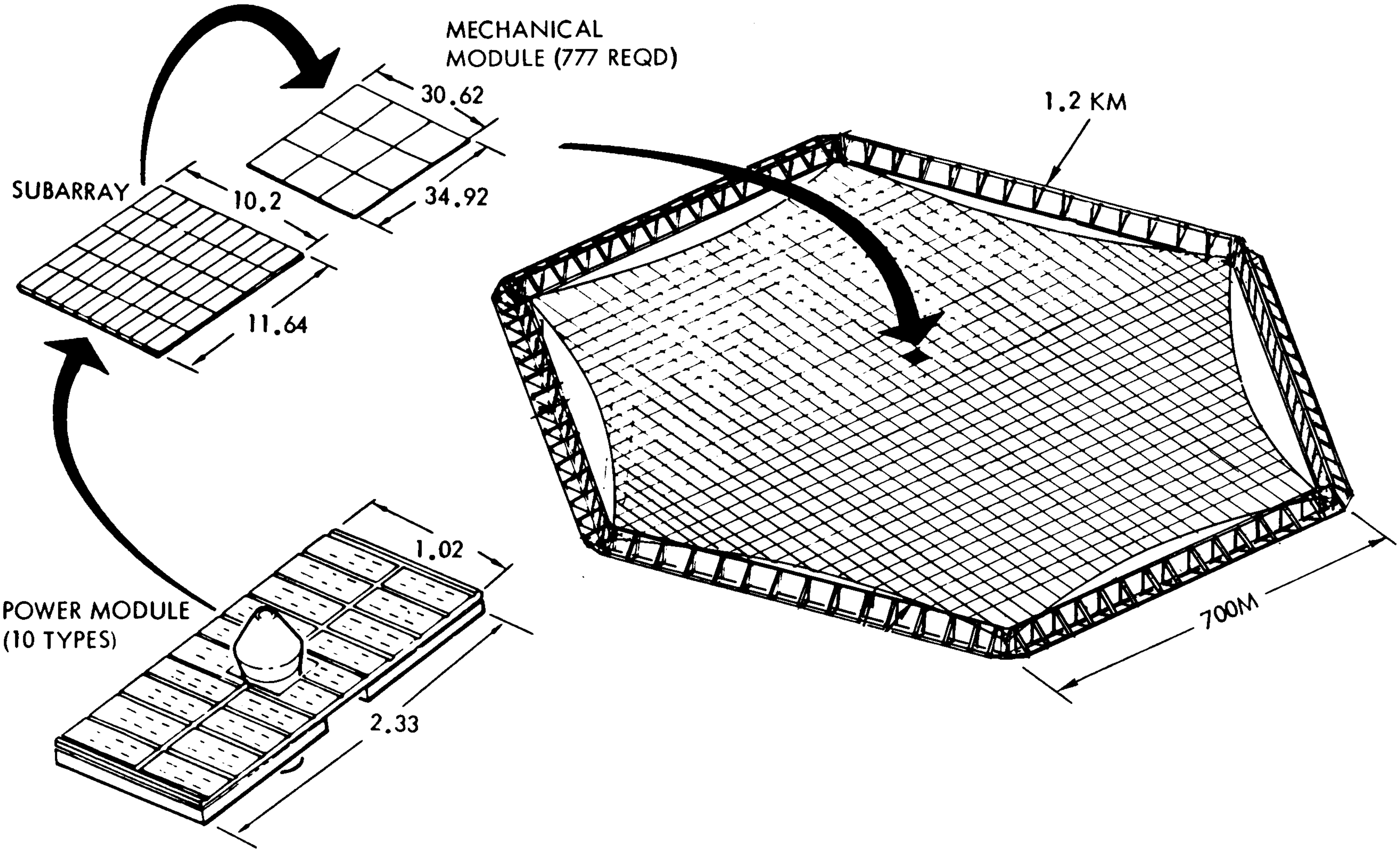


- Aluminum compression frame
- Composite tension web
- 21 KW/m$^2$ radiation at center
- 50 KW per klystron (136,000 klystrons)

Figure R-12. Satellite Antenna

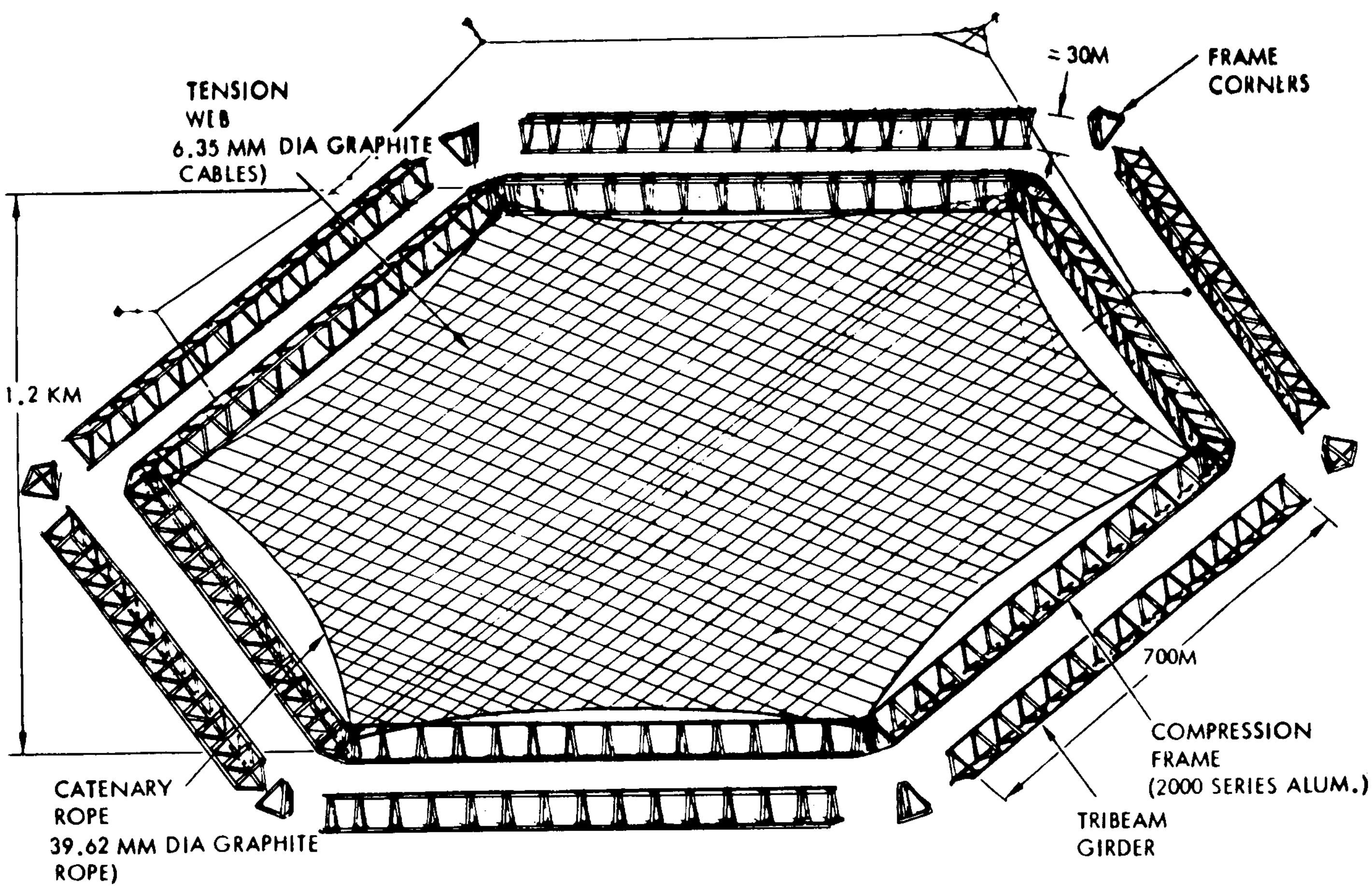


Figure R-13. Microwave Antenna Structure - Selected Design Concept

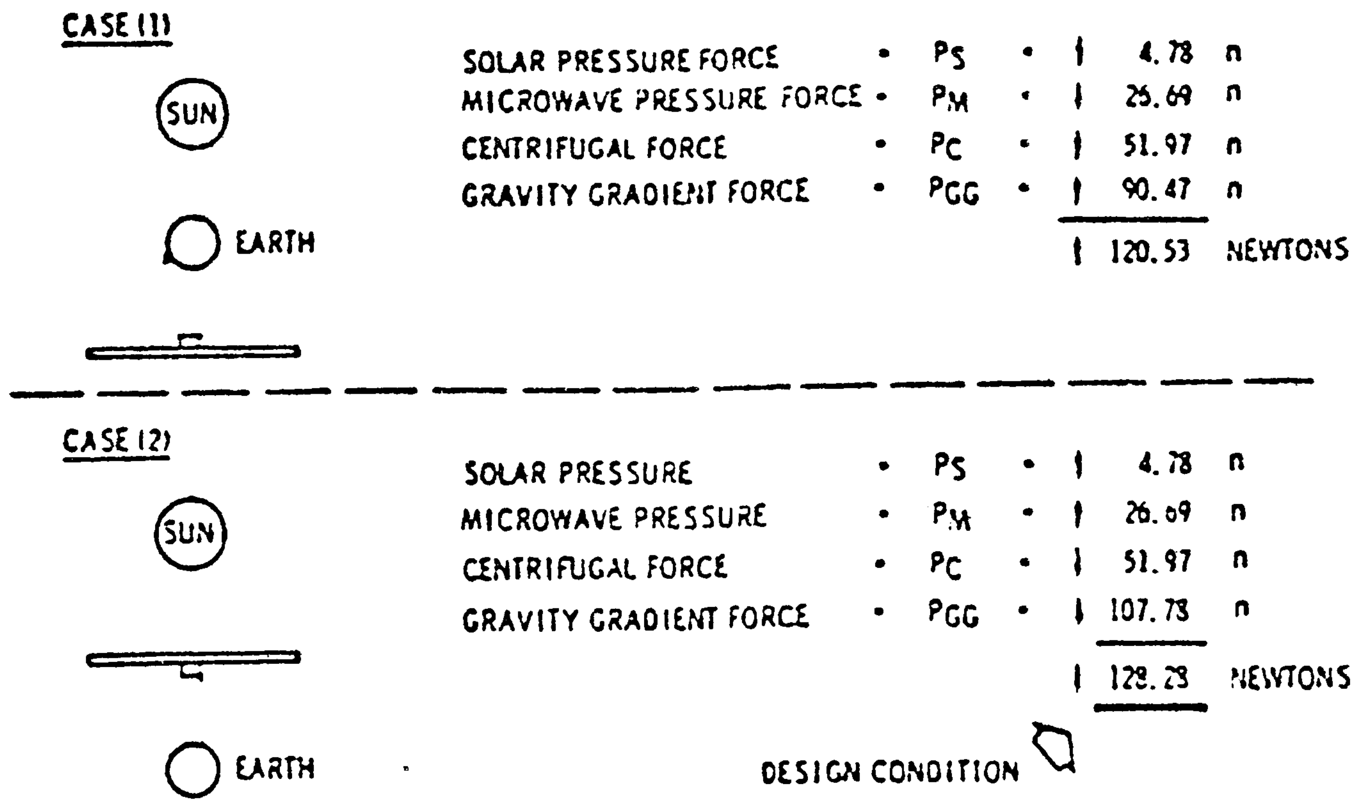


Figure R-14. Microwave Antenna Structure Design Condition

The basic design requirements for the compression frame tension web concept are as follows:

- o 1-km diameter surface (or equivalent)
- o Web angular misalignment: $\pm 0.08°$ under environmentally and operationally induced loads and temperatures
- o Optimize for light weight
- o Compatible with on-orbit fabrication and assembly
- o Compatible with operational equipment
- o Service life: >30 years

The tri-beam girder material thickness is $4.36 \times 10^{-4}$ m (0.17 in.) and its side dimension and bay length dimension are 30.57 m. The catenary cables and tension web cables are woven graphite, 0.0396 m (1.56 in.) and 0.0064 m (0.25 in.) in diameter, respectively.

Power Distribution - Figure R-15 illustrates the basic power distribution concept considered for the satellite antenna network. Sixteen independent power risers (one per slip-ring/brush are routed to sixteen dedicated high voltage, high-power dc-dc converters. The output of the dc-dc converters are summed on two independent summing power bus sets (each set consists of five different voltage levels from 8-40 kV). A network of secondary feeders then routes the power to the individual dc-RF converters distributed on the antenna surface.

A backup power system is located on the antenna structure with an emergency bus routed along side the regular network for operation during powered down periods such as may occur during solar eclipse periods. It must be emphasized that the emergency bus is separate from and cannot be used to supplement, in any configuration, the transmission of power.

Conditioning - The power conversion equipment converts the nominally 40 kV DC main bus voltage to the subsystem voltages required for the various subsystem loads. The major requirement is to supply the five basic voltages, (40 kV, 32 kV, 24 Kv, 16 kV and 8 kV) to the klystron DC-RF power converters. A secondary requirement is the need to supply low voltages (<100 V) to the various operating electronics.

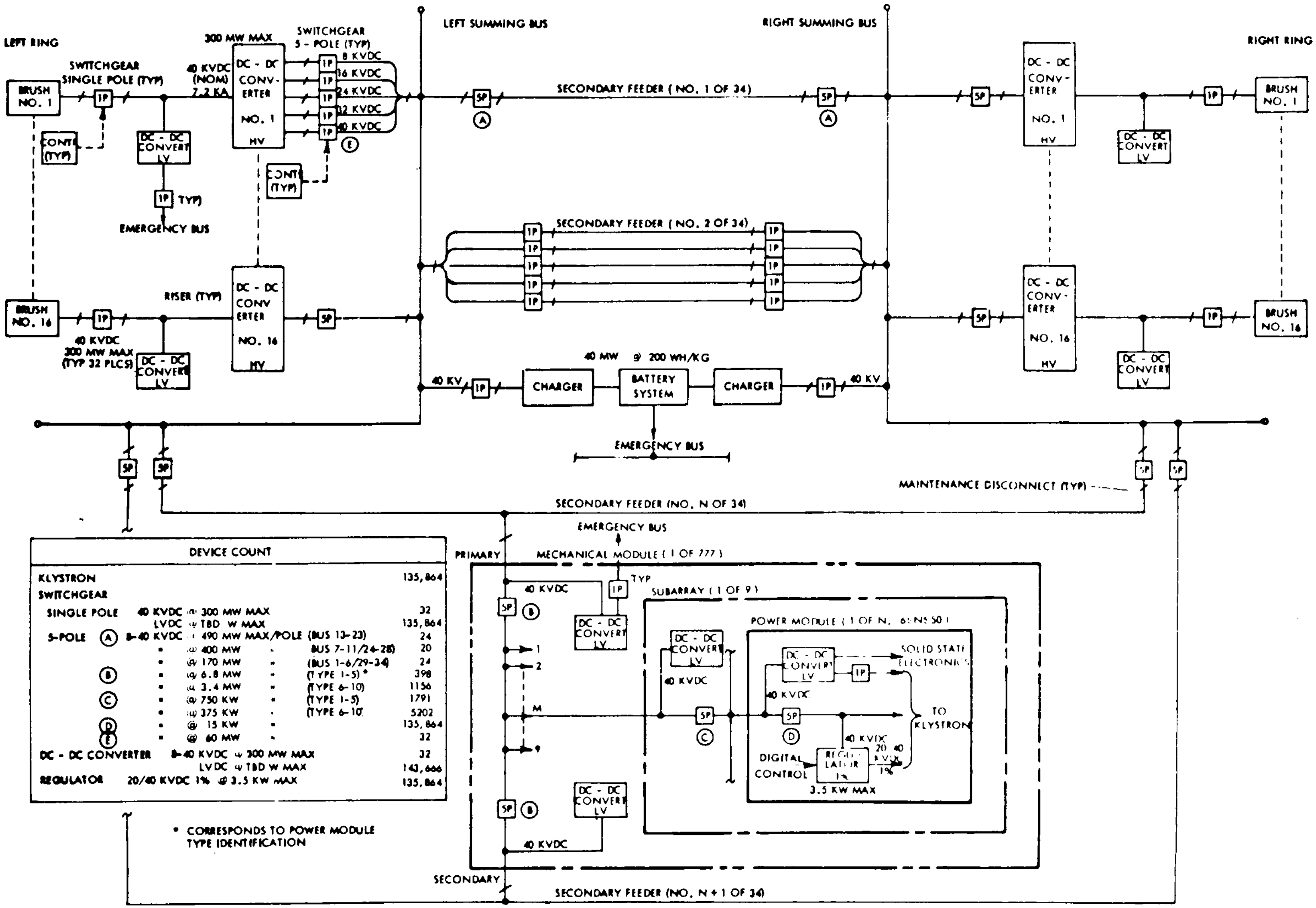


Figure R-15. Power Distribution - Microwave Antenna (Preliminary)

The high voltage conversion is provided by 32 converters located near the antenna gimbal joints (16 at each gimbal). These converters are sized at 271 megawatts (6.73 kA). The secondary or low voltage converters are located adjacent to the various subsystem loads and are presently estimated to provide a maximum of 3.5 kW at each location.

DC/RF Converters - The DC/RF conversion is performed by klystrons with an assumed efficiency of at least 85%. The klystron accepts the multiple level high voltage generated by the high voltage DC/DC converters and outputs a microwave segment at 2.45 GHz and at a nominal 50 kW level.

The proposed operational klystron is a variation of a Varian VKS-7773 utilizing a depressed, multiple voltage collector fabricated of a refractory material such as pyrolytic graphite, Figure R-16. Thermal control of the collector is by direct radiation to space. The baseline approach to cooling the klystron tube body is to utilize heat pipes with the radiating surfaces located on the front face of the resonant cavity radiator (RCR) associated with each klystron microwave generator. The baseline array specifies a makeup consisting of 135,864 klystron/RCR sets. With this number of converters, each unit will operate at a true value approaching 54.2 kW average.

Mechanical Module, Subarray, and Power Module - The 50 kW klystrons, selected as power converters, are mounted in resonant cavity radiators (RCR) with their collectors protruding from the array base as shown in Figure R-17. This assembly is a power module. Its area varies so as to set the radiated power densities required over the array surface. There are ten density steps and corresponding module designs. These modules are assembled to form ten subarray types.

The SPS antenna is composed of subarrays. A subarray is defined as a portion of the total antenna array which has been phase shifted to point in the direction of the pilot beam. The center of the subarray has a phase, set by a single retroelectronics assembly. In addition, there is a phase variation across the array face used to steer the subarray antenna pattern.

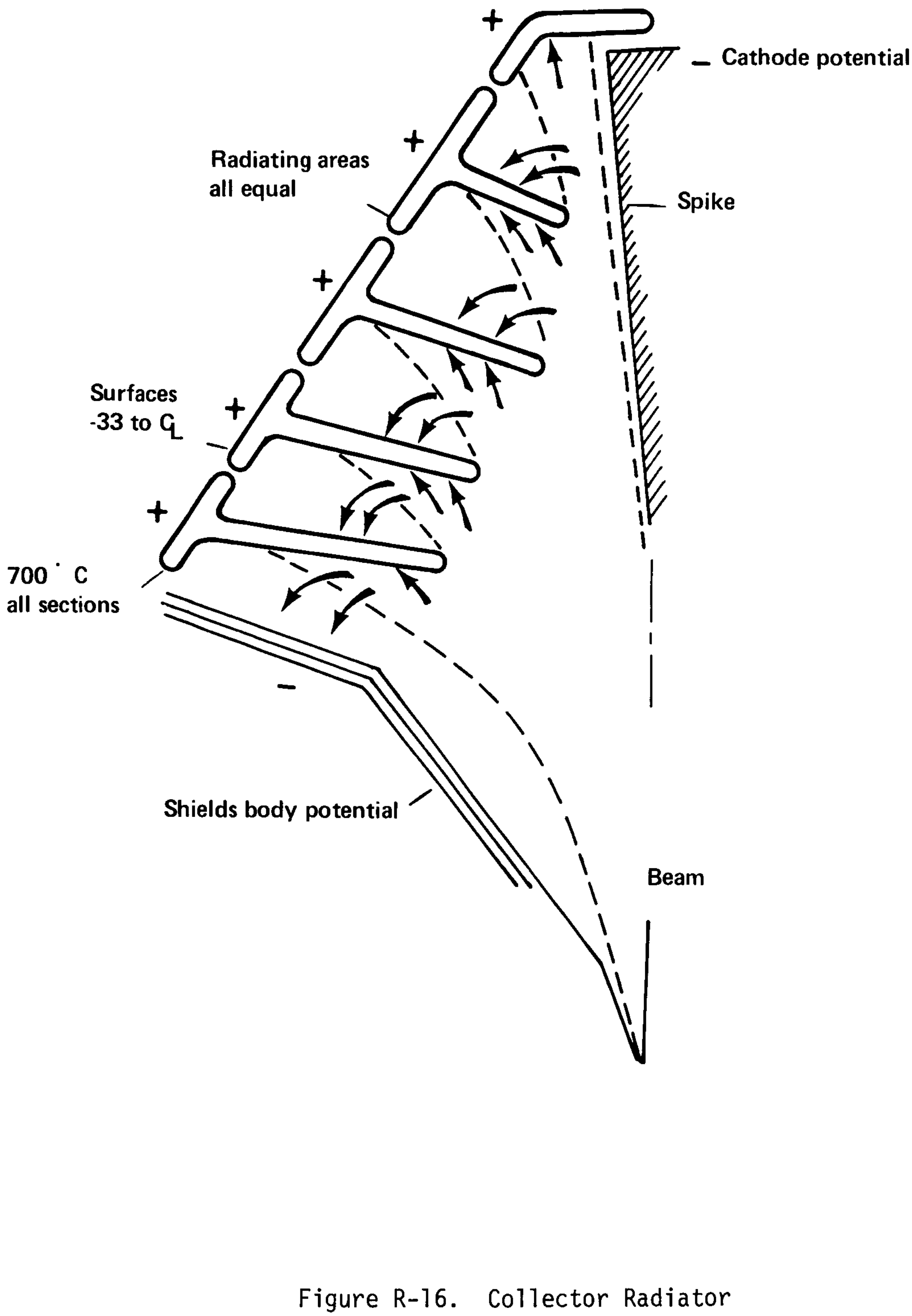


Figure R-16. Collector Radiator

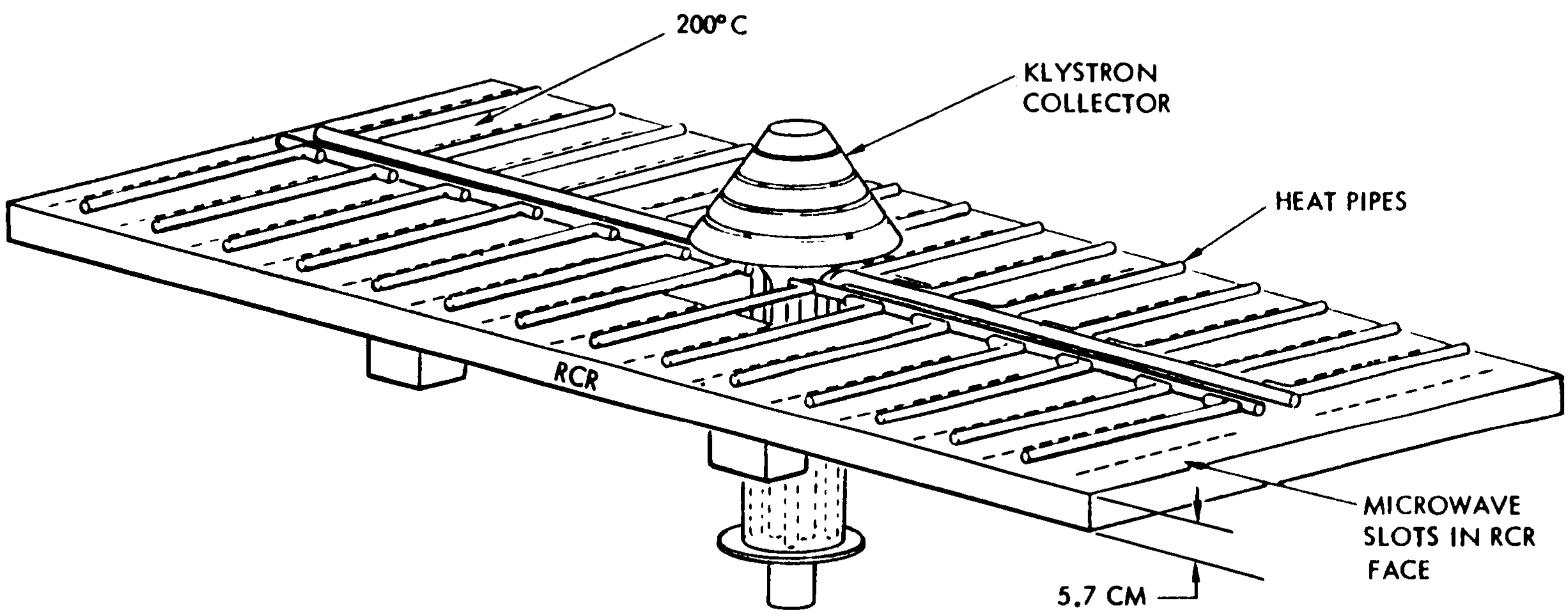


Figure R-17. Radiating Face of Power Module

The subarray size selected is 11.64 x 10.2 m. Sets of nine subarrays are then supported by a secondary structure to form a 34.92 x 30.6 m mechanical module. The module is supported by connections to the catenary tapes of the compression-frame/tension-web which forms the primary array structure. The characteristics of the ten mechanical module types is shown in Table R-3. Included are the number of each type required in the baseline antenna array.

Power Taper and Density on Antenna - The power level of all power module amplifiers is, by definition, the same. The size of the module radiating surface is varied to vary the power density over the total array area. For instance, with 50 kW klystrons and gaussian distribution, the number of modules per 11.64 x 10.3-m subarray varies from 50 at the array center to 6 at the array edge. The module area thus varies from 2.38 $m^2$ to 19.79 $m^2$. The power density for the modified gaussian power distribution resulting from the selection of a 10-step approximation is shown in Figure R-18.

Rectenna - The ground based element is the rectenna (Rectifying Antenna). The rectenna receives the energy transmitted from geosynchronous altitude at 2.45 GHz, converts the energy to dc power and subsequently transforms and routes the energy to a form and level compatible with commercial requirements.

Each rectenna is designed to accept power from a single satellite and provide 5 GW of power to the utility interface. As shown in Figure R-19, a typical rectenna site located at 34°N latitude covers an elliptical area 13 km in the north-south direction by 10 km in the east-west direction. This area contains 750 rows of rectenna panels tilted 40 degrees from the horizontal, providing an active intercept area of 78.2 $km^2$.

The phased array is comprised of stripline patterns of bow-tie dipoles, shown in Figure R-20. This selection was based primarily on the increased efficiency and decreased diode count.

A summary of the rectenna characteristics is given in Table R-4.

Figure R-21 presents an approximation of the power density at the surface of the rectenna array along the N-S axis. The limits of 23 $mW/cm^2$ at the center,

Table R-3. Mechanical Module Mass and Power Characteristics

| Type | No. of Mech'l. Mod. | Km/M2 per density | Wt (Kg) per Mech'l. Mod. |
|---|---|---|---|
| 1 | 17 | 21.05 | 756 |
| 2 | 32 | 18.84 | 725.7 |
| 3 | 44 | 16.64 | 674.5 |
| 4 | 44 | 15.18 | 651.6 |
| 5 | 62 | 12.83 | 610.3 |
| 6 | 68 | 10.52 | 671.9 |
| 7 | 82 | 8.42 | 626.1 |
| 8 | 110 | 8.31 | 601.1 |
| 9 | 175 | 4.21 | 476.2 |
| 10 | 142 | 2.52 | 406.6 |

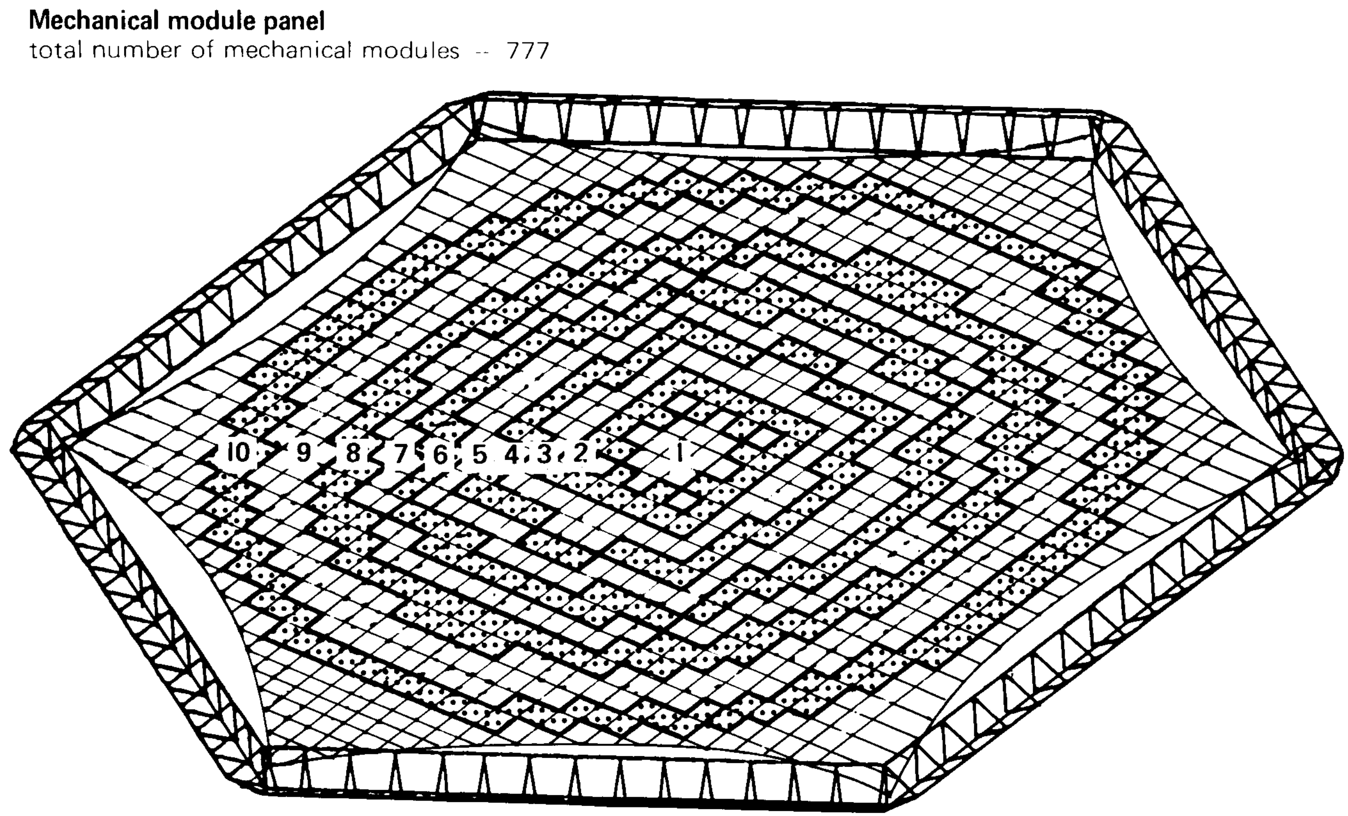


Figure R-18. Gaussian Beam Microwave Antenna

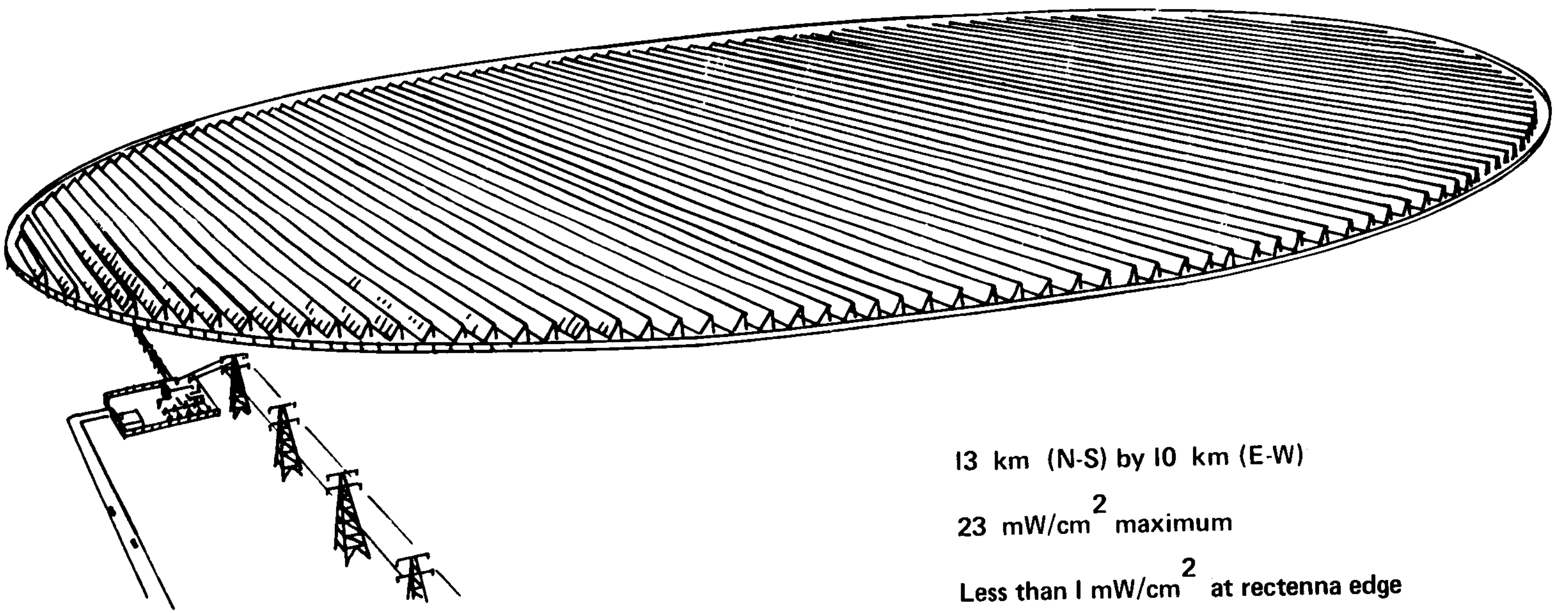


Figure R-19. Rectenna Site

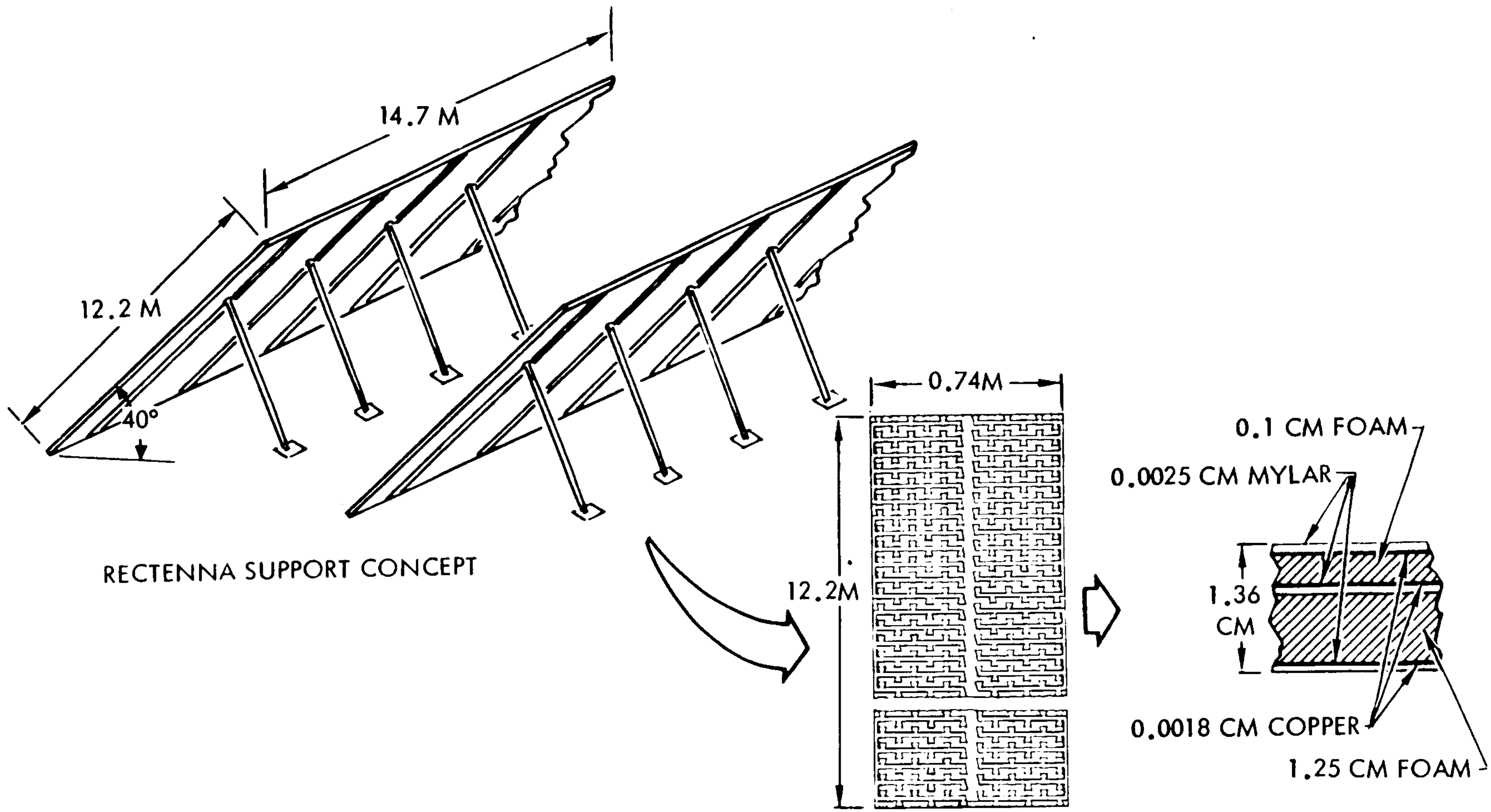


Figure R-20. Rectenna Construction

Table R-4. *Summary of Rectenna Definition*

| | |
|---|---|
| AREA AVAIL. (TOTAL | 102.1 $km^2$ |
| USED | 99 $km^2$ |
| PANEL AREA (ILLUMINATED) | 179.8 $m^2$ |
| INCIDENT POWER (TOTAL) | 5.53 GW |
| NO. PANELS USED | 390,500 |
| SPARE | ~12,200 |
| NO. 40 KV STRINGS | 368,672 |
| POWER PER STRING (OUTPUT) | 13.35 kW |
| NO. DIODES (597/STRING) | $220\times10^6$ |

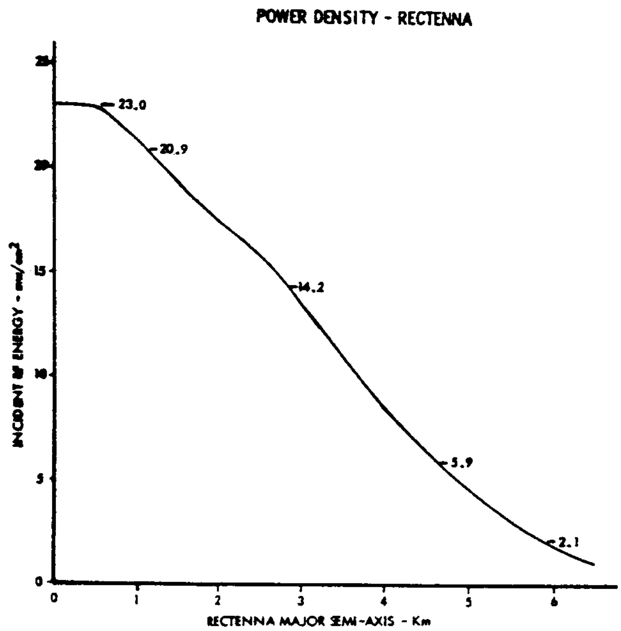


Figure R-21. *Rectenna Incident Power Density* reducing to 1 mW/cm at the perimeter of the rectenna is compatible with present environmental limit as stated in the program guidelines.

## I. Mass Statement

A summary of the satellite mass properties is presented in Table R-5. The two major segments, the collector array and the antenna section, are nearly equal in mass. The major contributor to the collector array mass is the power source, which includes the solar blanket and the concentrators. The solar blanket is the predominant mass. Antenna section mass properties are driven by the microwave power segment which includes the RF radiators and the klystrons. Total satellite mass, including a 25-percent mass growth factor, is 38.09-million kilograms. Propellant resupply for attitude control and stationkeeping is a very small annual mass compared to the satellite mass.

## J. Space Transportation

The transportation system operational regimes include earth to LEO, LEO to GEO, and on-orbit (for short distance and duration flight). These systems must be capable of transporting both crew and cargo.

HLLV - SPS transportation requirements from earth to LEO, environmental factors, element of risk and operations complexity and cost led to the selection of two HLLV concepts; a winged two-stage vertical takeoff-horizontal landing configuration (VTO) and a more advanced technology option; an HTO-SSTO configuration.

Winged VTO-HLLV - A potential HLLV candidate with equal size (volume) stages is depicted in Figure R-22. The vehicle is a parallel burn configuration with propellant crossfeed from the 1st to 2nd stage and is capable of placing a 225 x $10^6$ kg payload in an orbit of 500 km at an inclination of 28.5°. Both stages have fly-back capability; the 1st stage only employs air breathing engines. The boost phase uses LOX/RP in both stage engines. The 2nd stage employs

Table R-5. Photovoltaic Point Design Mass Statement

5 GW

| SUBSYSTEM | WEIGHT (MILLION KG) |
|---|---|
| COLLECTOR ARRAY | |
| STRUCTURES AND MECHANISMS | 3.825 |
| POWER SOURCE | 8.831 |
| POWER DISTRIBUTION & CONTROL | 1.347 |
| ATTITUDE CONTROL | 0.116 |
| INFORMATION MANAGEMENT & CONTROL | 0.050 |
| TOTAL ARRAY (DRY) | (14.17) |
| ANTENNA SECTION | |
| STRUCTURE AND MECHANISMS | 1.685 |
| THERMAL CONTROL | 2.457 |
| MICROWAVE POWER | 7.012 |
| POWER DISTRIBUTION & CONTROL | 4.516 |
| INFORMATION MANAGEMENT & CONTROL | 0.630 |
| TOTAL ANTENNA SECTION (DRY) | (16.3) |
| TOTAL SPS DRY WEIGHT | 30.47 |
| GROWTH (25%) | 7.62 |
| TOTAL SPS DRY WEIGHT WITH GROWTH | 38.09 |
| PROPELLANT PER YEAR (W/O GROWTH) | 0.093 |

**Mass Properties**

| | $10^6$ kg | $10^6$ LB |
|---|---|---|
| Glow | **6.804** | 15.00 |
| Blow | **5.443** | 12.00 |
| $WP_1$ | **4.627** | 10.2 |
| U low | **1.134** | 2.50 |
| $WP_2$ | **0.966** | 2.13 |
| Payload | **0.227** | 0.500 |

**Concept Features**

- LOX/RP 1st stage
- $LOX/LH_2$ (dual mode) 2nd stage
- Propellant crossfeed – Parallel burn
- Region of minimum glow
- Staging velocity 2377 m/sec (7800 ft/sec)
- Staging altitude 61 Km (200,000 ft)s.

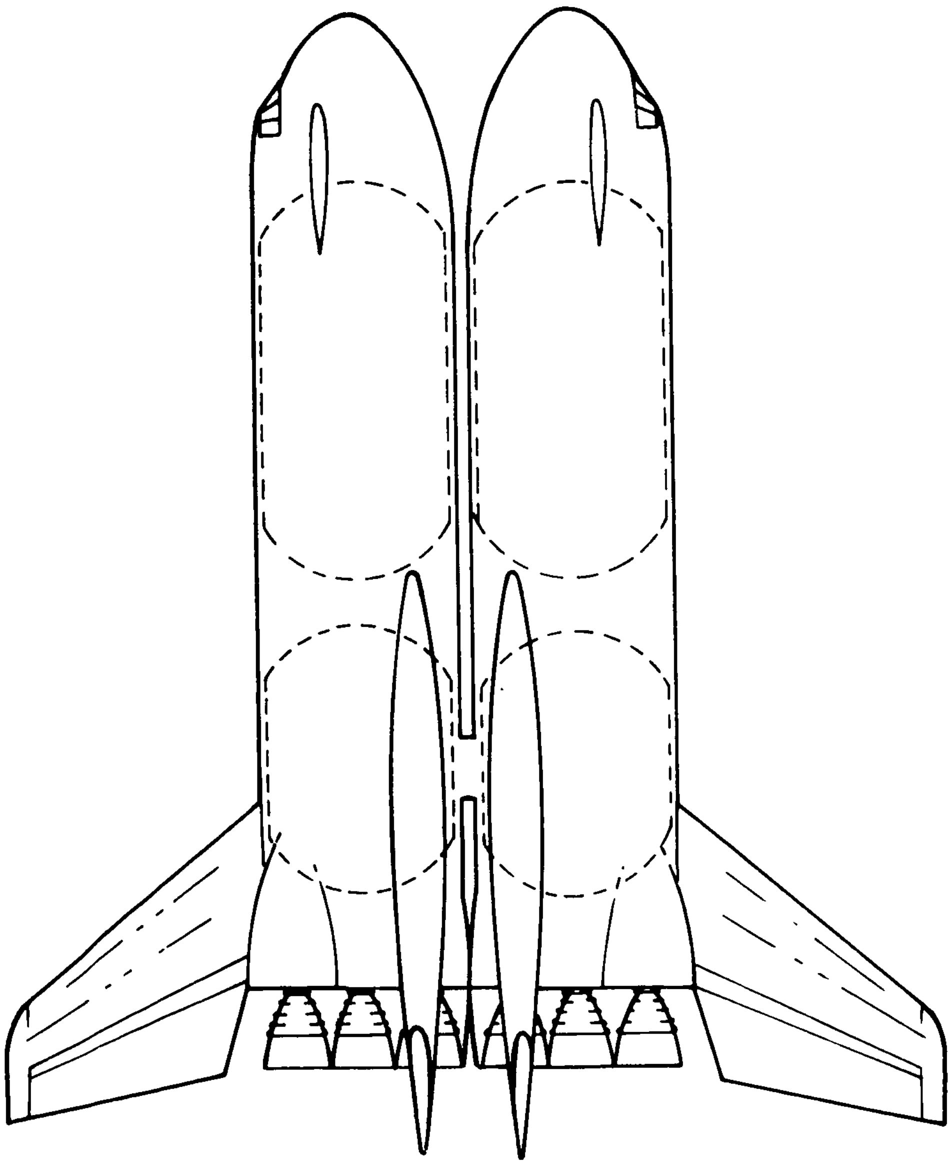

Figure R-22. Preliminary VTO HLLV Concept multi-mode engines which operate on LOX/$LH_2$ during 2nd stage burn only. The configuration very nearly approximates a minimum GLOW vehicle for the prescribed payload. Staging conditions are such that a "heat-sink" booster requiring minimum thermal protection may be utilized.

Horizontal Takeoff SSTO HLLV - The horizontal takeoff, single-stage-to-orbit concept represents a more advanced technology option for SPS. This concept was considered because of the operational problems related to multiple daily launches of very large vertical takeoff concepts and the overall operational flexibility. Without a commitment toward accelerated advanced technology programs, it is not apparent that this configuration can meet current SPS technology readiness requirements.

The winged vehicle, Figure R-23, is a delta flying wing consisting of a multi-cell pressure vessel. The wing contour is a supercritical air-foil with leading edge modified to improve supersonic and hypersonic performance.

The cargo bay floor is designed similar to the C5-A military transport to permit the use of Airlog cargo loading and retention systems. Cargo is deployed in orbit by swinging the forebody to 90 or more degrees about a vertical axis and transferring cargo from the bay on telescoping rails.

Ten high-bypass, supersonic-turbofan/air-turbo exchanger/ramjet engines with a combined thrust of $1.4 \times 10^6$ lb are mounted under the wing. The inlets are projected by retractable ramps that close the inlets and fair the bottom surface into a continuous surface suitable for reentry.

Three uprated SSME-type rocket engines (total thrust = $3.2 \times 10^6$ lb) provide the required thrust above the sensible atmosphere. The vehicle is capable of placing a 91,000 kg payload in a 550 km equatorial orbit.

Cargo Orbital Transfer Vehicle - The payload required for construction is transported to GEO using a dedicated electric OTV. This concept is illustrated in Figure R-24. The OTV is sized to carry $4 \times 10^6$ kg ($8.8 \times 10^6$ lb) of payload for a LEO-GEO trip time of 133 days. Approximately ten OTV flights are required to transport the mass required for the construction of each SPS. GaAlAs solar cells also are used in this concept to provide power for propulsion. As for

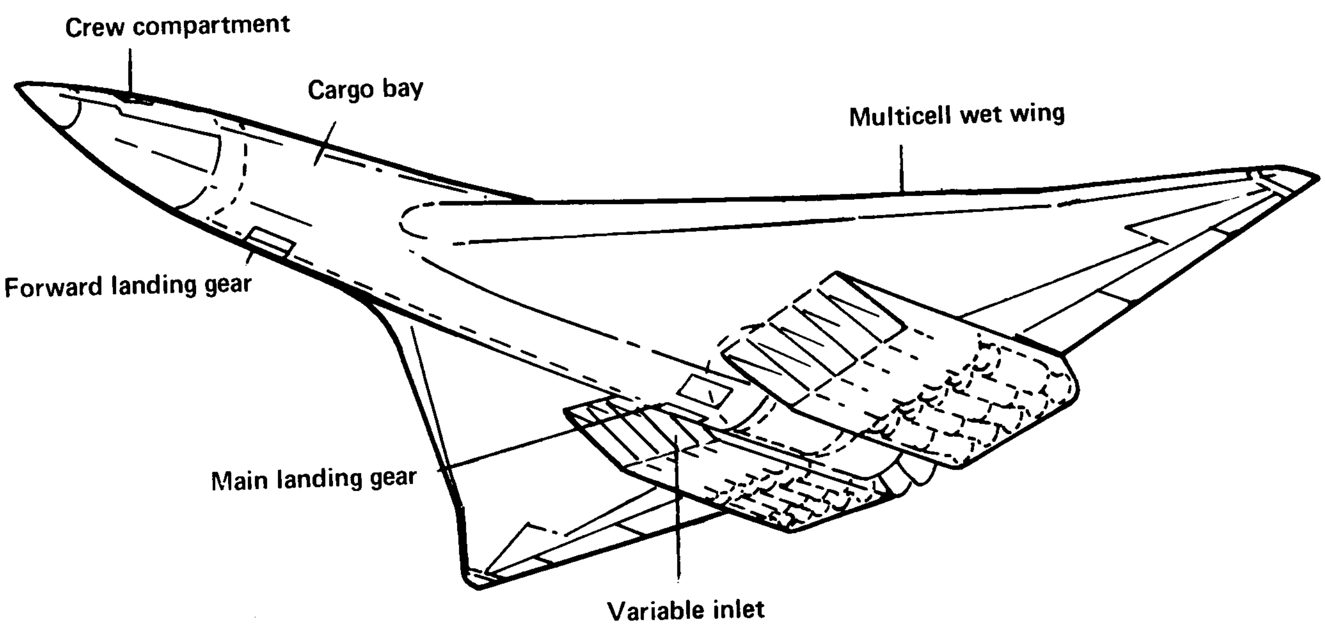


Figure R-23. Winged HLLV-HTO-SSTO Concept

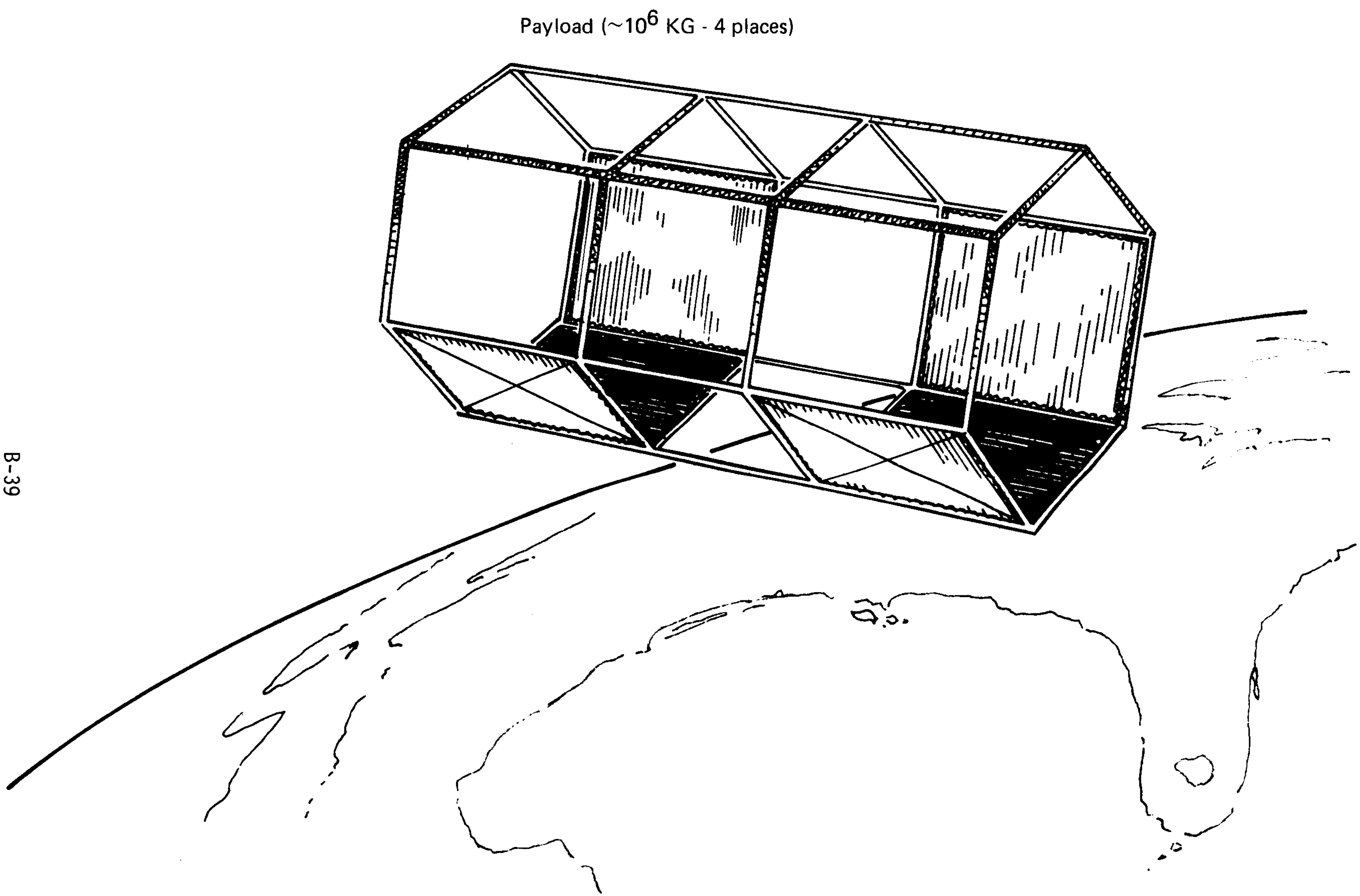


Figure R-24. Dedicated Electric OTV Concept for SPS Applications the self-propelled mode, the solar cells are self-annealing of the radiation damage occurring during transit and consequently, the dedicated OTV can be reused.

The OTV uses an ion bombardment thruster with an aperture diameter of 100 cm and argon propellant.

The power conditioners of the SPS propulsion system process only the low-voltage fixed power (278 W input per thruster). The other supplies are taken directly from solar arrays. The beam power is obtained from the OTV solar array. To avoid significant power loss from plasma discharge, the array voltage is maintained at 2000 V; this is stepped up to the beam voltage by dc-dc converters before collection by the main solar array power distribution lines.

The accelerator and discharge power sources are small arrays near the thrusters. This location reduces cabling mass. Because only 50 kW per thruster is generated, thermally induced voltage transients can be regulated by voltage limiters. An auxiliary power unit (APU), charged by the discharge supply solar array, furnishes 278 W to the thruster low-voltage supplies.

Because of the desire to minimize propellant requirements, the OTV design was based on a high specific impulse of 13,000 s.

Personnel Transport Systems (POTV) - The construction sequence developed for the SPS required a crew rotation every 90 days for crew complements in multiples of 48. A crew and resupply module (CRM) was synthesized on this basis. Based on previous Rockwell studies of passenger modules, a parametric sizing curve for passenger modules was developed. For a crew complement of 48 persons, the module would weigh approximately 200 kg (440 lb) per man, or 9,600 kg. Comparable data were extracted from these studies for consumables, passenger/personal effects, in-transit consumables, crew module, resupply module, and on-orbit habitable module spares.

A conceptual layout of the CRM is shown in Figure R-25. A command module area is provided to monitor and control OTV performance during crew rotation flights. Spacing and layout of the passenger module is comparable to current

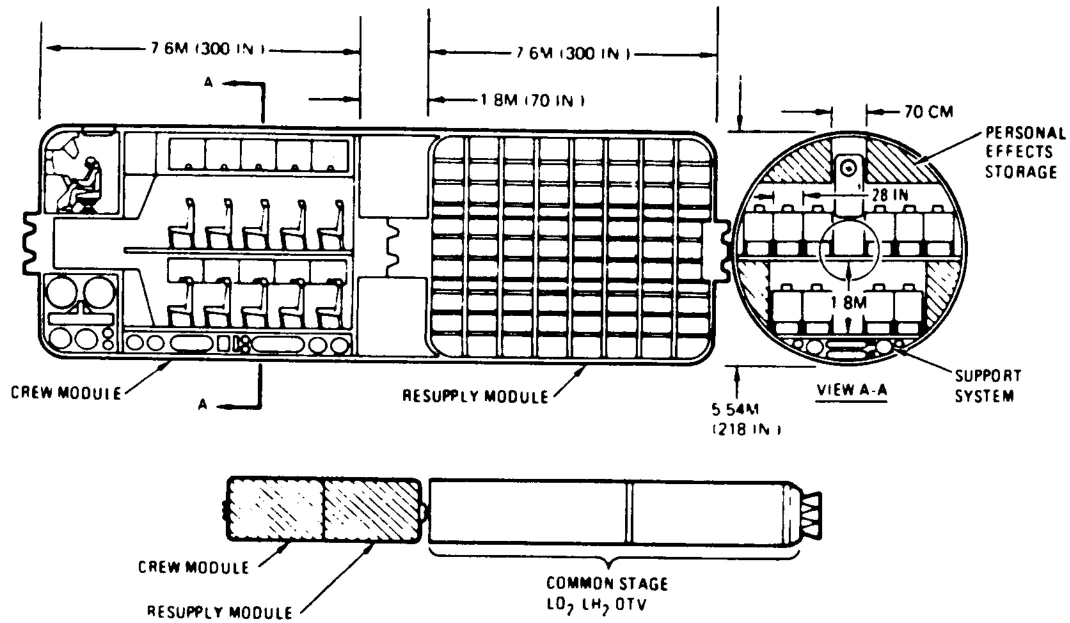


Figure R-25. Crew and Resupply Module

commercial airline practice. A nominal packing density of 160 kg/$m^3$ (10 lb/$ft^3$) is assumed for resupply consumables. The resupply modules are to be exchanged each mission. While at GEO, the resupply module may be used as the consumables storage module. Thus, multiple access aisles are included in the sizing. A gross packing density of 93 kg/$m^3$ (6 lb/$ft^3$) allows for a large growth factor.

The POTV is a common-stage chemical (two stages having the same propellant capacity) vehicle, utilizing LOX/$LH_2$ propellant. (See Figure R-26.) The propellant tankage for both stages is the same, but the propulsion system for the first stage has twice as many engines as the second. This allows the initial thrust/weight for both stages to be kept at about 0.15 g. The engines have a specific impulse of approximately 470 s at a mixture ratio of 6:1.

K. Natural Resources

Table R-6 identifies the type and amount of materials required in the construction of one satellite power system using GaAs solar cells at a concentration ratio of 2. NOTE: Totals do not reflect growth allowance.

L. Operations

a. Construction

This section describes the space-related aspects of SPS operations. The overall operations scenario is first described. This is followed by a description of the construction approach, including the construction base and the approach to handling cargo.

Overall Operations Scenario - Figure R-27 summarizes, by location (i.e., earth, LEO and GEO), the space-related operations required to support the construction and operation of the SPS satellites subsequent to establishment of the necessary ground and space bases. The right hand side of the figure identifies the four types of transportation vehicles used in the space operations: the HLLV transfers cargo and crew to LEO; the electric cargo orbital transfer vehicle (EOTV) transfers cargo between LEO and GEO; the personnel orbital transfer vehicle (POTV), which is a two-stage chemically propelled vehicle, transfers crew and priority cargo between LEO and GEO; and the intra-orbital transfer vehicle

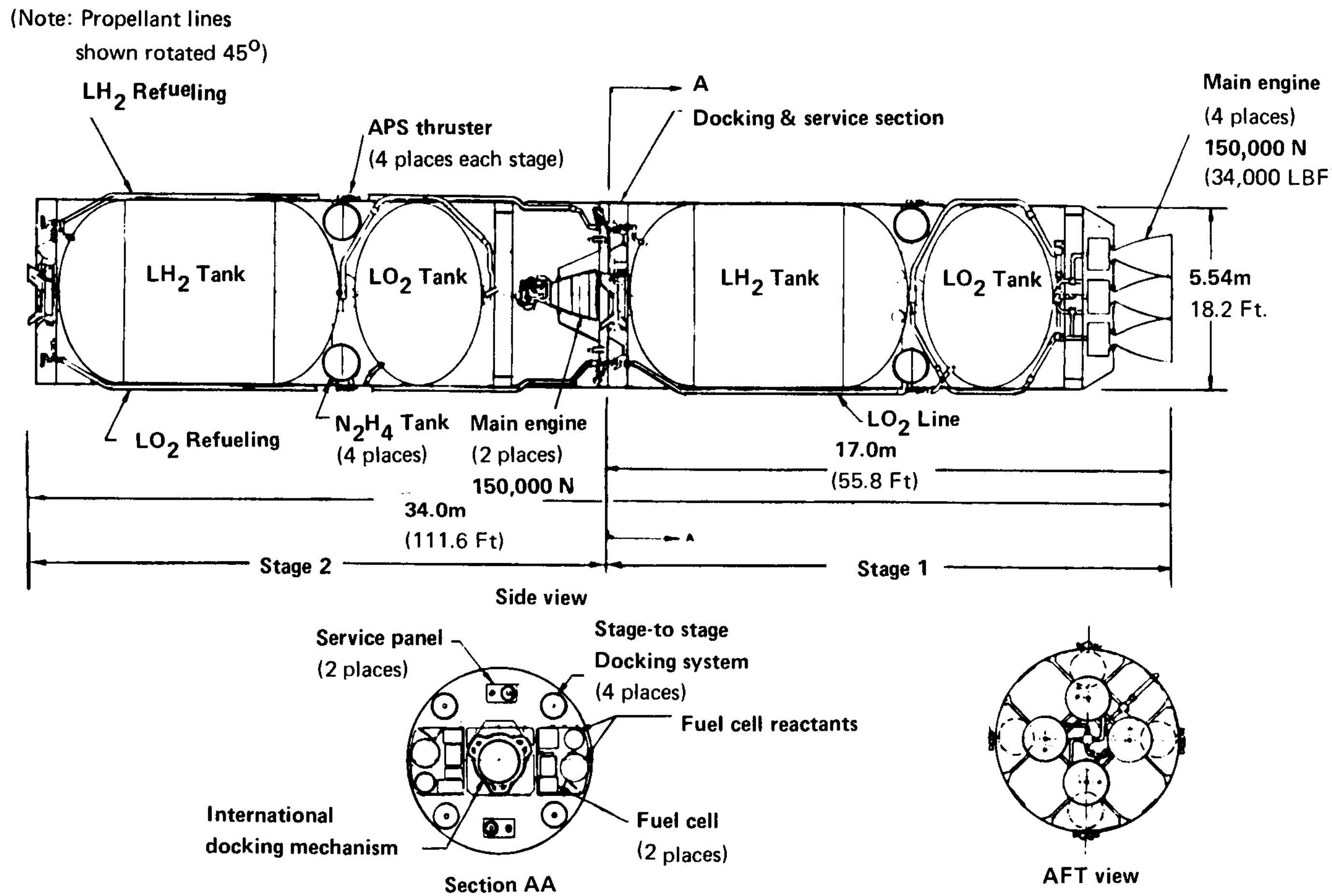


Figure R-26. Common Stage Chemical OTV Configuration

Table R-6. Summary - SPS Mass and Materials
(Photovoltaic GaAs, CR=2)

| MATERIAL | MASS (LESS GROWTH) $10^6$ kg | % |
|---|---|---|
| ALUMINUM | 12.104 | 39.72 |
| STEEL | 1.171 | 3.84 |
| TITANIUM | 0.026 | 0.08 |
| COPPER | 3.662 | 12.01 |
| ALNICO-V | 0.808 | 2.65 |
| SILICON | 0.006 | 0.02 |
| ALUMINUM OXIDE (CERAMIC) | 0.437 | 1.43 |
| KEVLAR/RESIN | 0.038 | 0.12 |
| GRAPHITE/RESIN | 2.590 | 8.50 |
| PLASTICS | 0.630 | 2.06 |
| SAPPHIRE | 3.087 | 10.13 |
| GALLIUM ALUMINUM ARSENIDE | 0.113 | 0.37 |
| GALLIUM ARSENIDE | 1.133 | 3.71 |
| TEFLON (FEP) | 1.055 | 3.46 |
| KAPTON | 2.536 | 8.32 |
| SILVER | 0.576 | 1.89 |
| SILVER-PALLADIUM-TITANIUM | 0.208 | 0.68 |
| SILVER MESH (INTERCONNECTOR) | 0.010 | 0.03 |
| CRYOGENIC ARGON | 0.042 | 0.14 |
| HEAT TRANSFER FLUID | 0.215 | 0.70 |
| TOTAL | 30.47 | 100.00 |

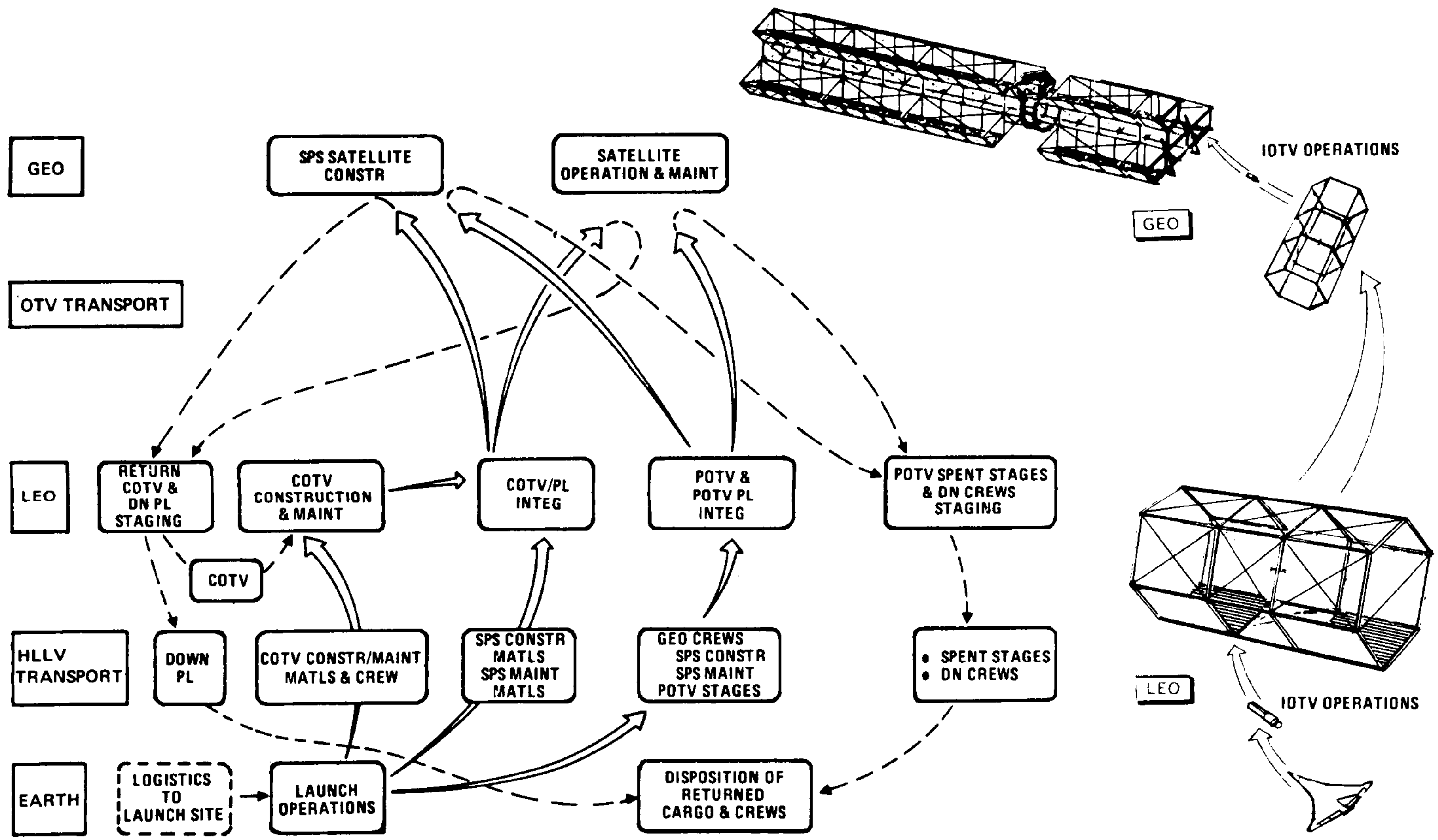


Figure R-27. Space Operations Concept

(IOTV) transfers cargo and crew between the HLLV and the EOTV/OTV/LEO base, and at GEO transfers cargo between the EOTV and the GEO bases.

All launch operations take place at a single launch site. In addition to HLLV launch facilities per se the launch site includes facilities for: receiving, storage and processing of satellite and EOTV construction materials, spares, and propellants; fabrication and subassembly of selected satellite elements; payload packaging; storage, refurbishment and checkout of the HLLV, POTV and IOTV fleets; space crew support operations; and space and ground crew administration.

The continuing operations taking place in LEO are: EOTV servicing and maintenance; IOTV servicing and maintenance; transfer of up and down payloads between HLLV's and OTV's; integration of POTV stages and assembly of crew/ payload modules to the upper stage; and staging of spent POTV stages and down crews and integration of same into HLLV's for the LEO-to-earth transfer. (Additionally, the EOTV's are constructed in LEO, an operation which takes place during the early program, with the possibility of additional units being constructed late in the program.)

Construction material for each satellite is transported to LEO in 175 separate HLLV flights. The HLLV flights will be scheduled to coincide with EOTV availability in LEO to permit direct cargo transfer. Five days are required for EOTV loading with their departure for GEO scheduled approximately every five days. The LEO-GEO-LEO transport cycle requires 161 days, which includes allowances for loading, unloading and refurbishment. Upon EOTV return to LEO the down cargo (packing materials, damaged equipment/materials, consumables containers) is off loaded to the HLLV and the scheduled EOTV maintenance of replacing thruster grids and replacing the empty argon tanks with full tanks is accomplished prior to rescheduling.

Satellite construction and maintenance crews are carried to LEO by HLLV's, utilizing crew modules which can accommodate 48 people each plus consumables for 90 days. For GEO-destined crews the module, is mated with two chemical propulsion stages in LEO to become a POTV which transfers the crew to

GEO. The fueled stages are also delivered to LEO by the HLLV and arrive concurrent with the crew module. Crews which have completed their 90-day GEO duty cycle are transported to LEO by returning POTV's. The crew module with its crew and the two spent stages are then returned to earth via HLLV's.

Featured in this scenario is the concept of direct transfer of cargo from the HLLV to the EOTV thus precluding the requirement for a large LEO staging depot and double handling of cargo and crews. Because the on-going LEO operations are primarily those of traffic control and light maintenance, only a small permanent base with a 30-man crew is currently projected.

At GEO a single integrated satellite construction base (SCB) is employed in building the entire fleet of satellites. The SCB is the location of all GEO construction activities. All EOTV cargo is transferred via the IOTV directly to the warehouse area on the SCB, POTV's dock directly with the SCB, and all construction crews live and work on the SCB.

Incorporated in each satellite is a small, permanently manned operations and maintenance base sized for a 24-man crew. Logistical support of these bases is through the same launch site and LEO base which supports satellite construction. Operational control of each satellite is through its designated rectenna site and is an integrated function of both the onboard crew and the ground rectenna site crew.

Satellite operations and maintenance crews are transported directly to their assigned satellite by POTV's and will be rotated at 90-day intervals. Maintenance materials are transported to the satellite via HLLV/EOTV.

GEO Satellite Construction Base (SCB) - Each satellite is constructed at its designated GEO longitudinal location. The satellite construction base (SCB) produces satellites at the rate of 4 per year during the mature portion of the program. Upon completion of one satellite, the base is moved to the operational location of the next satellite and construction is initiated.

The construction base, shown in Figure R-28,consists of the satellite construction fixture, the construction equipment, and the base support facilities

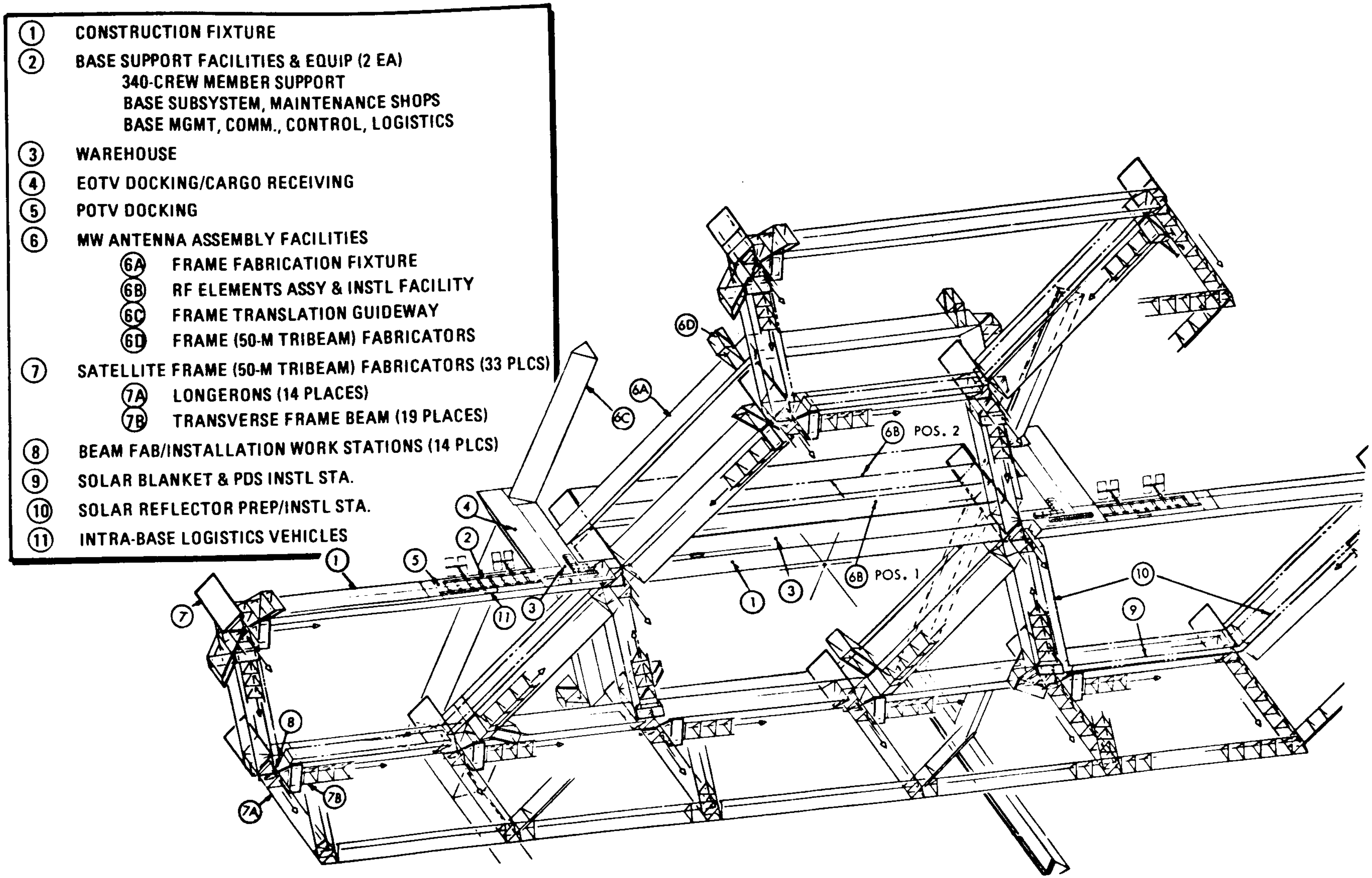


Figure R-28. Satellite Construction Base (SCB) and equipment. The construction fixture is a rugged heavy gage metal structure upon which all of the elements of the construction base are mounted. The fixture constitutes the reference surfaces for the construction operations and the locating jig for the equipment which either constructs or installs various elements of the satellite.

The location of the major construction equipment is shown on the figure. Thirty-three tri-beam fabricators, installed at thirteen different locations as indicated by 7A and 7B are required. Dispensing devices for the solar blankets, reflectors, solar array retention cables, and power distribution conductors 9 and 10 are located at the bottom and sides of each of the three troughs. The assembly facility for construction of the microwave antenna frame, denoted by 6A, including its tri-beam fabricators 6D is located in the center of the SCB. Also shown is the RF elements assembly and installation facility, 6B which translates towards the completed antenna frame and provides a platform from which the RF elements are attached to the antenna as it translates past the platform in guideways 6C.

Facilities for docking IOTV's and for storing cargo are provided on the platform 4 located to the left of the antenna fixture in Figure R-28. GEO construction base support facilities and their locations also are identified in Figure R-28. A crew size requirement of 680 has been estimated for accomplishing the construction in the scheduled time. The crew and their facilities are divided equally and are located on each side of the hex portion of the fixture as shown. One of these 340 men facilities shown in more detail in Figure R-29, consists of 7 three-module crew habitability complexes plus 2 base management modules, 2 pressurized storage modules and solar array power modules.

The modules of the crew habitability complex are described in more detail in the lower right of the figure. Each complex is composed of two of the crew hab modules, each of which provide staterooms, personal hygiene facilities and support subsystems for 24 crewmembers; and one crew support module which provides galley, recreational and medical facilities and subsystems for the 48 crewmembers of the two crew hab modules. The base management modules

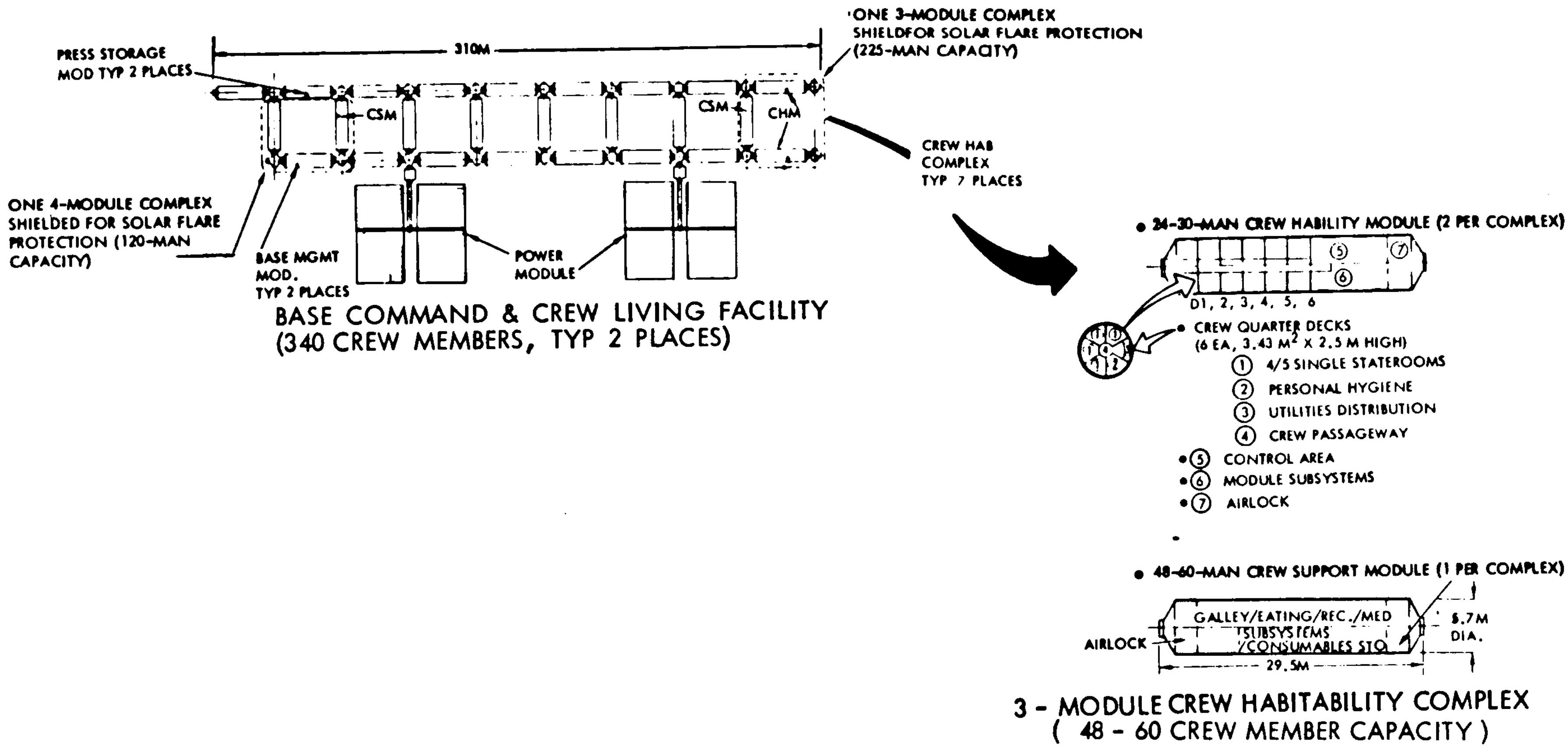


Figure R-29. SCB Support Facilities

house the communications and control systems for the construction base. The pressurized storage modules include workshops for maintenance of construction facility elements and satellite hardware as required.

Seven of the modules (enclosed by the dashed lines) are hardened against solar flare radiation and serve as temporary quarters for the entire crew when the base is subjected to that environment.

Satellite Construction Operations - Identification of the major construction operations and their time-phased relationship with each other and with the overall construction schedule for a single satellite are given in Figure R-30.

Construction starts at one wing tip and progresses toward the center section where the microwave antenna rotary joint is located, and thence continues outbound building wing No. 2 and terminating at that wing tip. The first eight days are designated for preparation of the construction facility. Prior to the eighth day sufficient materials have been delivered by the EOTV to satisfy the first several days of construction: primary structure material (beam machine cassettes) for 1/2 the satellite; solar blanket and reflector rolls, electrical conductors and switch gear for the first two bays; and antenna components. Since the rear side of the facility is always exposed to space with no interference from the main construction activities, it is implemented as the jig for building the antenna frame and as the location for assembly, and installation of the 30 x 30 m RF mechanical modules. Fabrication of the microwave antenna for this Nth satellite was started on the 50th day of construction of the previous (N-1) satellite and is continued up through the 48th day of construction of this satellite; at that time it is ready for installation into the slip-ring-mounted trunnions.

Each satellite wing consists of 12 bays 800 m long. These are constructed at the rate of one every two days using three 8-hour shifts. Prior to the start of longeron fabrication, the solar array blankets and reflectors for one bay are placed in position for deployment and attached to the frame of the preceding bay so that they may be unrolled as beam fabrication progresses.

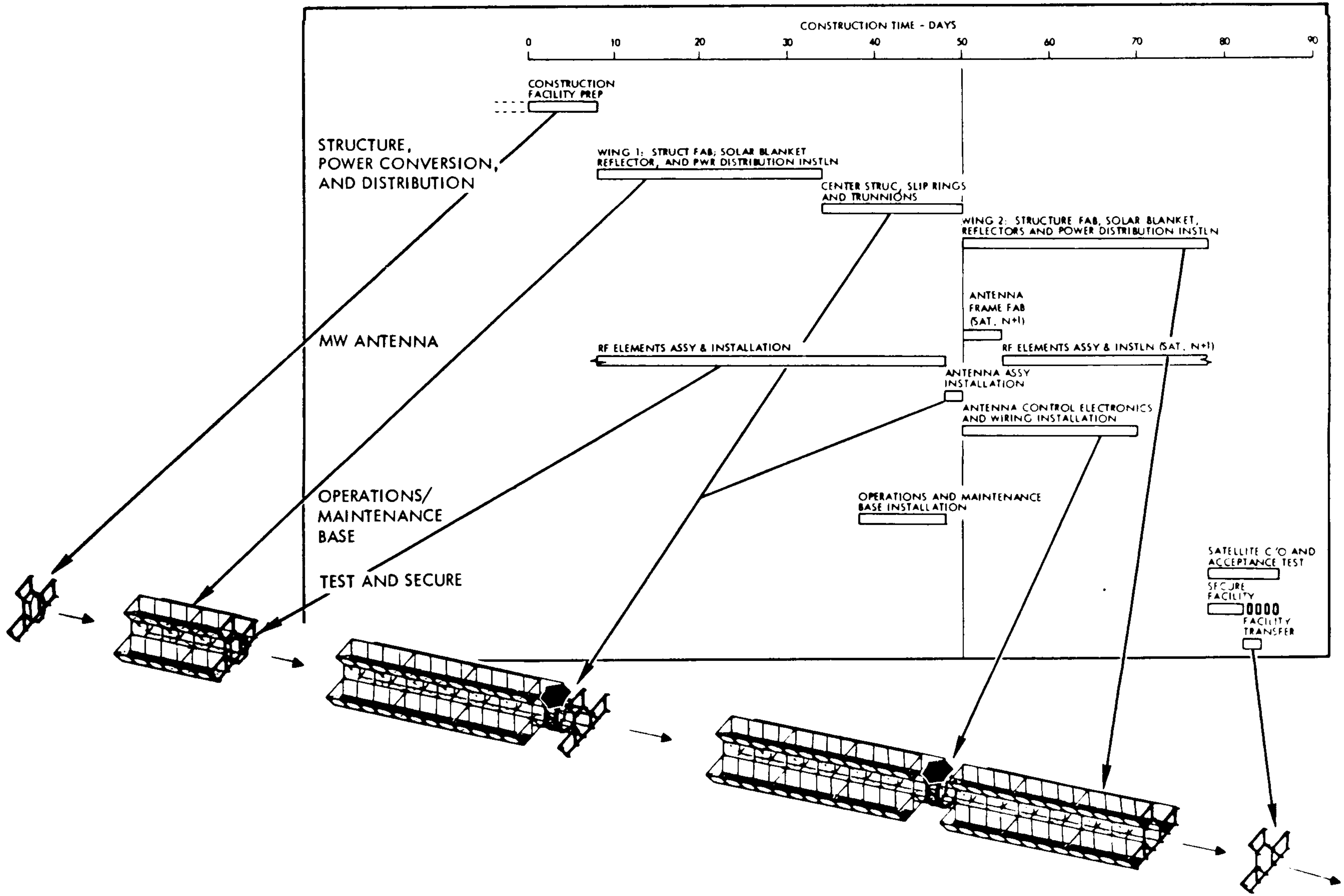


Figure R-30. Nth Satellite Construction Sequence

(Figure R-31 illustrates the solar blanket installation operation.) Similarly, power distribution system (PDS) switches are installed on the frame and main feeders are positioned for unrolling. These operations, requiring 39 men per shift, are accomplished during the first two and one-half shifts. During beam machine operation the same crew installs and fastens the various rolls to longerons and cables as they deploy.

The longerons are fabricated automatically during 2 shifts starting with the third shift. The beam machines produce longerons at the rate of 2 m/minute, or 800 meters in approximately one 8 hour shift. The operation is spread over 2 shifts to allow for fastening of blankets, cables, etc., as the longeron advances. The transverse beams are fabricated during the first of the two shifts. During the next shift, end fittings are added to them and the beams are translated, installed into position, and attached to the longerons. Installation of transverse beam end fittings, beam translation, and securing in place are remote-manual operations requiring manned manipulator modules at each beam end. All beam machines are shutdown during the transverse beam joining operations.

While the wing No. 1 construction is taking place, the antenna crews are proceeding with the assembly, test, and installation of the antenna elements into the antenna frames. (This activity was initiated during construction of the previous satellite.) The antenna assembly continues during construction of the center section. The synopsis of the antenna construction and assembly operations is shown in Figure R-32 which is described.

The antenna frame is constructed on its dedicated hexagonal work fixture located on the (otherwise) inactive side of the SCB, Panel A of the figure. Beam machines located at each corner of the hex fixture produce the antenna frame. The antenna corner elements are constructed initially, followed by the connecting beams. The catenary cables and suspension web cables upon which the antenna RF elements are subsequently mounted are then deployed and tensioned by two track-mounted vehicles operating on opposite sides of the frame and connected by a closed-loop cable conveyor.

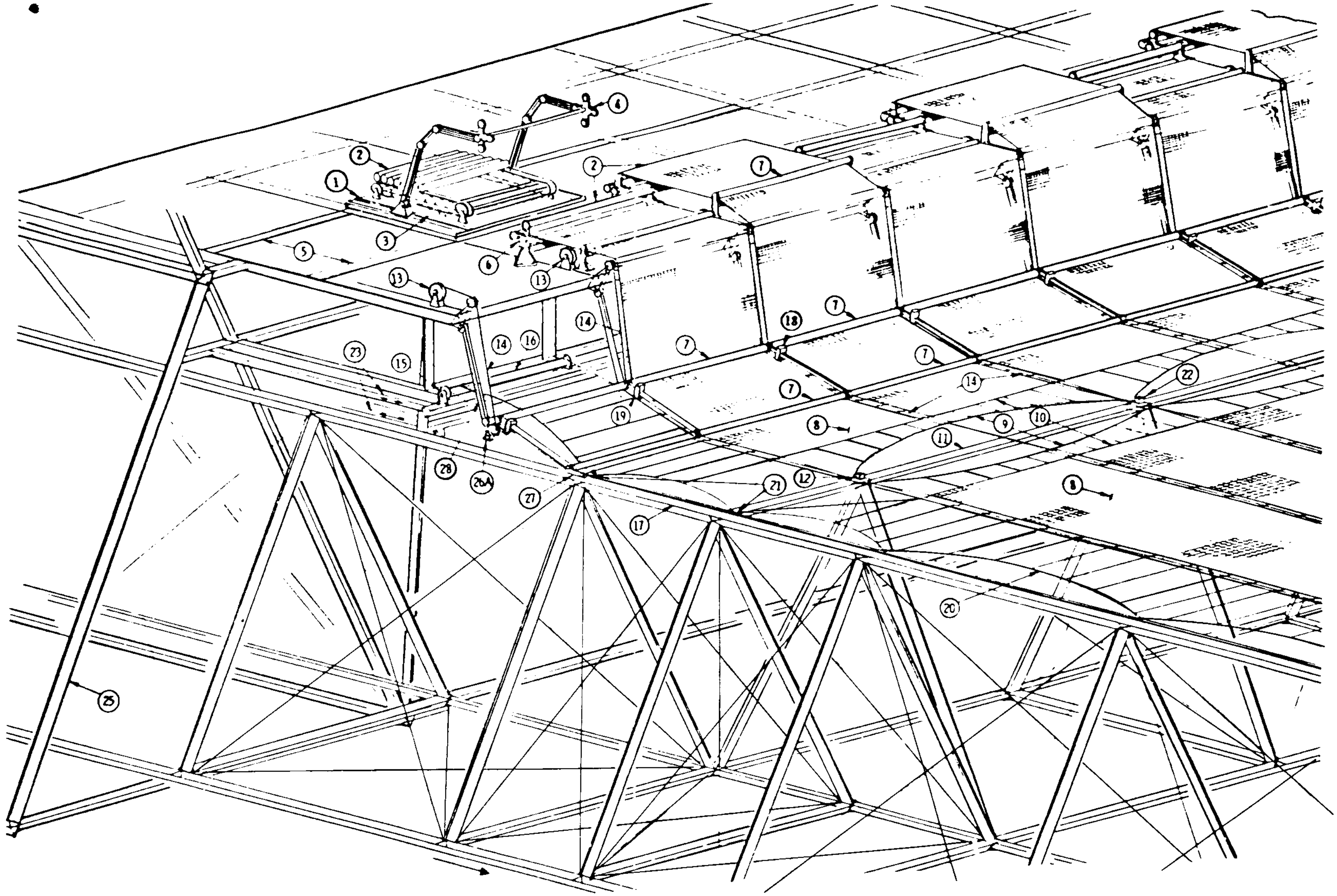


Figure R-31. Solar Blanket Installation Concept (continued)

Figure R-31 Solar Blanket Installation Concept (concluded)

1. S/A BLANKET ROLL TRANSPORTER - LOADER
2. S/A BLANKET ROLLS
3. USED ROLL CORES
4. BLANKET ROLL INSTALLER - REMOVER
5. TRANSPORTER TRACKS
6. S/A BLANKET DISPENSING SPINDEL QUAD
7. BLANKET STRIP GUIDE ROLLERS
8. DEPLOYED SOLAR BLANKET STRIP
9. LEADING TRANSVERSE CATENARY
10. BLANKET STRIP - TRANSVERSE CATENARY JOINT LINE
11. UPPER VERTEX OF SATELLITE (50 M TRIBEAM GIRDER) CROSS BEAM
12. TRANSVERSE-CATENARY-TO-CROSS BEAM ATTACH POINT
13. LONGITUDINAL CABLE DISPENSER
14. LONGITUDINAL CABLE
15. LONGITUDINAL CATENARY DISPENSING SPINDEL
16. LONGITUDINAL CATENARY ROLL
17. UPPER VERTEX OF SATELLITE (50 M TRIBEAM GIRDER) LONGERON IN BOTTOM CORNER OF TROUGH
18. BLANKET-EDGE-TO-CABLE ATTACH MACHINE
19. BLANKET-EDGE-TO-LONGITUDINAL CATENARY ATTACH MACHINE
20. DEPLOYED LONGITUDINAL CATENARY
21. CATENARY-TO-LONGERON ATTACH POINT
22. SWITCH GEAR MOUNTED ON CROSS BEAM
23. RETRACTING PLATFORM FOR SWITCH GEAR AND SECONDARY FEEDER INSTALLATION
24. MAIN FEEDER DISPENSER
25. CONSTRUCTION FIXTURE
26. TRANSVERSE CATENARY-TO-CROSS BEAM ATTACH MACHINE IN ATTACH POSITION; 26A NON-ATTACH POSITION
27. LONGITUDINAL CATENARY-TO-LONGERON ATTACH MACHINE IN ATTACH POSITION; 27A NON-ATTACH POSITION
28. ATTACH EQUIPMENT TRANSLATING SUPPORT ARM

(28A) TRANSLATING ARM IN CATENARY-TO-CROSS BEAM ATTACH POSITION

29. CROSS BEAM (50 M TRIBEAM GIRDER) FABRICATION FACILITY IN BEAM FABRICATION POSITION

(29A) 50 M CROSS BEAM IN FABRICATION POSITION

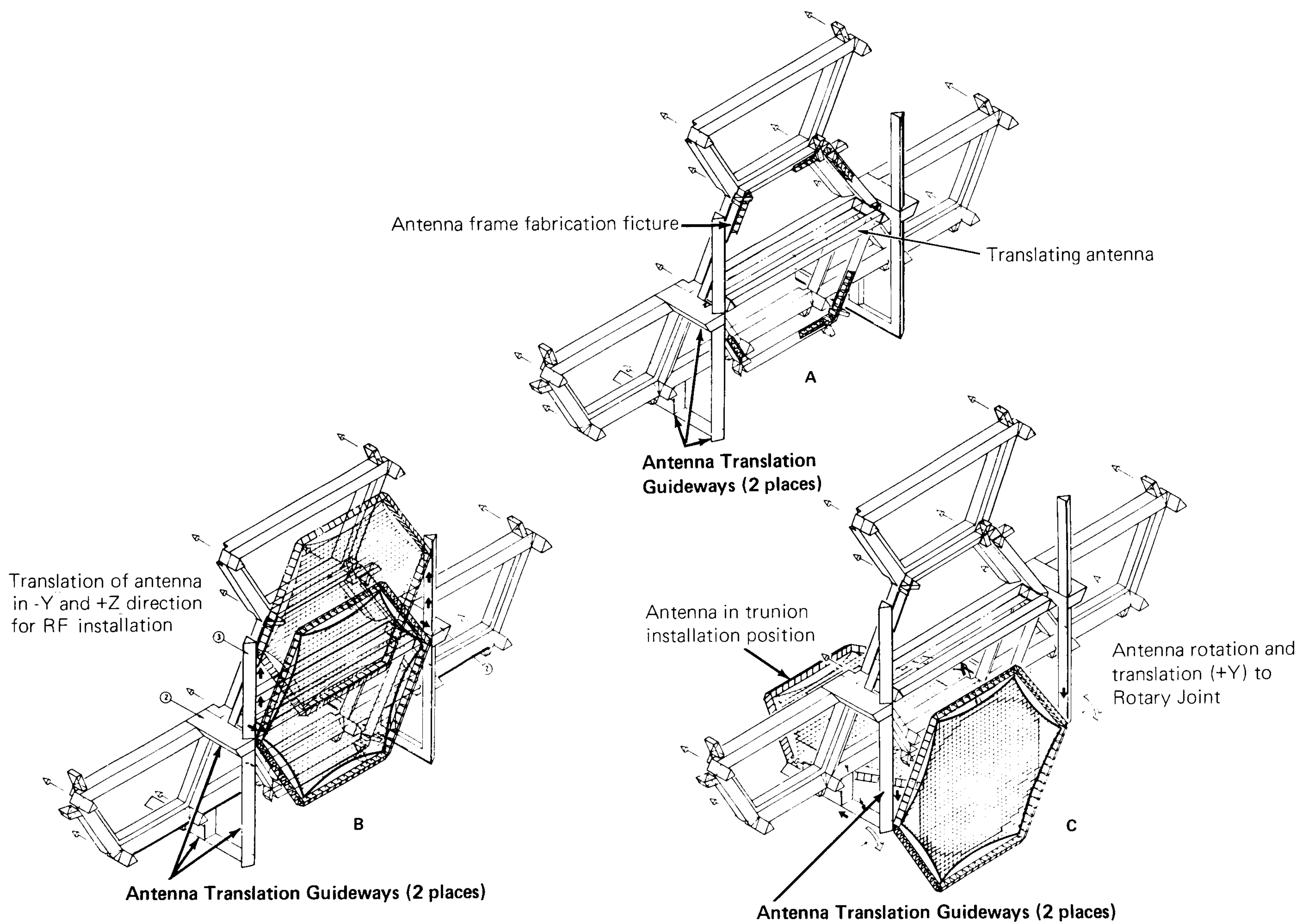


Figure R-32. Antenna Construction and Assembly Sequence

The movements of the antenna required to initiate installation of the RF elements are indicated in Panel B. Upon completion of the tension web installation the antenna structure is released from its hex fixture and translated in the -Y direction to the X-Y plane of the vertical section of translation track which allows the assembly to be moved in the $\pm Z$ directions. The RF assembly and installation facility is then extended in the -Y direction to be in close proximity to the plane of the tension web to support installation of the RF modules onto the web. The antenna is first moved in the +Z direction until the bottom row of the tension web is accessible to the RF facility and that row of modules is then installed. The antenna is subsequently translated row-by-row past the RF facility in the -Z direction for RF module installation; when all modules have been installed the antenna assembly is complete.

Completion of the antenna occurs simultaneously with completion of the rotary joint. In Panel C the antenna is first translated in the -Z direction to the end of the verticle section of track, rotated, and then translated in the +Y direction along the lower track to the position shown which locates it over its mounting trunnions for attachment to the rotary joint. The transfer/installation operations have been designed for minimal transfer distance of the completed antenna.

The entire structure and the power conversion system (solar blankets, reflectors and power distribution system), for wing No. 1 is completed on the 34th day. Subsequent to completion of wing No. 1 the construction facility constructs the longerons and frames in the center section, installs the slip-rings, constructs the trunnion supports, installs the trunnions, antenna and the power wiring in the center. Although 16 days are scheduled for this activity, the timeline requires only 12 days with two additional days scheduled for transfer of the antenna to the trunnion mounts and two days allowed for contingencies. Immediately upon completion of the center section primary structure the facilities for the operation and maintenance base are installed and the first operational maintenance crew arrives to support installation of the antenna control electronics and satellite checkout, which takes place from day 50 through day 69 as wing No. 2 is also being fabricated.

By the 51st day all satellite hardware has been delivered. On-site logistics activities are therefore greatly reduced freeing construction support personnel for subsystems hookup and checkout during the wing No. 2 construction period.

Use of the construction facility is completed on day 78 and it is transferred (flyaway) to the construction site of the next satellite on day 84. Final satellite checkout and acceptance testing is completed on day 86.

LEO Base - The continuous support functions of the LEO base include supervision of cargo and crew transfers between HLLV's and OTV's, scheduled maintenance of EOTV's (changeout of thruster screens and argon propellant tanks) and IOTV's, and up and down traffic monitoring. No depot function is provided for normal transfer of cargo and crew. It is estimated that these activities can be supported by a crew of 30. The permanent LEO base is shown in Figure R-33. It includes one crew habitat module and one crew support module which are of the same configurations as those modules used on the GEO SCB. The operations control and staging module provides multiple docking ports for emergency staging support.

Construction of the electric OTV's is scheduled to take place in LEO. The fleet buy for the entire program is 70 units based on a 10 year life. These vehicles can be constructed at the rate of 27 days per unit utilizing a crew of 188 men (36 construction workers plus 11 supporting crewmembers per shift). The EOTV construction facility will be manned early in the program (prior to initiation of satellite construction), but only intermittently thereafter.

Cargo Handling Mass Flow - Delivery requirements to meet the construction schedule of reference Figure R-30 are defined by the mass flow demand schedule of Figure R-34. This schedule requires that all materials except the antenna component be delivered in the first 72 days of construction. Payload compositions and delivery sequence must support the individual subsystems demands.

The aluminum cassettes, solar array blankets, and reflector rolls must be scheduled early in the traffic flow, since wing construction commences

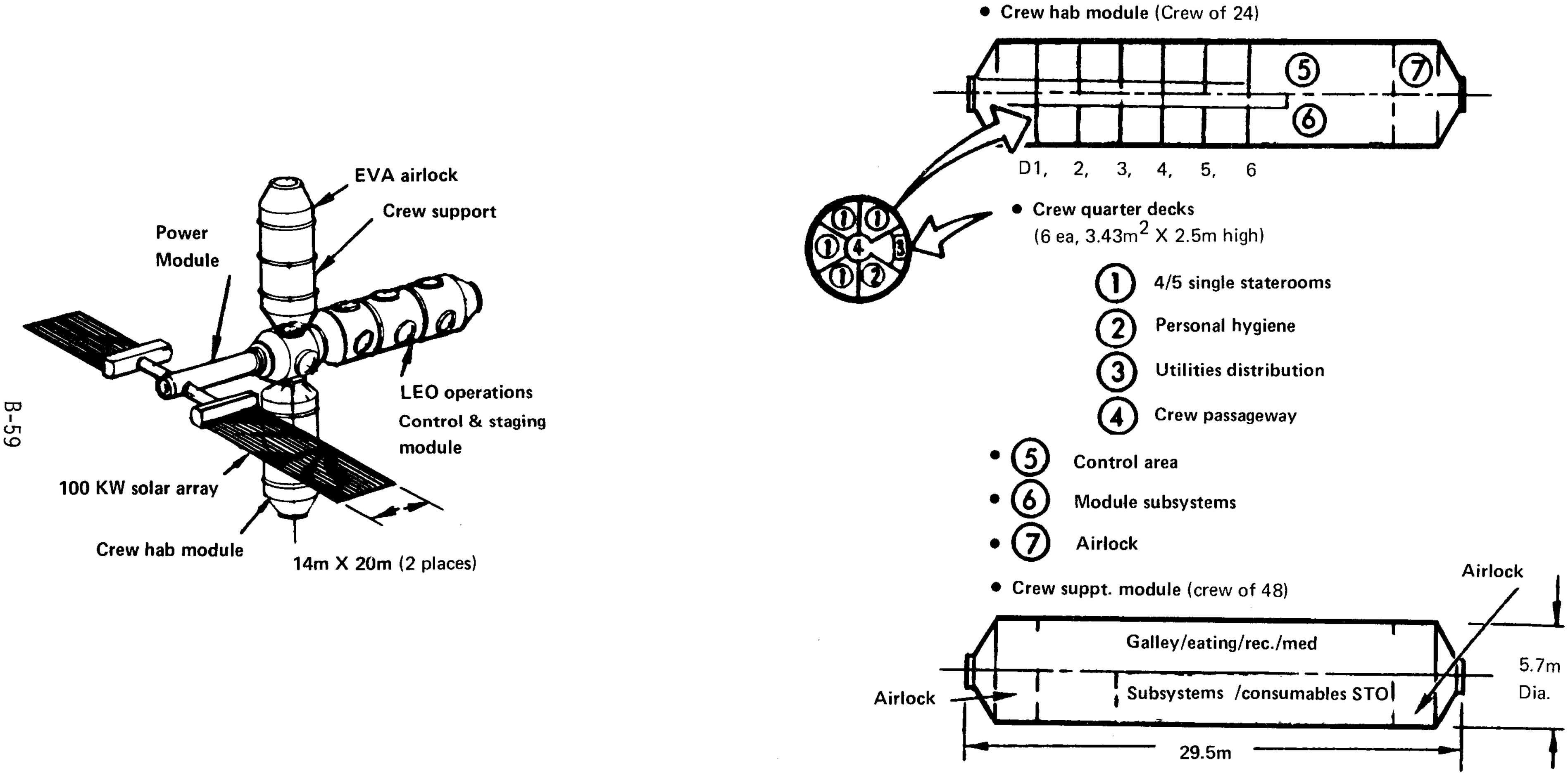


Figure R-33. LEO Base Concept

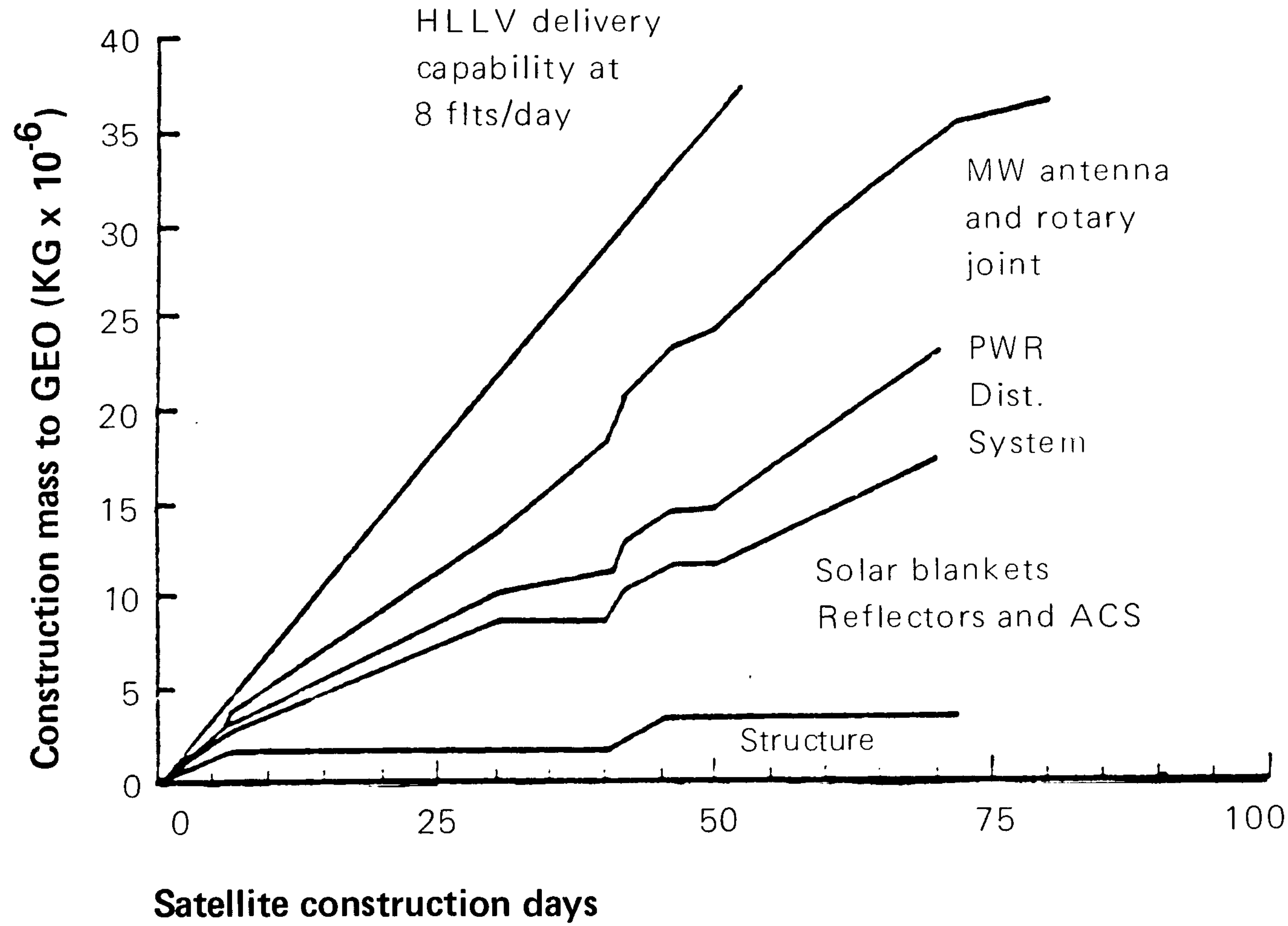


Figure R-34. Mass Flow Demands for Satellite Construction at approximately the eighth day of the 90 days allocated for fabrication and checkout of each satellite. The waveguide subarrays have different need dates, but their very low density characteristics make it necessary to include some arrays in almost every payload, thus complicating mass flow planning.

A total of 166 HLLV flights are required to transport $37.2 \times 10^6$ kg, representing the mass of one satellite, to LEO. ($37.2 \times 10^6$ kg is not necessarily the current satellite mass, which is subject to continual updating, but is a representative value.) Seven different payload mixes, averaging 225,000 kg each, have been defined and sequenced to support construction needs. An HLLV launch schedule averaging 3.2 flights per day has been postulated and is shown as the top line of the figure. The schedule is within the projected launch rate capability, considering other delivery requirements imposed on the transportation system such as maintenance materials and crews. This provides the potential for completion of deliveries to each satellite in 51 days thus providing a 21 day margin for contingencies.

Cargo Packaging - An analysis of cargo packaging was conducted to assure that the construction materials can be properly packaged in quantities consistent with construction requirements and in packages that fully utilize the payload weight capability of the HLLV, while not exceeding the volume constraints. Table R-7 illustrates packaging concepts for major elements of the satellite. These package configurations, sizes, and specified quantities per satellite are designed for compatibility with the satellite construction concept and construction equipment described earlier.

Three primary structure cassettes are installed in each beam machine to produce the 2-m triangular beam elements which comprise the basic building block for the 50-m girders. The cassettes contain enough material to complete one half of the satellite structure and are replaced only once subsequent to initial loading of the beam machine to complete the remainder of the structure. Therefore, sufficient cassettes must be on hand at the beginning of the first wing fabrication to support construction of the entire wing.

Each solar blanket roll is 750 m long - the length required for one bay. For a 600-m wide bay, 22 of these 25-m wide rolls are mounted side by side

Table R-7.  Cargo Packaging

| SPS ELEMENT | PACKAGING | PACKAGE DIMENSIONS | NO. REQUIRED | NOTES |
|---|---|---|---|---|
| STRUCTURES | CASSETTES OF ALUMINUM TAPES | 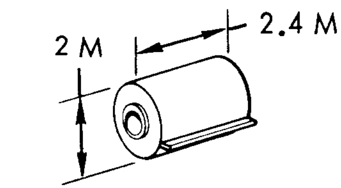 | 1188 | 6 DIFFERENT TAPE LENGTHS<br>2500 KG AVE MASS |
| SOLAR BLANKETS | ROLLS | 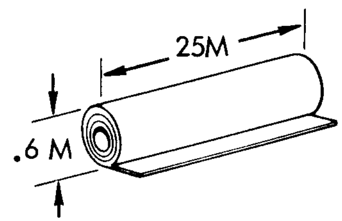 | 1632 | 750 M LENGTH/ROLL<br>7136 KG/ROLL |
| REFLECTORS | ROLLS OF FABRIC-HINGED ALUMINIZED KAPTON SHEET | 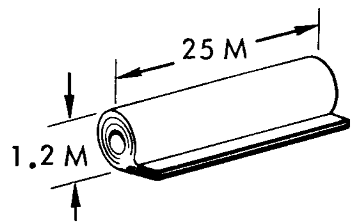 | 144 | 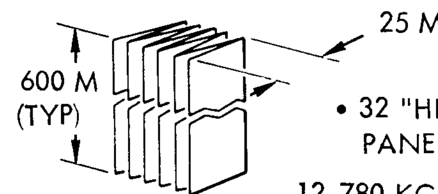<br>• 32 "HINGED" PANELS<br>•12,780 KG/ROLL |
| MW ANTENNA WAVEGUIDE PANELS | SUB ARRAYS | 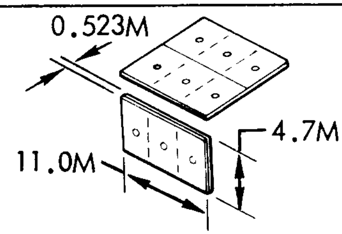 | 6993 | • ALL SUBARRAYS HAVE SAME OVERALL DIMENSIONS<br>• 10 DIFFERENT POWER MODULE SIZES - QUANTITY VARIES WITH SIZE<br>• SUBARRAY MASS (AVE) = 716 KG |

in the blanket layer and deployed simultaneously. End and side attachment materials and hardware are packaged separately.

The reflector panels are 600-m wide and 800-m long when deployed. When packaged, the reflectors have an accordian-fold 25 m wide. The resulting 25 x 600-m strip is then rolled for packaging as shown in Table R-7.

The 6993 waveguide panels are the lowest density payload item and, therefore, become a major driver in packaging and scheduling payloads. Based on the average panel shipping dimensions and mass given on the table, a maximum of 50 panels for a total mass of 35,000 kg can be carried in the HLLV cargo bay.

In addition, klystrons (which do not present a packaging problem) are a major payload item. The microwave antenna contains a large number of subarrays that, in turn, are composed of up to 50 power modules. Each power module has a klystron which is shipped to GEO separately and inserted before the subarray is secured to the antenna. Each klystron has an average volume of 0.092 $m^3$ and weighs 45 kg; 135,864 are required for each satellite.

b. Commercial Operations

Commercial operations consists of operating and control of the power system as it supplies power to a power grid and maintenance operations required to keep the system within performance limits.

Loss of total or partial power from the satellite would occur several times a year due to satellite routine maintenance, shadowing effect from the earth and from other SPS systems. When these outages are predictable and scheduled it should have a minimal effect on the utility systems integrity and operations since the timing of such outages would be during the low load periods.

However, assuming a significant penetration of SPS power systems in the future, the generation reserve needed to maintain the utility service reliability would be expected to increase to cover the emergency shutdowns of the satellite. More detailed utility system studies are needed to predict the impact on reserve levels from emergency SPS power system outages.

## DOCUMENTATION LIST

The Rockwell International Satellite Power Systems (SPS) Concept Definition Study, NAS 8-32475, was performed over a 12-month period and was documented in a seven volume final report. The final report documents are as follows:

| Volume | Title | Number | Date |
|---|---|---|---|
| I | Executive Summary | SD-78-AP-0023-1 | April 1978 |
| II | SPS System Requirements | SD-78-AP-0023-2 | April 1978 |
| III | SPS Concept Evolution | SD-78-AP-0023-3 | April 1978 |
| IV | SPS Point Design Definition | SD-78-AP-0023-4 | April 1978 |
| V | Transportation and Operations Analysis | SD-78-AP-0023-5 | April 1978 |
| VI | SPS Technology Requirements and Verification | SD-78-AP-0023-6 | April 1978 |
| VII | SPS Program Plan and Economics Analysis | SD-78-AP-0023-7 | April 1978 |

## 2. BOEING AEROSPACE COMPANY

The following is a description of the SPS concept produced by the Boeing Aerospace Company under contract to the NASA Johnson Space Center.

### A. Guidelines and Assumptions

The guidelines and assumptions for this study were essentially the same as for the Reference System. The only exception is that the SPS size is 10 GW using two 5 GW ground power output microwave transmission and reception systems.

### B. System Overview

Figure B-1 shows the satellite configuration, which is a photovoltaic SPS without solar concentrators employing glass-encapsulated, single crystal silicon solar cells.

The nominal ground output is 10 GW through two microwave power transmission links each rated at 5 GW. A summary of the nominal efficiency chain for this concept is presented in Table B-1. The satellite microwave antenna employs klystron microwave generators, a Gaussian power distribution and a maximum power density at the rectenna of 23 $mw/cm^2$. The rectenna land area, without a buffer zone, in 100 $km^2$. The satellite is constructed at low earth orbit in 8 elements employing a crew of approximately 500. The satellite elements are transferred to geosynchronous orbit using electric thrusters powered by partially deployed SPS solar arrays.

Elements of the approximately 100,000 metric ton SPS are launched into low earth orbit by 2-staged, winged, land-landing heavy lift launch vehicles, each with a 400 metric ton payload. Kennedy Space Center was assumed as the reference launch complex, pending further study.

Configuration - As illustrated in figure B-1, the configuration is a simple planar structure supporting approximately 102 $km^2$ of solar arrays. The solar blanket is divided into 256 bays, each 667.5 meters square. The bays are grouped into eight modules each having four by eight bays. A 1000-meter diameter transmitter antenna is located at each end of the 5300 m X 21280 m solar

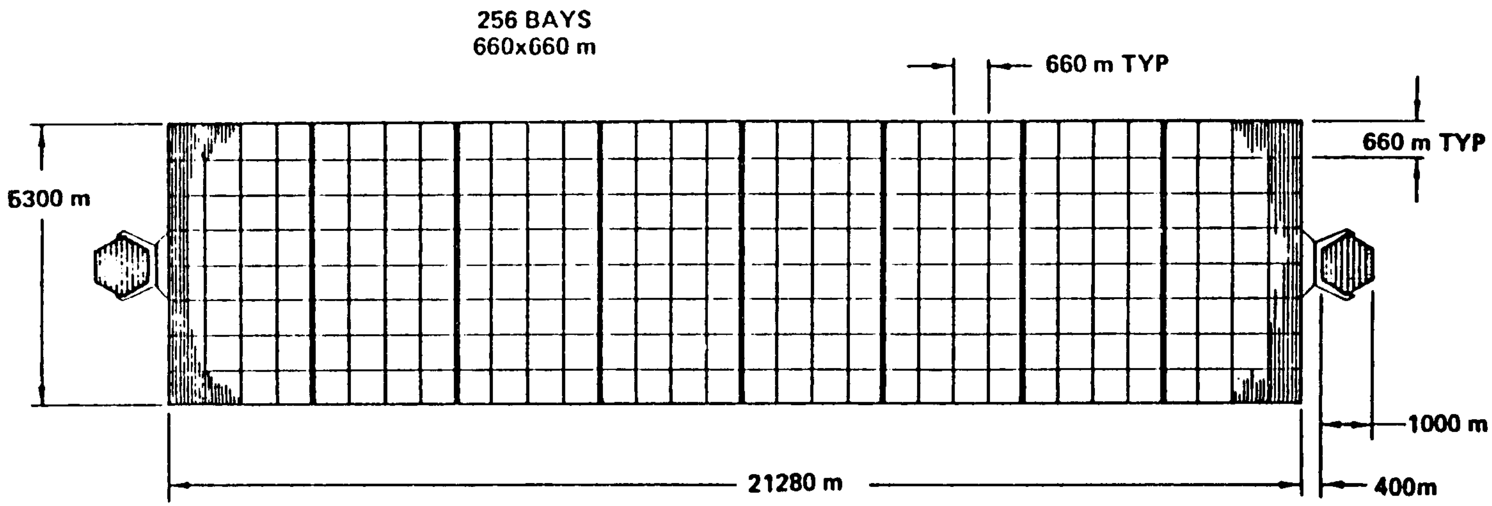


TOTAL SOLAR CELL AREA: 100 $Km^2$
TOTAL ARRAY AREA: 105 $Km^2$
TOTAL SATELLITE AREA: 113 $Km^2$
OUTPUT: 17 GW MINIMUM TO SLIPRINGS

CELL AREA = 390,000 $m^2$/BAY
PANEL AREA = 405,000 $m^2$/BAY
ARRAY AREA = 410,000 $m^2$/BAY
NO. OF BAYS = 256

Figure B-1 Photovoltaic Reference Configuration (5,000 MW Output Each Transmitter) array structure. The array primary structure is 470 meters in depth. Each transmitting antenna is mounted within a yoke structure which is, in turn, coupled to the solar array structure through a rotary joint/slip ring mechanism.

Table B-1 Efficiency Chain

| ITEM | EFFICIENCY | |
|---|---|---|
| Summer Solstice Factor | 0.9765 | |
| Cosine Loss (POP) | 0.919 | |
| Solar Cell Efficiency | 0.173 | |
| Radiation Degradation | 0.97 | |
| Temperature Degradation | 0.954 | 0.151 |
| Cover UV Degradation | 0.956 | |
| Cell-to-Cell Mismatch | 0.99 | |
| Panel Lost Area | 0.951 | |
| String $I^2R$ | 0.998 | 0.932 |
| Bus $I^2R$ | 0.934 | |
| Rotary Joint | 1.0 | |
| Antenna Power Distr | 0.97 | |
| DC-RF Conversion | 0.85 | |
| Waveguide $I^2R$ | 0.98 | |
| Ideal Beam | 0.965 | |
| Inter-Subarray Errors | 0.956 | 0.86 |
| Intra-Subarray Errors | 0.981 | |
| Atmosphere Absorp. | 0.98 | |
| Intercept Efficiency | 0.95 | |
| Rectenna RF-DC | 0.89 | |
| Grid Interfacing | 0.97 | |
| Products/Sums | 0.0712 | |
| Sizes ($Km^2$) | 108.8 | |

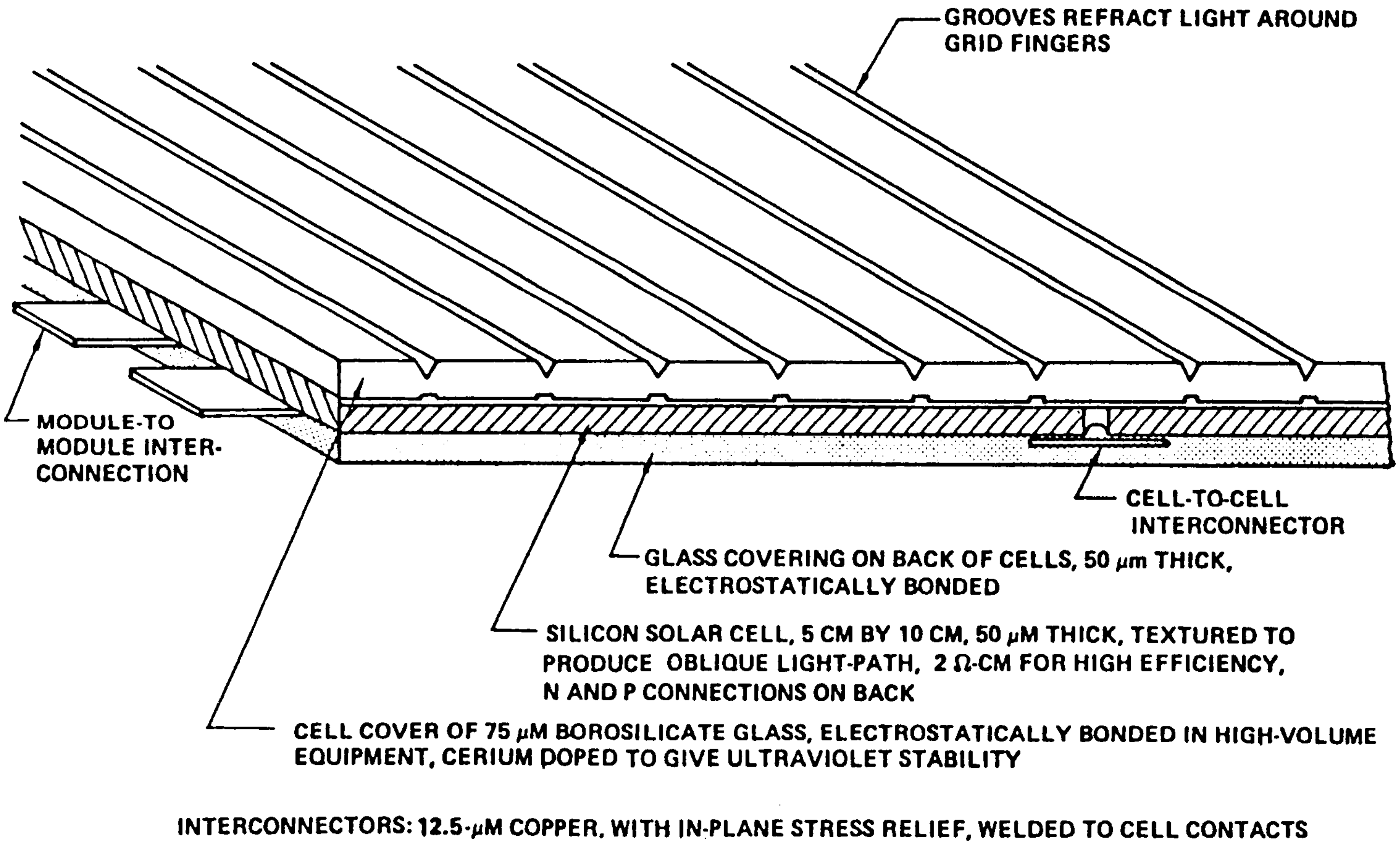


Figure B-2 Solar Array Blanket

## C. Solar Cells and Blankets

Figure B-2 shows details of the basic solar cell blank structure. The blanket consists of 50 μm thick single crystal silicon solar cells with borosilicate cover glass electrostatically bonded to the cells front and back. The cells are designed with both P and N terminals brought to the backs of the cells. This feature makes it possible to use 12.5 μm silver-plated copper interconnections which are formed on the substrate glass. Complete panels are assembled electrically by welding together the module-to-module interconnections. Other details and features of the blanket design are shown on figure B-2. The nominal cell efficiency is 17.3 percent (AMO, 28°C) at beginning of life. A key feature of the blanket design is the ability to perform in-situ annealing of the solar cells using a laser annealing concept. Annealing is required to recover radiation induced degradation of the cells.

## D. Solar Array and Structure

Figure B-3 shows the buildup of a solar array fundamental elements, which is a blanket panel. A blanket panel contains 224 solar cells (16 in series by 14 in parallel). Its dimensions are as shown. The blanket panels are assembled into installable blanket segments by welding the interpanel connectors and taping the panels together (see figure B-4). The blanket segments are 14.9 m wide by 656 m long (about one bay length) and are shipped accordion-folded in a suitable box. The method of supporting the solar blanket within the primary structural bays is shown in figure B-4. This method of support will provide a uniform tension to the end of each solar array segment by the use of constant force tensioning springs at each blanket support tape. These springs are also attached to a catenary cable that is then attached to the primary structure, (upper surface), beams at 15 meter intervals. The springs are in compression, for better reliability, and exert a uniaxial force of approximately 3.5N to each blanket support tape.

The buildup of high voltage in the solar array is accomplished by connecting approximately 78,000 sets of solar cells in series (a string). Solar cell strings approximately 5.1 km long were selected for the reference

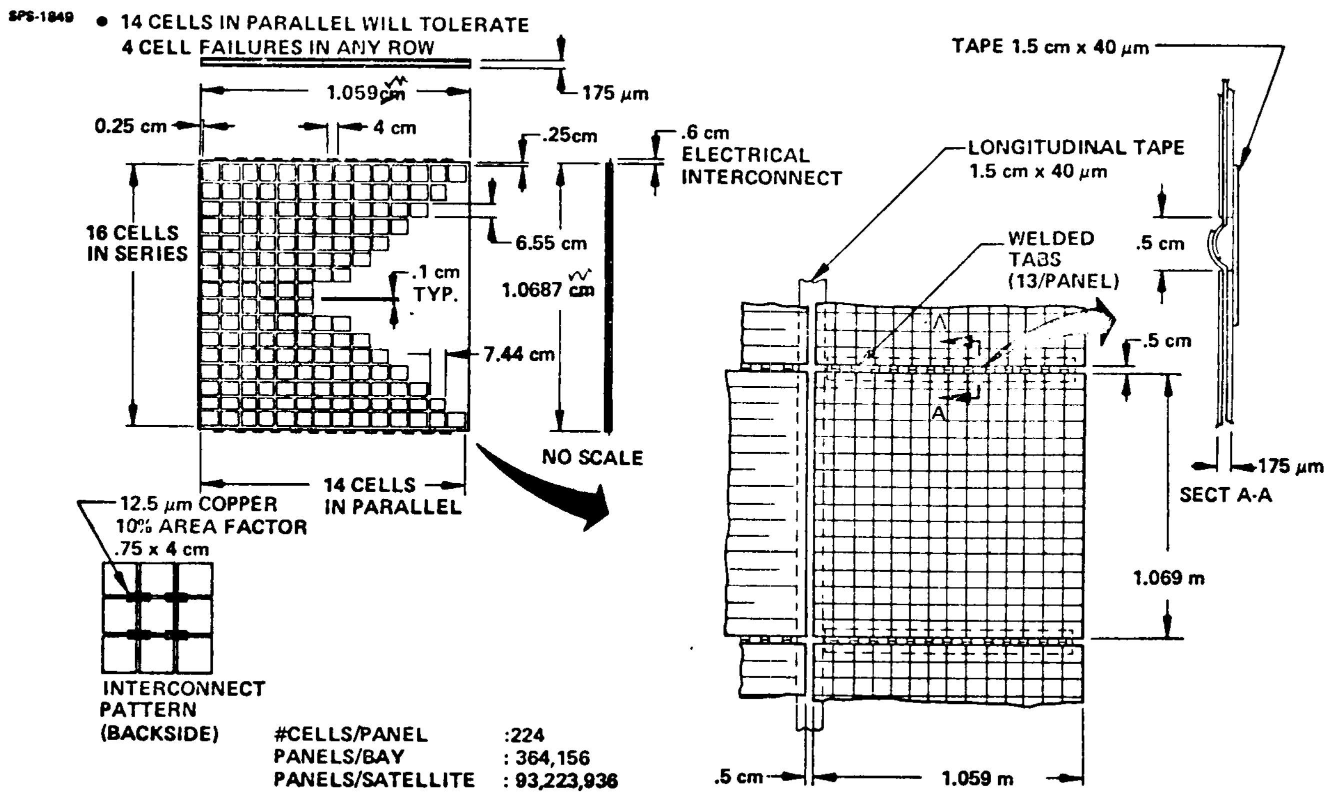


Figure B-3 Array Blanket Description

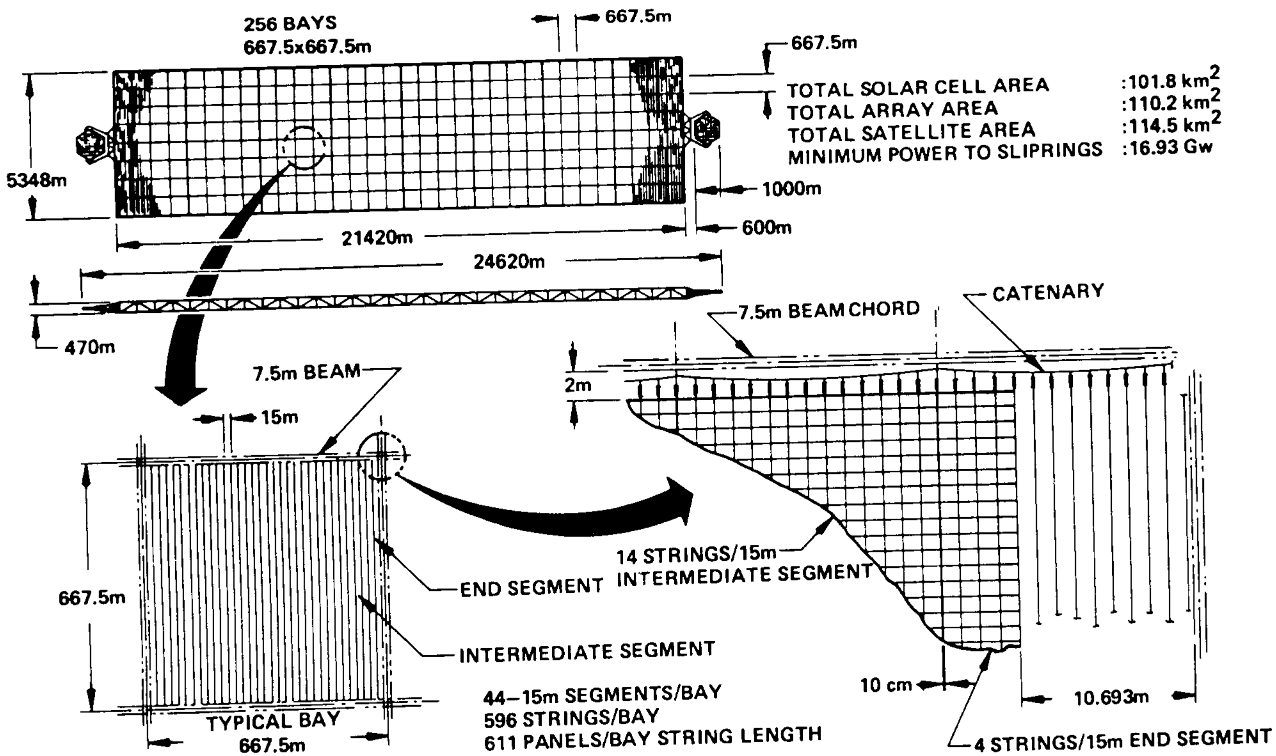


Figure B-4 Reference Photovoltaic System Description photovoltaic system configuration. This permits generating the required voltage directly from the solar array without intervening power electronics. All solar cell strings are identical. Current generated by the solar cells are carried by conductors or by the solar cells themselves. It is noted that no conductors are needed for bringing in the current from the edges of the array, the solar cell strings being arranged in loops which start from one center bus loop around the edge of the array, and return to the other bus at the center of the array. The strings of solar cells start at the centerline of the satellite and go to the outer edge and then back to the centerline. A string, therefore, must cross the primary structural beams, between bays, eight times. Interbay jumper mode of aluminum cable are used to electrically connect strings in one bay to the appropriate strings in the next bay of the string length. Figures B-5 and B-6 show sketches of the reference array blanket support method and the interbay jumper installation, respectively. The solar array primary structure is a truss-type design using 20 m triangular beams as the basic structural element. The structural material is graphite composite. The truss design load results from uniaxial tension of the solar blankets. The truss struts were sized by long column buckling and local crippling. Lightly loaded struts were sized by minimum gauge material.

E. Power Distribution

The prime function of the power distribution system is to accumulate and control prime power from the silicon solar cell collector panels; control, condition, and regulate the quantity and quality of the electrical power generated for the microwave generators; provide for the required energy storage during solar energy occultation or system maintenance shut-down; and provide for monitoring fault detection, and fault isolation disconnects. Figure B-7 shows a schematic diagram of the solar array power distribution system. The solar array is divided into 228 power sectors. Each power sector is switchable and can be isolated from the main power bus, facilitating solar cell annealing operations and/or other servicing.

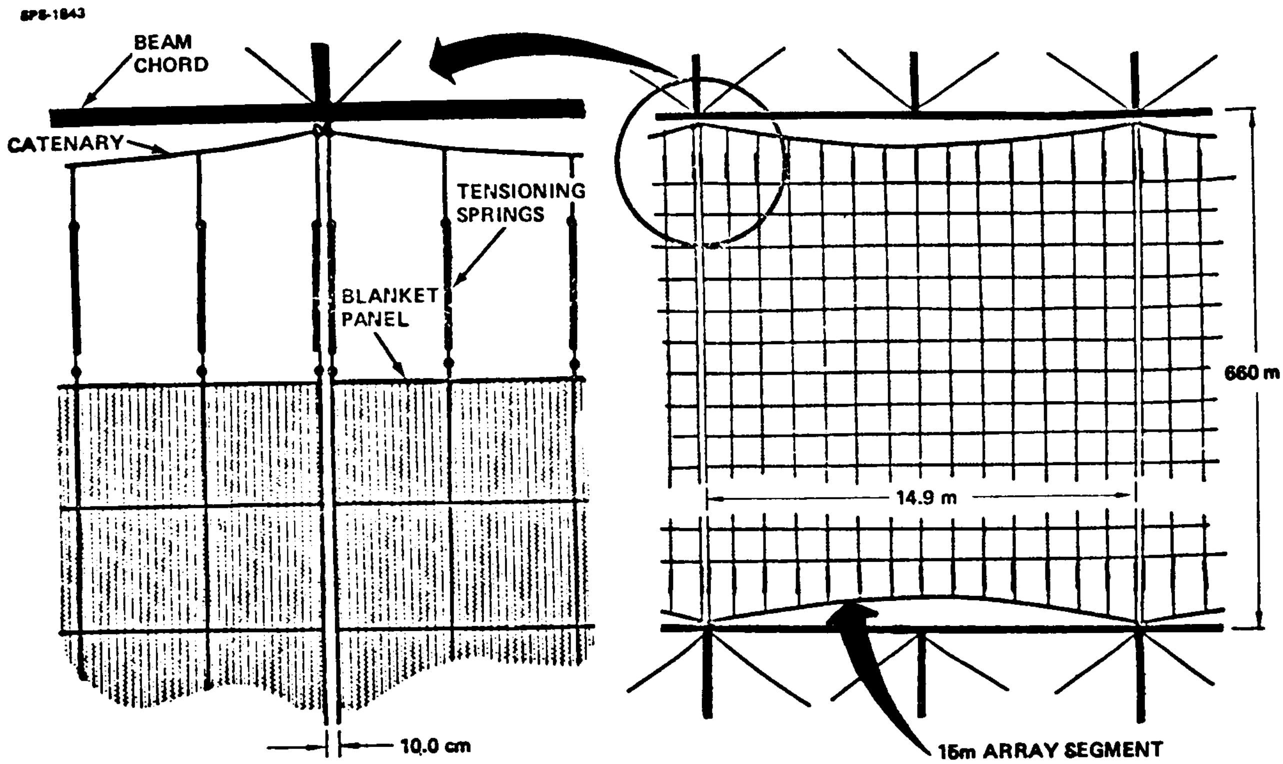


Figure B-5 Reference Array Blanket Support

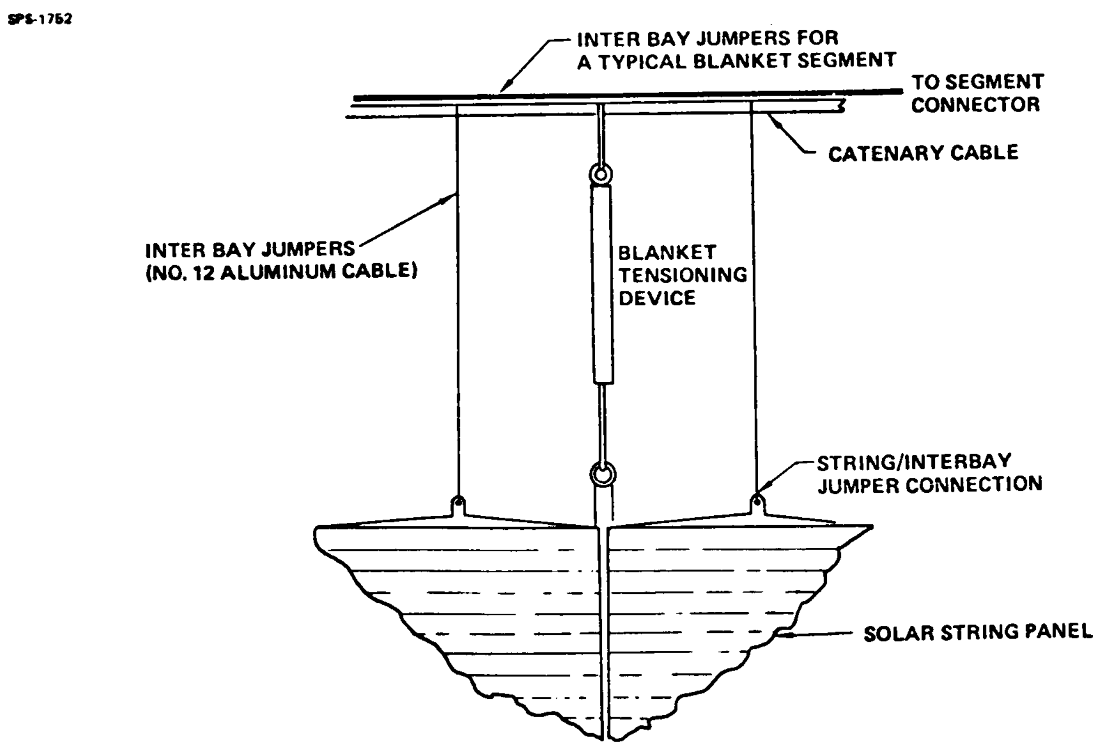


Figure B-6 Inter Bay Jumpers

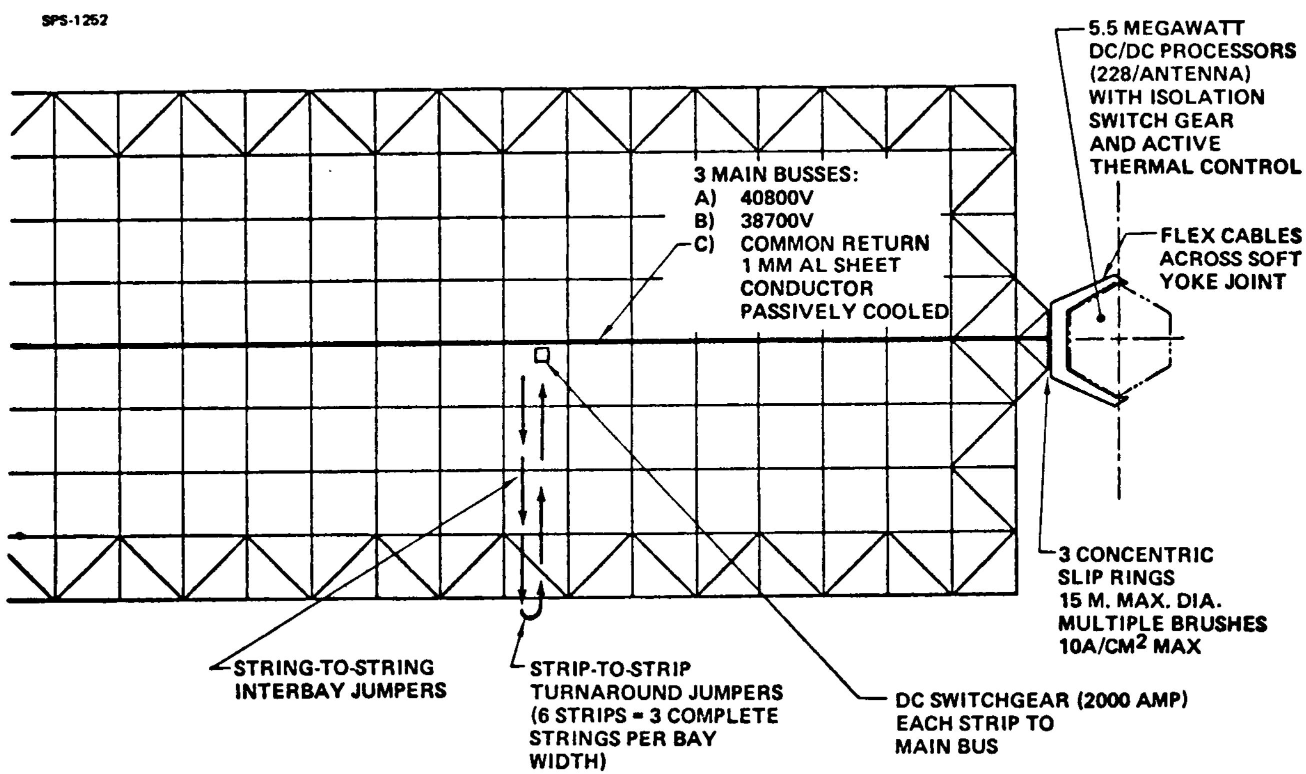


Figure B-7 SPS Power Distribution

Solar array power is controlled by vacuum circuit breakers near the buses. Voltage is controlled by turning groups of strings on or off, depending on load requirements. Two sections of the array provide the required voltage at the sliprings using the sheet conductor voltage drop to achieve the required voltage at the sliprings.

Power transfer across the rotary joint is accomplished by a slipring/brush assembly. Mechanical rotation and drive is provided by a mechanical turntable 350M in diameter. The antenna is suspended in the yoke by a soft mechanical joint to isolate the antenna from turntable vibrations.

F. Rotary Joint

As previously stated, power transfer from the solar array section to the microwave antenna is accomplished via a rotary joint (figure B-8) using a slip ring/brush assembly. Mechanical rotation and drive is provided by a mechanical turntable 350 m in diameter. The antenna is suspended in the yoke by a soft mechanical joint to isolate the antenna from turntable vibrations. The antenna is mechanically aimed by CMG's installed on its structure. A position feedback with a low frequency bandpass allows the mechanical turntable to drive the yoke to follow the antenna and also provide sufficient torque through the soft joint to keep the CMG's desaturated.

Figure B-9 illustrates the electrical components of the rotary joint. Coin silver (90% silver and 10% copper) was selected for the slip-ring material and a silver-molybdenum disulfide brush with 3% graphite was selected. With a design using a brush current density of 20 amps/$cm^2$ only about 40 kW of power is dissipated in the rotary joint. The projected brush/slip-ring wear is very small (.0289 to .0617 $cm^3$/year).

G. Attitude Control System

The attitude control system (ACS) includes all operational elements and software required to maintain orbit station keeping and attitude control of the SPS in the operational orbit or to establish attitude control from an initially uncontrolled condition. The ACS is an electric propulsion system with four installations, one at each corner of the SPS solar array system. A typical

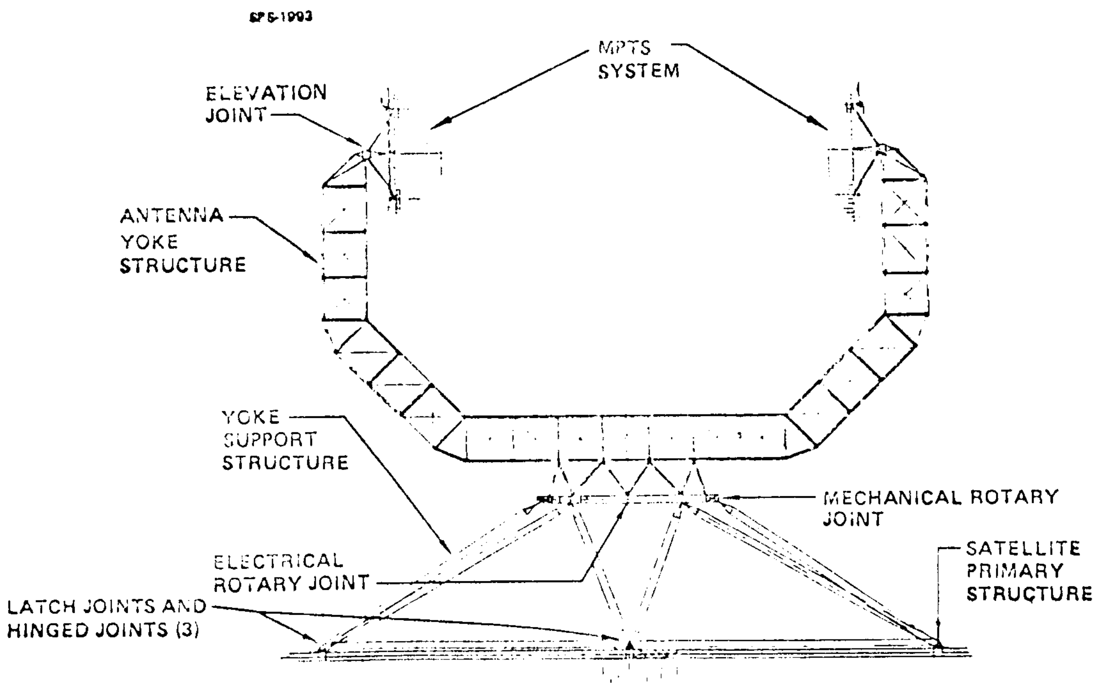


Figure B-8 Antenna Yoke and Turntables

SPS-1022

ELECTRICAL ROTARY JOINT MASS SUMMARY

| | |
|---|---|
| SLIP RINGS | – 11,810 kg |
| BRUSH ASSEMBLY | – 1,970 kg |
| FEEDERS | – 3,840 kg |
| STRUCTURAL SUPPORT | – 900 kg |
| ASSY. & INSTL. HARDWARE | – 200 kg |
| CONTINGENCY ALLOWANCE | – 900 kg |
| TOTAL | – 19,600 kg |

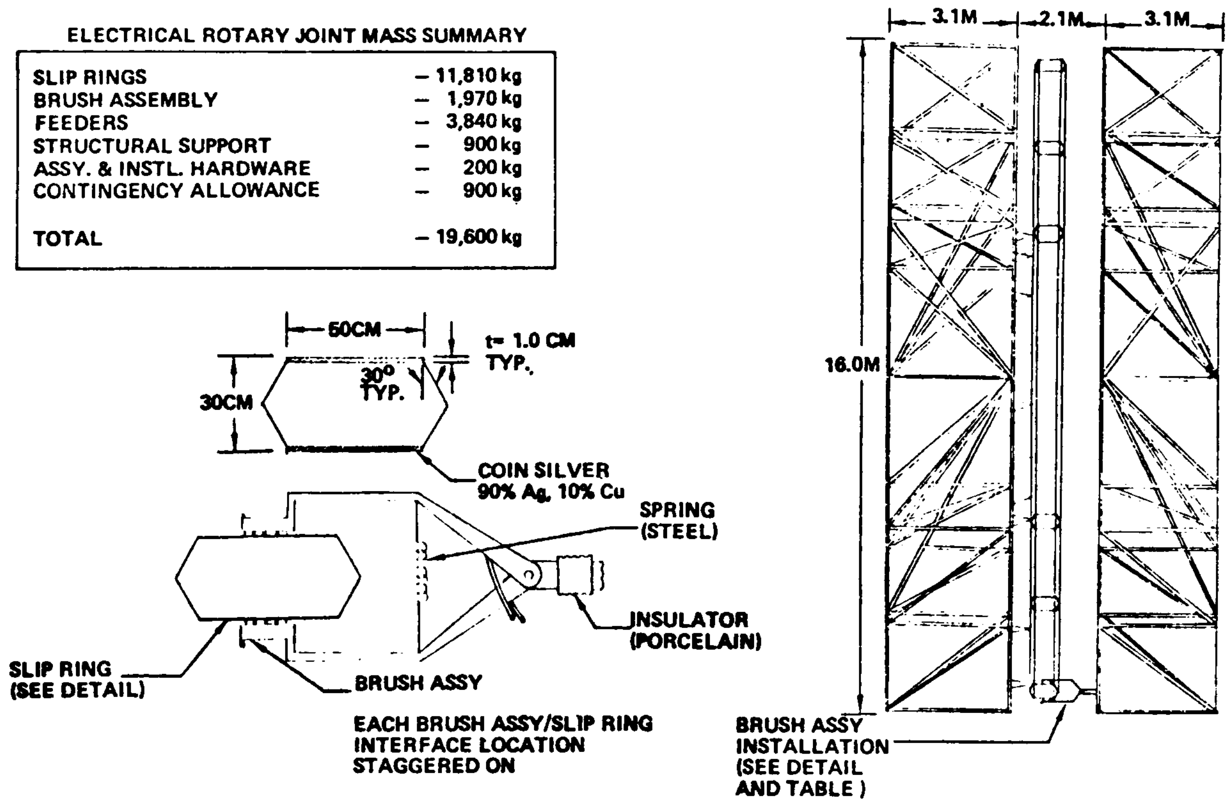


Figure B-9 Electrical Rotary Joint and Mass corner installation is illustrated in figure B-10. The ACS consists of thruster, power processor, structure, propellant feed, control systems, and instrumentation. The thrusters include the primary electric thruster and auxiliary chemical thrusters required for establishment of attitude control when electric power is not generated by the SPS.

The electric thrusters are 100 cm diameter ion engines using argon as primary propellant. Thruster Isp is 20,000 sec. Each panel contains 25 thrusters. The net thrust per panel is 150 newtons. The operating life of the system is 2 years with a 50% duty cycle and 80 amp beam current.

The chemical thrusters use $LO_2/LH_2$ as propellants and are used for control during equinoctal occultations. The engine Isp is 400 sec.

## H. Microwave Power Transmission System

General - The microwave transmission system includes the entire spaceborne array power transmitter which includes the dc distribution system from the rotary joint to the rf transmitters, the rf transmitters themselves (klystrons), their dc and rf control and monitor circuitry, and the rf antenna elements composed of slotted waveguides, support structure, rf feed circuits, mechanical pointing control, all the components required for distribution and control of the phase of the retrodirective antenna subarrays, and the ground receiving stations (rectenna). Figure B-11 shows sketches of the major components of the transmitter system. The design utilizes a retrodirective phased array powered by dc-rf klystron converters. DC power from the rotary joint is distributed in a manner to minimize $I^2R$ losses to the klystrons, utilizing 85% unprocessed power with a maximum voltage of 42 kv. The klystrons are combined to provide a tapered (10 db quantized Gaussian) illumination of the array resulting in low sidelobe levels and high antenna efficiency (over 95%). The thermal loading in the center of the array (22 kw/$m^2$rf) permits a design for a 1 km diameter array which provides roughly 5 GW of dc power on the ground per antenna. The phased distribution system is designed to minimize line lengths and cumulative phase errors in the distributing transmission lines by using a 3-node reference distribution system with line length compensation. The pilot

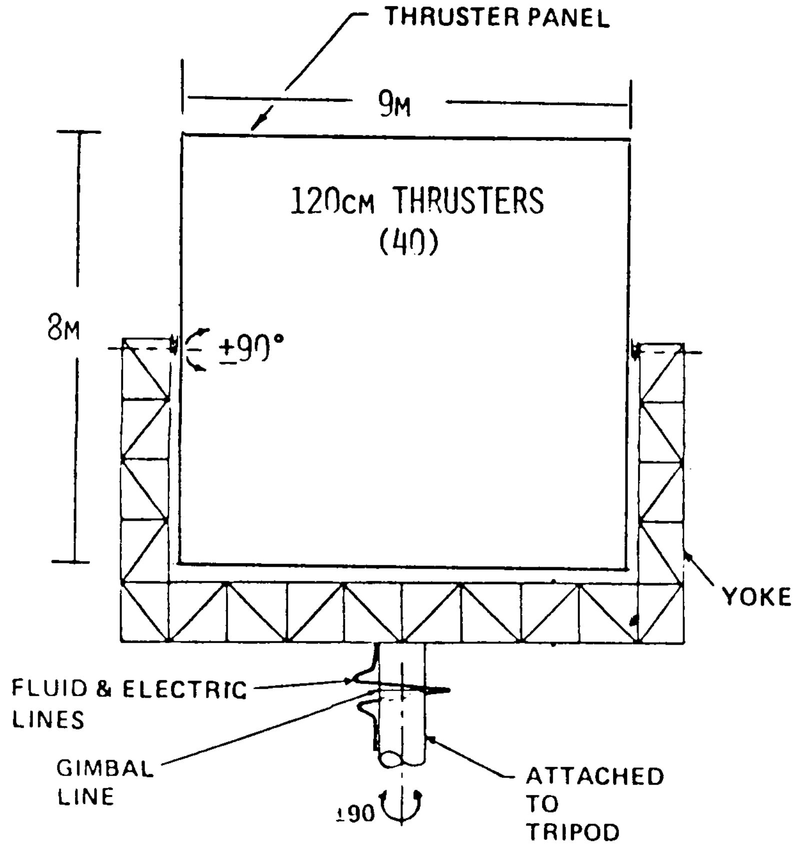


ELECTRIC THRUSTERS

- 4 PANELS (ONE AT EACH CORNER)
- THRUST/PANEL - 150N
- 25 OPERATING THRUSTERS/PANEL (40 TOTAL)
- $I_{SP}$ = 20,000 SEC
- ARGON PROPELLANT (41,000 - 80,000 KG/YEAR)
- OPERATING LIFE - 2 YEARS (0.5 DUTY CYCLE AND 80A BEAM CURRENT)

CHEMICAL THRUSTERS ($LO_2/LH_2$)

- CONTROL DURING EQUINOCTAL OCCULTATIONS
- $I_{SP}$ = 400
- 1500 - 3000 KG/YEAR

Figure B-10 Attitude Control System Thrusters

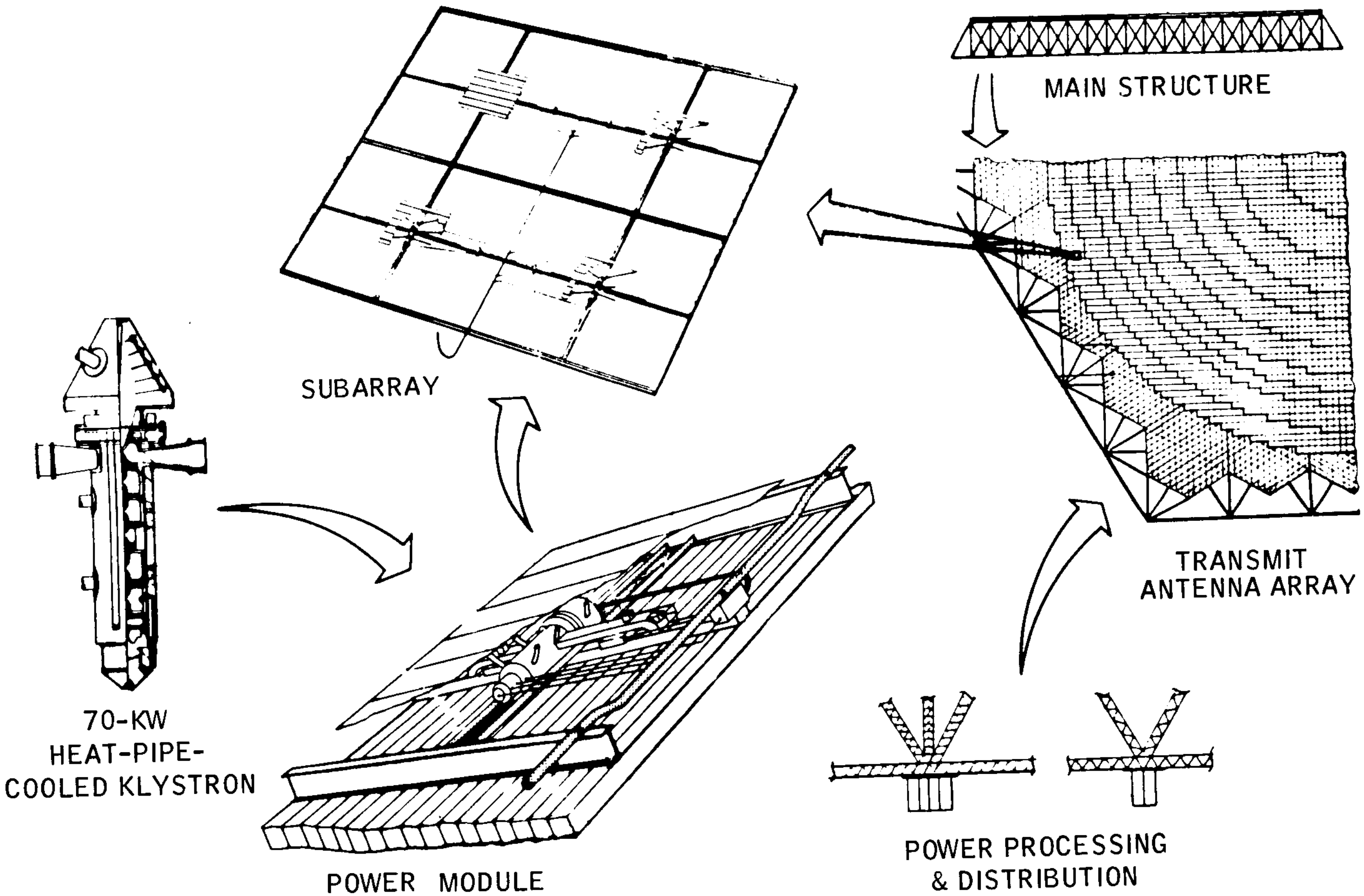


Figure B-11 Microwave Power Transmitter Design Concept reference signal from the ground utilizes 2-tone modulation with a suppressed carrier near the power beam frequency, to effect conjugation (i.e., electronic fine beam steering) in an efficient manner. Correction for some systematic propagation errors is provided through multiple pilot beam transmitting antennas.

Antenna Power Distribution - The power distribution system provides power transmission, conditioning, control, and storage for all elements of the microwave transmitting antenna. Figure B-12 shows a schematic diagram of this system. The antenna is divided into 228 power control sectors, each providing power to approximately 420 klystrons. Two of the kylstrons' depressed collectors "A" and "B" which require the majority of supplied power are provided with power directly from the power generation system to avoid the dc/dc conversion losses. All other kylstron element power requirements are provided by conditioned power from the dc/dc converter. System disconnects are provided for isolation of equipment for repair and maintenance. A nickel hydrogen battery system provides 12.186 megawatt hours of energy storage for klystron cathode heater power during solar occultations. Up to two hours capacity is provided.

DC/DC Converter and DC/RF Generators - Each dc/dc converter (figure B-13) provides power to approximately 0.5% of the total number of antenna klystrons. The klystron with five depressed collectors has a calculated tube efficiency of 85%. Figure B-14 shows a sketch of the reference 80 kw klystron unit. The selected design is a continuous wave (CW) amplifier operating at 42 KV. It uses a compact, efficient (82-85%) solenoid wound-on-body design. To achieve long life, a cathode loading of 0.15 amps/$cm^2$ was chosen.

Figure B-15 shows a drawing of the integrated klystron module. The figure shows the klystron mounted on the back of the slotted waveguide antenna array. The passive cooling system can be seen. Not illustrated here is the phase control system required to insure that the radiation from the modules will be in phase at the rectenna. This system will tie the modules within a subarray together with waveguide and all the subarrays together with coaxial cable or an equivalent transmission link. Each transmitting antenna contains 101,552 of the 70 kw amplifiers and operates with a gain of 83-85 db.

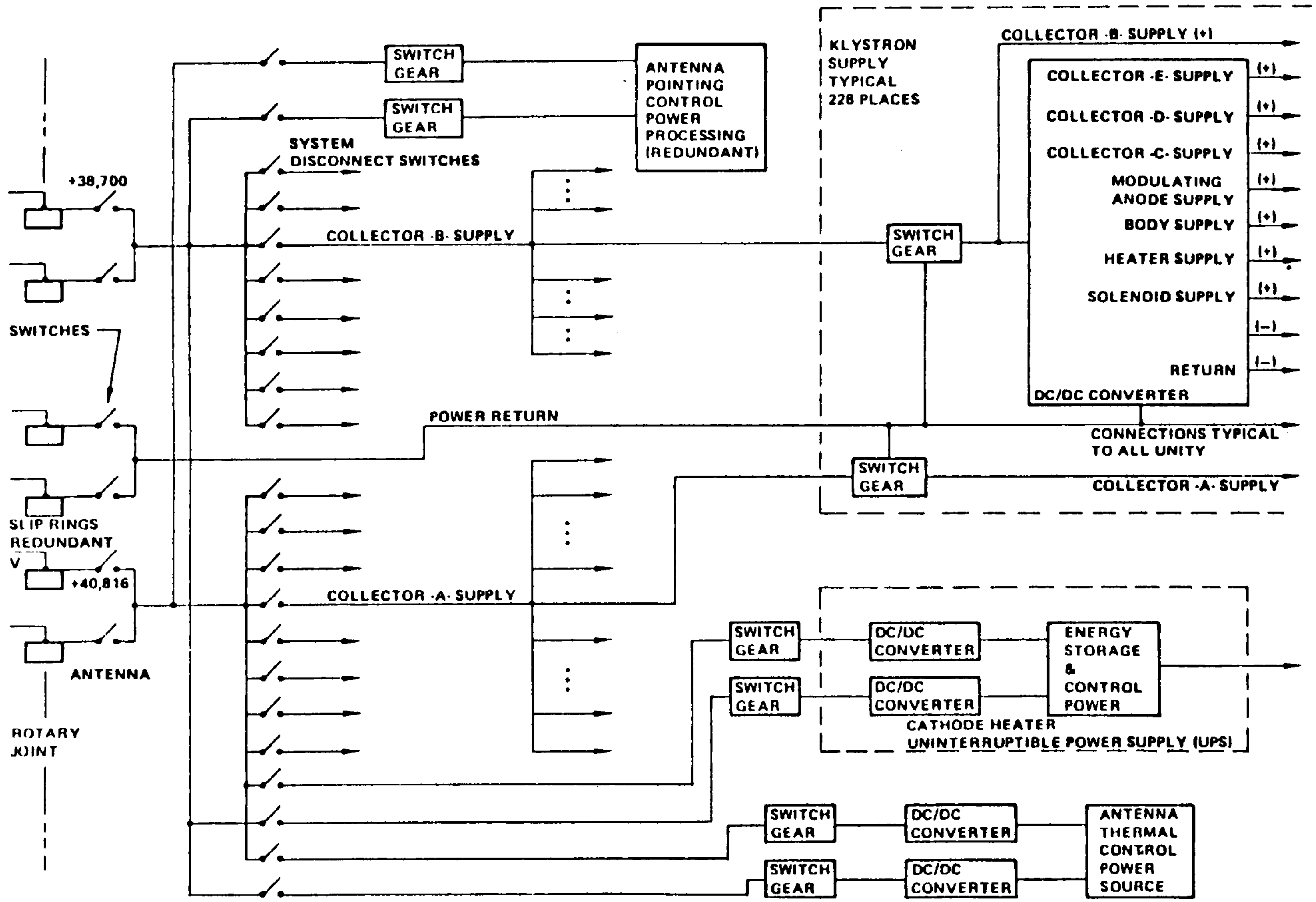


Figure B-12 MPTS Power Distribution System Block Diagram

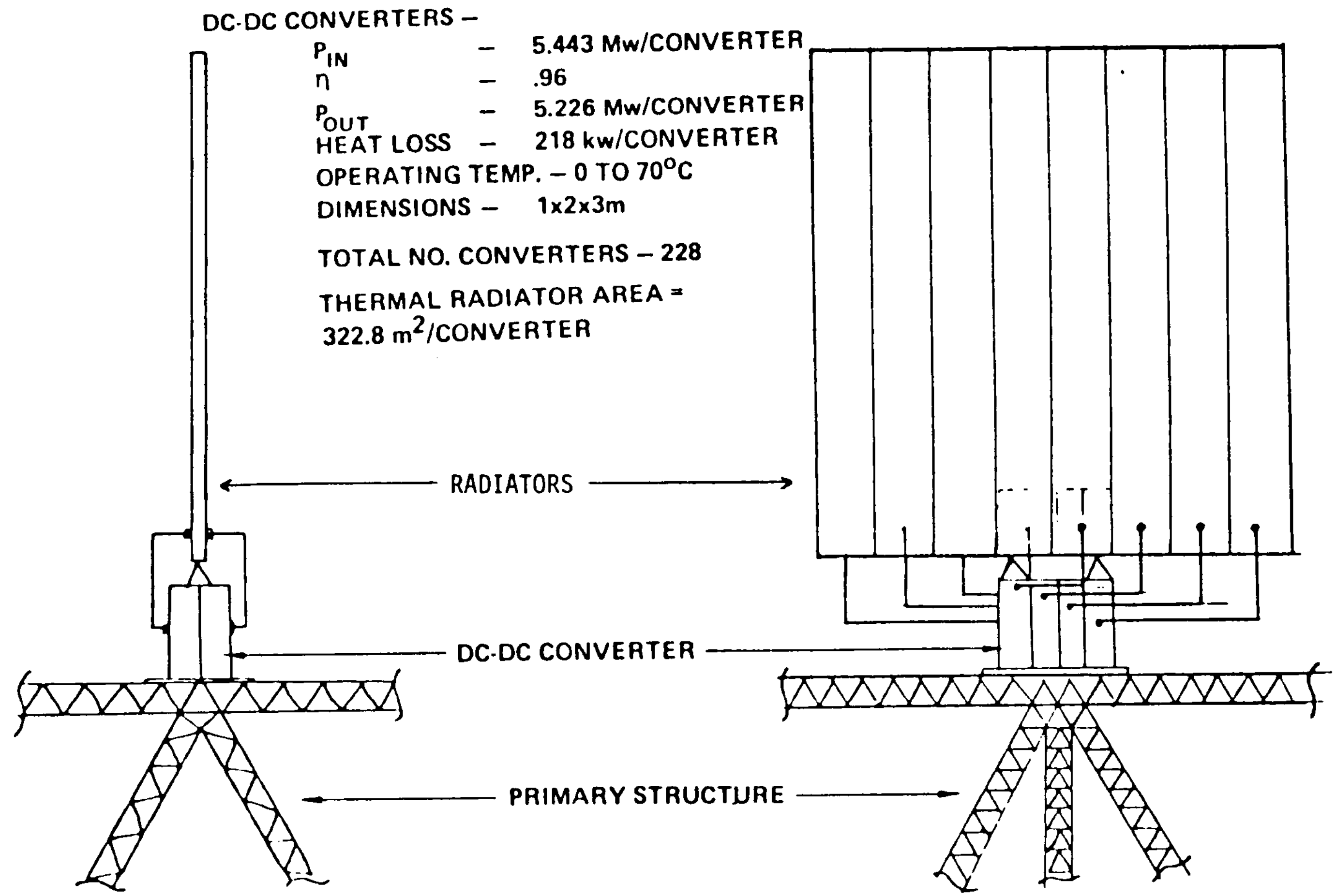


Figure B-13 MPTS DC-DC Converter

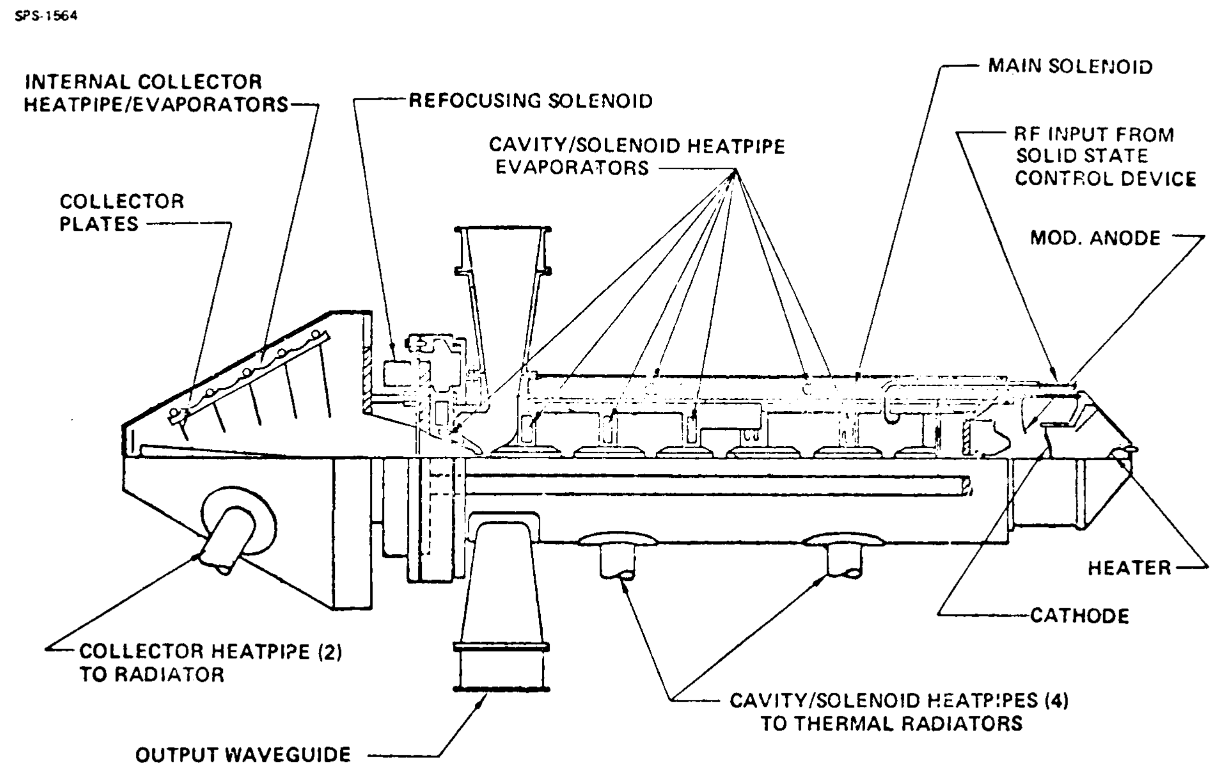


Figure B-14 70 Kw Klystron

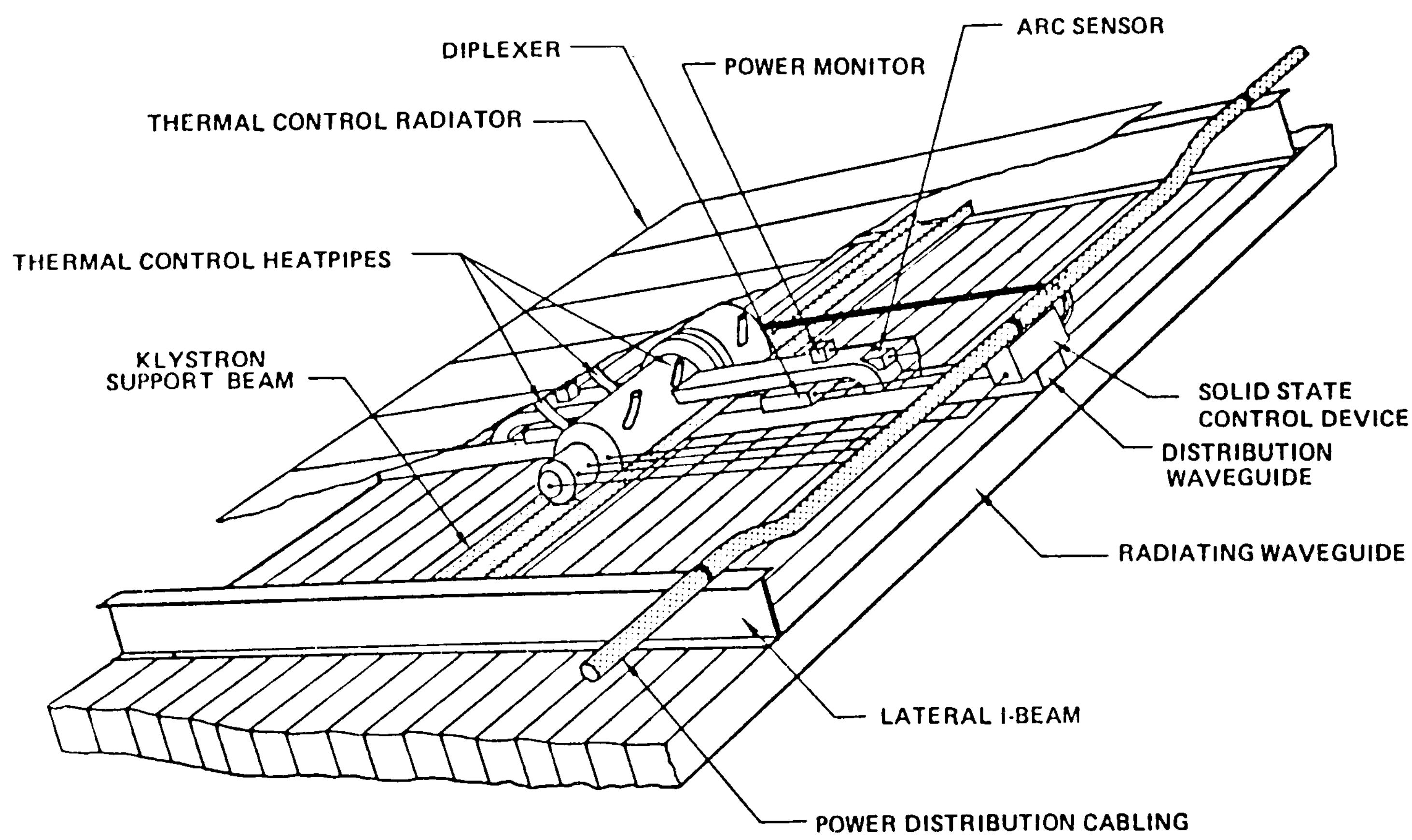


Figure B-15 Integrated Klystron Module

Integrated Subarray - The retrodirective phase array configuration utilizes 7220-10.4 x 10.4 meter subarrays arranged in a quantized 10 db taper configuration conforming to dimensional requirements which will result in a maximum RSS error associated loss of 2%. Figure B-16 shows a 4-module subarray which contains 4 klystrons, associated radiation waveguides, thermal control radiation, and control devices. The subarray support structure is composed of perimeter beams, lateral and longitudinal I-beams. Figure B-17 shows an antenna quadrant illustrating the arrangement of subarrays on the antenna to obtain the desired 10 db taper. The number of klystrons per subarray varies from 4 in the outer edge of the antenna to 36 per subarray in the center.

Figure B-18 shows a plot of microwave power density versus antenna radius illustrating a 10-step subarray distribution that closely approximates the desired Gaussian distribution.

Antenna Structure - The microwave power transmitter primary structure provides overall shape and form to the transmitter. The primary structure is an A-frame open truss structure, 130 meters deep, with a quasi-hexagonal shape in excess of 1,000 meters width and length. The primary structure and its relationship to the secondary structure and the rest of the power transmitter are shown in figure B-19. The A-frame elements of the primary structure are made up of 7-1/2 meter continuous chord beams composed of graphite polysulfone composite structure.

Secondary structure provides structural bridging over the primary structure with a sufficiently small repeating structure element interval to allow installation of the transmitter subarrays. The secondary structure, shown in figure B-20 is a deployable cubic truss, with telescoping vertical members to minimize packaging volume. The members are made from graphite composite materials and the joints all include a rigidizing mechanism or device to provide complete ridigity of the structure after deployment. Diagonal cross-members are removable as necessary to allow for maintenance of the subarrays.

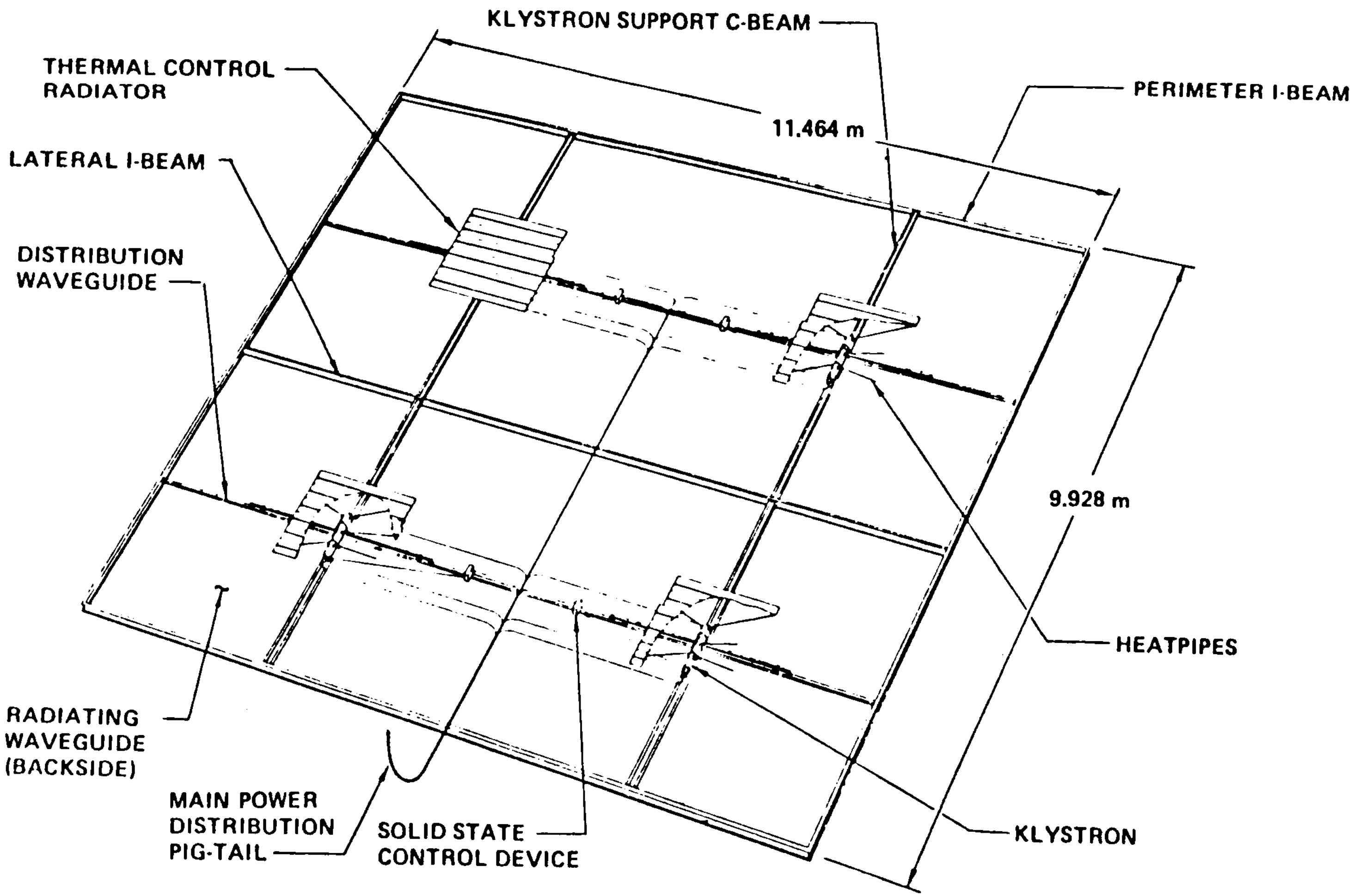


Figure B-16 Integrated Subarray

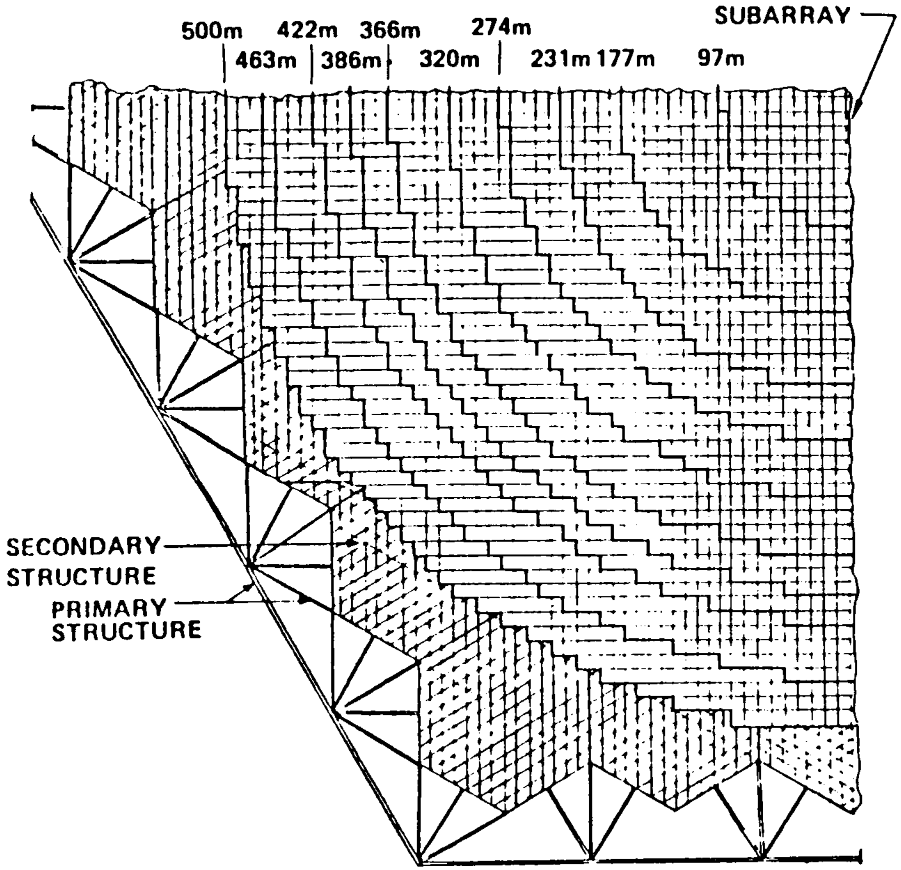


| STEP | NO. SUBARRAYS | NO. KLYSTRONS |
|---|---|---|
| 1 @ 36 | 272 | 9792 |
| 2 @ 30 | 580 | 17420 |
| 3 @ 24 | 612 | 14688 |
| 4 @ 20 | 612 | 12240 |
| 5 @ 16 | 756 | 12096 |
| 6 @ 12 | 864 | 10368 |
| 7 @ 9 | 628 | 5652 |
| 8 @ 8 | 576 | 4608 |
| 9 @ 6 | 1032 | 6192 |
| 10 @ 4 | 1000 | 4000 |
| TOTALS | 6,932 | 97,056 |

POWER OUTPUT: (ANTENNA) 7 GW
(GROUND) 5 GW

Figure B-17 Power Taper Integration

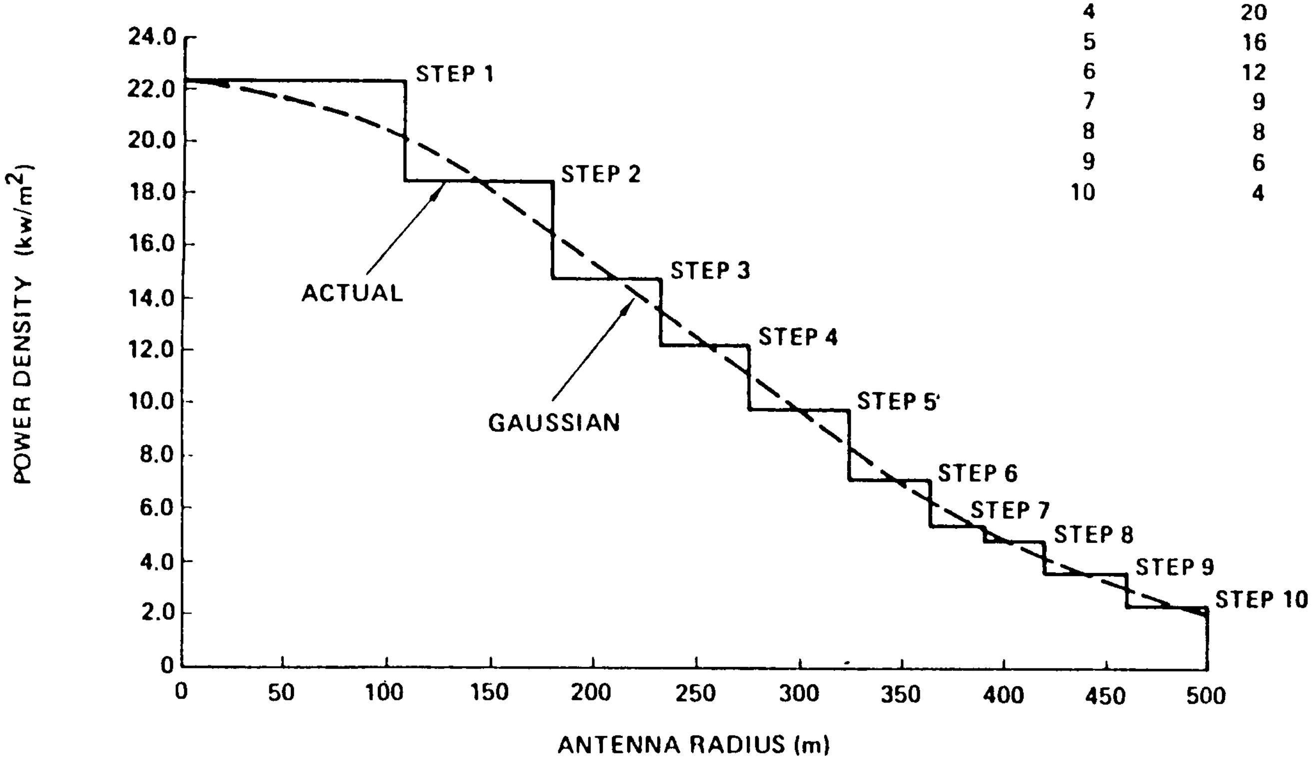


| STEP | ELEMENTS/ SUBARRAY | POWER DENSITY $kw/m^2$ |
|---|---|---|
| 1 | 36 | 22.14 |
| 2 | 30 | 18.45 |
| 3 | 24 | 14.76 |
| 4 | 20 | 12.30 |
| 5 | 16 | 9.84 |
| 6 | 12 | 7.38 |
| 7 | 9 | 5.54 |
| 8 | 8 | 4.92 |
| 9 | 6 | 3.69 |
| 10 | 4 | 2.46 |

Figure B-18 MPTS - Reference 10 dB Taper

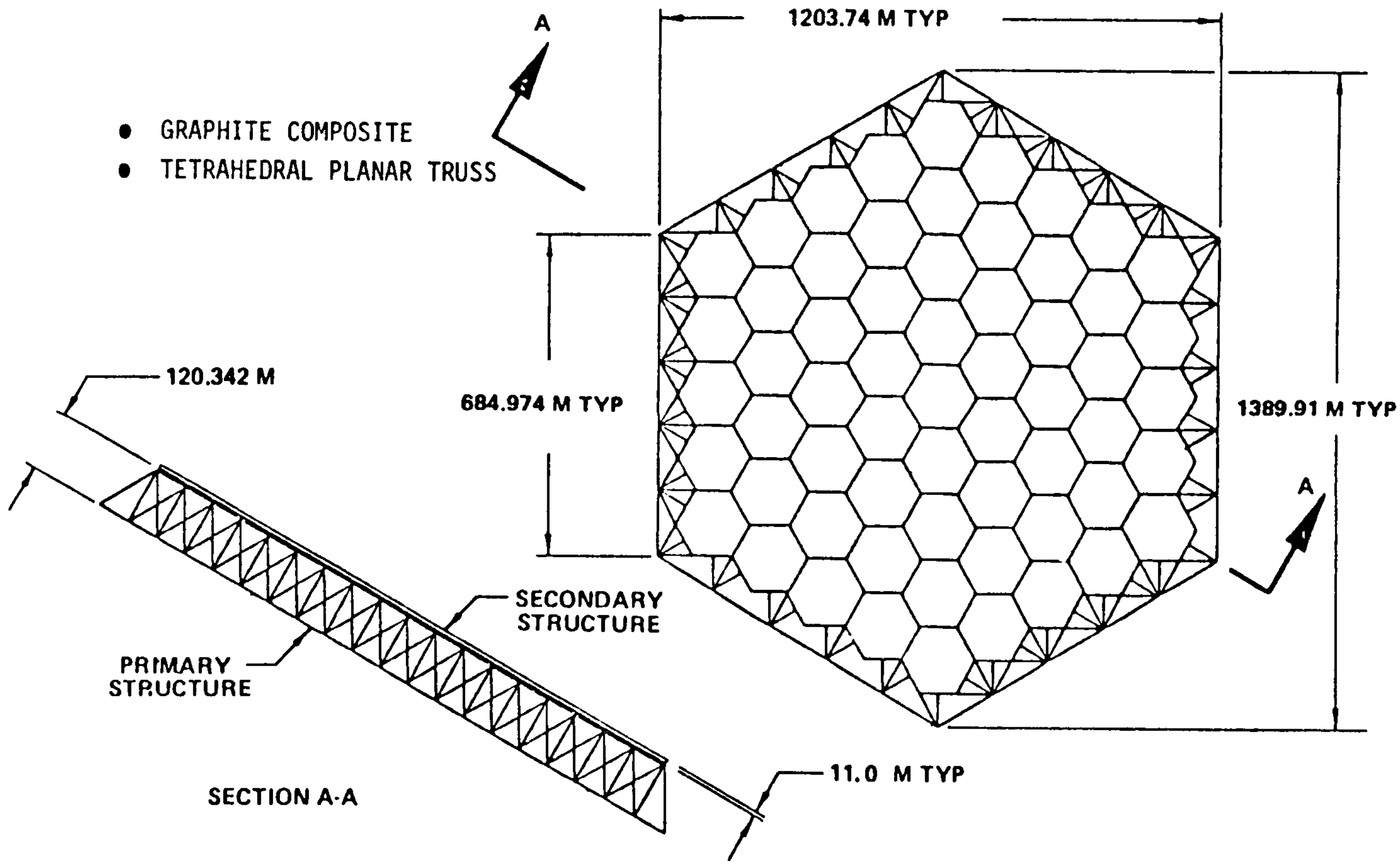


Figure B-19 Antenna Primary Structure

- GRAPHITE COMPOSITE

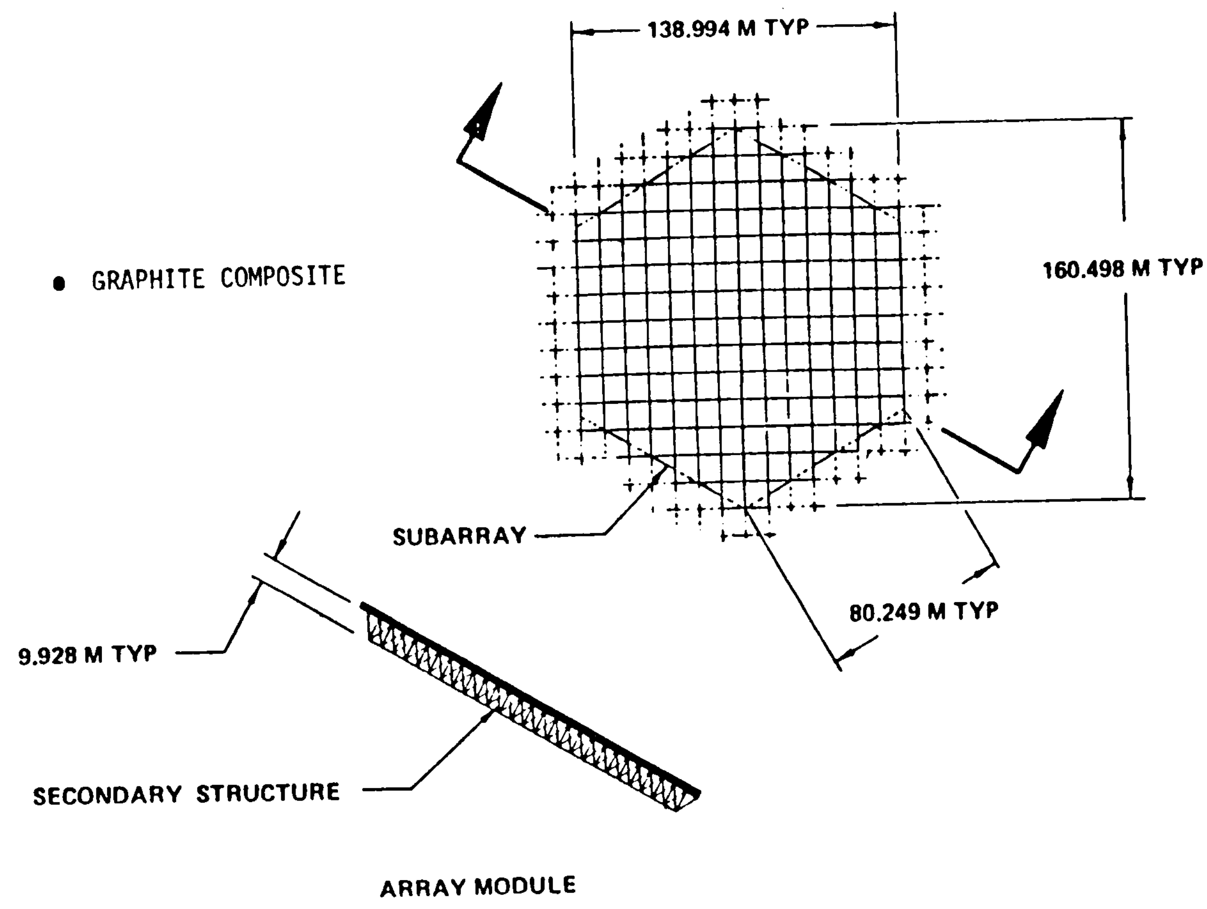


Figure B-20 Secondary Truss-Module

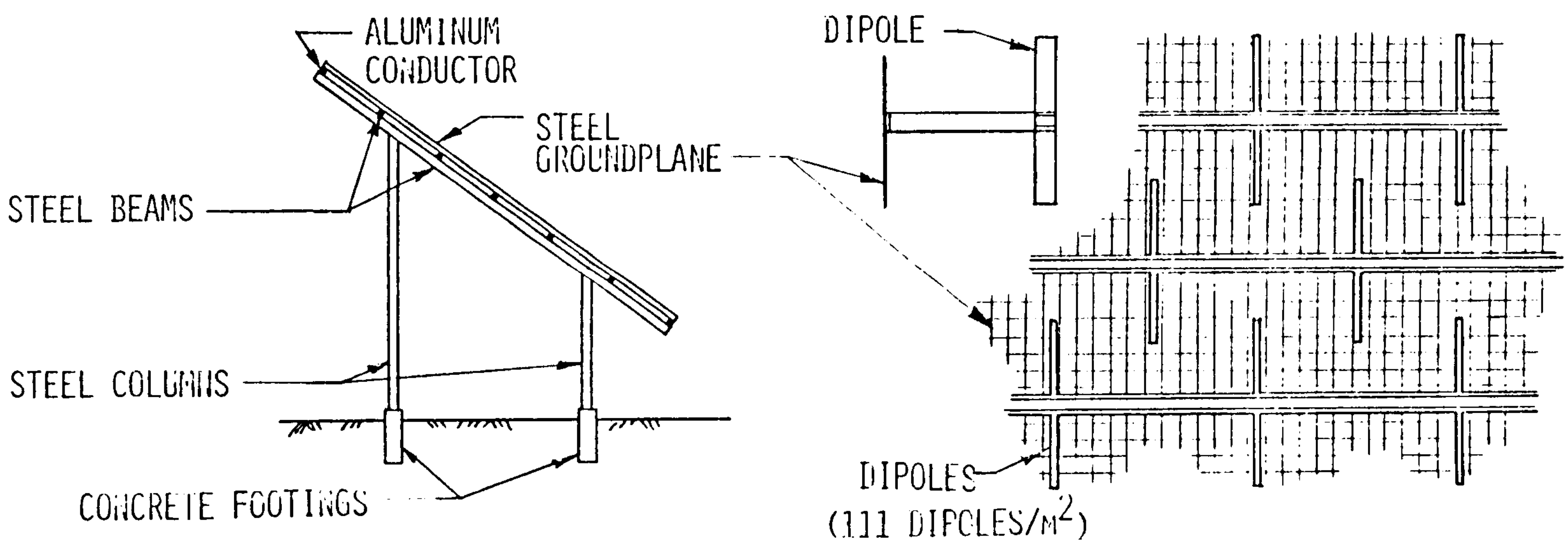


Figure B-21 Rectenna Components

The optimum efficiency of the rectifying elements is attainable at specific RF density levels and at specific DC load levels. The matching DC load increases for low RF density levels, which makes it needful to use different elements at different locations of the rectenna. Higher impedance elements are needed at the rectenna edge locations which is concomitant with the need to array more parallel elements to reach specific power levels. The receiving aperture cross-section area of such an element is approximately 50 $cm^2$. The conversion efficiency of the element is averaged to be 89%, with 86% efficiency at the periphery of the rectenna at power levels of approximately 1 $mw/cm^2$, and 94% at the center of the rectenna at power levels of 21 $mw/cm^2$.

The RF/DC converters are arrayed in units of 1 MW at a DC voltage at $\pm 2$ kV. These again are arrayed to form 2x20 MW primary units at the same DC voltage. The DC efficiency of arraying to the level of 40 MW units at $\pm 2$ kV is evaluated to be 97%, which leads to total RF/DC efficiency of approximately 85%. A 5000 MW rectenna contains 10.96 billion RF assemblies.

All the primary units of 40 MW along a radial line of the rectenna are locally converted to utility power levels and the power flow is directed radially to or out of the center of the rectenna.

Conversion to AC is performed in a total of 125 50 MW converter station/5 GW rectenna.

A moving factory concept would be utilized for rectenna construction. Materials brought in at one end of the factory are basic ingredients to high speed automated manufacture and assembly of rectenna panels which flow continuously through the factory. Detailed features of this concept have not yet been developed.

I. Mass Statement

Table B-2 shows a summary of the SPS mass on an elemental basis. The mass growth allowance was derived from a probablistic uncertainty analysis of SPS mass estimating factors.

Table B-2
PHOTOVOLTAIC CONFIGURATION MASS SUMMARY, WEIGHT IN METRIC TONS
10 GW

| Component | Mass |
|---|---|
| 1.0 SOLAR ENERGY COLLECTION SYSTEM | (55,747) |
| 1.1 Primary Structure | 7,155 |
| 1.2 Mechanical Systems | 67 |
| 1.3 Control | 323 |
| 1.4 Instrumentation/Communications | 4 |
| 1.5 Solar Cell Blankets | 45,773 |
| 1.6 Power Distribution | 2,425 |
| 2.0 MICROWAVE POWER TRANSMISSION SYSTEM | (25,546) |
| 2.1 Structure | 500 |
| 2.2 Attitude Control | 254 |
| 2.3 Comm/Data | 42 |
| 2.4 Power Distribution | 4,986 |
| 2.5 RF Generation and Distribution | 19,762 |
| SUBTOTAL | 81,293 |
| GROWTH | 17,590 |
| TOTAL . . . . . . . . . . . . | 98,883 |

## J. Space Transportation

This section provides a description of the space transportation system. Both launch and orbit transfer vehicles for cargo and personnel are included. In addition, launch facility requirements and operations/support are discussed.

The space transportation system includes a heavy lift launch vehicle (HLLV), a modified shuttle personnel launch vehicle (PLV), a personnel and supplies high-thrust orbit transfer vehicle (OTV), and low-thrust cargo orbit transfer vehicle (COTV) installed on the SPS modules constructed at LEO. The low-thrust OTS modules are reusable and are returned to LEO by a vehicle similar to the personnel OTV.

HLLV - The HLLV is a 2-stage, fully reusable winged launch vehicle. The launch configuration of the HLLV is shown in Figure B-22 with the overall geometry noted. This vehicle uses 16 $LCH_4/LO_2$ engines on the booster (first stage) and 14 standard SSME's on the orbiter (second stage). The $LCH_4/LO_2$ booster engines employ a gas generator cycle and provide a vacuum thrust of $9.79 \times 10^6$ newtons each. The SSME's on the orbiter provide a vacuum thrust of $2.09 \times 10^6$ newtons (100% power level). The gross lift-off weight of an HLLV is 11,040 metric tons with a payload to low earth orbit of 424 metric tons. A return payload of 15% (63.5 metric tons) of the delivered payload was assumed for the orbiter entry and landing conditions.

An airbreather propulsion system (aircraft jet engine) has been provided on the booster for flyback capability to simplify the booster operational mode. Its landing weight is 934 tons.

The HLLV is launched vertically using an erection system as illustrated in figure B-23. The stack height of the vehicle is 164 meters. The booster has a wing span of 60.6 meters.

The orbiter uses a glideback landing and has a landing weight of 439 metric tons.

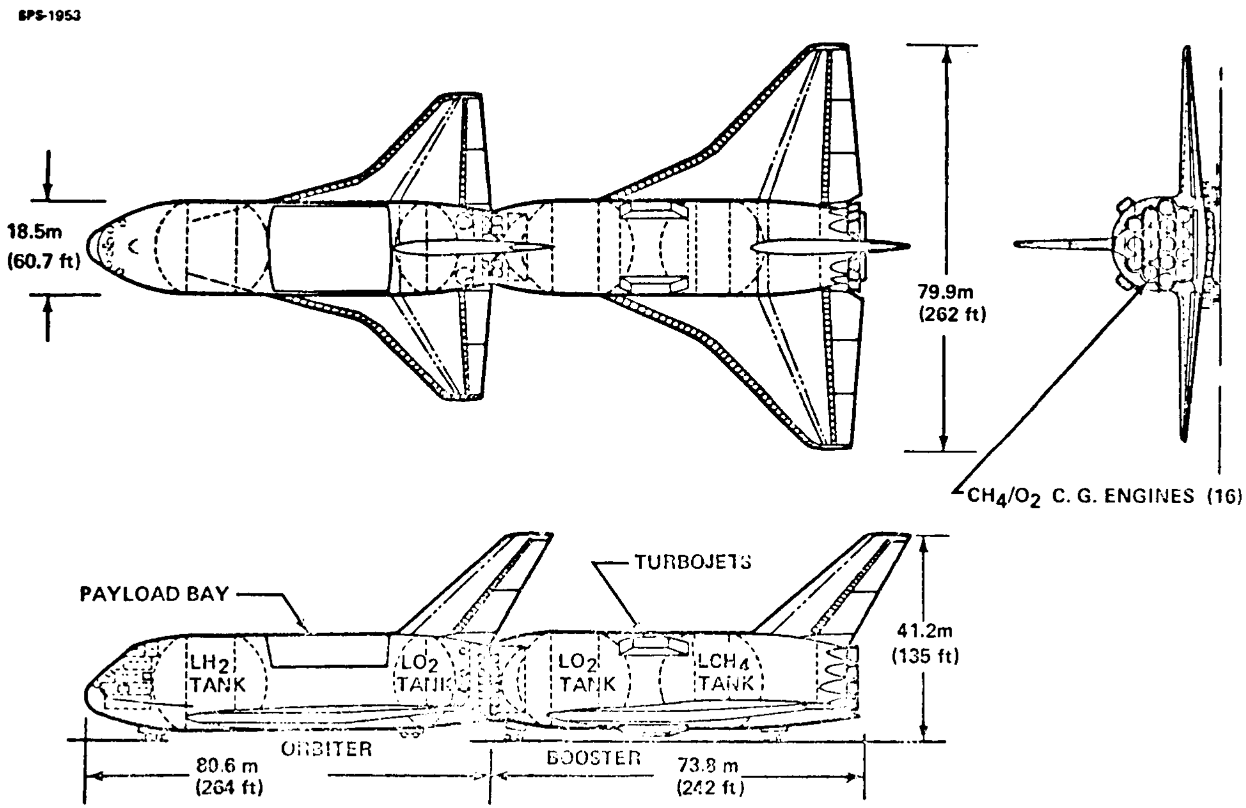


Figure B-22 Two-Stage Winged SPS Launch Vehicle (Fully Reusable Cargo Carrier)

SPS 1979

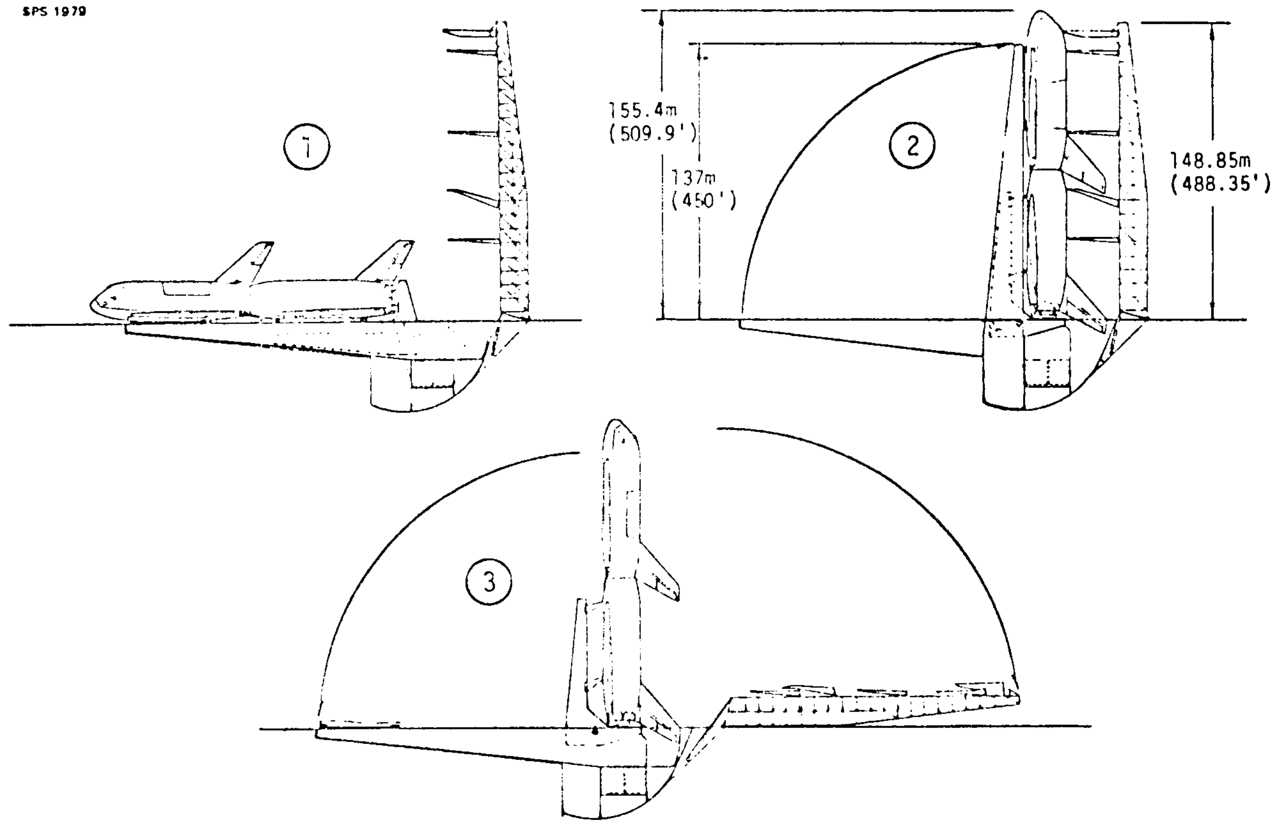


Figure B-23 Launcher/Erector Concept

Transportation Fleet Requirements - Table B-3 provides a summary of the total transportation requirements for the installation of one 10 GW SPS. Requirements are expressed in terms of flights/year for each vehicle, fleet size, and propellant requirements.

Personnel Launch Vehicle (PLV) - The personnel launch vehicle provides for the transportation of the crews between earth and low earth orbit. The vehicle is a derivative of the current space shuttle system which incorporates a liquid propellant booster in place of the Solid Rocket Boosters (SRB's). A series-burn ascent mode was selected and as a result External Tank (ET) propellant load is required.

The personnel launch vehicle, shown in figure B-24 incorporates a propane fueled booster, External Tank and Space Shuttle Orbiter. Overall vehicle geometry and characteristics are shown in the figure. The overall length of 60.92 m is due to the tandum arrangement rather than the side-mounted concept in the current shuttle system.

The vehicle transports 75 passengers to low earth orbit using a personnel module as depicted in figure B-25.

Personnel Orbit Transfer Vehicle (POTV) - The functions of the POTV is to deliver personnel and supplies from LEO to GEO and to return personnel from GEO to LEO at 90-day intervals.

The vehicle is a two-stage (common stage) $LO_2/LH_2$ configuration as illustrated in figure B-26. The vehicle transports 75 personnel per trip.

Cargo Orbit Transfer Vehicle (COTV) - The COTV includes all hardware, software, and consumables installed on SPS modules to equip them for orbit transfer from LEO to GEO. There are eight sets of this equipment as the SPS is transferred in eight modules. The modules are self-powered during the orbit transfer using portions of the on-board SPS solar array as the energy source for ion engines.

Table B-3 SPS Transportation Requirements

SPS TRANSPORTATION REQUIREMENTS

| VEHICLE | FLIGHT/YEAR | FLEET SIZE | PROPELLANT REQUIREMENTS METRIC TONS | |
|---|---|---|---|---|
| PLV 1ST STAGE | 36 (2) | 2 (5) | $O_2$<br>$CH_4$ | 44,000<br>12,500 |
| PLV 2ND STAGE | 36 (2) | 2 (5) | $O_2$<br>$H_2$ | 17,000<br>2,850 |
| POTV - BOTH STAGES | 5 (2) | 2 | $O_2$<br>$H_2$ | 2,160<br>360 |
| HLLV 1ST STAGE | 391 (1) | 6 (4) | $O_2$<br>$CH_4$ | $2.0 \times 10^6$<br>670,000 |
| HLLV 2ND STAGE | 391 (1) | 6 (4) | $O_2$<br>$H_2$ | 812,000<br>133,000 |
| COTV ~ LARGE PANELS | 8 (3) | 8 | AR<br>$O_2$<br>$H_2$ | 11,800<br>5,040<br>840 |
| COTV ~ SMALL PANELS | 24 (3) | 24 | AR<br>$O_2$<br>$H_2$ | 13,000<br>5,400<br>900 |
| | | TOTALS: | $O_2$<br>$H_2$<br>$CH_4$<br>AR | $\approx 3 \times 10^6$<br>$\approx$140,000<br>$\approx$700,000<br>$\approx$ 25,000 |

NOTES:

(1) PLUS 61 FLTS 1ST YEAR TO DELIVER LEO & GEO CONST. BASES

(2) 480 PEOPLE IN LEO, 60 PEOPLF IN GEO, 90 DAY STAY TIME, 80% LOAD FACTOR

(3) ASSUMED SINGLE FLIGHT/UNIT

(4) 4 DAY TURNAROUND, 25% SPARES

(5) 14 DAY TURNAROUND, 40% SPARES

SPS-681

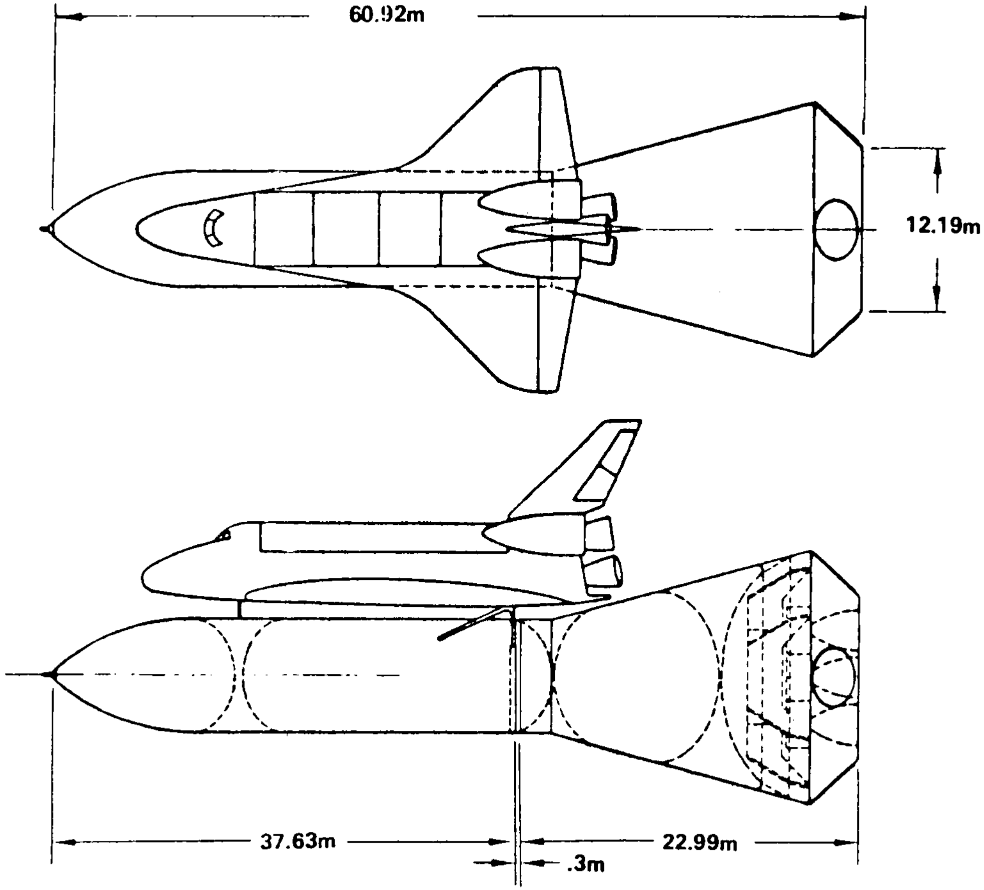


| | |
|---|---|
| GLOW | $2.512 \times 10^6$ KG |
| BLOW | $1.779 \times 10^6$ KG |
| $W_{p_1}$ | $1.560 \times 10^6$ KG |
| ULOW | $.659 \times 10^6$ KG |
| $W_{p_2}$ | $.547 \times 10^6$ KG |
| PAYLOAD | $.074 \times 10^6$ KG |
| T/W AT LIFTOFF | 1.238 |

MAIN PROPULSION

| STAGE | $\varepsilon$ | NUMBER/TYPE | THRUST/ENGINE (VACUUM) $10^6$ N | THRUST/ENGINE (VACUUM) $10^6$ lbf | $I_{sp}$ SEC |
|---|---|---|---|---|---|
| 1 | 40 | $4 \cdot C_3H_8$ | 8.523 | 1.916 | 340.0 |
| 2 | 77.5 | 3 SSME | 2.091 | .470 | 455.2 |

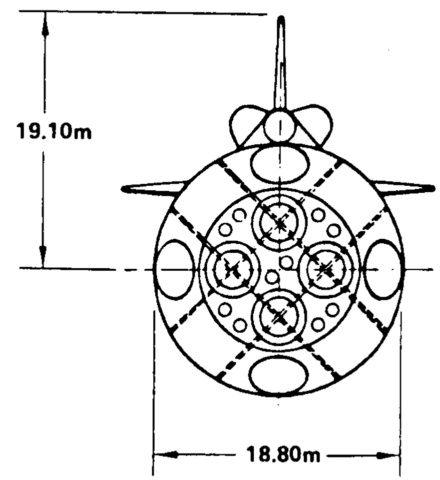


Figure B-24  Personnel Launch Vehicle

SPS-926

| | |
|---|---|
| EMPTY MASS | 9,958 KG |
| MASS OF CREW (50) | 7,938 KG |
| TOTAL MASS | 17,896 KG |

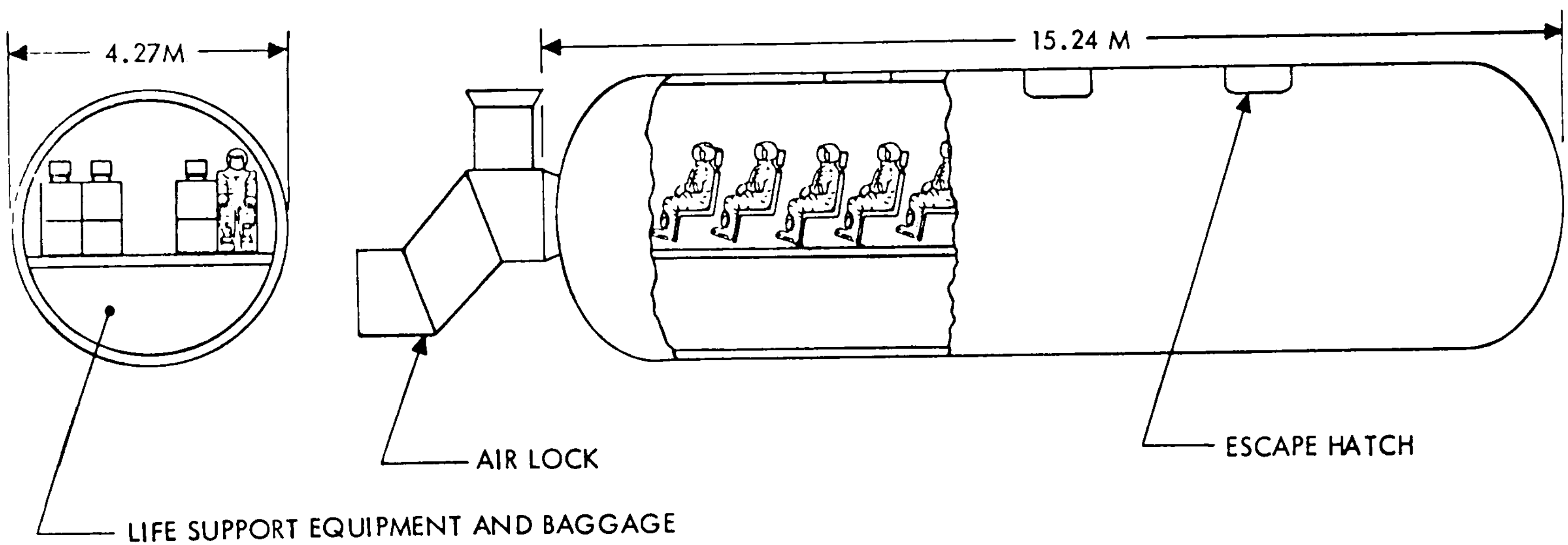


Figure B-25 Shuttle Personnel Module

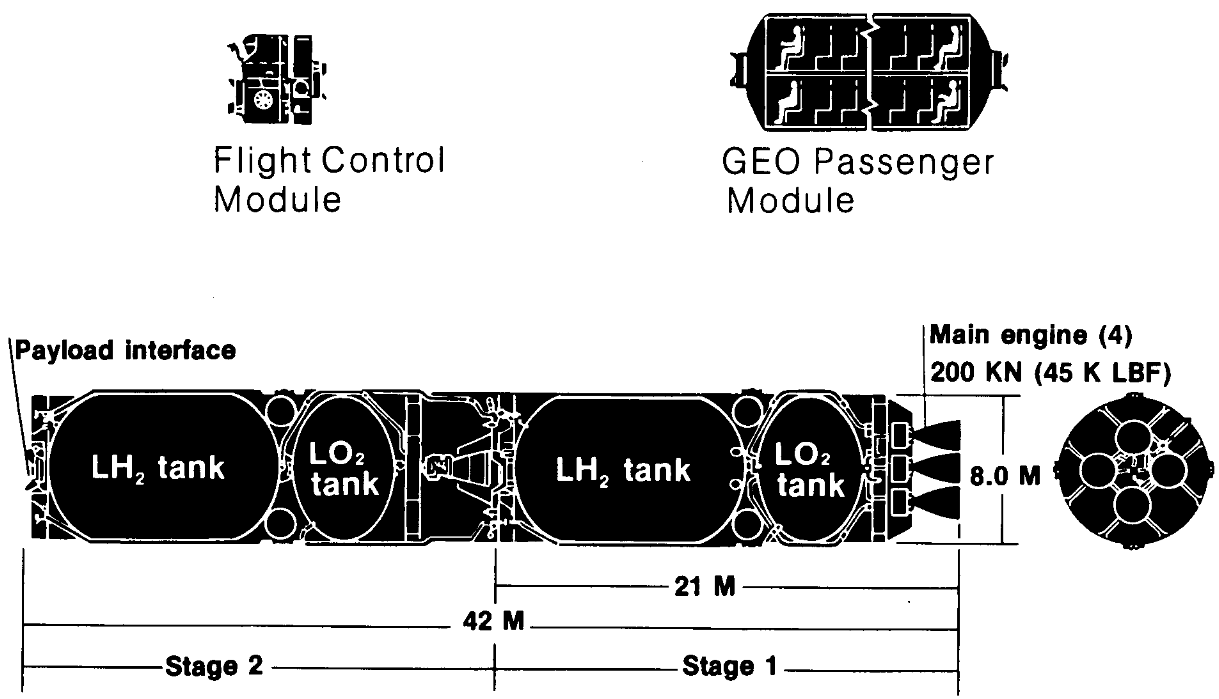


Figure B-26 Personnel Orbit Transfer Vehicle (POTV)
Common Stage $LO_2/LH_2$

The configuration arrangement and characteristics of the system elements used in the transfer of each satellite module are shown in figure B-27. Each module is 2.7 x 5.4 km. Six of the modules are transferred without a microwave antenna attached. Their mass is 8700 metric tons each. The other two modules each have a fully constructed microwave antenna attached making their mass 23,700 tons each. Propulsion for the orbit transfer is provided by a combination of electric powered ion thrusters (argon propellant) and $LO_2/LH_2$ thrusters. The ion thrusters provide most of the orbit transfer energy whereas the chemical system is used to counteract gravity gradient torques on the module and to maintain desired attitude during the transfer. Power for the ion thrusters is provided by partially deployed SPS solar array. The 8,700-ton modules require 13% of the SPS array deployed to power four panels of 600 ion thrusters. The heavier modules (with antenna) require 36% of the on-board solar array to power four panels of 1,600 ion thrusters. The trip time for each module is 180 days.

The SPS solar array was oversized 5% to compensate for the radiation degradation of the silicon solar cells during passage through the Van Allen radiation belt. This also compensates for the inability to anneal out all of the damage after reaching GEO.

L. Operations

1. Satellite System Construction Operations - The integrated construction, maintenance and transportation operational concept for low earth orbit (LEO) construction of the CR=1 photovoltaic satellite is shown in figure B-28. Space operations crews and all hardware and consumables required in space are delivered to LEO by launch vehicles. The crew launch vehicle was assumed to be an improved space shuttle with the solid rocket boosters replaced by a reusable liquid propellant booster. The cargo vehicle is a two-stage wing-wing vehicle capable of delivering approximately 400,000 Kg of payload per flight. Crew flights occur every two weeks while three cargo vehicle flights are required every two days to each construction facility for the case of constructing one 10 GWe satellite per year.

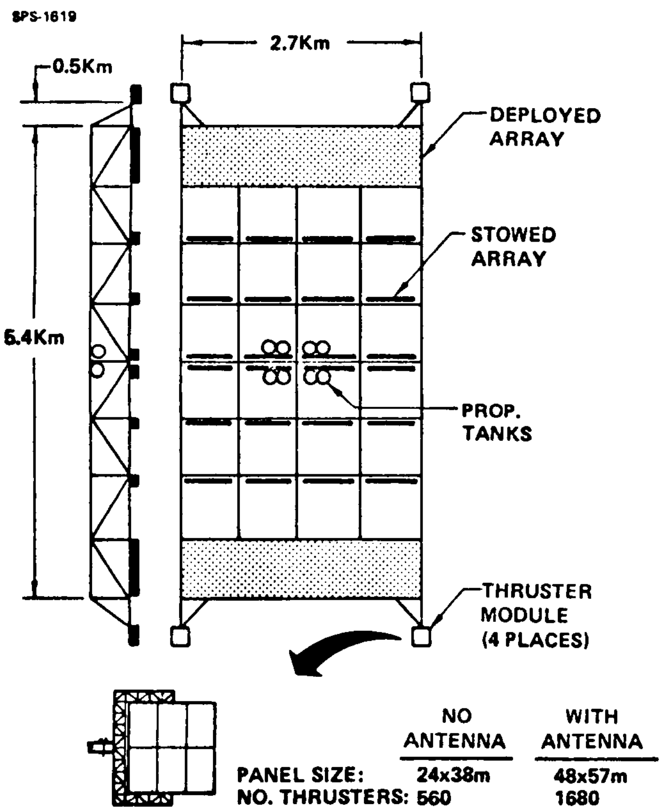


| | NO ANTENNA | WITH ANTENNA |
|---|---|---|
| PANEL SIZE: | 24x38m | 48x57m |
| NO. THRUSTERS: | 560 | 1680 |

GENERAL CHARACTERISTICS

- 5% OVERSIZING (RADIATION)
- TRIP TIME = 180 DAYS
- ISP = 7000 SEC

| MODULE CHARACTERISTICS | NO ANTENNA | WITH ANTENNA |
|---|---|---|
| • NO. MODULES | 6 | 2 |
| • MODULE MASS ($10^6$KG) | 8.7 | 23.7 |
| • POWER REQ'D ($10^6$Kw) | 2.38 Km$^2$ | 0.81 |
| • ARRAY % | 13 | 36 |
| • OTS DRY ($10^6$KG) | 1.1 | 2.9 |
| • ARGON ($10^6$KG) | 2.0 | 5.6 |
| • $LO_2/LH_2$ ($10^6$KG) | 1.0 | 2.8 |
| • ELEC THRUST ($10^3$N) | 4.5 | 12.2 |
| • CHEM THRUST ($10^3$N) | 12.0 | 5.0 |

Figure B-27 Self Power Configuration Photovoltaic Satellite

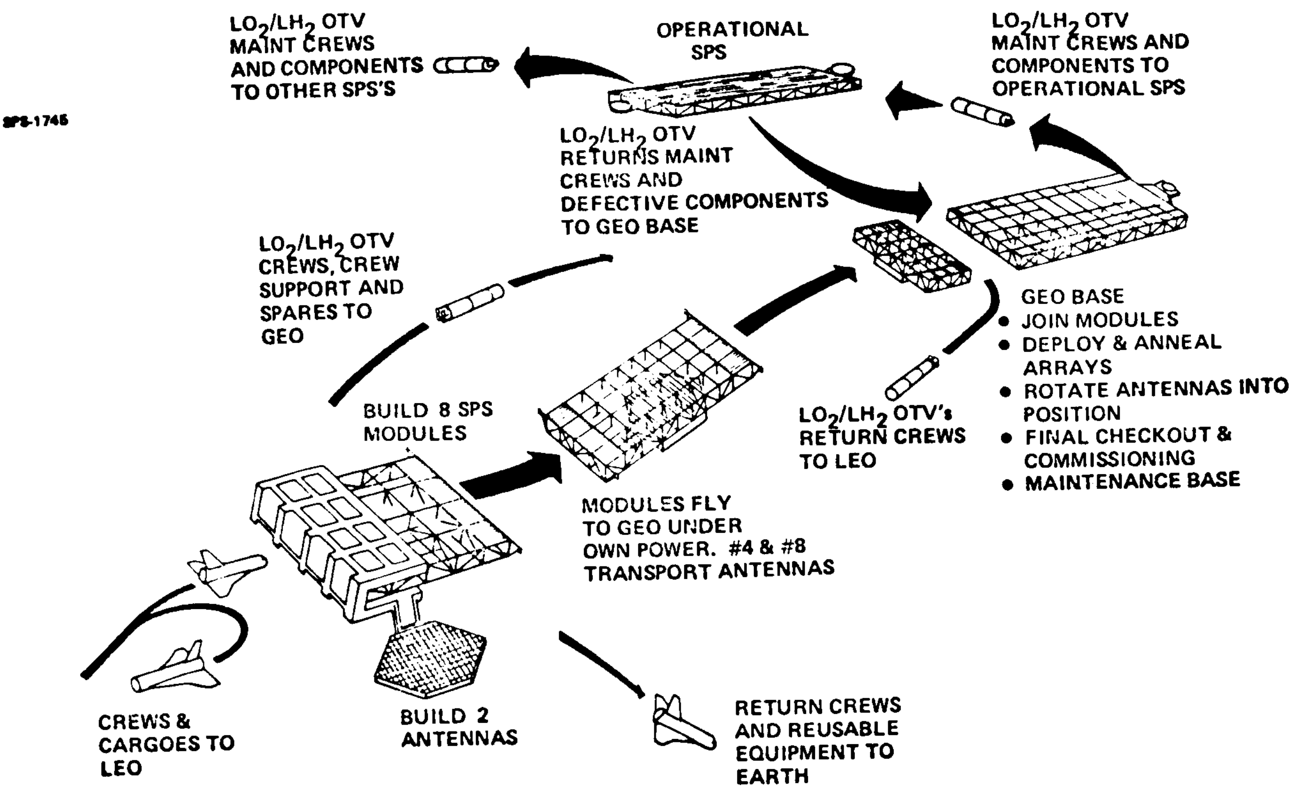


Figure B-28 Integrated Space Operations

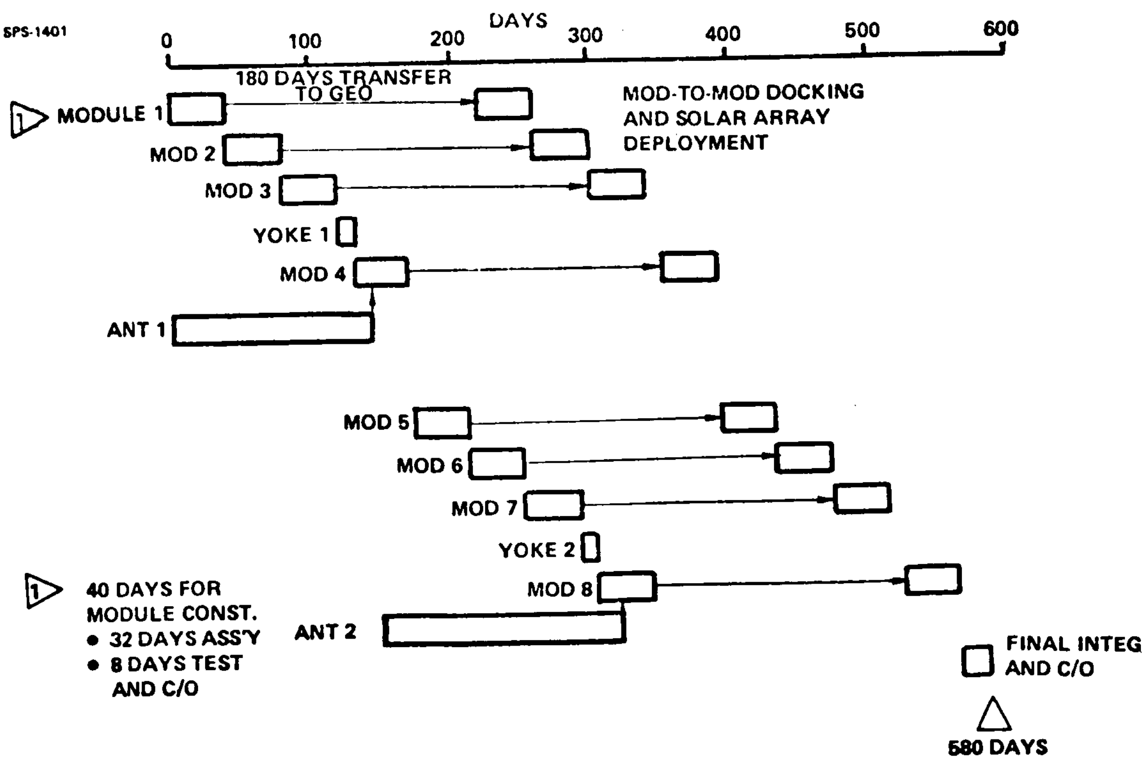


Figure B-29 Photovoltaic Satellite LEO Construction Timeline

The LEO construction base is nominally located in a 478 Km circular orbit at 31° inclination. This base houses a crew of 480 with overflow quarters for transients, e.g., those crew members awaiting transportation to some other location. The primary purpose of the LEO base is construction of eight SPS power generation modules and two antennas. The satellite construction timeline is shown in figure B-29. The base also serves as a staging depot for orbit transfer vehicles used to carry construction and maintenance crews, crew supplies and replacement parts to the GEO base. A construction crew OTV flight to the GEO base normally occurs once every three months. Maintenance crew and replacement components are also transferred to GEO every three months.

The satellite modules are equipped with electric propulsion systems and flight control systems for the self-powered trip to GEO.

The GEO base is used for final assembly and maintenance operations. The final assembly operations include module berthing, antenna placement, and deployment of solar array. The maintenance operations include refurbishment of failed SPS hardware. The GEO base is also used as a staging area for the satellite maintenance crews, mobile habitats, spare parts, and their orbit transfer vehicles. The GEO base houses 60 final assembly crew members and up to 240 SPS maintenance crew members.

The maintenance crews are dispatched from the GEO base in an OTV-propelled crew module along with an OTV-propelled replacement parts module destined for an operational SPS that is scheduled for regular maintenance. The maintenance crew will visit each SPS two times per year and will spend four days replacing defective components before returning to the GEO base or proceeding to the next SPS.

<u>Construction Base LEO</u> - The LEO construction base for the photovoltaic satellite consists of two interconnecting facilities. One of the facilities is used to construct the module and the other is used to construct the antennas as shown in figure B-30 and B-31.

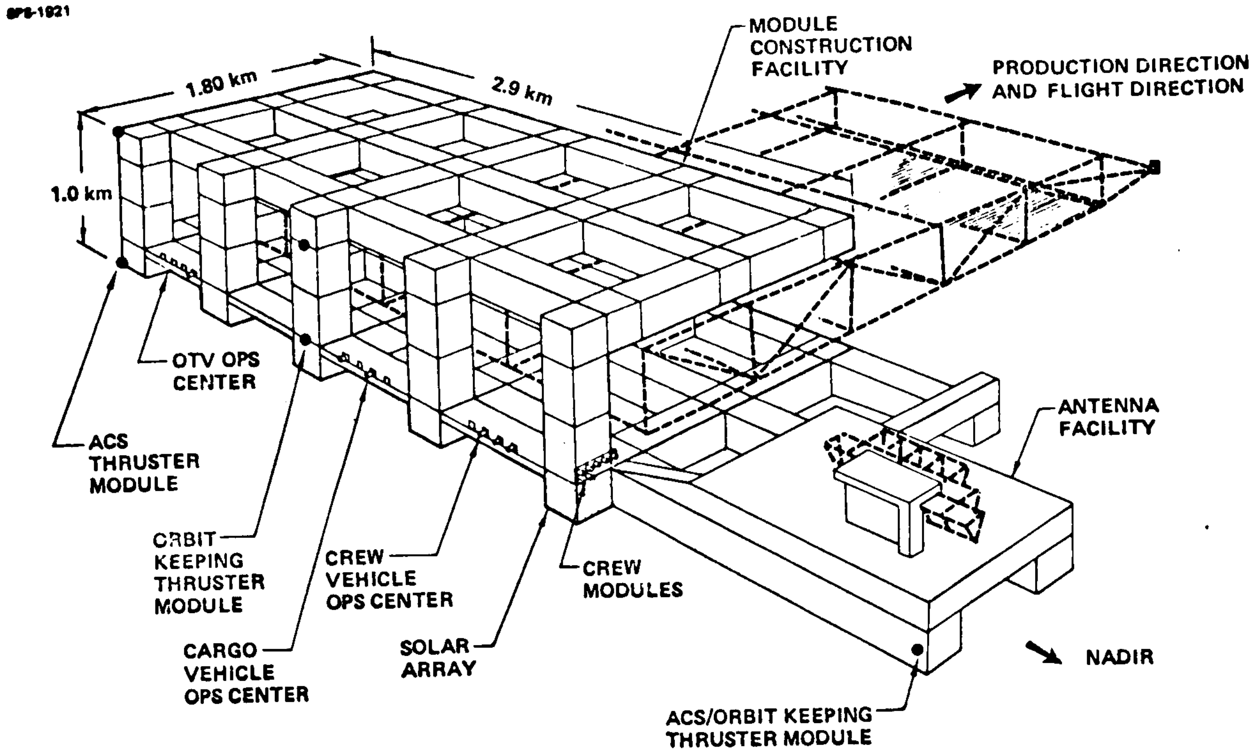


Figure B-30 LEO Construction Base Photovoltaic Satellite

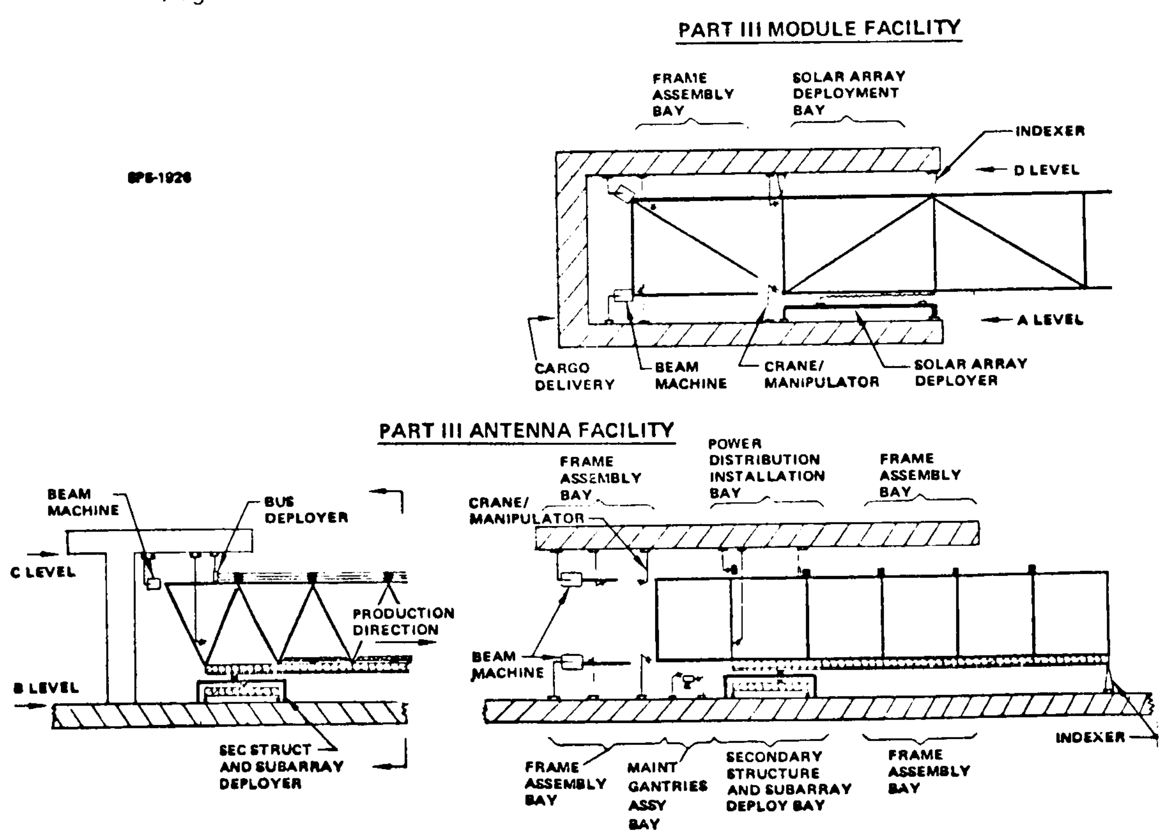


Figure B-31 Construction Base Equipment/Operations

The module construction facility is an open-ended structure which allows a 4-bay-wide module to be constructed with only longitudinal indexing. There are two sets of internal working bays. The aft bays are used for structural assembly using moving beam machines and crane/manipulators attached to both the "A" level and "D" level surfaces of the facility (see figure B-31). Solar array and power distribution components are installed from equipment located on the "A" level in the forward bays. The satellite module is supported and indexed by movable towers located on the "D" level of the facility.

The antenna facility is located with respect to the module facility in such a way that the antenna is constructed at a location where the completed antenna can be mated to the yoke without any vertical movement. The antenna construction facility (also shown in figure B-31) is configured in an open-ended structure that is five antenna bays wide which allows the antenna to be constructed using both lateral and longitudinal indexing. The two end bays are used to assemble the primary structure and the inner bays are used to deploy the secondary structure and subarrays, and to install the power distribution system and maintenance gantries. Construction equipment operates from both the "B" and "C" levels of the antenna facility.

The module construction sequence for the structure, solar array and power buses begins with building the first end frame of the structure. This completed end frame is indexed forward one structural bay length. Machines can then form the remainder of the structure in each of the bays. The first row of four bays is then indexed forward to allow construction of the second row of structural bays in parallel with installation of solar arrays in bay 1 through 4. Solar array installation and construction of structure occurs simultaneously across the width of the module although neither operation depends on the other. At the completion of the 16 bays (four rows of bays in length), the power buses and propellant tanks are installed. Construction of the structure and installation of solar arrays of the remaining four bay lengths of the module are done in a similar manner to that previously described.

Thruster modules for the self-power system are attached to each of the four corners of the module. An annealing device gantry is installed on each module.

Construction of the antenna takes place in parallel with module construction. The first antenna is completed during construction of the fourth satellite module; the second antenna is completed with the eighth module. The antenna is indexed laterally through the facility one bay at a time. When a full width of bays is constructed the antenna is indexed longitudinally out of the facility so that the next strip of bays can be assembled. When the antenna is completed, it will be located at the proper position so that it can be mated to the yoke.

The yoke for the antenna is constructed in the module construction facility because of its large dimensions. This requires the yoke to be made between the third and fourth module and between the seventh and eight modules. Following yoke construction, it is moved to the side of the module facility. At that time, either the fourth or the eighth module will be constructed. During the construction of these modules, the antenna is completed so that it can then be attached to the yoke. After five bays of either the fourth or eighth module have been completed, the antenna/yoke combination can then be attached to the module in its required location. Construction of two more rows of bays pushes the antenna outside the facility where it then can be hinged over the module for its transfer to GEO.

In addition to the construction base facilities, the LEO base includes crew modules, work modules, cargo handling/distribution equipment/ vehicles and base subsystems.

The LEO construction base includes five primary crew modules. The modules have an earth atmosphere environment and are sized to accommodate crew sizes between 50 and 100. The modules have dimensions of 17m diameter and up to 23m in length.

Work modules are used for operations, maintenance, and training. They are similar in design to crew modules but have specialized functions which include clinic, satellite components maintenance and checkout, and new personnel training.

Base subsystems include electrical power and flight control systems. The total power requirement estimated for all LEO base operations is 3725 kw. The primary power supply is solar arrays similar to those used in the SPS with nickel hydrogen batteries used for occultation periods.

The flight control system includes guidance/navigation/attitude type sensors such as IRU, star trackers, horizon sensors and the propulsion system ($LO_2/LH_2$) to perform attitude and orbit maintenance maneuvers.

Construction Base GEO - The GEO construction base is a 2 x 2 bay-wide platform that is attached to and indexed across the solar array side of the modules, as shown in figure B-32. This platform has four solar array deployment machines that are used to deploy the undeployed solar arrays. There are also a variety of crane/manipulators, logistics and SPS maintenance equipment aboard.

The first operation to occur once the modules reach GEO is that of the berthing (or docking) of the modules. The modules are berthed along a single edge as indicated in figure B-33. The major equipment used to perform these berthing operations are shown. The concept employs the use of four docking systems with each involving a crane and three control cables. Variations in the applied tension to the cables allows the modules to be pulled in, provide stopping control and provides attitude control system involving thrusters which are not shown.

During the transfer from LEO to GEO, the antenna is attached below the module with a single hinge line. Once GEO is reached, the antenna is rotated into position followed by the final structural and electrical connections, as indicated in figure B-34.

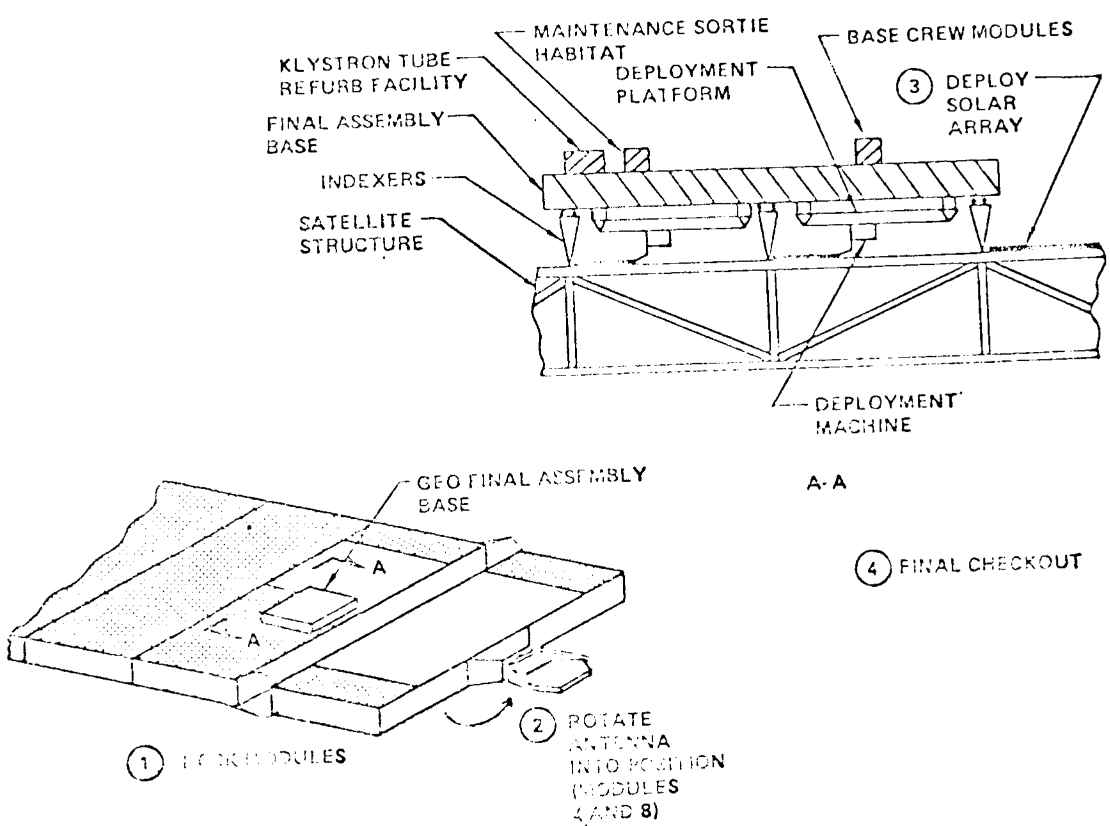


Figure B-32 GEO Final Assembly Base/Operations

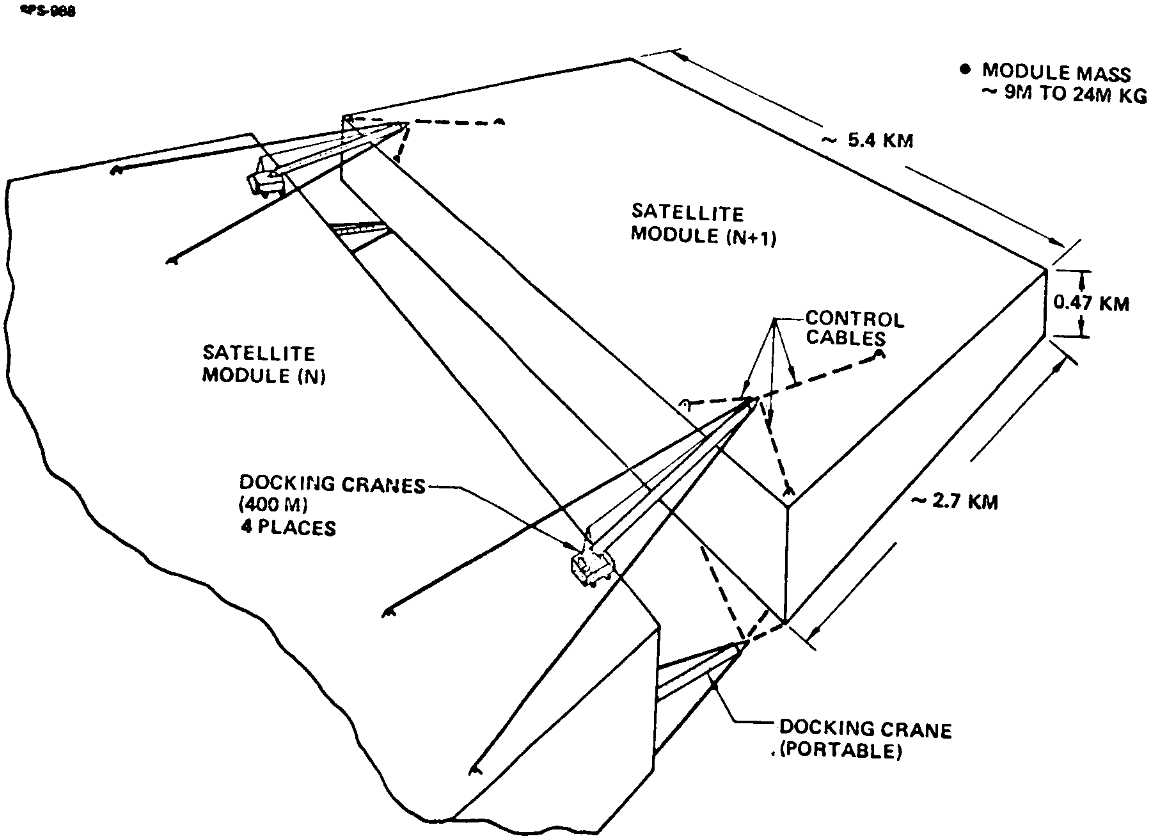


SPS-1487 Figure B-33 GEO Berthing Concept-Photovoltaic Satellite

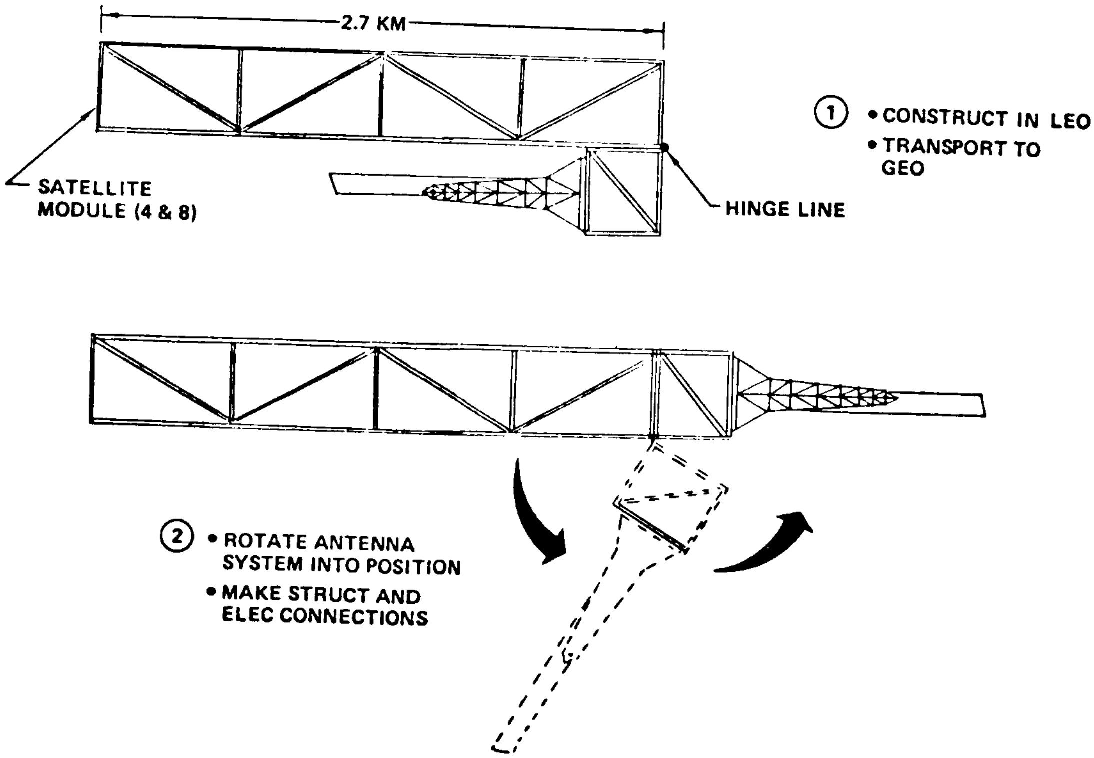


Figure B-34 Antenna Final Installation-Photovoltaic Satellite

The GEO base has overall dimensions of 1400m x 1600m with two decks of operation. The upper deck supports the crew and maintenance modules and docking facilities for transportation systems and payloads. The lower surface of the facility supports the four solar array deployment machines. Docking cranes used in berthing the modules are also attached to the base when not in use or when the GEO base is transferred to another longitudinal location.

GEO base primary subsystems include electrical power (260 Kw solar array) and flight controls systems consisting of attitude control and station keeping systems, which use $LO_2/LH_2$ propulsion.

Other major elements of the base include construction equipment, satellite maintenance systems, and crew modules. Construction equipment is similar to LEO base construction equipment except for docking cranes, which are not needed on the LEO base. The major maintenance systems center around microwave antenna klystron tube replacement and solar array annealing operations. Both require special equipment and provisions for access to maintenance areas and for repair/refurbishment operations.

The GEO base has a construction crew size of 65 and only a minimum of construction operations so, consequently, all functions can be incorporated into a single crew module. Transportable maintenance crew modules are also based at the GEO facility. The construction crew module includes structure, electrical power, environmental control, life support, crew accommodations, and information systems. The crew modules are similar in design to the crew quarters modules used at the LEO construction base. The major modifications to the LEO modules are as follows: (1) incorporation of an operation deck in place of one of the three personnel decks since only 65 rather than 100 people are housed in the module, and (2) add an eighth deck which serves as a solar flare radiation shelter. Assuming a shielding requirement of 20 to 25 $gm/cm^2$, the shelter will add an additional 115,000 Kg to the basic module mass. Within the shelter will be provisions for up to five days and controls to operate the complete base on standby status. Subsystems used within the modules are the same as for the LEO base modules described previously.

Figure B-35 shows a summary of crew requirements for the LEO and GEO construction base operations.

Component Packaging for Launch - Component packaging for launch is a very significant factor in construction as well as space transportation. Packages must not only meet dimensional and weight constraints of the launch vehicle, but must have appropriate mass density to far cost effective transportation. Figure B-36 illustrates the dimensions, density, and part count of various SPS components. As indicated, densities vary from a low of 12 $kg/m^3$ for antenna subarray elements to about 2500 $kg/m^3$ for power conductor. To obtain desired densities, components must be packaged in appropriate mixes as indicated in figure B-37. Such packaging minimizes the number of launches, thereby reducing transportation costs.

Crew Considerations - Figure B-28 illustrates the integrated space operations. The satellite construction phase requires 580 days as indicated on the construction timeline shown in figure B-29. During construction, a crewman will be located in geosynchronous orbit.

The reference crew scheduling concept is summarized below.

- 90 day staytime
- 6 days on/1 day off per week
- 10 hours work shift per day
- 2 shifts per day (2 crews)
- 0.75 operator productivity factor

Radiation protection is provided to limit crewmen to 35 REM/year exposure. Shielding of 2 to 3 $gm/cm^2$ in LEO and 20 to 25 $gm/cm^2$ in GEO will provide this protection. Habitat walls will provide the 2 to 3 $gm/cm^2$ shielding, however, special "storm shelter" facilities must be provided to obtain 20 to 25 $gm/cm^2$ shielding. This type of facility would be needed during solar flares only.

CONSTRUCTION CREW

- 480 IN LOW EARTH ORBIT (250-300 NM)
- 60 IN GEOSYNCHRONOUS EQUATORIAL ORBIT
- MAXIMUM CREW STAY TIME - 90 DAYS
- WORK SCHEDULE - 2 SHIFTS<br>6 DAYS/WEEK<br>10 HOURS/DAY

Figure B-35 Space Operations

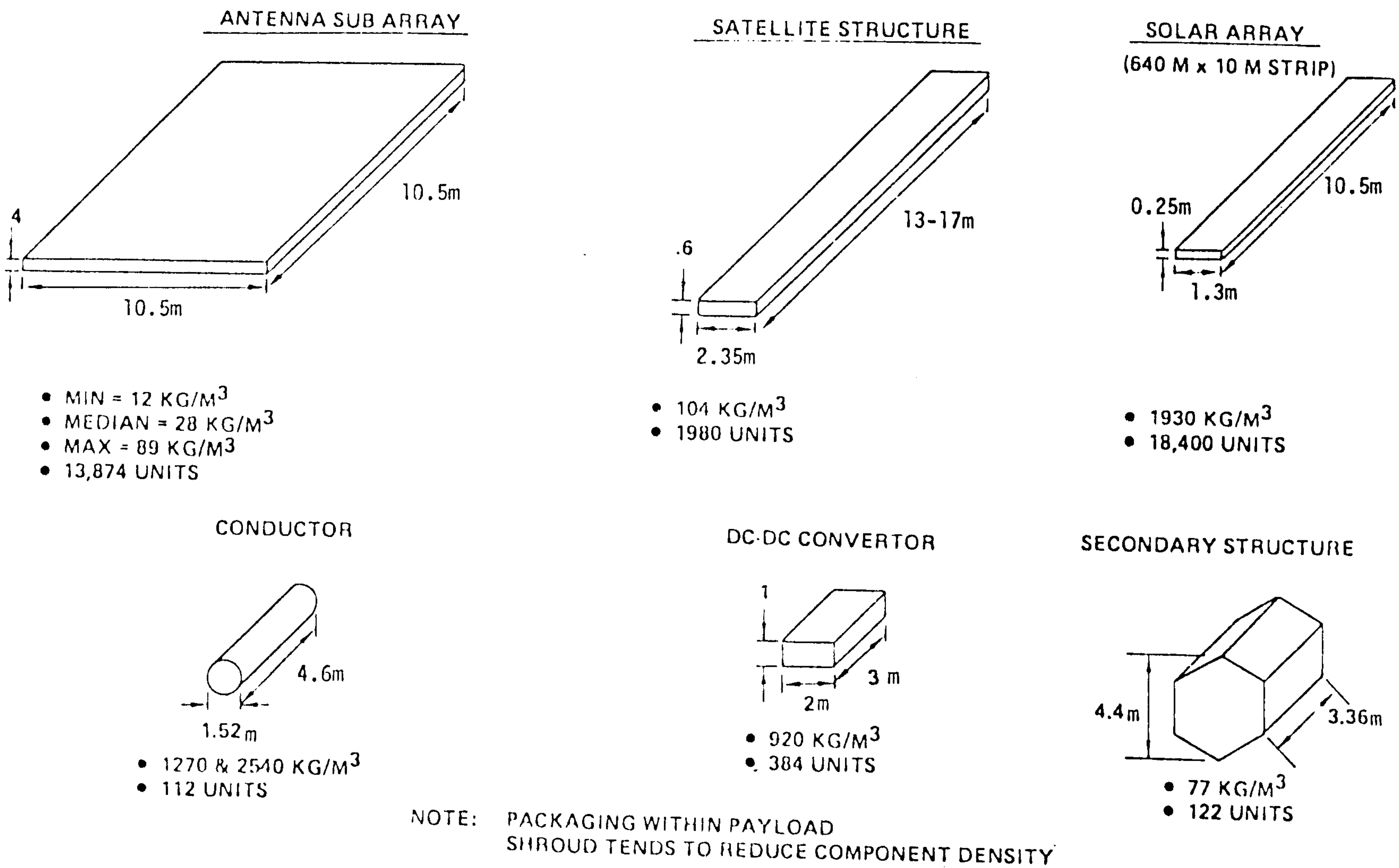


Figure B-36 Component Packaging Characteristics

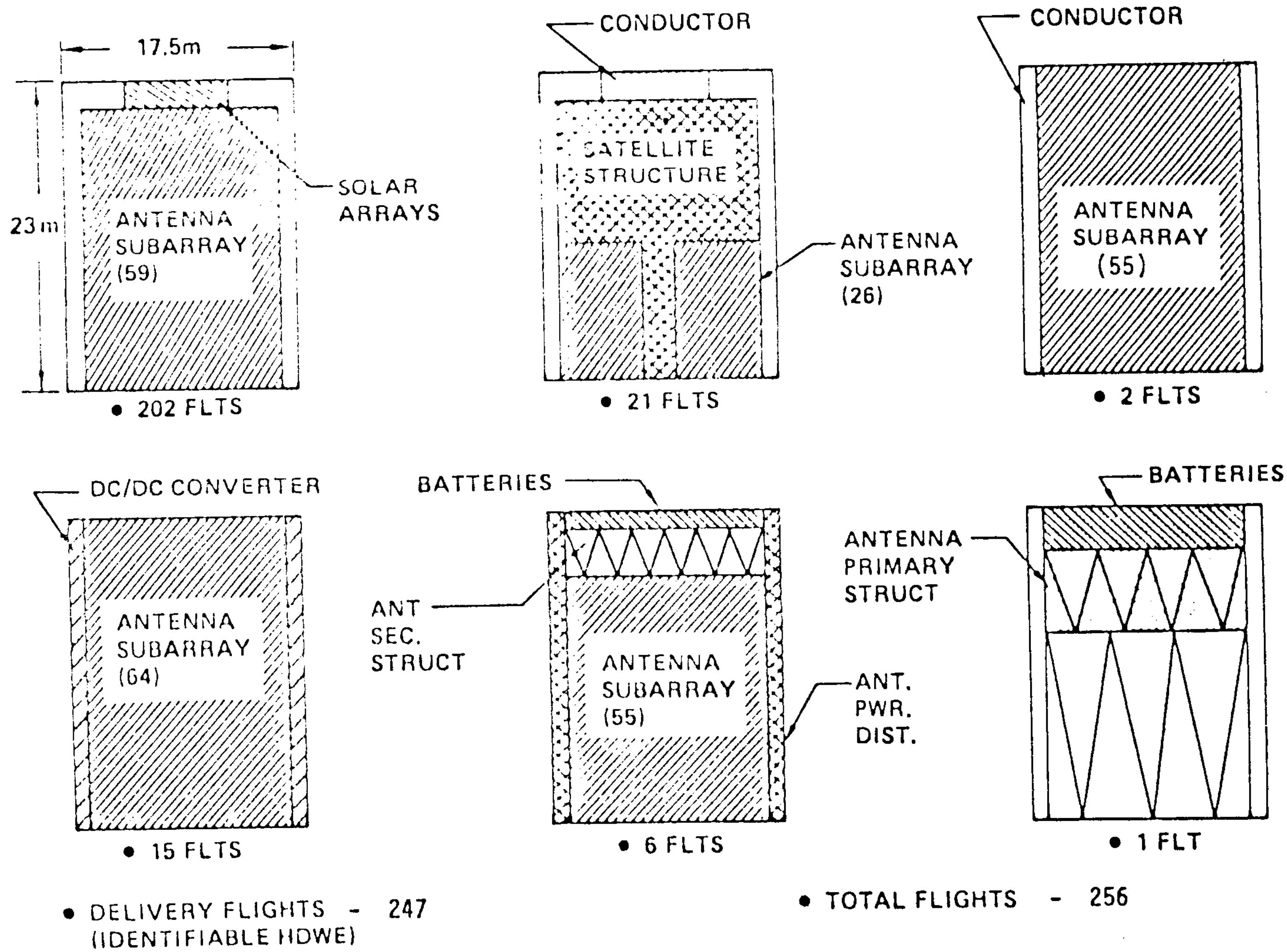


Figure B-37 Typical Component Mixing

Ground Station (Rectenna) - The rectenna concept utilizes a weather proof matched dipole configuration which is amenable to mass production. All materials required are readily available and of low cost. To achieve low construction costs, a moving rectenna factory is envisioned. Materials brought in at one end of the factory are basic ingredients to high speed automated manufacture and assembly of rectenna panels which flow continuously from the moving factory.

2. Commercial Operations - Commercial operations consists of operating and control of the power system as it supplies power to a power grid and maintenance operations required to keep the system within performance limits.

Loss of total or partial power from the satellite would occur several times a year due to satellite routine maintenance, shadowing effect from the earth and from other SPS systems. When these outages are predictable and scheduled it should have a minimal effect on the utility systems integrity and operations since the timing of such outages would be during the low load periods.

However, assuming a significant penetration of SPS power systems in the future, the generation reserve needed to maintain the utility service reliability would be expected to increase to cover the emergency shutdowns of the satellite. More detailed utility system studies are needed to predict the impact on reserve levels from emergency SPS power system outages.

# DOCUMENTATION LIST

The Boeing Solar Power Satellite System Definition Study, NAS 9-15196, was performed and documented in three parts as follows:

| | | | |
|---|---|---|---|
| **Part I** | | | |
| Vol. I | Executive Summary | D180-20689-1 | Jun 28, 1977 |
| Vol. II | System Requirements and Energy Converstion Options | D180-20689-2 | Jul 29, 1977 |
| Vol. III | Construction, Transportation and Cost Analyses | D180-20689-3 | Aug 8, 1977 |
| Vol. IV | SPS Transportation System Requirements | D180-20689-4 | Aug 1, 1977 |
| Vol. V | SPS Transportation: Representative System Descriptions | D180-20689-5 | Jul 28, 1977 |
| **Part II** | | | |
| Vol. I | Executive Summary | D180-22876-1 | Dec 1977 |
| Vol. II | Technical Summary | D180-22876-2 | Dec 1977 |
| Vol. III | SPS Satellite Systems | D180-22876-3 | Dec 1977 |
| Vol. IV | Microwave Power Transmission System | D180-22876-4 | Dec 1977 |
| Vol. V | Space Operations | D180-22876-5 | Dec 1977 |
| Vol. VI | Evaluation Data Book | D180-22876-6 | Dec 1977 |
| Vol. VII | Study Part II Final Briefing Book | D180-22876-7 | Dec 13, 1977 |
| Vol. VIII | SPS Launch Vehicle Ascent and Entry Sonic Overpressure and Noise Effects | D180-22876-8 | Dec 1977 |
| **Part III** | | | |
| | Preferred Concept System Definition | D180-24071-1 | Mar 1978 |
| | (Final Briefing) | D180-24071-3 | Mar 7, 1978 |

NASA-JSC